SPECIATION MODELLING OF COPPER(II) IN THE THIOMOLYBDATE – CONTAMINATED BOVINE RUMEN

A Thesis Submitted to the College of
Graduate Studies and Reasearch
In Partial Fulfillment of the Requirements
For the Degree of Doctor of Philosophy
In the Department of Chemistry
University of Saskatchewan
Saskatoon

By

Joseph Essilfie - Dughan

PERMISSION TO USE

In presenting this thesis in partial fulfillment of the requirements for a Postgraduate degree from the University of Saskatchewan, I agree that the Libraries of this University may make it freely available for inspection. I further agree that permission for copying of this thesis in any manner, in whole or in part for scholarly purposes may be granted by the professor who supervised my thesis work or, in his absence, by the Head of the Department or the Dean of the College in which my thesis work was done. It is understood that any copying or publication or use of this thesis or parts thereof for financial gain shall not be allowed without my written permission. It is also understood that due recognition shall be given to me and to the University of Saskatchewan in any scholarly use which may be made of any material in my thesis.

Request for permission to copy or to make other use of material in this thesis in whole or part should be addressed to:

Head of the Department of Chemistry
University of Saskatchewan
110 Science Place
Saskatoon, Saskatchewan
S7N 5C9
CANADA.

ABSTRACT

Copper is one of the most vital trace elements in ruminant nutrition. It is required for several metabolic activities and it is also an essential component of several physiologically important metalloenzymes. Thus copper deficiency in ruminants results in distinctive pathologies, and hence in significant economic losses to farmers. Copper deficiency results from very low copper in diet (primary copper deficiency) and interference with Cu absorption in the animal due to Mo and S in food or water (secondary copper deficiency). The molybdenum-induced copper deficiency that affects ruminants can be attributed to the formation of thiomolybdates (TMs) ($MoO_xS_{4-x}^{2-}$; x = 0,1,2 or 3) from molybdate and sulfide in the rumen. The TMs formed then react irreversibly with copper to form insoluble Cu-TM complex which ultimately end up being excreted, thus reducing copper bioavailability to the ruminant.

In this study, an attempt has been made to use computer simulations to model speciation of copper in rumen fluid in the presence of TMs with the aim of understanding the extent to which TMs affects the levels of copper in the rumen.

This was done by initially refining the computer model of copper speciation with respect to low molecular mass (LMM) ligands in bovine rumen with the aim of correcting the discrepancy that was observed during experimental validation of the computer model in a previous study. To this end, mass balance equations which describes the distribution of Cu(II) amongst the different ligands were encoded into a spreadsheet to calculate equilibrium concentration of all species. Formation constants obtained from literature as well as those obtained from studies in our group were used as input values in the spreadsheet. Results show that at average ruminal pH, the metal would be present mostly as carbonate and phosphate complexes. The results obtained from the computer model in the present study were validated using ^{1}H NMR experiments on simulated rumen fluid as well as actual rumen fluid containing Cu(II); using acetic acid chemical shift as the probe for monitoring the speciation pattern. Excellent agreement was observed between the computer model and experimental

results. Discrepancy was however observed upon introduction of copper lysine as copper source into the model. Incorporation of a mixed ligand complex of Cu(II), acetate and lysine into the computer model gave an excellent agreement between the computer model and experimental results

The study was extended to include glycine, histidine, methionine and EDTA complexes as the copper source in both rumen saliva (McDougall's solution) and rumen fluid. Results show that only the histidine and EDTA complexes persist to any significant extent, in spite of the large number of competing ligands present in these matrices.

In this study, success has also been achieved in the integration of the slow (kinetically controlled) formation of TMs and copper-tetrathiomolybdate (TM4) complexation into the previously developed model for the rapidly equilibrating copper-ligand speciation. To simulate the formation of the TMs and Cu-TM4 complex with respect to time, the differential equations representing rate expressions for each chemical species were solved to obtain an analytical solution using the Laplace transform method. The analytical solutions obtained were encoded in a spreadsheet and calculated as function of time to obtain time – dependent concentrations of TMs and Cu-TM4 complex. This was then integrated with previously developed model for the rapidly equilibrating copper-ligand speciation in the rumen. The kinetic data used in the simulation of the formation thiomolybdates was obtained fron literature wheras that for Cu-TM4 complexation was obtained from our lab using Cu(II) - Ion Selective Electrode. The results show that that in the presence of TM4 the, Cu(II) bound to low molecular ligands in the rumen is drastically reduced confirming the effect TM4 on Cu(II) observed in several *in vitro* studies.

The study shows that in thiomolybdate contaminated rumen environment, the bioavailability of copper is considerably reduced. Though metal bioavailabilities are hard to predict this approach could help better our understanding of this process.

ACKNOWLEDGMENTS

I would first like to thank God for his grace, goodness and inspiration. I am very grateful to my supervisor Dr. R. S. Reid, for all the assistance, guidance and support throughout the course of this study. His criticisms and suggestions were invaluable for the successful completion of this work. I would like to thank him for his patience, which was instrumental in seeing this thesis in its present form.

I would also like to thank the members of my supervisory committee for their helpful suggestions and discussions: Dr. H. B. Kraatz, Dr. D. A. R. Sanders and Dr. M. J. Hendry.

I also gratefully acknowledge the help and support of the past and present members of the Reid group: Dr. E. K. Quagraine, Ms Mildred Budu, Mr. M. Bagonluri, Mr. R. Clark, and Miss D. Slamova. The friendly atmosphere in the lab made work a lot easier. I also wish to thank the many friends I made in Saskatoon, who are too numerous to mention, in particular Mr. Michael Nketia, Ms Irene Bediako-Amoa, Dr. K. Amoako, Dr. Francis Appoh, Dr. S. Gyepi-Garbrah, Dr. P. Ahiahonu, and Dr. G. K. Quainoo.

To my wife Stella and daughters Abigail and Eva, I dearly appreciate your various sacrifices that were very instrumental in the completion of this thesis.

The financial support of the University of Saskatchewan, The Department of Chemistry and The Agricultural Development Fund (ADF) of the Province of Saskatchewan is gratefully acknowledged.

To

My beloved hardworking wife, Stella and my lovely daughters Abigail & Eva.

TABLE OF CONTENTS

LIST OF TABLES

LIST OF FIGURES

LIST OF ABBREVIATIONS

ADC	Analog to digital converter
A_x	Absorbance of species x
a_x	Activity of species x
$\mathbf{B}_1$	External magnetic field
$\mathbf{B}_o$	Radio frequency magnetic field
DM	Dry matter
DSS	Sodium dimethyl –2-silapentane-5-sulphonate
E	Electrode potential
E^0	Standard electrode potential
EDTA	Ethylenediaminetetraacetic acid
Exp	Experimental
FID	Free induction decay
GIT	gastro-intestinal tract
HMM	High molecular mass
hr	Hour(s)
HySS	Hyperquad Simulation and Speciation
Hz	Cycles per second
I	Ionic strength
ISE	Ion Selective Electrode
JESS	Joint Expert Speciation System
K_f	Formation constant
KHP	Potassium hydrogen pthalate
LMM	Low molecular mass
M	Molarity = moles solute/L solution
MHz	MegaHertz
min	Minutes
m**M**	Millimolar
^{95}Mo NMR	Molybednum-95 nuclear magnetic resonance

NIST	National Institute of Standards and Technology
NMR	Nuclear magnetic resonance
Obs	observed
pH	Negative log of the hydrogen ion activity
pK_a	Negative log of the acid dissociation constant
pK_w^c	Negative log of the experimental autoionisation constant for H_2O
ppm	Parts per million
R	Residual factor
R^2	Correlation coefficient
SIT	Specific ion Interaction Theory
T	Tesla
T_1	Spin-lattice relaxation time
T_2	Spin-spin relaxation time
TM	Thiomolybdate
TM1	Monothiomolybdate ($MoSO_3^{2-}$)
TM2	Dithiomolybdate ($MoS_2O_2^{2-}$)
TM3	Trithiomolybdate (MoS_3O^{2-})
TM4	Tetrathiomolybdate (MoS_4^{2-})
UV	Ultraviolet
VFA	Volatile fatty acid
z_x	Charge of the ion x
α_i	Molar fraction of species i
δ	Chemical shift
δ_{obs}	Observed chemical shift
μ	micro
λ	Wavelength
Σ	Sum
^oC	Degree Celsius

1. INTRODUCTION

1.1 OBJECTIVES OF THE STUDY

The molybdenum-induced copper deficiency that affects ruminants can be attributed to the formation in the rumen of thiomolybdates (TMs) ($MoO_xS_{4-x}^{2-}$; x = 0,1,2 or 3) from molybdate and sulfide. The TMs then react irreversibly with copper, thus reducing its bioavailability. Although the kinetics of the formation of TMs and their reactions with copper in solution have been the subject of several *in vitro* studies, it has not hitherto been possible to apply this to understanding the biological situation, i.e., how the presence of TMs affects copper speciation in the presence of the many competing ligands in the rumen.

In this study, computer simulations, ^{1}H NMR as well as potentiometry will be used to model speciation of copper in rumen fluid in the presence of TMs with the aim of understanding the extent to which TMs affects the levels of copper in the rumen

Initial attention will be focused on reviewing the computer modeling of Cu(II) with respect to low molecular mass (LMM) ligands in the bovine rumen fluid with the aim of correcting a discrepancy that was observed during experimental validation of the computer model in a previous study (see Section 1.14). Mass balance equations which describes the distribution of Cu(II) amongst the different ligands will be encoded into a spreadsheet to calculate the equilibrium concentration of all species. Formation constants obtained from literature as well as those obtained from studies in our group will be used as input values in the spreadsheet.

The results obtained from the computer model in the present study will be validated by performing ^{1}H NMR experiments on simulated rumen fluid as well as actual rumen fluid containing Cu(II); using acetic acid chemical shift as the probe for monitoring the speciation pattern.

Lysine will be introduced into the rumen model as an exogenous ligand with the aim of investigating the cause of the discrepancy between the predicted and the experimental results observed in the previous study in our group

Upon successful investigation and solution of the above mentioned discrepancy, studies will be conducted on speciation modeling of other copper compounds (Cu glycine, Cu methionine, Cu histidine and Cu EDTA), which are being used as Cu supplement for ruminants, in McDougall's solution (bovine saliva) and rumen fluid. The aim of this study is to find out which of the chelated supplements mentioned above holds on to Cu in the presence myriad of competing ligands. Results from the computer models will also be validated using ^{1}H NMR experiments as described above.

The rumen model developed will be expanded to include the formation of thiomolybdates as well interaction of the thiomolybdates with Cu(II) in the presence of the presence myriad ligands present in the rumen. This is to find out the effect of the presence of thiomolybdates in rumen on the bioavailability of Cu(II) in the rumen. Results from solution chemistry studies conducted on individual TMs, and their interactions with Cu(II) ions from a previous study in our group as well as kinetic data from literature will be used in this study.

1.2 CHEMICAL SPECIATION

1.2.1 Chemical Speciation Defined

In all living systems, the biochemical functions of both essential and toxic metals are mediated through specific chemical species, or complexes, and it is the concentrations of these particular species which are important for the biochemical reactions and not just the total concentration of the metal in the system [1]. For instance some elements can be highly toxic to various life forms; others are considered essential, but can become toxic at higher doses. Many of these effects depend strongly on the particular form in which the element is present in the system. For example, Cr(VI) ions are considered far more toxic than Cr(III) [2]. On the other hand, while both methyl mercury and inorganic mercury are toxic, they show different patterns of toxicity. Often these different chemical forms of a particular element or its compounds are referred to as "species". The notion that the distribution among its various species will have a major effect on the behavior of a particular element has been accepted in such diverse fields as toxicology, clinical chemistry, geochemistry, and environmental chemistry.

New developments in analytical instrumentation and methodology now often allow the identification and measurement of the species present in a particular system. Because of these possibilities, numerous publications have appeared in which the term "speciation" is employed. However, this term has been used in a number of different ways, including the transformation of species, the distribution of species, or the analytical activity to determine the concentrations of species.

In an attempt to end the confusion regarding the usage of the term speciation IUPAC commissioned an interdisciplinary committee to consider the issue and came out with the recommendation in 2000 that chemical compounds that differ in isoptopic composition, oxidation or electronic state, or in the nature of their complexed or covalently bound subsituents, can be regarded as distinct chemical species. This recommendation leads to the following definitions:

i. *Chemical species*; specific form of an element defined as to isotopic composition, electronic or oxidation state, and/or complex or molecular structure.

ii. *Speciation analysis*; analytical activities of identifying and/or measuring the quantities of one or more individual chemical species in a sample.

iii. *Speciation of an element;* distribution of an element amongst defined chemical species in a system under specified conditions.

Strictly speaking, whenever an element is present in different states in terms of i., it must be regarded as occurring in different species. In practice, however, it will depend on the relevance of the species differences for our understanding of the system under study, and on our ability to distinguish between the various species analytically, whether different species should be grouped or can be measured separately. Various conformations, excited states, or transient forms of an element, its coordinated atoms, and the molecules of which they are part technically constitute unique species (eg., see Figure 1.1). Nevertheless, analytical methodology and practical considerations dictate that the speciation analysis of a system yields a profile of sufficiently different and measurable species for the desired level of understanding of the system's behavior. Various aspects of structure contribute to identifiable species for a particular element, and may differ in importance depending on the reasons for which a speciation analysis is undertaken [3].

1.2.2 Chemical Speciation in Biological Systems

Of the 92 naturally occurring elements, about 30 are thought to be essential to animal or plant life at either bulk or trace levels. The remainder of the elements of the Periodic Table may display toxicological properties that will change as a function of the

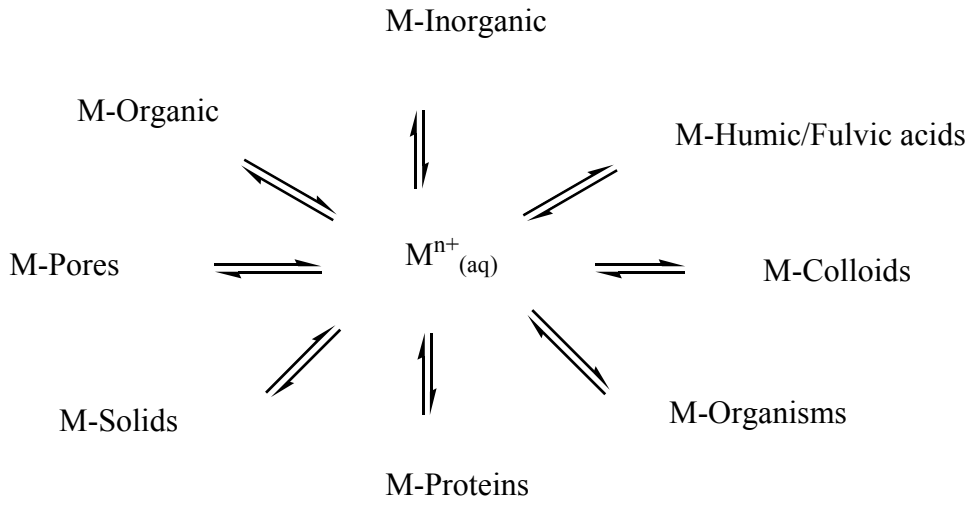

Figure1.1 Speciation scheme suggesting the possible distribution of metal ions (M) in the environment [4]

concentration and distribution within the organism, and the nature of the particular element in question. However even the essential elements may be associated with pathological situations where the concentrations of the element is either too high or too low, or as is often unrecognized, present within the wrong cellular 'compartment' of the organism.[5].

The 30 elements believed to be essential to life forms can be divided into four major categories: (1) bulk elements (H, C, N, O, P, S); (2) macrominerals and ions (Na, K, Mg, Ca, Cl, PO_4^{3-}, SO_4^{2-}); (3) trace elements (Fe, Zn, Cu); and (4) ultratrace elements, comprised of nonmetals (F, I, Se, Si, As, B) and metals (Mn, Mo, Co, Cr, V, Ni, Cd, Sn, Pb, Li). Other essential elements may be present in various biological species. A trace element is considered essential if it meets the following criteria: (1) Its withdrawal from the body induces, reproducibly, the same physiological and structural abnormalities regardless of the species studied; (2) its addition either reverses or prevents these abnormalities; (3) the abnormalities induced by deficiency are always accompanied by pertinent, significant biochemical changes; and (4) these biochemical changes can be prevented or cured when the deficiency is corrected [6, 7].

A high degree of chemical speciation can exist for any trace element in biological systems. Due to the predominantly aqueous nature of biological systems, biochemically active forms of all metallic elements tend to be ionic, these elements being complexed by molecules possessing electron-donating functional groups. Metal ions in biological systems tend to be distributed between four different states *in vivo* as illustrated in Figure 1.2. First, there is the inert ("non-labile") form of the metal complex which describes those molecules in which the metal ions is integrated into a molecular function, e.g. metal-activated enzymes or storage proteins. The "labile" protein-bound fraction is used to denote metal ions complexed to large molecules whose primary function is metal ion transport. The low-molar-mass fraction consists of metal ion complexes with inorganic anions, amino acids and carboxylic acids of molecular mass less than 2000. In the majority of situations, the free aquated metal ions, $[M(H_2O)_x]^{n+}$, is present at vanishingly low concentrations.

The last two complexes and the free aquated metal ions are in equilibrium such that a rise in metal ion concentration present in the biological fluid will bring about an across-the-board increase in labile protein, low molecular mass, and aquated metal ion concentrations without necessarily increasing the amount of metal complexing to the inert protein. To build a metal into, or to extract a metal from, an inert protein usually involves a sophisticated biochemical process such as occurs in the liver or the spleen. Table 1.1 indicates some examples of metal ions complexed in these four different types of species *in vivo*[8].

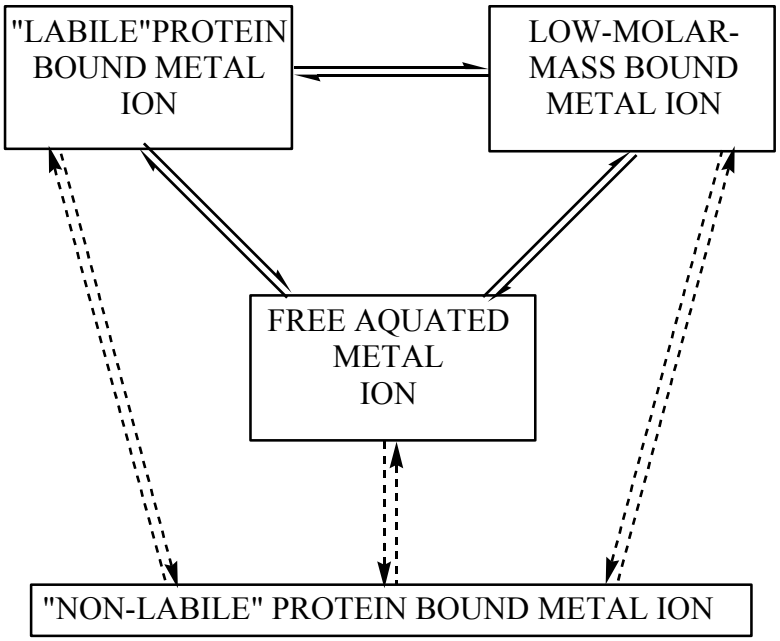

Figure 1.2 A general scheme showing potential interactions between metal-ion containing fractions in biological compartment. "Labile" equilibria are denoted by solid arrows, whilst "non labile" equilibria are represented by broken arrows.

Table 1.1 Examples of metal species in humans as illustrated in the scheme in Figure1.2

Inert and/or thermodynamically non-reversible	*Labile and thermodynamically reversble*
Iron Haemoglobin Myoglobin (Ferritin)	Transferrin $\rightleftharpoons$ Low molecular mass Fe^{3+} complexes $\rightleftharpoons$ $[Fe(H_2O)_6]^{3+}$
Copper Ceruloplasmin (Metallothionein)	Serum albumin $\rightleftharpoons$ Low molecular mass Cu^{2+} complexes $\rightleftharpoons$ $[Cu(H_2O)_6]^{2+}$
Zinc α_2 Macroglobulin (Metallothionein)	Serum albumin $\rightleftharpoons$ Low molecular mass Zn^{2+} complexes $\rightleftharpoons$ $[Zn(H_2O)_6]^{2+}$

1.2.3 Speciation Analysis

Before speciation analysis of biological samples is attempted, it is essential first to measure accurately and precisely the total metal concentration in the samples. Even total metal analysis is often a formidable task, and the accepted concentrations of some metals in biological systems have consistently fallen over the years as superior analytical techniques become available and, particularly, as more care has been taken to avoid contamination during sampling and analysis [6].

Whereas determination of total metal contents is sometimes challenging, the determination of species concentrations tends to be even more challenging due to (i) difficulties associated with isolating the compound(s) of interest from complex matrices; (ii) most of the speciation techniques available perturbing (to some extent) the equilibria existing between the various chemical species present in the system under study; (iii) for species present in ultra-trace levels, few analytical procedures possessing the degree of sensitivity required; and (iv) suitable standard reference materials often being unavailable. The nature of the challenges varies with matrix type, that is, different approaches are required for speciation analysis in waters, or biological materials, or soils/sediments [5].

Regardless of the approach chosen for a particular study, it is essential that the results of the experiments reflect the true situation as found *in vivo*. The structural and chemical integrity of the species under study must be maintained throughout any physical or chemical manipulation steps. Care must be taken not to disturb the equilibria involved in the interconversion of labile species, as this will naturally lead to false information. Both chemical and biological contamination which could lead to problems with the interpretation of the results, have to be controlled. Furthermore, the techniques that are chosen for the analysis of the various constituents must have the required sensitivity and specificity [9].

Determination of the actual concentrations of the individual species in a biological or environmental system is complicated and time consuming. Standard analytical techniques for trace metal determination such as radiometric analysis, colorimetric determination, atomic absorption, and mass spectroscopy, cannot normally be applied directly as they determine the total concentration of an element, not the concentrations of the individual species. The matrix may contain other metals and ligands, thus much work may have to be done on species separation before concentration determination.

Ultrafiltration and dialysis are useful separation techniques for initial separations. Ultrafiltration processes utilize a membrane with specific molecular mass cut-off; any species with molecular mass greater than that of the filter cut-off remains on the filter whilst all remaining species pass into the filtrate. Dialysis may be used to remove any unwanted inorganic salts from the system.

Improved species separation can be gained using electrophoresis. This technique is primarily used in the study of metal protein binding. The location of the metal following electrophoresis on polyacrylamide or agarose gels can normally be correlated with protein concentration. Improvement in separation can be achieved using two dimensional electrophoresis or iso-electric focusing in conjunction with electrophoresis.

Gel filtration and its related techniques, *e.g.* ion exchange, gel affinity chromatography and chromatofocusing, have been used to separate the different protein fractions in a given sample. Gel filtration separates according to weight; ion exchange according to charge; in gel affinity chromatography proteins are bound to the gel surface and eluted in different fractions using a buffer gradient; and finally chromatofocusing which is a column method for the separating proteins by taking advantage of their isoelectric points [1].

Having achieved the separation, it is still necessary to characterize the trace metal-containing species. Techniques that are generally used to characterize trace metal-containing species are listed in Table 1.2.

Experimental analysis of biological systems is, as stated earlier, complicated by the fact that the metal concentrations may be orders of magnitude below those which can be readily determined in the laboratory. Also measurement of a species concentration without upsetting the equilibrium and thus changing the species concentrations is difficult. A further complication in biological speciation is the complexity of the system which tend to perturb instrument sensitivity, precision and accuracy [10]

The aforementioned difficulties regarding speciation analysis can be circumvented by modeling the metal–ligand interactions occurring in the biological system under steady state conditions using computer simulation programs [10]. Computer models are able to describe concentrations much lower than those which can be successfully measured in the laboratory, and hence they can be used to gain insight into the speciation of metals in biological systems which are much more accurate than the information gained from experimental methods.

1.3 SPECIATION BY COMPUTER MODELING

Chemical Speciation is often studied using experimental methodology; however, an alternative approach involves the application of theoretical chemical concepts to predict the distribution and transformations of chemical species, usually by calculating the concentrations of species in equilibrium. Two main approaches have been used.

For gas-phase equilibria, it is convenient to minimize the free energy of the system by adjusting the partial pressures of the reagents, using either stoichiometries based on explicit chemical reactions or a nonstoichiometric approach in which chemical reactions are not used explicitly [11]. Such an approach is convenient because there are

Table 1.2 Techniques for the Characterization of Trace Metal-containing Species [9]

Information	Techniques and methods	Comments
Trace metal content	Anodic stripping voltammetry	Complete mineralization of samples is necessary before analysis.
	Atomic Absorption Spectrometry Plasma Emission Spectrometry Inductively Coupled Plasma/Mass Spectrometry	Both on-line and off-line analysis of sample fractions without further pretreatment is possible. However increase sensitivity of analysis is obtained for some elements when samples are mineralized and converted into hydrides, e.g. antimony, arsenic, bismuth, lead, mercury, selenium, tellurium and tin.
	Neutron activation analysis	Time-consuming sample preparation required, and long delays, up to Several weeks, before results are available.
Identification of volatile Thermally stable, low-molar -mass trace element-containing species.	Gas Chromatograhy/Mass Spectrometry Gas Chromatography/Atomic Absorption Spectrometry	Identification is possible if standards are available for comparison. Derivatization can convert relatively non-volatile species into species that are amenable to separation by GC.
Identification of water-soluble, high-molar-mass species	Liquid Chromatographic Techniques/ Atomic Spectrometry	Poor chromatographic resolution does make it difficult to identify individual species in complex biological matrices. Multi-fractionation steps may be necessary for unequivocal identification.
The environment around the trace element-containing sites	Electron paramagnetic resonance (EPR) spectroscopy, Magnetic susceptibility Visible Absorption Spectroscopy Mössbauer Spectroscopy Nuclear Magnetic Resonance (NMR)	Techniques useful in the study of some trace metal-containing species.

extensive databases of standard free energies of formation for compounds in the gas phase, and (for ideal-gas mixtures) there is a simple relationship between the chemical potential of a species, its standard free energy of formation and its partial pressure.

For equilibria in solution, it is usual to measure the equilibrium constants for the individual reactions and to calculate the species' concentrations by solving the equations of mass-balance. This approach was pioneered in the programs HALTAFALL [12] and COMICS [13]. These programs were written to solve sets of equations that typically might arise with systems of one or two metal ions and one or two ligands. Although they could be adapted to deal with slightly larger numbers of components, they could not be greatly expanded. In particular, they were both rather limited in respect of the way they stored data and in respect of their equation-solving algorithms [14].

Since the development of these programs and with advances in computer speed and availability, a number of computer programs for the simulation of metal-ligand equilibria in aqueous systems have been developed. These include ECCLES [15], MINEQL [16], SCOGS[17], SOLMNQ [18], COMPLOT [19], SPE [20], ESTA [21], GEOCHEM[22], JESS [23-25] Visual MINTEQ [26], CHEAQS [27] and HySS [28]. These are static models which calculate the chemical equilibrium distribution of aqueous species in a solution and, in some cases, the saturation indices for solid phases. Other programs such as PHREEQC [29] and EQ3/6 [30] perform the same function as the chemical speciation models but, in addition, they may be used as dynamic models capable of predicting the path of a reacting system. For example, mass transfer in and out of a system, or changes in the distribution of an aqueous species, either as a reaction progresses or with time.

Although the speciation models mentioned above vary in sophistication, the basic components of each of the models is the same (Figure 1.3). The models use the Laws of Mass Action and Mass Balance and thermodynamic formation constants for all of the possible metal-ligand species, in conjunction with defined parameters such as pH, redox potentials and total metal and total ligand concentrations.

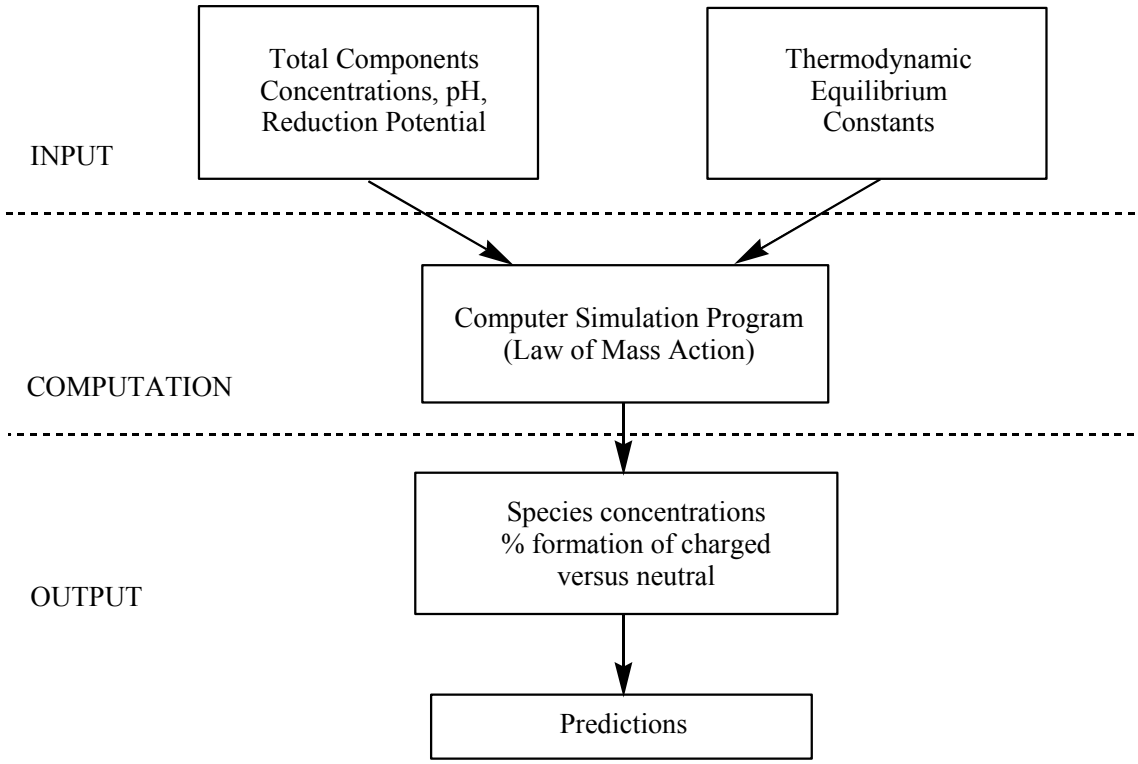

Figure 1.3 The basic components of a chemical speciation model

In any assessment of "real-life" processes made using simulation techniques, there are three major sources of uncertainty. These have been referred to [31] as "modeling", "data", and "completeness" uncertainties. Modeling uncertainties stem from an imperfect understanding of the processes being modeled and/or from numerical approximations used in the mathematical representations of processes. Data uncertainties arise as a result of poor quality and/or applicability of data and parameters used as input to a mathematical model. Completeness uncertainties refer to possible omissions from the model because of lack of knowledge.

The contribution of each type of uncertainty to the overall uncertainty which is intrinsic to a given simulation exercise will vary depending upon the process(es) being modeled. The total of these three uncertainties associated with a model can be quantified

by a combination of uncertainty analysis and exercises in verification and validation [31]. Verification and validation exercises compare the models and their predictions with experimental results, thereby checking both the mathematics and the input data. These procedures, and especially verification, are also used in "inter-code" comparisons to further assess the success, or otherwise, of calculation procedures [32].

In simulations of chemical speciation in aqueous media, the main source of uncertainty is normally the quality of the input data, specifically that of the formation constants and the composition of their associated complexes. Thus, it is essential that the formation constants used in any chemical speciation modeling are critically evaluated. In evaluating formation constants from any source, factors that are considered include: experimental method, purity of reagents, background electrolyte, reagent concentrations, ionic strength and computational procedures.

Formation constant data is readily available from databases such as The IUPAC Stability Constants Database (SC-Database), NIST Critically Selected Stability Constants of Metal Complexes and the Joint Expert Speciation System (JESS) thermodynamic database. SC-Database is a compilation of literature data, intended to direct the user to the original literature reference. It contains all significant stability constants and associated thermodynamic data published from 1887 to the present day, including all stability constants included in the book volumes published by the Chemical Society, London (now the Royal Society of Chemistry) and by IUPAC. It is maintained and kept up-to-date through regular upgrades. The NIST Critically Selected Stability Constants of Metal Complexes Database is a reference work covering a tremendous number of interactions for aqueous systems of organic and inorganic ligands with protons and various metal ions. The informational scope of the NIST Critically Selected Stability Constants of Metal Complexes Database is very similar to that of the six-volume set by Martell and Smith [33] except that most of the data have been rescrutinized, errors corrected, and some 50% new material has been added, effectively superseding the values found in the published hardbound volumes. The JESS Thermodynamic Database system, called JTH, provides a powerful and versatile means of storing and

retrieving the thermodynamic data associated with chemical reactions. Data in the JESS Parent Database provides the backbone for equilibrium calculations and thus for the determination of speciation. The database details the interactions in solution of over 100 metal ions with more than 3,000 ligands [34].

Where equilibrium constants from a database or literature were obtained at a different temperature from the one used in the current modeling study, the Van't Hoff's equation can be used to correct them (see Appendix A.1.2):

$$\ln K_2 = \ln K_1 + \frac{\Delta H}{R}\left[\frac{1}{T_1} - \frac{1}{T_2}\right] \qquad \textbf{(1.1)}$$

K_1 and T_1 represent the literature value of the formation constant and the temperature under which it was measured. T_2 represents the temperature at which the formation constant is desired and K_2 is the constant under the required temperature.

Values that were obtained under different ionic strength can be corrected using a modification of the Davies equation (Equation 1.2) (see Appendix A.1.1).

$$\log \beta'_{p,q,r} = \log \beta^{o}{}_{p,q,r} + a_i\left(\frac{\sqrt{I}}{1+\sqrt{I}} - 0.3I\right) \qquad \textbf{(1.2)}$$

where $\beta^{\circ}_{p,q,r}$ is formation constant at zero ionic strength, $\beta'_{p,q,r}$ the formation constant at the desired ionic strength, $a_i = A\Sigma z^2$, A the Debye - Huckel limiting slope ($0.509M^{-1/2}$), Σz^2 the square of the charge on each species summed over the formation reaction and I the desired ionic strength of solution [35].

Equilibrium constants obtained under different temperature and ionic strength conditions can also be corrected using *The Adjustment, Estimation and uses of Equilibrium reaction constants in Aqueous solution suite of programs* (Aq_solutions) *©2004* [36]. This is a package of programs for the quantitative treatment of equilibria in solution. The

software consist of programs for the correction of formation constants for changes in ionic strength, prediction of the temperature dependence of equilibrium constants using thermodynamic equations, the calculation and display of species distribution curves for complexes (including insoluble species) and the simulation of metal-ligand titration curves in real time and the dynamic display of speciation.

1.3.1 Hyperquad Simulation and Speciation: A Chemical Speciation Program

Hyperquad Simulation and Speciation (HySS) [37] is a typical utility program for the investigation of equilibria involving soluble and partially soluble species. HySS is written for the Windows operating system running on personal computers. It provides (a) a system for simulating titration curves and (b) a system for providing speciation diagrams. The calculations relate to equilibria in solution and also include the possibility of formation of a partially soluble precipitate.

At the centre of any calculation the concentrations of the free reagents, [A], [B] etc., are determined by solving the equations of mass-balance

$$T_A = [A] + \sum_i a_i \beta_i [A]^{a_i} [B]^{b_i} \ldots + \sum_j p_j C_j$$

$$T_B = [B] + \sum_i a_i \beta_i [A]^{a_i} [B]^{b_i} \ldots + \sum_j q_j C_j \qquad \textbf{(1.3)}$$

where A, B, etc. are reagents, a, b,… p, q, etc. are stoichiometric indices, β values represent equilibrium constants and the quantities C represent molar concentrations of insoluble species (quantity of solid divided by the volume of the solution) if any are present. Associated with each insoluble species there is a solubility product.

$$K_j = [A]^{pj} [B]^{qj} \ldots \qquad \textbf{(1.4)}$$

Initially it is assumed that there is no precipitate present and the free concentrations are calculated with the C terms omitted from the equations of mass-balance. If there is the possibility of the formation of a precipitate the concentration product is compared with the corresponding K_j. If it is larger not only is the C term included, but an additional equation is added to the set

$$\ln K_j = p_j \ln[A] + q_j \ln[B] \ldots \quad \textbf{(1.5)}$$

and the free concentrations are recalculated. When a solid is present the set of mass-balance and solubility equations is solved, according to the Newton–Raphson method, by iteratively solving the set of linear equations.

$$\begin{bmatrix} \frac{\partial T_A}{\partial [A]}[A] & \frac{\partial T_A}{\partial [B]}[B] & \ldots & \frac{\partial T_A}{\partial C_j} & \ldots \\ \frac{\partial T_B}{\partial [A]}[A] & \frac{\partial T_B}{\partial [B]}[B] & \ldots & \frac{\partial T_B}{\partial C_j} & \ldots \\ \ldots & \ldots & \ldots & \ldots & \ldots \\ \frac{\partial \ln K_j}{\partial [A]}[A] & \frac{\partial \ln K_j}{\partial [B]}[B] & \ldots & \frac{\partial \ln K_j}{\partial C_j} & \ldots \\ \ldots & \ldots & \ldots & \ldots & \ldots \end{bmatrix} \begin{bmatrix} \frac{\Delta [A]}{[A]} \\ \frac{\Delta [B]}{[B]} \\ \ldots \\ \frac{\Delta C_j}{C_j} \\ \ldots \end{bmatrix} = \begin{bmatrix} \Delta T_A \\ \Delta T_B \\ \ldots \\ \Delta \ln K_j \\ \ldots \end{bmatrix} \quad \textbf{(1.6)}$$

Now, because $\partial T_A/\partial T_B = (\partial \ln K_j/\partial[A])[A] = p_j$, etc. the matrix of coefficients is symmetric and we can use the numerically stable Choleski factorisation for the solution whether or not a precipitate has formed: when a solid has dissolved the corresponding row and column of the equations will simply be omitted.

A further complication can arise in a speciation calculation since it is possible to specify either the analytical concentration, T_A, or the free concentration [A] of any reagent. For example, the pH may be specified rather than T_H. In that case the corresponding equation of mass balance is omitted and the given value of that free concentration is used to solve the remaining set.

The main novelty in HySS is the complete flexibility with which the conditions may be specified for speciation calculations and the simple interface to other Windows applications, such as word-processors or spreadsheets, for the results of the calculations. Also, there are no restrictions as to the number of reagents that may be present or the number of complexes that may be formed and the titration simulation option can be used effectively in didactic situations.

1.3.2 Computer Simulation of Chemical Speciation using Spreadsheet

A spreadsheet is a computer application program that simulates a physical spreadsheet by capturing, displaying, and manipulating data arranged in rows and columns. In a spreadsheet, spaces that hold items of data are called cells. Each cell is labelled according to its placement (for example, A1, A2, A3...) and may have an absolute or relative reference to the cells around it. The cells are functionally equivalent to variables in a sequential programming model. Cells often have a formula, a set of instructions which can be used to compute the value of a cell. References between cells can take advantage of spatial concepts such as relative position and absolute position, as well as named locations, to make the spreadsheet formulas easier to understand and manage. Spreadsheets automatically update cells when the cells on which they depend have been changed.

Spreadsheet software allows one to: manipulate data through built-in or user-defined mathematical functions; interpret data through graphical displays or statistical analysis; perform various curve fitting procedures, either built-in (linear or nonlinear regression) or user-defined through the power add-ons like Solver (Microsoft Excel); and write user-defined macros or Visual Basic for Applications (VBA) routines to automate or enhance a spreadsheet for a particular purpose [38].

Thus computer spreadsheets provide the means of carrying out a large number of calculations, as required in chemical speciation simulation, with the same ease as a single calculation. In computing chemical speciation in a spreadsheet, an initial

"intelligent guess" is made for the concentrations of each of the free components and the required formation constants (corrected for temperature and ionic strength variations) and other required constants are input into the mass balance equations. Using an iterative procedure this value is varied till one gets the minimum residual for the calculated total concentration of the component j ($[T_j]^{cal}$) and the analytical concentration of the component j, ($[T_j]$). In other words, the concentration of the free concentration is obtained when $[T_j]^{cal}$ - $[T_j]$ is closest to zero. The concentration of each of the species and hence the mole fraction of each species can done be calculated as a function of variables such as pH and subsequently plotted in the spreadsheet.

The main advantage of using a spreadsheet in chemical speciation simulation as compared to other chemical speciation simulation programs is that, one can watch the value at each iteration. Observing progress towards convergence makes the method more understandable, and often reveals some of the subtleties involved.

1.4 THE CHEMISTRY OF COPPER

Copper (Cu), a nonferrous metal, is the twentieth most abundant element present in the Earth's crust, at an average level of 68 parts per million (0.11 kg/metric ton). It is the 29th element on the Periodic Table, located between nickel and zinc in the first row of transition elements and the same subgroup as the other so-called coinage metals, silver and gold. Copper has eleven known isotopes, of which only two, ^{65}Cu and ^{63}Cu, are present in significant amounts, with natural abundances of 30.91 and 69.09% respectively, resulting in an atomic weight of 63.546. The ground state electronic configuration of elemental copper is $1s^2 2s^2 2p^6 3s^2 3d^{10} 4s^1$ or $[Ar]3d^{10}4s^1$. Although copper can exist in oxidation states ranging from +1 to +4, the common oxidation forms are copper(I), Cu^+; and the generally more stable copper(II) state, Cu^{2+}, which forms blue or blue-green salts and solutions due to the partially filled 3d orbitals ($[Ar]3d^9$) [39].

Most Cu(I) compounds are fairly readily oxidized to Cu(II) compounds. The redox properties of the Cu(I)/Cu(II) systems are associated with three principal processes shown below [40]: (a) electrolytic oxidation or reduction (b) disproportionation and (c) the oxidation of Cu(I) with O_2 to yield H_2O ultimately. As with any cation with variable oxidation

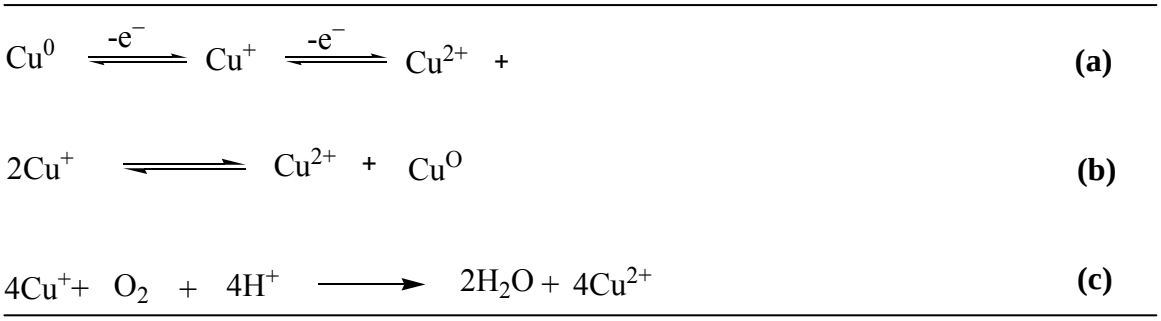

states, the relative stabilities of the various oxidation states of copper are very sensitive to the chemical environment; the redox properties of copper are strongly influenced by the ligands present, their disposition in space and the solvent [41].

The copper(I) ion is an extremely soft acid; this means that its complexes are strongest with the heavy halogens, with sulfur ligands, and with unsaturated ligands. Complexes with the softer ligands often also bind carbon monoxide and sometimes dioxygen reversibly. Tetrahedral coordination dominates, with two and three coordination much less common. The tetrahedral coordination is preferred because Cu (I) has fully filled 3d orbital (resembles a nontranstion metal) which leaves it with the empty 4s and the three 4p orbitals for bonding to ligands [42]. The coordination number rarely exceeds four although five coordination is known and may have to be considered in biological situations (in hemocyanin, for example) [43].

The copper (II) ion is classified as borderline hard acid, thus its chemistry is dominated by N-type and O-type ligands. A fair number of complexes with sulfur ligands are also known. There are few isolated complexes of Cu(II) with either phosphine, arsine and stibine, probably as a result of their soft nature [41]. In common with most first-row transition metal(II) cations, the coordination number 2 is rare, except

for gaseous phase compounds. Cu(II) readily forms coordination complexes involving mainly the coordination numbers 4, 5, and 6. The coordination number six is certainly the most common. The d^9 configuration makes Cu(II) subject to Jahn – Teller distortion if placed in an environment of cubic (i.e., regular octahedral or tetrahedral) symmetry, and this has profound effect on all its stereochemistry. The Jahn-Teller theorem requires that any nonlinear system with an electronically degenerate ground state will undergo geometrical distortion, i.e. a lowering of the symmetry to remove the orbital degeneracy. This also has the effect of lowering the overall energy of the complex.

To illustrate, consider an octahedrally coordinated Cu^{2+} ion. There is one vacancy in the e_g orbitals, in either d_{x2-y2} or the d_{z2} orbital. If the coordination is strictly octahedral, the two configuations $d^2_{x2-y2}d^1_{z2}$ and $d^1_{x2-y2}d^2_{z2}$, are of equal energy. This is the sense in which the electronic state of the Cu^{2+} ion is doubly degenerate. However, this is a state which, according to the Jahn – Teller theorem, cannot be stable. Suppose the actual configuration in the e_g orbitals is $d^1_{x2-y2}d^2_{z2}$. The ligands along the z axis are much more screened from the charge of the Cu^{2+} ion than are the four ligands along the x and y axes.The z-axis ligands will therefore tend to move further away. As they do so, however , the d_{z2} orbital will become more stable than the d_{x2-y2} orbital thus removing the degeneracy, as shown in Figure 1.4 .In the extreme case of this distortion, of course, the elongation leads to a square planar coordination [42]

5-coordinated Cu(II) complexes generally involve distorted square pyramidal and distorted trigonal bipyramidal stereochemistry. In the distorted square pyramidal geometry there is both an elongation of the four-fold axis and a trigonal in-plane distortion or, less frequently, a tetrahedral distortion. It rarely involves a regular square pyramidal stereochemistry. Regular trigonal bipyramidal geometry can occur but is more frequently distorted towards square pyramidal geometry.

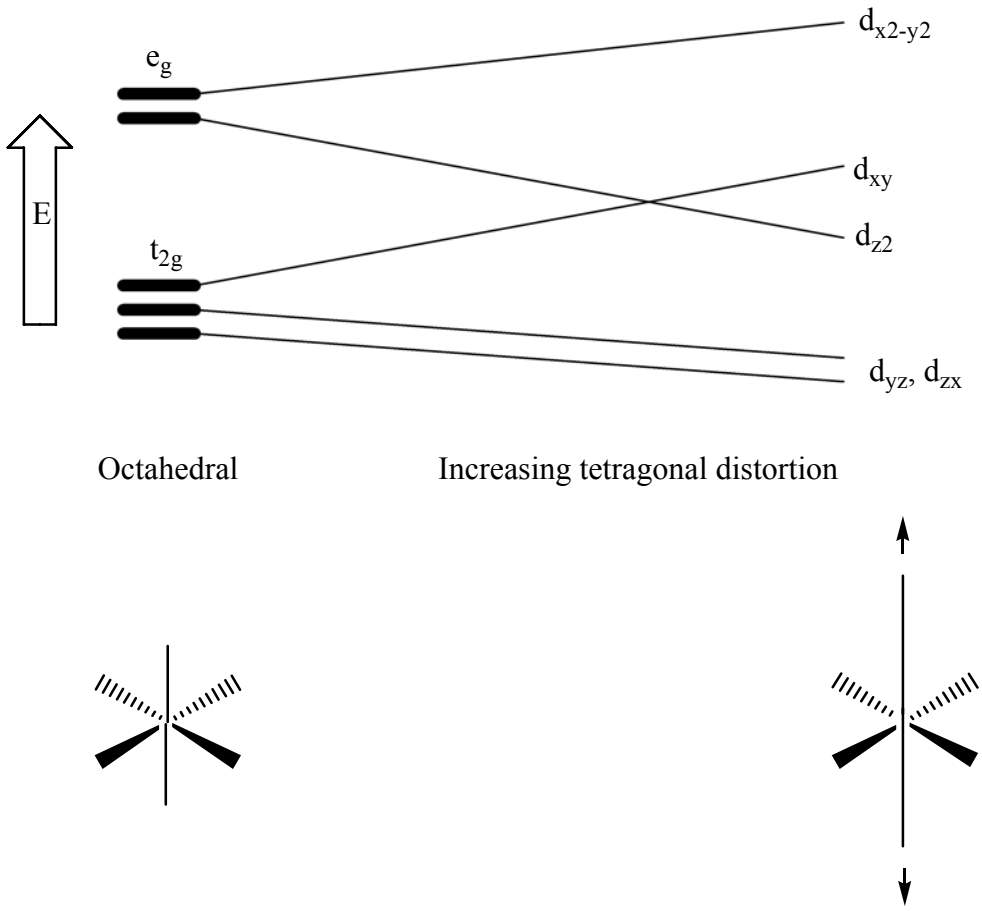

Figure 1.4 An energy-level diagram showing the further splitting of the d orbitals as an octahedral array of ligands becomes distorted by progressive withdrawal of two trans ligands along the z axis [42].

Coordination number four, an accurately square planar configuration, is not all that common: solvent molecules or, in the solid state, adjacent molecules are often close enough along the axes perpendicular to the plane to make the shape better described as square pyramidal or tetragonally elongated octahedral. Although distorted toward a tetrahedron is quite frequent, no regular tetrahedral complexes of copper(II) are known or would be expected to be stable [41].

Cu(I), having a closed shell configuration, $[Ar]3d^{10}$, is diamagnetic. Thus it has no vacant d orbitals, to enable it undergo d-d transitions. Hence Cu(I) compounds are mostly colorless. However, there are some that are colored, due to charge-transfer

transitions (both ligand to metal charge transfer (LMCT) and metal to ligand charge transfer (MLCT)) or intraligand-orbital transitions [41]. Cu(II) complexes show d-d transitions. Such d-d transition is as a consequence of light absorption in the visible region of the electromagnetic spectrum (~400 to 800 nm) and the origin of color is due to partially filled d orbitals where such transitions are possible. Virtually all Cu(II) complexes or compounds are blue or green in color. The single unpaired electron in the case of Cu(II) ([Ar]$3d^9$) makes it paramagnetic. Cu(II) compounds therefore show EPR (electron paramagnetic resonance) signals, and in nuclear magnetic resonance (NMR) spectroscopy the binding of Cu(II) to ligands results in paramagnetic line broadening and shift effects for the ligand resonances (see Section 1.12.3) [40].

The aqueous chemistry of copper(II) is dominated by the blue $[Cu(OH_2)_6]^{2+}$ ion. This ion has a significant Jahn-Teller distortion from a regular octahedral symmetry. There are two weakly bonded water ligands in the axial positions, with the overall molecule undergoing a rapid fluxional change resulting in equivalence and rapid exchange at all of the waters. The stability of $[Cu(OH_2)_6]^{2+}$ to hydrolysis and mobility in the physiological pH range, coupled with its tendency to form complexes with a variety of biological ligands, are responsible for the toxicity caused by free copper in the body.

Addition of ligands to aqueous Cu(II) leads to the formation of complexes by successive displacement of water molecules. These complex formations can be represented as:

$$[Cu(OH_2)_6]^{2+} + nL^{m-} \longrightarrow [Cu(OH_2)_{6-n}L_n]^{2-nm} + nH_2O$$

where L represents any ligand. Copper is known to possess relatively high formation constants for such complexes compared with the other divalent first row transition elements. As expected, multidentate ligands (chelates) form stronger complexes than monodentate complexes (see Table 1.2) due to the chelate effect (see Section 1.9.1). In general a dissociative SN_1 mechanism is involved for the formation of copper complexes. Ligand field activation energies predicts this to be a more likely mechanism

than the associative SN_2. The kinetics of these ligand exchange reactions are generally fast, usually taking less than a millisecond.

Table 1.3 Formation constants of complexes of copper(II) with nitrogen donor ligands of different denticity [44]

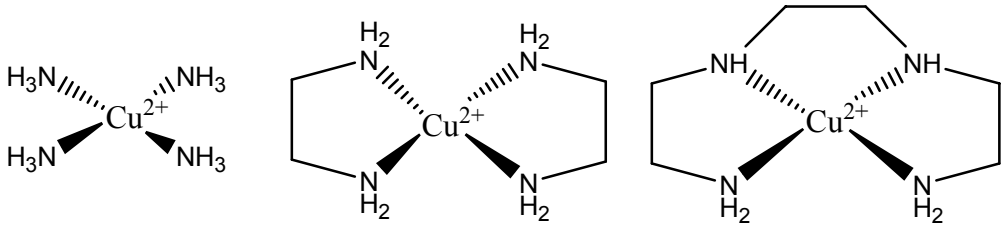

Ligand:	ammonia	ethylenediamne	triethylenetetramine
Denticity:	1	2	4
	$\log\beta_4 = 13.0$	$\log\beta_2 = 19.6$	$\log K_1 = 20.1$

Cu(II), with its 6 coordination sites, can also form mixed ligand complexes in the presence of more than one potential ligand. Mixed ligand complexes are those in which more than one kind of ligand, other than the solvent molecule, are present in the innermost coordination sphere of the central ion and can be represented by the general formula Cu(AB). Where A and B represent different ligands [45]. Mixed chelation occurs commonly in biological fluids. The formation of low-molar mass complexes in biofluids results from multimetal-multiligand equilibria involving exchangeable metal ions and amino acids, peptides, nucleotides or other biomolecules. Because potential bioligands greatly exceed biological transition metal ions in number and quantity, mixed-ligand complexes are more common than binary and multinuclear complexes. They play important roles in metal ion transport, enzyme reactions and other biological functions [46]. Reviews covering the various aspects of copper mixed ligand complexes can be found in literature [45-48].

There are two convenient ways to characterize the stability of mixed-ligand complexes. One is based on the difference of log stability constants, Δ log K (Equations 1.7-1.9), and the other on the "disproportionation" constant, log X (Equations 1.10 and 1.11).

$$CuA + B \rightleftharpoons CuAB, \quad K^{CuA}_{CuAB} = \frac{[CuAB]}{[CuA]\,[B]} \qquad \textbf{(1.7)}$$

$$Cu + B \rightleftharpoons CuB, \quad K^{Cu}_{CuB} = \frac{[CuB]}{[Cu]\,[B]} \qquad \textbf{(1.8)}$$

$$\Delta \log K = \log K^{Cu\,A}_{CuAB} - \log K^{Cu}_{CuB} \qquad \textbf{(1.9)}$$

$$CuA_2 + CuB_2 \rightleftharpoons 2CuAB, \quad X = \frac{[CuAB]^2}{[CuA_2][CuB_2]} \qquad \textbf{(1.10)}$$

$$\log X = 2\log \beta_{CuAB} - (\log \beta_{CuA2} + \log \beta_{CuB2}) \qquad \textbf{(1.11)}$$

Generally one would expect to observe negative values for Δ log K (Equation 1.9), since usually it holds that $K^{Cu}_{CuB} > K^{CuB}_{CuB2}$. This is because more coordination positions are available for bonding of the ligand given metal ion than for the second ligand. The equilibrium constant corresponding to the addition of ligand A to MB is given by Equation 1.12

$$CuB + A \rightleftharpoons CuBA, \quad K^{CuB}_{CuBA} = \frac{[CuBA]}{[CuB]\,[A]} \qquad \textbf{(1.12)}$$

For kinetically labile systems, the species [CuAB] and [CuBA] are identical. The overall stability constants given by Equation 1.7 and 1.12 is usually determined experimentally although they can be estimated by calculation from the equilibrium

constants of the corresponding binary complexes by assuming that the mixing of ligands in such complexes is purely statistical, *e.g.* [49].

$$CuA_2 + CuB_2 \rightleftharpoons 2CuAB$$

If ligands A and B give complexes with same number of donor atoms, the probabilities for the various reactions are as summarized below [49]:

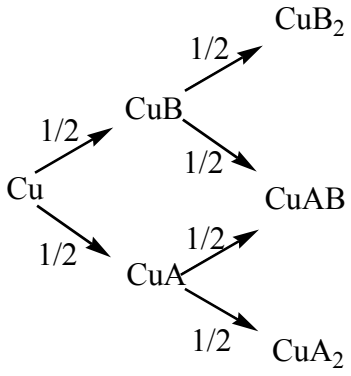

That is, the probabilities of the formation of CuA_2 and CuB_2 are both proportional to ½ x ½ = ¼ , while the probability of formation of CuAB is proportional to 2 x ¼ = ½. The statistical value for the equilibrium constant is then (½)^2 / (¼)^2 = 4 or

$$\beta^2_{CuAB} = 4 \times \beta_{CuA2} \times \beta_{MB2} \qquad \textbf{(1.13)}$$

Equilibrium or stability constants so determined have been found not differ significantly from experimentally determined values for simple ternary complexes such as the one described above [47, 49]. However for more complex systems there can be significant deviations from the experimental value. This due to the fact that formation of mixed ligand complexes and its stability does not only depend on statistical reasons but also charge neutralization, steric factors, π-bond formation and intramolecular ligand-ligand interactions [47].

1.5 BIOLOGICAL IMPORTANCE OF COPPER

Though the use of copper dates back to antiquity, the recognition of its biological importance is of a more recent origin. Copper has been found to be required essential trace element for the normal functioning of plants, animals and most microorganisms. As a trace metal, it is present in tissues and fluids at parts per million (ppm) or parts per billion (ppb) concentrations [40]. The essentiality of copper is due to its presence in several enzymes and proteins widely distributed in animals and plants where it performs central functions in various fundamental biological processes.

In plants copper participates in the process of photosynthesis, assists in the assimilation of starch and nitrogen, enhances the stability of chlorophyll, and stimulates respiration. The vegetative parts of plants contain more copper than the reproductive parts. Its content varies with the plant species, soil type, vegetative stage and the use of copper-containing fertilizers.

In animals, copper is involved in the body's protective functions; pigmentation and keratinisation of hair and feathers; and the formation of copper-containing proteins with enzymatic functions [50]. Copper proteins play two main functions, namely electron transport and dioxygen transport and activation. Typical are the cases of cytochrome c oxidase, the protein which represents the final step in the respiratory chain (that is, permits formation of adenosine triphosphate (ATP) in mitochondrial energy production) and hemocyanins, which act in several organisms as dioxygen transport proteins. Several other fundamental functions of copper proteins have been described:

- Copper oxidases help to produce the extracellular matrices of living eukaryotic organisms (e.g. lysyl oxidase, which catalyzes the deamination of Lys residue in peptides to form peptidyl α-aminoadipic-δ-semialdehyde residues, an aldehyde derivative)
- In plants, the copper oxidases (free radical oxidases) perform defensive roles such as the formation of protective films when the tissues are damaged (phenol oxidases).

- Protection by copper against the toxic effect of free radicals is further found in the cell cytoplasm and outside cell (e.g. Cu/Zn Superoxide Dismutase (SOD) protects intracellular components from oxidative damage by converting the superoxide radical to hydrogen peroxide and molecular oxygen) [51].
- Other copper oxidases remove excess of amine neurotamsmitters (copper amine oxidases) but are also used for the synthesis of adrenalin, one of the main transmitters of the nervous system (dopamine β-hydroxilase) [52].

Reviews covering the various aspects of copper in biological systems, especially copper proteins and their function(s), are found in the literature [40, 43, 51, 53-56].

1.6 DIGESTION IN RUMINANTS

For a proper understanding of the fate of a trace metal administered to a ruminant, an understanding of the digestive system is essential. This is because most of these trace metals are administered orally. Digestion in the cow is accomplished by a combination of chemical, mechanical and microbial action. The major distinctive feature of the digestive system of the cow, and ruminants in general, is the four-chambered stomach (Figure 1.5) that enables them to ruminate between periods of eating. It also facilitates the breakdown of cellulose and other resistant polysaccharides which is undoubtedly the most important digestive process taking place in a ruminant, and the one which distinguishes ruminants from non-ruminants. The four stomach compartments are the reticulum, the rumen, the omasum and the abomasum. The fore stomach compartments - the reticulum, rumen and omasum - serve to store and delay the passage of ingested food. They are also sites of anaerobic microbial fermentation of plant material and of absorption, mainly of the fermentation products.

Digestion begins at the mouth. Once food is ingested by the animal, it is mixed with lavish amounts of saliva in the mouth, and passed onto the stomach through the oesophagus. The major part of the stomach is the reticulo-rumen which comprises about

85% of the total volume of the stomach in an adult. The great size and location of the rumen make it the major site of digestion in the cow. Food and water entering the rumen is partially fermented to yield principally short chain acids like acetic, propanoic and butanoic acids. These are referred to in animal nutrition as the volatile fatty acids (VFAs). The gases methane and carbon dioxide are also produced. The chemical breakdown of food here is brought about mainly by enzymes, secreted not by the animal itself, but by the microbes present therein. The gases are lost by belching, while the volatile fatty acids are mainly absorbed through rumen wall. Bacteria and protozoa are the major micro-organisms present in the rumen.

Fermentation in the rumen is brought about by both the chemical and microbial action that takes place in the rumen. Significant amounts of ammonia are produced in the rumen via microbial degradation of dietary protein. Ruminants culture the microbial

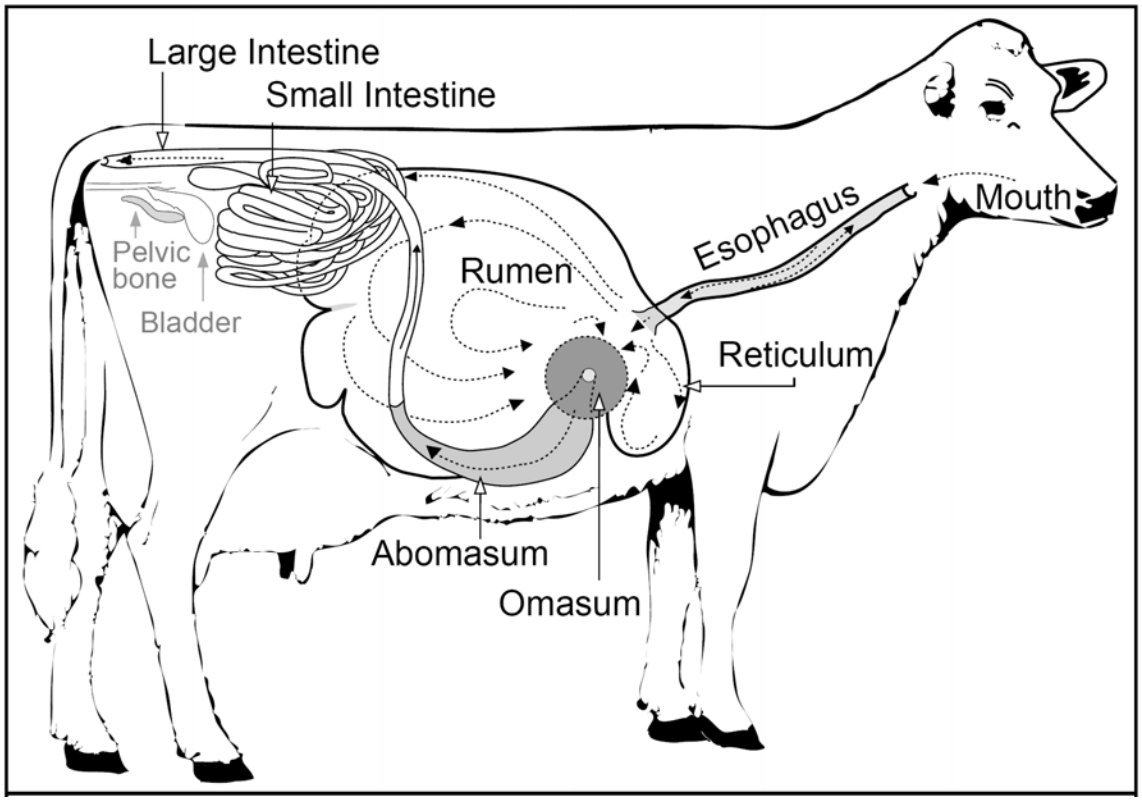

Figure 1.5 The digestive system of a ruminant [57].

population in the rumen by supplying and masticating feed regularly, by adding buffers and removing acids produced by flushing out microbial products and indigestible foods, and by maintaining conditions (pH, temperature, and moisture) appropriate for microbial growth. The contents of the rumen are discussed in more detail in Section 1.5.1.

Postruminal digestion is much the same as in other mammals. Digestion and absorption in the abomasum and small intestine are particularly important. The partially digested food leaving the stomach enters the small intestine, where it is mixed with secretions from the duodenum, liver and pancreas. The inner walls of the intestine are lined with villi which are the main sites of absorption of the end products of digestion. By the time the food material has reached the colon most of the nutrients will have been absorbed. Extensive microbial activity, similar to that in the rumen, occurs in the large intestine. This, however is not as effective, because the digesta is not held for sufficient time and many of the products of digestion are not absorbed. The byproducts are then excreted [58].

1.6.1 Rumen Contents

The rumen contents do not have a uniform composition; the composition is markedly influenced by the diet fed to the ruminant. Rumen contents are generally more viscous with concentrate diets as compared with forage diets.

Rumen dry matter (DM) is estimated to be between 10 and 15 percent of the total weight of the contents. This is greatly influenced by the feed and length of time since drinking.

A dome of gas is formed in the upper part of the rumen mostly made of the gases carbon dioxide and methane [59]. Carbon dioxide is produced from the acid-base chemistry of the bicarbonate buffer in saliva and from bacterial fermentation. It is invariably produced as a by-product, mainly of the fermentation processes. Methane is another end product of fermentation in the rumen. Hydrogen sulfide can also be formed

either by the reduction of sulfates or by the decomposition of sulfur-containing amino acids by the rumen micro-organisms.

The VFAs are an important constituent of rumen contents. The principal fatty acids in descending order of abundance are acetic, propionic, butyric, isobutyric, valeric and isovaleric. The proportions of the different VFAs are markedly influenced by diet and the microbial population in the rumen [60]. Although some VFA leave the rumen with digesta flowing to the lower gastro-intestinal tract, nearly all are absorbed across the rumen wall in the free form, apparently without active transport. At normal rumen pH, only small amounts of VFA are in the free acid form. However, removal of free acid is balanced by formation of more free acid through the reversal of the ionization equilibrium by mass action. Free acid is favoured by lower pH and higher concentration. The intracellular pH of the rumen wall and blood is ordinarily more alkaline than that of the rumen, favouring movement of acid toward the blood through the free energy of neutralization. The gradient similarly discourages flow of fatty acid anion. Bicarbonate, sodium ions and some urea flow in a reverse direction toward the rumen. The mechanism of VFA absorption in the lower tracts of ruminant and non-ruminant animals is similar to that of the rumen.[60]. Ammonia is one of the most abundant nitrogen compounds. The ammonia produced is utilised by microbes in biosynthesis of amino acids. However, most is absorbed through the rumen wall strictly by passive diffusion; the quantity absorbed is related to ruminal ammonia concentrations and to rumen pH [59].

The flora of the rumen is extremely complex and heavily diet-dependent. The digestion of plant materials like grasses and leaves is a slow process and the rumen provides the ruminant with a large vessel where digestion can proceed at a slow rate.

1.6.2 Rumen Conditions

Rumen temperature is generally considered to be normal within a range of 38 ^{o}C to 40 ^{0}C. Consumption of feeds such as alfalfa hay may result in temperatures as high as 41 ^{0}C. Rumen temperature is also influenced by the ingestion of water, which is at a

lower temperature than normal rumen temperatures. It might take two or more hours for the temperature to rise back to normal levels [61].

Rumen pH varies depending on the nature of the diet and the time that it is measured after ingestion. Fluctuations of rumen pH are a result of changes in accumulated VFAs. Depending on the nature of the diet fed, the rumen pH is lowest 2-6 hours after feeding. The rumen pH lies between within a normal range of 5.8 to 6.8 due to the effect of the alkaline saliva and the VFAs. It can be as low as 4.0 with intake of high carbohydrates and as high as 7.5 with poor rations [62].

Rumen conditions are known to be anaerobic and very little oxygen is found in rumen contents. The rumen is known to provide a highly reducing environment. The E^0 measured between platinum and calomel electrodes lies between –360 and –420mv [63]. The bubbling of oxygen *in vitro* causes no alteration in the E^0 values [64].

Rumen liquor has a high pH buffering capacity between 6.8 to 7.8; beyond that the buffering capacity is reduced. At normal rumen pH the buffering capacity comes principally from the bicarbonate and phosphate moieties of saliva.

1.6.3 Copper in the Rumen

The rumen is a multi-component, multi-phase medium where different metal-ligand interactions can take place. There is a huge excess of ligands compared to the metal concentration present there. This situation leads to ligand competition for the metal ions.

For a complete characterisation of the equilibrium situation (more correctly, the steady-state situation) in the rumen environment, it is essential to consider the adsorption and complexation that takes place in the rumen with the high molecular mass (HMM) fractions as well as the low molecular mass (LMM) fractions.

Complex formation between metal ions in general, and carbohydrates and monosaccharides in particular, has been studied [65]. Generally the interactions are weak, and their biological significance is thought to be minor [66]. Proteins are the most significant macromolecules that bind copper. This binding could be through a number of sites, using the side chains of the amino acids, the carbonyl oxygen, and the amide N of the peptide bond or the N and C of the terminal amine and carboxylate groups respectively. Significant amounts of copper could also be associated with dissolved high molecular weight organics. In addition to metal-organic complexes, there might as well be metal-organic precipitates. There might also be adsorption as well as surface complexation with the living biota. The metal can thus occur in a considerable number of different forms. To fully account for the copper speciation it is necessary to take into consideration the fraction of the metal that could be associated with dietary ingredients.

Though quantitatively the bulk of copper is attached to the macromolecular forms, our main interest lies in the low molecular mass ligands (LMM), as it is in these forms that copper can be transported. In particular, in these forms it can traverse the cell membranes and be readily absorbed [58].

1.7 COPPER METABOLISM IN RUMINANTS

Metabolism is a broad term that encompasses all events and components that take part in that post digestive transfer of copper from a food source to its ultimate location in a tissue or cell. A single copper atom may encounter numerous biochemical agents in the blood, capillaries, cell membrane, and cytosol before arriving at its final destination, usually an enzyme, or a binding or storage protein. These biochemical agents together form a metabolic pathway for copper within important body organs.

Once ingested, the copper distributes itself into different fractions in a body of a ruminant. The different fractions of copper metal ions that are present in free and bound forms have different functions to perform. Knowledge of the concentrations of these

fractions and their distribution in different biological fluids is of the utmost importance in understanding their functions in these fluids. Copper forms a variety of strong complexes, and hence all measurable amounts of copper exist in tissues as complexes [41]. Because of the multiplicity of factors that control the distribution of metal ions, ligands and their complexes in different biological fluids, it is not possible to easily predict in which specific fluid compartment they will be found. The distribution of metal ions into different fractions has physiological implications; this distribution helps specify the functions to be performed by the metal ion, and helps regulate the metal's homeostasis.

Copper species can be divided into low molecular mass (LMM) and high molecular mass (HMM) fractions. The LMM ligand fraction consists mainly of simple organic acids, amino acids and their derivatives, small peptides, carbohydrates and nucleotides. Other LMM ligands could be molecules such as citrate, pyruvate, oxalate and succinate. The HMM fraction consists mostly of proteins, nucleic acids, polysacharrides and lipids. The LMM fraction plays a vital role in transporting the metal ion between biological binding sites. In the intracellular fluids, LMM species can also serve as intermediate pools to provide metal ions for incorporation into proteins

The HMM fraction is represented essentially by the large proteins in the fluids. Complexes involving these could be either loosely bound, where they are exchangeable, or tightly bound (non-exchangeable), where the proteins bind the metal ion essentially irreversibly. Albumin is one of the chief ligands involved in the exchangeable HMM fraction. Such ligands are often present in relatively high concentrations and, therefore act as buffers for copper ions in addition to their functions in the transport or detoxification of the metal ion [58].

1.7.1 Copper Absorption

In most animals species copper is poorly absorbed; the extent of absorption is influenced by its chemical form. Generally not more than 5-10% of the Cu in the diet is

absorbed by adult animals, while young animals may absorb 15-30%. Often only 1-3% of Cu is absorbed in ruminants [67].

Copper absorption is limited to the stomach and small intestine in most mammals. The anatomical sites of dietary Cu absorption in the rat are the stomach and small intestines. Although studies on the absorption of Cu in ruminants have been less consistent, Cu has been found to be absorbed mostly from the abomasum, small intestine and colon, and to a lesser extent from the rumen-reticulum [68]. Absorption is a two step process, which involves copper uptake into the mucosal cells and subsequent transfer across the membranes for entry into the blood and internal tissues. Studies in a number of species have shown that the intestinal absorption of Cu is influenced by its chemical form, valence state, and the relative concentrations of competing metals (Ca, Fe, Zn, Cd, or Mo). Fe is thought to interfere by competing for sites on carrier proteins. Cd and Zn are thought to interfere by stimulating the synthesis of a Cu-binding protein in the intestinal mucosa. The half life of this protein, called metallothionein, is about the same as an intestinal cell, and so Cu is bound up in the intestinal mucosa and prevented from being transported into the blood. Sodium ions also play a role in the overall transmembrane movement. Fibres in fruits and vegetables as well as phytate in grains have been noted to impair intestinal absorption of copper. Ascorbic acid is also thought to inhibit absorption by reducing copper(II) to copper(I). In ruminants the significant antagonists of Cu absorption are Mo and S; these issues are discussed in detail below (Section 1.10). Agents that are thought to enhance intestinal copper absorption are amino acids and citrates [54].

Although the biochemical mechanisms of copper absorption are not completely understood, copper appears to be absorbed by two mechanisms; simple diffusion and active transport. Simple diffusion involves the movement of copper from a region of high concentration to one of low concentration. Active transport involves an intermediate – the carrier system. The carrier system possesses binding sites to which the metal is attached. The active form is used primarily for the transport of low concentrations of copper. Metallothionein synthesised in mucosal cells has been

identified as a regulator of Cu absorption and as a site of intestinal interaction between Cu and Zn [67].

1.7.2 Copper Transport

Transport implies the movement of copper toward a defined target from remote location. In plasma, two proteins, albumin and transcuprein, have been implicated in transporting copper to the liver from the intestine.

Copper entering the blood plasma from the gastrointestinal tract becomes bound to albumin and transcuprein. Although the concentration of albumin in plasma greatly exceeds the concentration of transcuprein, the affinity of transcuprein for Cu is much greater than that of albumin, with the result that about one-third of cupric ions entering the blood plasma is bound to transcuprein. Albumin- and transcuprien-bound Cu is cleared rapidly by the liver [68].

The liver has long been recognised as the main storage organ of body Cu and as a key organ in the metabolism of Cu; liver concentrations reflect intake and the Cu status of the organism as a whole. The storage form of Cu seems to be a mitochondrial cuprein. Within the liver, Cu is distributed amongst mitochondria, microsomes, nuclei, lysosomes and the soluble fraction of the liver parenchymal cells in proportions which vary with age, species and Cu status of the animal. The initial contact of Cu in the cells appears to be with glutathione (GSH), a cysteine-containing tripeptide. Copper is released from the cellular and subcellular fractions of the liver primarily for hepatic synthesis of ceruloplasmin, for synthesis of erythrocuprein by normoblasts of the bone marrow, and the incorporation into many enzymes. Nearly 90% of the Cu in mammalian plasma is in the form of the Cu metalloprotein, ceruloplasmin. Ceruloplasmin is the carrier for the tissue-specific export of Cu from liver to the target organs [67]. Its role in transport of Cu has been considered analogous to that of transferring, the iron transport protein. In transporting Cu, ceruloplasmin recognizes receptors on plasma membranes of cells and tissues and organs. Copper is believed to be released at the membrane site, and the

protein itself does not penetrate, a mechanism that differs from endocytotic mechanism used by transferrin [54]. In ruminants, the half-life of plasma ceruloplasmin varies with the biological species. It is estimated to be 70 h in sheep, 37 h in cattle. In the lactating dairy cow, though, it was found that 24% of milk Cu was derived directly from the diet and not from ceruloplasmin-bound Cu, indicating that the significance of ceruloplasmin as a transport form of Cu may vary with the biological species [68].

1.7.3 Copper Excretion

A high proportion of ingested Cu appears in the faeces. Most of this is unabsorbed Cu but active excretion occurs via bile, a further testament to the liver's role in maintaining balance and homeostasis. Very little is known about the mechanism of biliary Cu excretion in ruminants. Intermediate quantities are excreted through urine, milk, and intestine, and small amounts in perspiration [67].

1.8 COPPER DEFICIENCY IN RUMINANATS

The essentiality of Cu for ruminants was first established in 1931 when Cu deficiency in grazing cattle was demonstrated in Florida [67]. Copper has now been established as one of the most abundant trace elements in the body of ruminants. It is required for cellular respiration, bone formation, proper cardiac function, connective tissue development, myelination of the spinal chord, keratinisation, and tissue pigmentation. Also Cu is an essential component of several physiologically important metalloenzymes, including cytochrome oxidase, lysyl oxidase, superoxide dismutase, dopamine-β-hydroxylase, and tyroxinase.[9] Thus distinctive pathologies results from a deficiency in copper resulting in significant economic losses to livestock producers where it occurs.

Widespread copper deficiencies occur in many parts of the world. By the early 1950's, copper (Cu) deficiency in cattle was reported in Europe, Australia, New Zealand,

and the United States. Since then Cu deficiency has also been reported [67] in 34 tropical countries of Latin American, Africa and Asia with reported deficiencies, more than those of any mineral except P. In Canada, a Cu-responsive disease was described in cattle in the Swan River Valley of Manitoba in 1953. Since then Cu deficiency has been reported in Saskatchewan, eastern Ontario, British Columbia, northern Ontario and Alberta [69].

Copper deficiency in cattle is complicated because it can be the result of:

- very low copper in the diet-**a primary copper deficiency**, or
- interference with copper absorption due to the presence of antagonists in the diet of the animal -**a secondary copper deficiency**. Of all the antagonists mentioned in Section 1.7.1, the significant antagonist is molybdenum and/or sulfates which is present in the food or water of ruminants.

Of the numerous world reports of Cu deficiency in ruminants, only a few are concerned with a primary Cu deficiency, the majority with a secondary Cu deficiency [67]. Regardless of the reason for the copper deficiency, the problems exhibited by the animals are the same. Signs of Cu deficiency can be overt or non-specific. Often, the only sign seen is depression in production of milk. Furthermore, cattle can be clinically normal although their liver and plasma Cu concentrations may indicate a deficient state; clinical signs seldom occur until the body's Cu reserves are depleted and a biochemical dysfunction has been created.

The type and severity of clinical signs depend on such factors as dietary Cu availability, age and breed of cattle, season of the year, and climatic conditions [69]. A very sensitive index of a Cu deficiency is achromotrichia, or loss of pigment in hair and wool. For instance the pigmentation of sheep is so sensitive to changes in Cu intake that alternating bands of unpigmented and pigmented wool fibres can be produced, as copper is withheld from and added to the diet. Other symptoms seen in ruminants with copper deficiency include unthrifty appearance, diarrhoea, poor weight gains, light hair coats, swollen and painful joints, broken bones, rear leg weakness or paralysis in calves,

infertility, anaemia, and decreased resistance to disease. The problems seen will vary from herd to herd and are not easily predictable. However, when copper deficiency does occur, it invariably causes losses in production, health, and profits [67].

1.9 COPPER SUPPLEMENTATION IN RUMINANTS

Copper deficiency is generally corrected by supplementing diets of ruminants with additional copper [67]. In many areas of Canada, Cu supplementation of the diet is essential to maintain normal Cu status in ruminants. Before the type and amount of Cu supplementation is chosen, the nutritionist must not only know the Cu concentration in the feed, but also the concentration of all dietary elements which might influence dietary Cu availability [69]. For instance, for meaningful recommendations of copper requirements it is necessary to make reference to molybdenum and sulfur concentrations in the feed, pasture or soil. Nonetheless, for cattle a dietary level of 10 mg Cu / Kg of dry matter (DM) is recommended, with a range of 4 to 15 and a maximum of 100 mg Cu / Kg. With very low levels of Mo (below 1.5 mg /Kg), 4 mg /Kg has been found to be adequate. Other important factors such as interactions with other minerals should also be taken into consideration. A Cu:Mo ratio of 3.0 is regarded as a minimum, 4.3 is adequate and 6 to 10 is ideal [70]. It must however be noted that, prolonged excessive supplementation can result in Cu toxicity [69].

There are a number of ways of administering supplemented Cu to ruminants. When ruminants are pen-fed or in a dry lot feeding, supplementary copper is best supplied by incorporation of the element into a concentrate mixture. This method is not, however, recommended for grazing ruminants, as it is extremely expensive. Copper can also be supplemented in drinking water, however this method was found to be less satisfactory than other methods of supplementation. Other techniques involve dosing or drenching animals with copper compounds, or injection of organic complexes. Subcutaneous or intramuscular injection of some forms of copper, those that are slowly absorbed, is a satisfactory means of treating copper deficiency. For severe cases of

molybdenum-induced copper deficiency, injection of copper compounds is the recommended procedure, as it circumvents the gut – the main site of copper/molybdenum interactions [67]. It must however be noted that parenteral injections of Cu can cause mild to severe local tissue reactions, particularly after repeated injections. The severity of the reactions depends on the preparation used. Cu EDTA caused minimal reaction, whereas generally Cu amino acids can cause severe reactions. These preparations are useful when oral supplementation is impractical [69]. Copper oxide needles have been shown to supply available copper when administered orally to ruminants. The needles were retained in the digestive tract and released copper for several weeks [71].

In addition to the above-mentioned supplementations, there also exists a wide variety of other copper supplements. These types of supplements range from simple inorganic supplements to forms in which the metal is bound to large organic molecules. The most common form of copper supplementation in Canada involves the use of copper sulfate [71]. It is considered as the standard form, against which other inorganic and "chelated" supplements are compared.

1.9.1 "Chelated" Copper Supplements

It is necessary to define the term "chelate" carefully, since it is used slightly differently by chemists and by animal nutritionists and the feed industry.

In chemistry, a **complex** is formed when one or more entities or **ligands** containing electron donor (Lewis basic) groups surround an electron-deficient (Lewis acidic) central atom, often a metal ion. A ligand that attaches to a metal ion through only one atom is called a unidentate ("one-toothed") ligand. If it attaches through more than one atom, it is polydentate. In the latter case, the complex is referred to as a **chelate.** (Note that though all chelates are complexes, not all complexes are chelates). The name derives from the Greek word 'chela', which translates into claw, as an analogy to the clipper-like groups that hold the central metal atom in the ring. Chelates are of particular importance due to their greater stability compared with similar unidentate complexes. This is known as the chelate effect. It enables polydentate ligand to form

thermodynamically more stable complexes than analogous unidentate ligands. The chelate effect has both an enthalpy and an entropy contribution [44]. The functional groups in the ligand(s) are located in positions that enable stable ring structures to be formed.

However, the Association of American Feed Control Officials (AAFCO) defines an amino acid metal chelate as the product resulting from the reaction of a metal ion from a soluble metal salt with amino acids with a mole ratio of one mole of metal to one to three (preferably two) moles of amino acids to form co-ordinate covalent bonds. The average weight of the hydrolysed amino acids must be approximately 150 and the resulting molecular weight of the chelate must not exceed 800 [72]. A metal amino acid complex is defined as the product resulting from complexing a soluble metal salt with an amino acid. Since this definition does not consider the actual binding in the complex, it is possible that a complex considered a chelate by animal nutritionists might not be considered as such by a chemist.

To further confuse the issue, various supplements are referred to as chelated minerals, usually in promotional literature, though by either definition they are not. In this thesis, the strict chemical definition of chelation will be adhered to. The nutritional use of the word will be placed in quotes, i.e. "chelated".

"Chelated" minerals have been proposed as superior alternatives to inorganic supplements as they are thought to overcome two of the major limitations of inorganic supplements – low bioavailabilities at low concentrations and toxicity at high levels. Inorganic copper supplements are absorbed with rates of between 1 and 3 % [73]. Chapman and Bell [74] report over 80% excretion in cattle of unabsorbed copper from inorganic copper sources.

The increasing utilisation of these supplements centres around the theory that they are more bioavailable, as a result of the stability of the complex, which protects the copper from further reaction with antagonists that inhibit the absorption of the metal.

Many potential advantages have been attributed to the use of "chelated" minerals. Some of these advantages include increased gain, higher reproduction efficiency, and lower levels of mineral requirement. An enhanced immune system and better general access to metabolic systems and tissues are some of the other advantages suggested [75-77]. The major limitation of these products is their higher cost. Although this varies from company to company, they are estimated to cost between six to thirty times the cost of their inorganic counterparts [78].

Research comparing the effectiveness of the different modes of supplementation remains inconclusive. Some investigations suggest that "chelated" minerals are superior [79-81]. Other reports indicate equal bioavailabilities from "chelated" minerals in comparison to inorganic sources. Some of the differences in finding here were ascribed to differences in age, weight and breed of animals investigated. The form and sources of the supplements were also different in many of these experiments.

Early work by Kirchgessner and Grassman [82] found greater bioavailability from rats supplemented with copper-amino acid supplements. In a more recent investigation Debonis and Nockels [83] concluded that copper lysine was better retained than copper sulphate in steers. Similar results were reported by Kincaid et al. [79]. Their findings agree with those of Debonis and Nockels [83], they found the bioavailability of copper proteinate to be greater than that of copper sulfate.

Baker et al. [84] report equal bioavailability for copper lysine supplement compared with copper sulphate. Ward and Spears [85] concluded that the two supplements behave similarly in the rumen using an *in vitro* study. In another study Ward et al [86] also concluded that the bioavailability of copper from copper sulfate and copper lysine is similar in steers in the presence and absence of supplemental molybdenum and sulfur. They used growth, plasma copper and ceruloplasmin activity as indicators of copper status. In another study Kegley and Spears [87] found similar bioavailabilities for copper lysine and copper sulfate in calves. Similar results were obtained by Wiittenberg et al [88]

who showed that copper proteinate was equally bioavailable as copper sulfate in growing steers.

Ellwood [89] in assessing the availability of copper in steers from copper proteinate and copper (II) oxide, Used liver and plasma levels in addition to perfomance. It was concluded that copper proteinate was an effective copper supplement compared to CuO. Aoyagi and Baker [90] reported equal copper availability from commercially available copper lysine supplement (Cu-Lys) compared with $CuSO_4$ using chicken bile Cu levels as the response variable. CuO has been reported to result in low bioavailability in growing cattle [87, 91] and sheep.

Research results suggest that there might be certain circumstances where organic supplements are metabolised differently [80, 85]. It is also not certain if "chelated" supplements stimulate certain biological processes. The inconsistent literature findings regarding the use of these compounds indicate the need for clarification on the apparent advantages of using them, and determining the particular circumstances where they may be beneficial. In particular, it is necessary to assess situations or conditions where performances or health response justify the additional cost involved in using them [85]. At this stage, it appears questionable if the claimed increase in availability justifies the large cost differential. Some researchers suggest that it might be more practical to add an inorganic supplement at a lower cost and lower availability if simple elemental levels are the sole purpose of the supplement [91] (see Section 1.14).

1.10 THE CHEMISTRY OF THIOMOLYBDATES

1.10.1 Molybdenum

Molybdenum (Mo), is the 42nd element on the Periodic Table; located between niobium and technetium in the second row of transition elements. It is either a dark-grey/black powder with metallic luster or a coherent silver white mass. The average abundance of Mo in the earth's crust has been placed at 1 ppm, but individual rock types may range from zero to as high as 3000 ppm [67]. Mo occurs chiefly as *molybdenite* (MoS_2), but also as molybdates such as *wulfenite* (PbMoO4) and *powellite* (CaMoO4). It has seven stable isotopes; ^{92}Mo, ^{94}Mo, ^{95}Mo, ^{96}Mo, ^{97}Mo, ^{98}Mo and ^{100}Mo with natural abundances of 14.84%, 9.25%, 15.92%, 16.68%, 9.55%, 24.13% and 9.63% respectively resulting in an atomic weight of 95.94 [92]. The ground state electronic configuration of elemental Mo is $1s^2 2s^2 2p^6 3s^2 3d^{10} 4s^2 4p^6 4d^5 5s^1$ or $[Kr]4d^5 5s^1$. Mo exhibits many properties which are due to its partially filled 4d orbitals. For instance, it can exist in variable oxidation states, can play catalytic roles and can form colored complexes.

Mo has a wide variety of stereochemistries in addition to the variety of oxidation states, so its chemistry is among the most complex of the transition elements. The stereochemistries of Mo compounds in the various oxidation states are well outlined in the literature [43] and complexes of coordination numbers 4 to 9 are all known. The numerous stable oxidation states of Mo as well as its ability to form metal-metal bonds in clusters underlie its versatility as a biological redox catalyst. Valence states ranging from +2 to +6 are known, although in biological systems, the +6, +5 and +4 states are most commonly encountered. In biological systems, Mo is generally found with oxygen and sulfur ligands [93].

Mo is very important in the biochemistry of animals, plants, and microorganisms. It is the only element in the second transition series known to have natural biological functions. It occurs in more than 30 enzymes. Enzymes containing molybdenum are of two types: (1) Nitrogenases, which are found in bacteria in legumes,

and are involved in the pathways of nitrogen fixation (*i.e.* conversion of nitrogen in air N_2, to biologically useful ammonia). The molybdenum atom is present in a characteristic cluster which includes iron and sulfur atoms and it is known as the iron-molybdenum cofactor, FeMoco. (2) Molybdopterins, which include all other known molybdenum enzymes. The name molybdopterin is misleading as the group of enzymes includes tungsten-containing enzymes, and the word "molybdopterin" does not actually refer to the metal atom. The group may also be referred to as the "mononuclear molybdenum enzymes" as the metal atom is not present in a cluster. This group of enzymes is involved in a variety of processes, as part of the global sulfur, nitrogen and carbon cycles and are very crucial for the metabolism in bacteria, plants and animals [39, 43].

The presence of molybdenum in a biological system can also induce Mo antagonistic behaviour. In ruminants, the molybdenum antagonism occurs if the animals graze on soil rich in molybdenum, but poor in copper. The molybdenum causes excretion of copper reserves from the animal, leading to copper deficiency. The presence of sulfate in the diet of the animals is found to exacerbate the Mo antagonism. Evidence points to the formation of thiomolybdates, $MoO_xS_{4-x}^{2-}$(x = 0, 1, 2 or 3), in the rumen which inhibits Cu absorption by reacting irreversibly with Cu resulting in the formation of an insoluble product which is subsequently excreted [94].

1.10.2 Thiomolybdate Formation

Thiomolybdates are tetrahedral sulfido- (i.e., thiolate-) molybdenum(VI) complexes formed from molybdate ion (MoO_4^{2-}) and sulphide salts by the sequential replacement of the O atoms by S resulting in the formation of MoO_3S^{2-}, $MoO_2S_2^{2-}$, $MoOS_3^{2-}$ and ultimately MoS_4^{2-} as shown on the next page. The higher S-content thiomolybdates, particularly TM4, have been the most intensively studied because of their ease of preparation, their relatively greater thermal and hydrolytic stabilities and their biological roles [95].

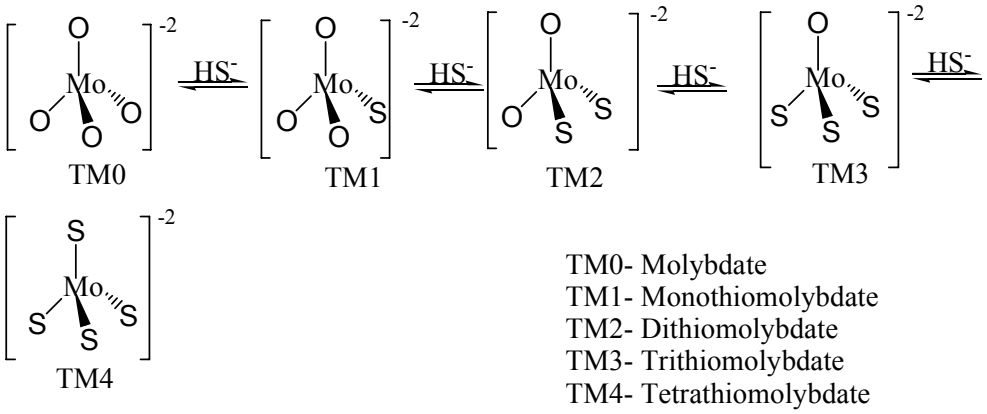

The synthesis of TMs can be traced back to the early 19th century when Berzelius [96] reported the formation of $(NH_4)_2MoS_4$ by evaporating a solution of molybdic acid in ammonium sulfide, and later Debray described the formation of $(NH_4)_2MoO_2S_2$ by treating ammonium molybdate with ammonium sulfide [97]. However, the true composition of the products was not established until fairly recently by Diemann and Müller [98]. They have done major work in the synthesis and characterization of each of the thioanions of molybdenum. By varying concentrations, solution pH, reaction times, and methods of isolation, they were able to prepare all four TMs (MoO_3S^{2-}, $MoO_2S_2^{2-}$, $MoOS_3^{2-}$ and MoS_4^{2}) from MoO_4^{2-} and H_2S in basic solution. All except TM1 are well characterized as crystalline solids. On the basis of qualitative observations, Müller et al. [98] concluded that H_2S and not S^{2-} might be involved in the formation reactions.

Although bonding and spectroscopic studies (full assignment of the UV/Vis and IR bands) of TMs were thoroughly reported by Müller et al. [98], only qualitative evidence on the reaction rates of these thioanions was given. Much of the initial quantitative work on the formation of TMs was carried out by Harmer and Sykes [99]. They observed that the rate of formation of TMs from the sequential displacement of O^{2-} with S^{2-} depends on $[H^+]$. The reverse reaction (hydrolysis) was found to be $[H^+]$ independent at pH > 8. Based on these observations and other trends in their kinetic study of TM formation and

hydrolysis, they proposed a mechanism for the sequential displacement of O^{2-} (in TM1) where these are first protonated before HS^- acts as a nucleophile. The prior protonation leads to a subsequent weakening of the Mo-O. An associative type mechanism is presumed. The reverse reaction is also assumed to be an associative process, involving H_2O, where an opportunity is provided for proton transfer to the departing S^{2-}. Harmer and Sykes [99] also observed that at lower pHs (3.6-5.6), the hydrolysis of TM3 was $[H^+]$-dependent as opposed to what was observed at higher pHs as mentioned above. They hence suggested an alternative mechanism where H_2S was presumed to be the nucleophile. This pathway is therefore relevant only at lower pHs (< 6) only. In an independent but concurrent study on the quantitative aspects on the formation of TMs [100] the results obtained were not much different from that obtained by Harmer and Sykes. Discrepancies observed in the rate constants obtained from both were as a result of different conditions used. A quantitative study of formation of TMs carried out later by Laurie et al. [101] obtained comparable results which were in good agreement with those obtained by earlier workers. However differences were reported in mathematical treatment of data and in interpretation of the mechanism of hydrolysis of TMs. Recently the synthesis of all TMs using a single route (which hitherto has been difficult) has been achieved using $(NH_4)_2S$ as the sulfide source. Detailed characterization of the TM products to ascertain their purity (which had also been previously lacking) was also achieved and for the first time TM1 has been successfully isolated in the pure form as the cesium salt in a study by Quagraine & Reid [102].

In the reducing environment of the rumen, TMs are formed from molybdates and sulfide, which is formed from reduction of both inorganic and organic sulfur by sulpholytic bacteria [103]. Which TM or TMs can be formed in the rumen has long been an issue of contention in the literature. The controversy over the presence or absence of TM4 is particularly significant, because this is the only form that has been shown to affect rats and sheep to the extent of inducing signs of Cu deficiency or of decreased Cu absorption. Various feed studies in cattle ([104], [105], [106], [107]) and sheep ([104], [107]) have detected radioactive labeled TM2 and TM3 (but not TM4) in the blood of animals, which were originally given the TM in the rumen. Earlier solution experiments [103] also

could not detect the presence of TM4 on mixing S^{2-} and MoO_4^{2-} at lower S:Mo ratios. This has led to the conclusion by some that TM4 is not formed in the rumen. However the characteristic absorption spectrum of TM4 has been detected by a variety of authors in rumen liquor incubated *in vitro* with Mo and S ([108], [94]) although the levels of Mo and S used in these studies have been criticized as being above their normal levels. Using Mo and S concentrations which are closer to those normally pertaining in the rumen, and in a fermentative system, substantial conversions of MoO_4^{2-} to TM4 were observed (35, 30 and 25% at S:Mo ratios of 12, 7.2 and 3.6 respectively) [109]. It should however be noted at the outset that, the inability to detect TM4 (or any other TM) spectrophotometrically in rumen fluids at normal dietary Mo levels does not necessarily mean that it is absent. High background absorbances may make such measurements difficult [94].

A recent study [102] of TM formation under rumen-like conditions with respect to time is shown Figure 1.6. Within 5 min about 85% of the TM formed is TM2, in agreement with an earlier observation that TM2 is rapidly formed for S:Mo > 10:1 [103]. There is then a steady decline of TM2 (slowing down only between 60 to 90 min), with a concomitant increase in TM3. A substantial amount (35%) of TM3 is formed within 30 min of reaction. The graphs for the levels of TM2 and TM3 are almost symmetrical, and the two stay almost constant between 90 to 150 min, suggesting that TM3 is formed from TM2. The mean residence time of sulfide in the rumen of sheep, reported [110] to be 107 min, falls within the time period where the percentages of TM2 and TM3 are almost constant, at ~28 % and ~ 48% respectively. Formation of TM4 is slow but noticeable within 30 min. TM4 then increases steadily, constituting about 18% at the mean sulfide residence time and 30% after 3 hr. TM1 formation is gradual under the conditions employed in this study, up to about 60 min, then its level begins to decline. No unreacted molybdate was found beyond 5 min [102].

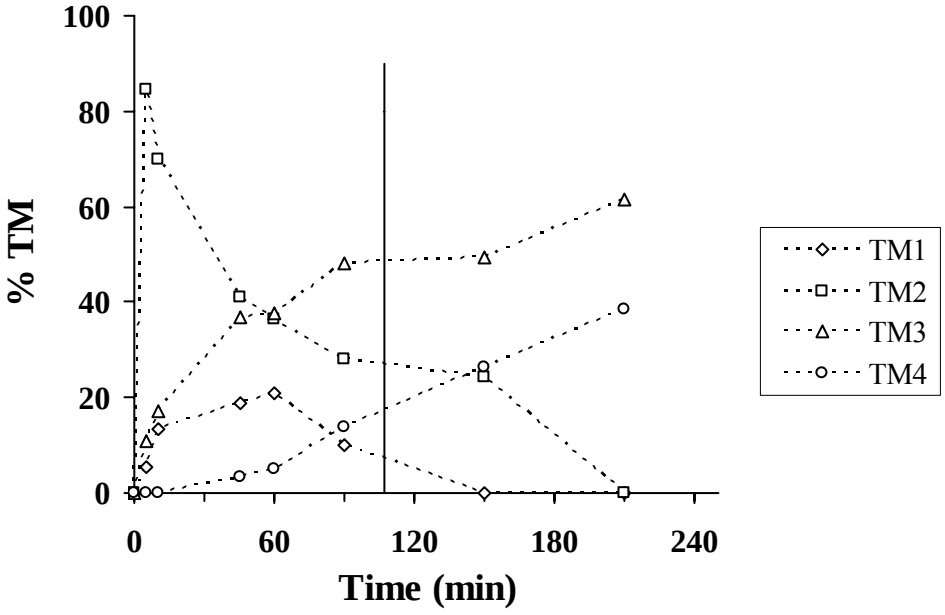

Figure 1.6 TMs as a fraction of total Mo present at different times after mixing Na_2MoO_4 in solution with ammonium sulfide solution to give an S:Mo ratio of 22:1, pH 7.0, ionic strength 0.2 **M**, and a temperature of 38°C. Initial concentration of molybdate in the mixture was 1x 10^{-4} **M**. The vertical line represents the mean residence time of S^{2-} in the rumen [102].

Formation of TM4 from MoO_4^{2-} clearly proceeds via successive replacement of oxygen, as evidenced from the color sequence change in solution: MoO_4^{2-} (colourless) to MoO_3S^{2-}(yellow) to $MoO_2S_2^{2-}$(orange) to $MoOS_3^{2-}$(orange-red) to MoS_4^{2-}(red). This colour sequence is shown in the UV/Vis absorbance spectrum (Figure 1.7). The strong colors are as results of S $\rightarrow$ M charge transfer which are of relatively low energy and lie in the visible region. Linear relationships in fact have been established between the energy of the longest wavelength electronic transition with the M-S stretching force constant and with the optical electronegativity of the metal centre (for closely related species). In the latter case the transition energy increases as the χ_{opt} value decreases — consistent with charge transfer being in the S $\rightarrow$ M direction [95].

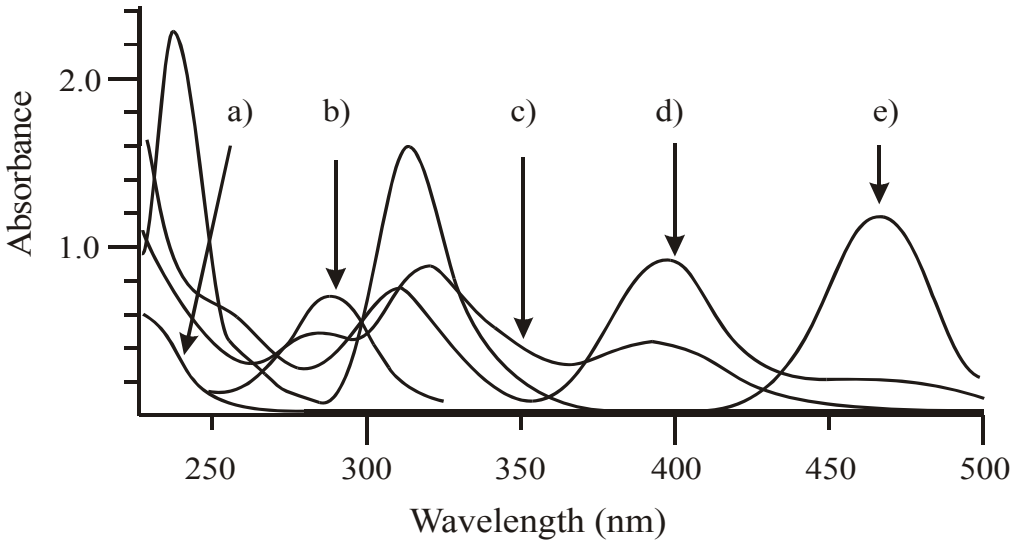

Figure 1.7 UV/visible spectra of molybdate and the thiomolybdates.
(a) TM0, (b) TM1, (c) TM2, (d) TM3, (e) TM4 [102].

The strong UV/Vis and IR absorption bands are particularly useful diagnostic tools in determining the purity of the TMs and in following their reactions. The distinctive UV/Vis spectra of TM4 and the TM3 anions have thus been used to determine the rate constants for the formation (pseudo-first order with S^{2-} in excess) and hydrolysis of the ions [95]. The intensities of ^{95}Mo NMR signals could also be used to determine the level of cross-contamination of the various TMs, but with lower precision. Discrepancies in some properties of the TMs described in the literature can now be ascribed to differences in purity of the TM samples prepared and used by different researchers [102].

TMs are not very stable in aqueous solution, especially at low pH. The stability decreases with increasing O content [98]. Hence, the lower S containing TMs (i.e. TM1 and TM2) are less stable. Under oxygen-free nitrogen atmosphere TM4 aqueous solution was found to be stable up to 1 day at 38 ^{o}C while TM3 showed a 33% decrease in

overall absorbance in the first 3 hr. An aqueous solution of TM4 even under normal conditions can be stable over 2.5 hr at 25 ^{o}C [102].

By far the most important property of the TMs, in particular TM4, is their role as ligands in a range of complexes. In these the $MoO_xS_{4-x}^{2-}$ moieties are mostly retained. It is the sulfide ions that play the key role as bridging ligands in which they can bridge two, three or four metal centres. The complexes formed range from simple linear structures, to small cubanes and to more complex clusters. In these cases the thiometallate anions act as the building blocks. Both the metal centres and the S ligands are redox active — either acting separately or, of more interest, acting in concert. Oxidation of S^{2-} can result in a number of species with oxidation states ranging up to VI, e.g. S_2^{2-}, S_4^{2-}, S_8, SO_2, SO_3 as well as the various oxyanions. All of these are also potential ligands [95].

The ability of TMs to act as bridging ligands in its formation of complexes has been implicated in their roles in Mo-induced Cu deficiency [111].

1.11 COPPER ANTAGONISM BY THIOMOLYBDATES IN RUMINANTS

Both Cu and Mo are well-known essential elements occurring in a range of metalloenzymes. Although their enzymatic functions primarily involve redox processes there is no evidence of any direct biological interactions between them as there is, for example, between Cu and Zn and Cu and Fe; this would be as expected from their different coordination chemistry behaviour and from their very different naturally occurring forms. However, there is one exception to this, and that is the well documented Mo-induced Cu deficiency that can afflict ruminants; more correctly this should be expressed as a Mo-S-Cu interaction [95].

Molybdenum was found to cause severe diarrhea in cattle in 1938 by Ferguson and co-workers [67]. However the three-way interaction between copper, molybdenum and

sulfur was recognized in 1953 by Dick [112] who first established the metabolic interrelationships among Cu, Mo and inorganic sulfate for ruminants. The involvement of S^{2-} in the Mo-Cu antagonism was not recognized until Dick et al. [113] and Suttle [114] proposed that thiomolybdates form spontaneously in the rumen. These workers suggested that TM would react with Cu in the rumen to form insoluble Cu-TM complex and that most of the complex would not be absorbed.

The first component of the complex digestive system of ruminants (e.g. cattle and sheep), the rumen, has a high microbial content and is anaerobic. Under these conditions both inorganic and organic sulfur are reduced to sulfide. Rumen sulfide levels of up to 6.0 ppm have been observed [95]. The sulfide produced in this way reacts with molybdate present in the diet of the ruminants to form TMs. Tms associated with solid rumen digesta (bacteria, protozoa and undigested feed particles) form insoluble complexes with copper that do not release copper even under acidic conditions [115].

The role of ruminal TM in the induction of Cu deficiency has been confirmed by many researchers. Addition of Cu(II) to a solution of TM4 in strained rumen contents resulted in the loss of the TM4 UV/Vis spectrum, with a complete loss of spectrum at an approximately 1:1 Cu:Mo ratio [116]. Other studies [103, 117] have confirmed that a rapid reaction occurs between Cu(II) ions and its complexes with TM4 and with the oxythiomolybdates: in fact, taking into account the rapidity of the reaction and the rumen concentrations it was concluded that the oxythiomolybdate ions $MoO_xS_{4-x}^{2-}$ (x = 1,2) were the more likely reactants. Studies by Mason and co-workers show that the TM2, TM3, and TM4 all have an effect on Cu metabolism when given intravenously to ruminants and have a reversible inhibitory effect on caeruloplasmin oxidase [118]. Despite these observations the majority of studies on the biological effects of the thiomolybdate ions have concentrated on TM4 because of its greater aqueous stability. Price et al. [94] found predominately TM3 and TM4 in the solid phase of ruminal, duodenal and ileal digesta. TM2 and TM3 were detected in the plasma of sheep after ruminal administration of ^{99}Mo-labeled molybdate ([94],[104]) and indicate that thiomolybdate species can be absorbed. This has been supported by the fact that Cu depletion caused by

TM4 appears to result from a decreased absorption from the diet and the formation of a non-bioabsorbable form. The latter has been identified as a ternary Cu-Mo protein form in both blood plasma and in liver cells, the proteins involved being albumin and metallothionein, respectively. ^{95}Mo NMR spectroscopy shows that TM4 can bind to serum albumin protein [119]. Other studies, using membrane filtration and UV/Vis spectroscopy, suggest this association to be a relatively weak, mainly ionic, binding between albumin and TM4, there was certainly no evidence of any S cross-linking. With Cu-albumin, however, there was rapid formation of a ternary TM4-Cu-Albumin complex with similar characteristics to the polymeric compound that we isolated in vitro, i.e. EPR evidence of Cu(I) and Mo(V) centres [117]. While we could find no evidence of any interaction between the Zn-thionein protein and TM4, with Cu(I)-thionein TM4 was strongly bound; the other thiomolybdates were found to behave in a similar manner [117].

Systemic effects on copper metabolism that have been attributed to thiomolybdates include (i) limiting Cu absorption, (ii) strong binding of copper to plasma albumin, resulting in a reduced transport of available copper for biochemical processes, (iii) depleting liver Cu, (iv) altering liver Cu and Cu from other tissues to a less available form, (v) increasing biliary excretion of Cu, (vi) limiting reabsorption of biliary Cu, (vii) increasing urinary Cu excretion and (viii) removal of Cu from metalloenzymes [68, 120].

Formation of thiomolydates also affects the kinetics of S metabolism by affecting sulfide formation and absorption. Thiomolybdates rapidly react with particulate matter and proteins to form complexes that bind Cu strongly, reducing its solubility, decreasing the H_2S concentration and thereby the rate of sulfide absorption [67].

Independent from its role in the molybdenum-copper interaction, sulfur may also reduce copper bioavailability[71]. Increasing dietary sulfur in the inorganic (sulfate) or organic (methionine) form from 1.0 to 4.0 g of sulfur/kg of diet reduced copper bioavailability in hypocupremic ewes fed low-molybdenum diets by 30–56%. Much of

the evidence obtained supports the idea that the utilization of Cu is impaired through the formation of insoluble, unabsorbed Cu sulfide (CuS) in the gut [121]. The exact site in the gut for the interaction of Cu and S is still a debate in literature. Whereas Huisingh and Matrone[122] and Suttle[123] have theorized that sulfide produced by ruminal microorganisms through the reduction of dietary S, interacted with Cu to reduce its availability, Allen and Gawthorne [115] found that the addition of sulfide to rumen contents in vitro did not change the distribution of Cu between the fluid and solid phases and that the critical site for CuS formation farther down the GI tract.

Although the total sulfide concentration in rumen liquor of ewes, 2 hr after been given inorganic supplement and organic supplement, to correspond to the proportions found in a herbage containing total S = 4 g kg^{-1}, was found to be 24 mg L^{-1} (7.5 x 10^{-4} **M**) [121] rising to 4.0 x 10^{-3} **M** under extreme dietary S value of 21.1 g kg^{-1} [102], the critical site for CuS formation to affect Cu bioavailability has been suggested [121, 124] to be probably farther down the GI tract. Although little is known about the metabolism of sulfide beyond the rumen, the fact that sulfide concentrations are as high in omasal as in ruminal digesta after S supplementation and that CuS is very insoluble at a pH of 2**,** suggests that any soluble Cu released during digestion in the omasum and possibly the abomasum will continue to be largely precipitated as CuS [121] possibly at the proximal duodenum and terminal ileum which have high pH [124].

1.12 NMR FOR AQUEOUS COMPLEXATION STUDIES

1.12.1 Introduction to NMR spectroscopy

Nuclear magnetic resonance (NMR) is a phenomenon exhibited when atomic nuclei in a static magnetic field absorb energy from a second oscillating magnetic field (usually a radio-frequency field) of certain characteristic frequencies. Some nuclei experience this phenomenon, and others do not, dependent upon whether they possess an intrinsic magnetic property called spin [39]. All nuclei that contain odd numbers of

nucleons and some that contain even numbers of nucleons have this intrinsic magnetic property. Nuclear magnetic resonance was first described independently by Felix Bloch and Edward Mills Purcell, in 1946, when they noticed that magnetic nuclei, like ^{1}H and ^{31}P, could absorb RF energy when placed in a magnetic field of a specific strength. Both of them shared the Nobel Prize in Physics in 1952 for their discovery.

Spectroscopy is the study of the interaction of electromagnetic radiation with matter. Nuclear magnetic resonance spectroscopy is the use of the NMR phenomenon to study physical, chemical, and biological properties of matter. As a consequence, NMR spectroscopy finds applications in several areas of science. It is one of the principal techniques used by chemists to obtain physical, chemical, electronic and structural information about a molecule [125].

The technique known as Fourier transform nuclear magnetic resonance spectroscopy (FT-NMR) revolutionalized the use of NMR by decreases the time required for a scan by allowing a range of frequencies to be probed at once. It was pioneered by Richard R. Ernst, who won a Nobel Prize in Chemistry in 1991. In FT–NMR spectroscopy, the entire spectrum of interesting frequencies is stimulated by a pulse of radio frequency (RF) energy, and response of the system is measured as a function of time using a digital computer. The frequency spectrum is generated mathematically in the computer using a Fourier transformation which converts the time domain data into a classical frequency domain spectrum [126]. The route is as summarized in Figure 1.8.

1.12.2 Principles of NMR Spectroscopy

When a nucleus, for instance a proton (^{1}H nucleus), is placed in a magnetic field in typical FT-NMR experiment, the nuclear spin of the proton interacts with the applied magnetic field. The proton, with a nuclear spin quantum number I = ½ can either align with or against the magnetic field of strength $\mathbf{B}_o$. Thus, two energy levels are generated

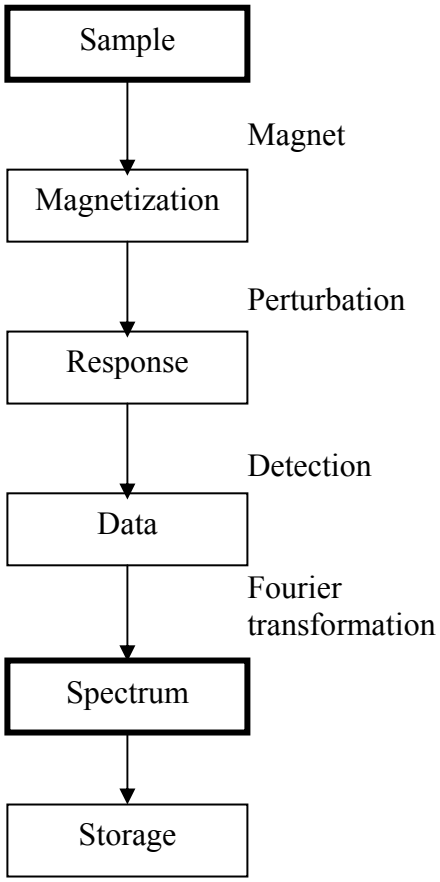

Figure 1.8 A conceptual block diagram of the pulsed FT-NMR experiment [126]

in the magnetic field. These energy states can be characterized by the nuclear spin quantum number, m_I, and are separated by an amount of energy, ΔE, which is field dependent. ΔE is given by:

$$\Delta E = \mathbf{B}_o \gamma h /2\pi \qquad \textbf{(1.14)}$$

where γ is the magnetogyric ratio and h is Planck's constant.

Considering now a large number of such protons, the two energy states will be unequally populated, the ratio of the populations being given by the Boltzman equation:

$$N_\beta/N_\alpha = \exp(-\Delta E/kT) \quad \textbf{(1.15)}$$

where N_β is the population of the upper state, N_α the population of the lower state, k the Boltzman constant and T the absolute temperature. The population difference is dependent both on the field and also the nuclear species under observation. This population difference corresponds to a bulk magnetization which can, in principle, be measured directly [126]. The signal in NMR spectroscopy results from the difference between the energy absorbed by the spins which make a transition from the lower energy state to the higher energy state, and the energy emitted by the spins which simultaneously make a transition from the higher energy state to the lower energy state. The signal is thus proportional to the population difference between the states [125].

The behaviour of magnetization in a magnetic field can be conveniently described using vector diagrams. A rotating frame of reference with co-ordinates (X`, Y` and Z) is used instead of the conventional ('laboratory') Cartesian co-ordinates (X, Y and Z). The X` and Y` axes rotate about the Z axis at a frequency of $\gamma\mathbf{B}_o/2\pi$ (the Larmor frequency). The applied magnetic field $\mathbf{B}_o$ points along the Z axis.

An individual magnetic moment, precessing at the same frequency in the laboratory frame as X' and Y', appears static in the rotating frame. The experimentally observed or 'bulk' magnetisation, **M**, is the vector sum of the individual magnetic moments. Since the individual magnetic moments are randomly distributed round the precession "cone", **M** is aligned along the Z axis.

Figure 1.9 shows the position of **M** as a pulse of radio-frequency radiation strikes the sample. **M** will experience a torque from the force generated by $\mathbf{B_1}$ (the magnetic field component of the electromagnetic radiation; This torque rotates the sample magnetic moment towards the X'Y' plane, the extent of rotation depending on the length of the pulse. For many experiments, the pulse length is chosen so as to correspond to a flip angle of 90^o (a '$\pi/2$ pulse'). A 90^0 pulse puts **M** in the X'Y' plane, as shown. Its

exact orientation will also depend on the direction in which B_1 points (the 'phase' of the pulse); we will consider pulses which rotate M round X', so that a 90^o pulse places M along the Y' axis.

When the pulse ends, **M** returns to its equilibrium position. The radio receiver in the spectrometer detects the components of magnetisation in the X and Y directions ($\mathbf{M}_x$ and $\mathbf{M}_y$); these decay away as equilibrium is restored. This decay is called the **Free Induction Decay** (FID): *Free* of the influence of the radiofrequency field, *Induced* in the coil and *Decaying* back to equilibrium [126]. Samples with several types of protons give FID's that consist of the various decay curves superimposed, with interference occurring between the FID's. This results in an interferogram. An interferogram cannot be easily interpreted. Therefore, the FID is converted to a frequency domain signal (i.e. a spectrum) using a mathematical operation, the Fourier Transform

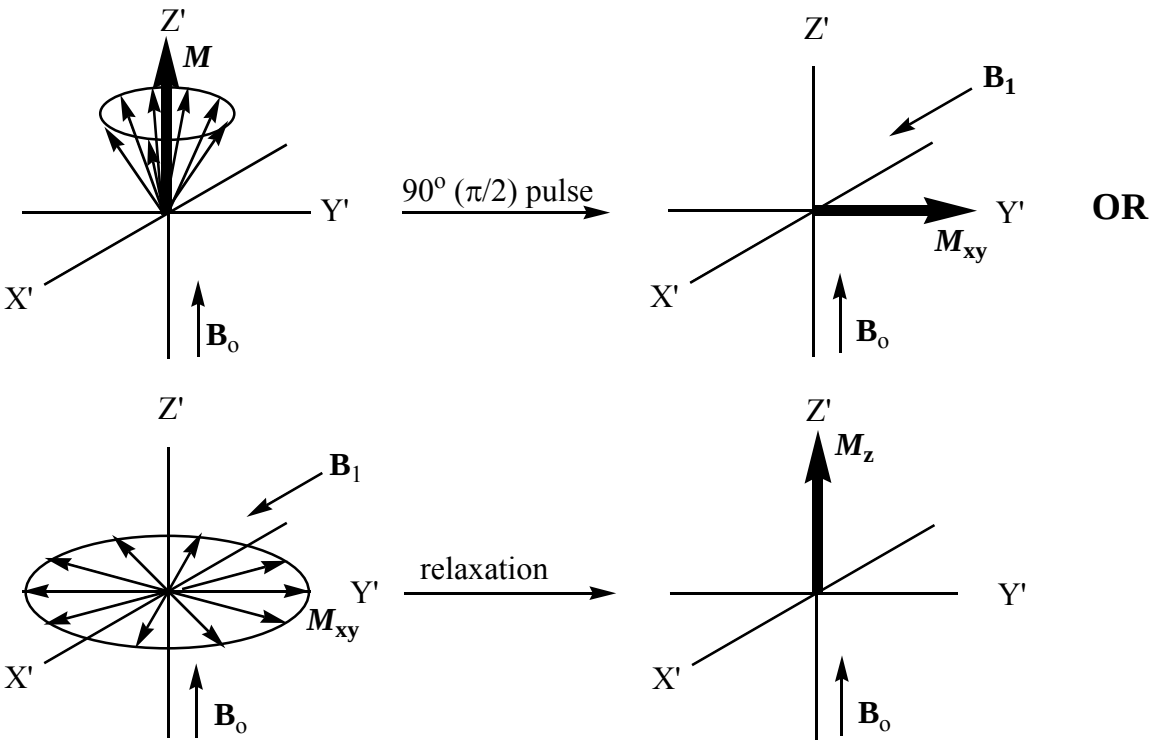

Figure 1.9 Behaviour of magnetic moments of nuclei in a rotating field of reference 90° (π/2) pulse experiment

1.12.3 NMR Relaxation

Relaxation is the process by which **M** returns to its equilibrium state, with $\mathbf{M}_z$ returning to its original value ($\mathbf{M}_0$) while M_x and M_y approach zero. The mathematical analysis of the complex behaviour NMR relaxation has been provided by Bloch [127]. The analysis leads to a set of equations which describe the variation with time of M_x, M_y, and M_z. The time constant which describes how M_Z returns to its equilibrium value is called the spin lattice or longitudinal relaxation time (T_1). The equation governing this behaviour as a function of the time t after its displacement is:

$$M_z(t) = M_z(0)\,(1 - e^{-t/T1}) \qquad \textbf{(1.16)}$$

The time constant which describes the return to the equilibrium value (i.e., to zero) of the transverse magnetization, M_{xy}, is called the spin-spin relaxation time, T_2.

$$M_{xy}(t) = M_{xy}(0)\, e^{-t/T2} \qquad \textbf{(1.17)}$$

T_2 is always less than or equal to T_1. The net magnetization in the XY plane goes to zero and then the longitudinal magnetization grows in until we have M_0 along Z [125]. The reciprocals of the relaxation times correspond to the rate constants for the two relaxation processes.

T_1 is by definition, the component of relaxation which occurs in the direction of the ambient magnetic field. This generally comes about by interactions between the nucleus of interest and unexcited nuclei in the environment, as well as electric fields in the environment (collectively known as the 'lattice'). Thus the name "spin-lattice" relaxation. T_2 by definition is the component of 'true' relaxation to equilibrium that occurs perpendicular to the ambient magnetic field. Because of this, the relaxation is dominated by interactions between spinning nuclei which are already excited [128]. This results in exchange of spin energy with one another so that some now precess faster than

the Larmour frequency, while others travel more slowly. The result is that the spins begin to fan out in the XY plane. Thus the name "transverse" or "spin-spin" relaxation [129].

Since relaxation times can be related to structural features of molecules and molecular motion, consideration of relaxation processes is important in the design of NMR experiments, as it is the decay of the magnetisation through the relaxation that we are observing during the free induction decay. The value of T_1 and T_2 can be controlled to some extent. Addition of a paramagnetic substance such as Cu^{2+} ions shortens T_1 and T_2 values, as the unpaired electrons provide an effective stimulus for NMR transitions [58]. This is as a result of the interaction between the unpaired electron spin and the nuclear spin under observation by NMR. The electron has magnetic moment about 10^3 times that of nuclear moments and generates strong magnetic field. It is the fluctuation of this field that results in the shortening of the nuclear spin relaxation resulting in the broadening of resonance peaks in NMR in spectrum. It is not uncommon for lines to be broadened into the baseline such that only a very broad line is observed if it is detectable at all. However there are applications where the presence of paramagnetic species can be used to probe the hydration shell of a nucleus and to obtain information on the binding sites of metal ions in biological systems.

1.12.4 Use of the NMR Chemical Shift

The exact frequency at which absorption of energy occurs depends on the identity of the nucleus concerned, and its chemical environment, as well as the magnetic field strength. The effective magnetic field actually experienced by the nucleus, $\mathbf{B}_{eff}$, is always less than that of the applied field:

$$\mathbf{B}_{eff} = \mathbf{B}_o (1- \sigma) \qquad \textbf{(1.18)}$$

where σ is the shielding parameter. (The nuclei are colloquially said to be 'shielded' from the full effect of $\mathbf{B}_o$. In fact, the circulation of electrons in the applied field gives rise to an induced field that tends to oppose the applied field).

Thus, nuclei that are not chemically equivalent (i.e. have different electronic environments) are shielded to different extents and give separate resonance signals in the spectrum. The frequency difference is measured between the resonance signals of the sample and that of a reference compound. A dimensionless quantity, δ, the chemical shift, is used instead of frequency by dividing the frequency difference in Hz by the mean operating frequency of the instrument being used. This makes the chemical shift independent of the field strength of the instrument, so that the same value is recorded on different instruments. Chemical shifts are usually quoted in parts per million (ppm). For this work, as with most NMR investigations in aqueous media, Sodium 2,2-dimethyl-2-silapentane-5-sulfonate (DSS), a water-soluble analog of the tetramethylsilane (TMS) used in non-polar solvents, is the standard reference used.

One of the unique properties of NMR is that it affords the opportunity to study systems actually at equilibrium, whereas most other analytical techniques displace the system from equilibrium. NMR can monitor the exchange of atoms within the same molecule. If equilibrium exists between two environments for the same nucleus and the exchange between them is quite fast, the signals of the resonance are merged into one. The condition for fast exchange is that the exchange rate must be greater than the difference in absorption frequency between the two states. If the exchange occurring between the two environments A and B is at a rate of k_{exc}, fast exchange occurs if $k_{exc} >> |\Delta\nu|$. Similarly slow exchange is when $k_{exc} << |\Delta\nu|$.

For a ligand with acid-base chemistry, the chemical shifts of the acid and the conjugate base forms are different. The exchange in most such instances is fast, such that only one peak is observed. The observed chemical shift is given by:

$$\delta_{obs} = \Sigma\, \delta_i \alpha_i \qquad \textbf{(1.19)}$$

where δ_{obs} is the observed chemical shift and δ_i is the chemical shift of species i while α_i refers to the fraction of species i [130]. The fraction of the different species in solution can be determined from a knowledge of the relevant equilibrium constants. In the course of a titration of an acid, the observed chemical shift for any NMR-active nuclei of a non-labile atoms on the acid, progresses monotonically from a value that represents the acid form to one that represents the conjugate base form. If the dissociation constants of the acid are known it is possible to obtain the chemical shift values of the individual species by using equation 1.12 to fit the experimental values.

With the introduction of copper, metal complexes are now introduced into the solution. The observed chemical shifts are still the weighed average of those of all the species including the complex species if under a fast exchange regimen. The chemical shift is now a function of the equilibrium constants, stoichiometry and pH values. Here again, the chemical shifts of the copper complexes can be obtained from fitting the observed chemical shift data. It is then possible to gain an insight into the speciation pattern prevailing in solution.

1.12.5 Solvent Suppression

It is necessary to convert the analog signal in NMR to digital form. An Analog to Digital (ADC) converter is used for this purpose. The number of bits (12 or 16) used by the digitizer limits the dynamic range and precision by which the signals can be represented. For instance, using a 12-bit digitizer, if a large signal produced an output of 4095 ($2^{12} - 1$), the smallest signal that can be recognised would correspond to 1 or .02% of the largest signal. Thus the smallest signal recognisable in an NMR spectrum is only a certain fraction of the largest signal. When the dynamic range in the spectrum exceeds that of the digitizer, the weakest signal will not be displayed. Such a situation is most frequently encountered in proton NMR of dilute solutes in aqueous solution. In aqueous solutions the water hydrogen atom concentration is of the order of 110 **M**, and the solutes of interest could be in the millimolar range or less.

This difficulty can be overcome either by chemical means, increasing the concentration of the solute used or by using deuterated solvents, as deuterium is a different nucleus. Often neither approach is feasible. Many chemicals are only sparingly soluble in solvents other than water and are often available only in very small quantities As in these studies a particular solute concentration may be of interest. And information in D_2O solutions may not reflect the situation in aqueous solutions [131]. For instance, the information on the exchangeable protons of proteins and nucleic acids cannot be obtained from D_2O solutions [132]. Moreover, the use of D_2O does not guarantee the elimination of dynamic range problems as significant residual HDO resonances may still exist. The body of a ruminant is composed of aqueous solutions and the data obtained for the copper(II) ligand system from potentiometry was also obtained in aqueous solutions. To allow for direct comparison between NMR and potentiometric data, it is thus advantageous to carry out the studies under aqueous conditions, the shortcomings notwithstanding.

There are over a hundred published experimental methods, collectively termed solvent suppression (SS) techniques, that have been devised to solve these dynamic range problems [133]. Most SS techniques either saturate the solvent signal or selectively excite others. Ideally, the technique should suppress the solvent signal and leave all others unchanged; this is however never completely attained in practice. Particular methods prove better in a given circumstance. Each SS technique has its own advantages and shortcomings. The spectrometer design, the operator skill and the system being investigated determine the optimum choice. For the present studies the Binomial "1 $\underline{3}$ 3 $\underline{1}$" sequence [134, 135] was found to give good results, and is simple to implement.

A Binomial pulse sequence consists of a series of pulses, equally spaced and alternating the direction in which they tip the magnetisation, and with amplitudes given by the binomial coefficients (e.g. 1$\underline{1}$, 1$\underline{2}$1, 1$\underline{3}$3$\underline{1}$, etc.). The alternation in direction between successive pulses is executed so that if the delay is short compared to the relaxation time, there is still no net excitation at the carrier frequency [126]. Figure 1.10a and 1.10b show the effect of a $\pi/2$ 1$\underline{3}$3$\underline{1}$ pulse sequence on the magnetisation for the

water proton resonance and for a solute proton respectively. The frequency of irradiation is placed on the solvent peak.

The first pulse (P1) rotates both solvent and solute magnetisation vectors by 11.25^0 about the Z axis. During the first delay τ, the solute magnetisation rotates by 180^0 about the Z-axis while the water magnetisation remains stationary. The next pulse (P3) rotates the solute magnetisation by an additional 33.75^0 towards the X'Y` plane, but rotates the water magnetisation 33.75^0 back towards the Z-axis. During the next delay τ, the solute magnetisation rotates by 180^0 about the Z-axis while the water magnetisation remains stationary. The next pulse (P3) rotates the solute magnetisation by an additional 33.75^0 towards the X'Y' plane, while the water magnetisation rotates by 33.75^0 towards (and past) the Z-axis. Once more during τ, the solute magnetisation rotates by 180^0 with the water magnetisation unperturbed. The final pulse (P1) flips the solute magnetisation vector by 11.25^0 into the X'Y' plane, and returns the solvent magnetisation to the Z-axis. Thus the solute experiences an overall rotation angle of 90^0 ($11.25^0 + 33.75^0 + 33.75^0 + 11.25^0$) while the solvent experiences an overall rotation angle of 0^0 ($11.25^0 - 33.75^0 + 33.75^0 - 11.25^0$), i.e. no excitation at all. In practice however the solvent does experience some excitation, as it is not an infinitely narrow peak, and part of the peak is off-resonance.

The 1331 pulse sequence was preferred to other binomial sequences as it combines good performance with simplicity. The experimental set up is fairly simple. The transmitter frequency is tuned to the exact frequency of the solvent peak to be suppressed and the pulse lengths are set so that their sum gives the desired pulse angle. The interpulse delays are chosen so as to only excite the desired spectral region. The pulses are separated by equal intervals of time τ. The Fourier transform of the sinusoid function that describes this pulse is given by:

$$S_n = \sin^3(\Delta\omega\tau/2) \qquad \textbf{(1.20)}$$

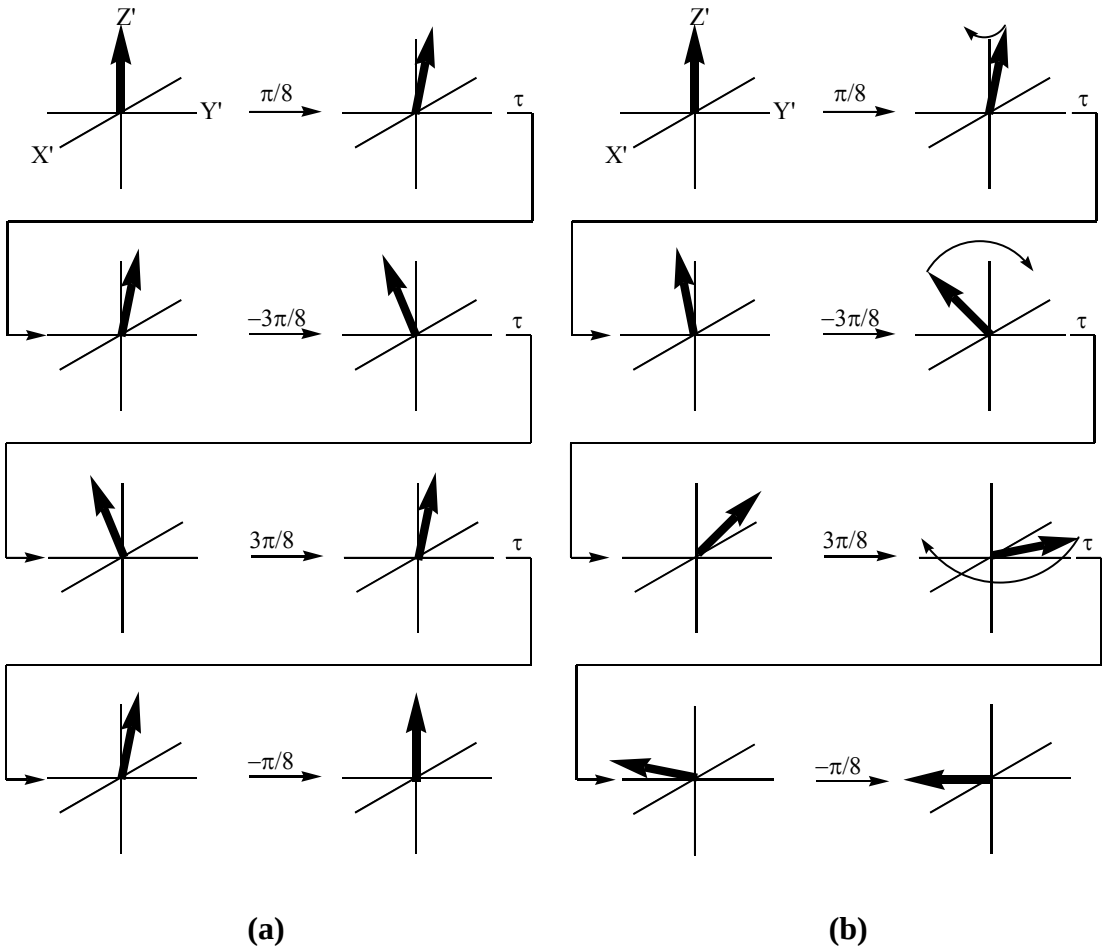

Figure1.10 (a) The effect of a 1331 pulse on the magnetisation for water and (b) for solute protons

where S_n is a frequency domain excitation function, and $\Delta\omega$ is the offset from the transmitter frequency. A broad maximum in the excitation spectrum occurs at offsets near $\pm\frac{1}{2}\tau$ One of the essential features of this sequence is that the null condition (where no excitation is experienced) is relatively broad because of the $\sin^3$ dependence. This however occurs at the expense of narrowing the frequency range for maximum excitation of solute resonance. The broader excitation null of this pulse makes it less sensitive to slight inaccuracies in the placement of the carrier frequency. This enables higher suppression factors, compared to the other binomial pulse sequences, to be achieved. The efficiency of this pulse sequence is not particularly sensitive to imperfection in the radiofrequency field.

The major shortcoming of this technique is a 180^0 phase discontinuity at the transmitter frequency. This produces a rolling baseline in the spectra. This owes its origin to the fact that these pulses were originally devised from a linear approximation system for which the response produced is proportional to the excitation magnitude obtained by FT of the time domain signal. There are however some non-linear effects, which are not taken into account. This approximation produces a pseudo-linear phase correction, which together with residual solvent signal produces a baseline roll. The spectrometer used has a baseline routine (ABS) that minimises this effect. This could provide a major source of variation in chemical shift values as the baseline drift is not exactly replicated in different runs, due to the non-exact placement of the transmitter frequency. The variation in the baseline drift introduces some error into the measured chemical shifts. It is for this reason that chemical shifts far away from the water signal are monitored.

1.13 POTENTIOMETRY

Potentiometry is an electroanalytical technique based on measuring the potential of electrochemical cells in the absence of appreciable current. Since the beginning of the twentieth century, potentiometric techniques have been used for the location of end points in titrimetric methods of analysis. Of more recent origin are methods in which ion concentrations are obtained directly from the potential of an ion selective membrane electrode. Such electrodes are relatively free from interference and provide a rapid and convenient means for quantitative estimates of numerous important anions and cations. The equipment required for potentiometric methods is simple and inexpensive and includes an indicator electrode, a reference electrode and a potential measuring device [129].

An indicator electrode is an electrode that serves as a transducer responding to the excitation signal (if any) and to the composition of the solution being investigated,

but that does not affect an appreciable change of bulk composition within the ordinary duration of a measurement [136]. An ideal indicator electrode responds rapidly and reproducibly to changes in activity of the analyte ion. Although no indicator electrode is absolutely specific in its response, a few are now available that are remarkably selective. There are two types of indicator electrodes: metallic and membrane.

Four types of metallic electrodes can be recognized: electrodes of the first kind, electrodes of the second kind, electrodes of the third kind and redox electrodes. Further information about metallic electrodes can be found in literature [129]. Membrane electrodes, also known as ion-selective electrodes (owing to their high selectivity towards particular ion of interest), fall into one of the following classes: (i) glass membrane for H^+ and certain monovalent cations, (ii) solid-state electrodes based on inorganic salt crystals, (iii) liquid-based electrodes using a hydrophobic polymer membrane saturated with a hydrophobic liquid ion exchanger and (iv) compound electrodes with a species-selective electrode enclosed by a membrane that is able to separate that species from others or that generates the species in a chemical reaction [137].

When compared to many other analytical techniques, Ion-Selective Electrodes (ISEs) are relatively inexpensive and simple to use and have an extremely wide range of applications and wide concentration range. The most recent plastic-bodied all-solid-state or gel-filled models are very robust and durable and ideal for use in either field or laboratory environments. They are invaluable for the continuous monitoring of changes in concentration: e.g. in potentiometric titrations or monitoring the uptake of nutrients, or the consumption of reagents. This makes them ideal for measuring rates of reaction. ISEs can be used in aqueous solutions over a wide temperature range. Crystal membranes can operate in the range 0 °C to 80 °C and plastic membranes from 0 °C to 50 °C [138]. ISEs measure the activity (or effective concentration) of ions in a solution, rather than the actual concentration; the activity is usually less than the concentration because of inter-ionic interactions and the difference between concentration and activity increases as the Ionic Strength increases. In practice, however, the measured activity is not significantly different from the concentration in dilute solutions (i.e. with total Ionic Strength of less than about 0.01 **M** for monovalent ions and 0.001 **M** for divalent ions),

and steps can be taken to minimize the difference at higher concentrations (e.g. by adding Ionic Strength Adjustment Buffer, diluting the sample, or, most effectively, by using Standard Addition or Sample Addition techniques) [138].

The most serious problem limiting use of ion-selective electrodes is interference from other, undesired, ions. No ISEs are completely ion-specific; all are sensitive to other ions having similar physical properties, to an extent which depends on the degree of similarity. Most of these interferences are weak enough to be ignored, but in some cases the electrode may actually be much more sensitive to the interfering ion than to the desired ion, requiring that the interfering ion be present only in relatively very low concentrations, or entirely absent. In practice, the relative sensitivities of each type of ISE to various interfering ions is generally known and should be checked for each case; however the precise degree of interference depends on many factors, preventing precise correction of readings. Instead, the calculation of relative degree of interference from the concentration of interfering ions can only be used as a guide to determine whether the approximate extent of the interference will allow reliable measurements, or whether the experiment will need to be redesigned so as to reduce the effect of interfering ions.

The Cupric ISE used for this study has a solid-state crystal membrane. The crystal membrane is made up of Ag_2S and this makes it responsive to Ag^+ and S^{2-}. However by doping the electrode with CuS, it is possible to prepare an electrode sensitive to Cu^{2+} [137]. The functioning of this material is the result of the response to the Ag^+ activity, which is itself affected by the S^{2-} activity, which in turn depends on the Cu^{2+}activity in the analyte [139].The electrode is designed for the detection of cupric ions (Cu^{2+}) in aqueous solutions and is suitable for use in both field and laboratory applications.

In order to measure the change in potential difference across the ion-selective membrane as the ionic concentration changes, it is necessary to include in the circuit a stable reference voltage which acts as a half-cell from which to measure the relative deviations. The most common and simplest reference system is the silver / silver

chloride single junction reference electrode. This generally consists of a cylindrical glass tube containing a 4 **M** solution of KCl saturated with AgCl. The lower end is sealed with a porous ceramic frit which allows the slow passage of the internal filling solution and forms the liquid junction with the external test solution. Dipping into the filling solution is a silver wire coated with a layer of silver chloride ("chloridised") which is joined to a low-noise cable which connects to the measuring system. In electrochemical terms, the half-cell can be represented by:

$Ag / AgCl_{(Saturatedd)}, KCl_{(Saturated)}$

and the electrode reaction is:

$$AgCl\ (s) + e^- \rightleftharpoons Ag\ (s) + Cl^-$$

The electrode potential for this half-cell is + 0.2046 V relative to the Standard Hydrogen Electrode at 25°C

One problem with reference electrodes is that, in order to ensure a stable voltage, it is necessary to maintain a steady flow of electrolyte through the porous frit. Thus there is a gradual contamination of the test solution with electrolyte ions. This can cause problems when trying to measure low levels of K, Cl, or Ag, or when using other ISEs with which these elements may cause interference problems. In order to overcome this difficulty the double junction reference electrode was developed. In this case the silver / silver chloride cell described above forms the inner element and this is inserted into an outer tube containing a different electrolyte which is then in contact with the outer test solution through a second porous frit. The outer filling solution is said to form a "salt bridge" between the inner reference system and the test solution and is chosen so that it does not contaminate the test solution with any ions which would affect the analysis. Commonly used outer filling solutions are: potassium nitrate - for Br, Cd, Cl, Cu, CN, I, Pb, Hg, Ag, S, SCN; sodium chloride - for K; ammonium sulphate - for NO_3; magnesium sulphate - for NH_4. One disadvantage with double junction reference electrodes is that they introduce an extra interface between two electrolytes and thus give the opportunity for an extra liquid junction potential to develop [138].

In a typical ion analysis, the ISE is immersed in an aqueous solution containing the ions to be measured, together with a separate, external reference electrode. (NB: this external reference can be completely separate or incorporated in the body of the ISE to form a Combination Electrode.) The electrochemical circuit is completed by connecting the electrodes to a sensitive milli-volt meter using special low-noise cables and connectors. A potential difference is developed across the ISE membrane when the target ions diffuse through from the high concentration side to the lower concentration side.

At equilibrium, the membrane potential is mainly dependent on the concentration of the target ion outside the membrane and is described by the Nernst equation

$$E = E^0 + (2.303RT/ nF)\ Log_{10}(a) \qquad \textbf{(1.21)}$$

Where E = the total potential (in mV) developed between the sensing and reference electrodes.E^0 = is a constant which is characteristic of the particular ISE/reference pair. It is the sum of all the liquid junction potentials in the electrochemical cell 2.303 = the conversion factor from natural to base10 logarithm. R = the Gas Constant (8.314 joules/degree/mole). T = the Absolute Temperature. n = the charge on the ion (with sign). F = the Faraday Constant (96,500 coulombs per mole). $Log_{10}(a)$ = the logarithm of the activity of the measured ion. Note that the activity is equivalent to the concentration in dilute solutions but becomes increasingly lower as the ionic strength increases.

Briefly, the measured voltage is proportional to the logarithm of the concentration, and the sensitivity of the electrode is expressed as the electrode Slope - in millivolts per decade of concentration. Thus the electrodes can be calibrated by measuring the voltage in solutions containing, for example, 10 ppm and 100 ppm of the target ion, and the Slope will be the slope of the (straight) calibration line drawn on a graph of mV versus log concentration, i.e.

$$S = [\ E_{100ppm} - E_{10ppm}\ ] / [\log_{10}100 - \log_{10}10] \qquad \textbf{(1.22)}$$

Thus the slope simply equals the difference in the voltages - since log100 - log10 = 1. Unknown samples can then be determined by measuring the voltage and plotting the result on the calibration graph. The exact value of the slope can be used as an indication of the proper functioning of an ISE; the following (in mV) are typical values: Monovalent: Cations +55 ± 5, Anions -55 ± 5. Divalent: Cations +26 ± 3, Anions -26 ± 3 [138].

Since ISE electrodes are ideal for long term monitoring of changes in ion concentration, Cu^{2+}-ISE have been used in this study to monitor the consumption of Cu^{2+} in the presence TM4 to determine the rate of reaction with respect to Cu^{2+}.

1.14 PREVIOUS STUDIES IN OUR GROUP

1.14.1 Mohammed Attaelmannan

Previously in our group [58] speciation of copper-lysine ('chelated' copper) and copper sulphate (inorganic copper) which are used as copper supplement for ruminants, has been successfully studied in McDougall's solution (simulated ruminant saliva) and satisfactorily in rumen fluid.

Mass balance equations were used to describe the distribution of copper(II) amongst different ligands. These equations were encoded into a spreadsheet to calculate all equilibrium species. Formation constants determined were used as input values into the spreadsheet. The results of the distribution of copper(II) ions in McDougall's solution (a simulated form of bovine saliva), indicate no significant differences in the distribution of copper using the different form of supplements. The metal was mainly present as carbonate and phosphate complexes.

^{1}H NMR was used to validate the results from the computer model, using the chemical shift as an indicator of the equilibrium position. Using a combination of the results from the saliva simulation model and the chemical shifts from the NMR studies,

the chemical shift changes that accompanied the addition of copper(II) to McDougall's solution were predicted. Results from the models did not show any appreciable differences from experimental values.

The spreadsheet was expanded to include the low molecular mass ligands in the rumen. Speciation calculation indicated that the bulk of the copper would be bound to ammonia in the rumen. ^{1}H NMR was once again used for validation. Rumen samples were collected. Important peaks in the ^{1}H NMR spectrum were assigned. The spectrum indicated that acetic acid, resulting from the fermentation in the rumen, was a good probe for monitoring the speciation pattern. Studies were conducted to monitor the chemical shifts of the acetate species. Using these together with the model, changes in chemical shifts that result from the introduction of copper (II) to the rumen contents were predicted. Results were compared with experimental values. Agreement between the two sets of results was found to be satisfactory. Some discrepancy was found between the model and predicted values as lysine was introduced into the model. That is at higher concentration of lysine, there was increasing deviation between the predicted and experimental values as shown in Figure 1.11.

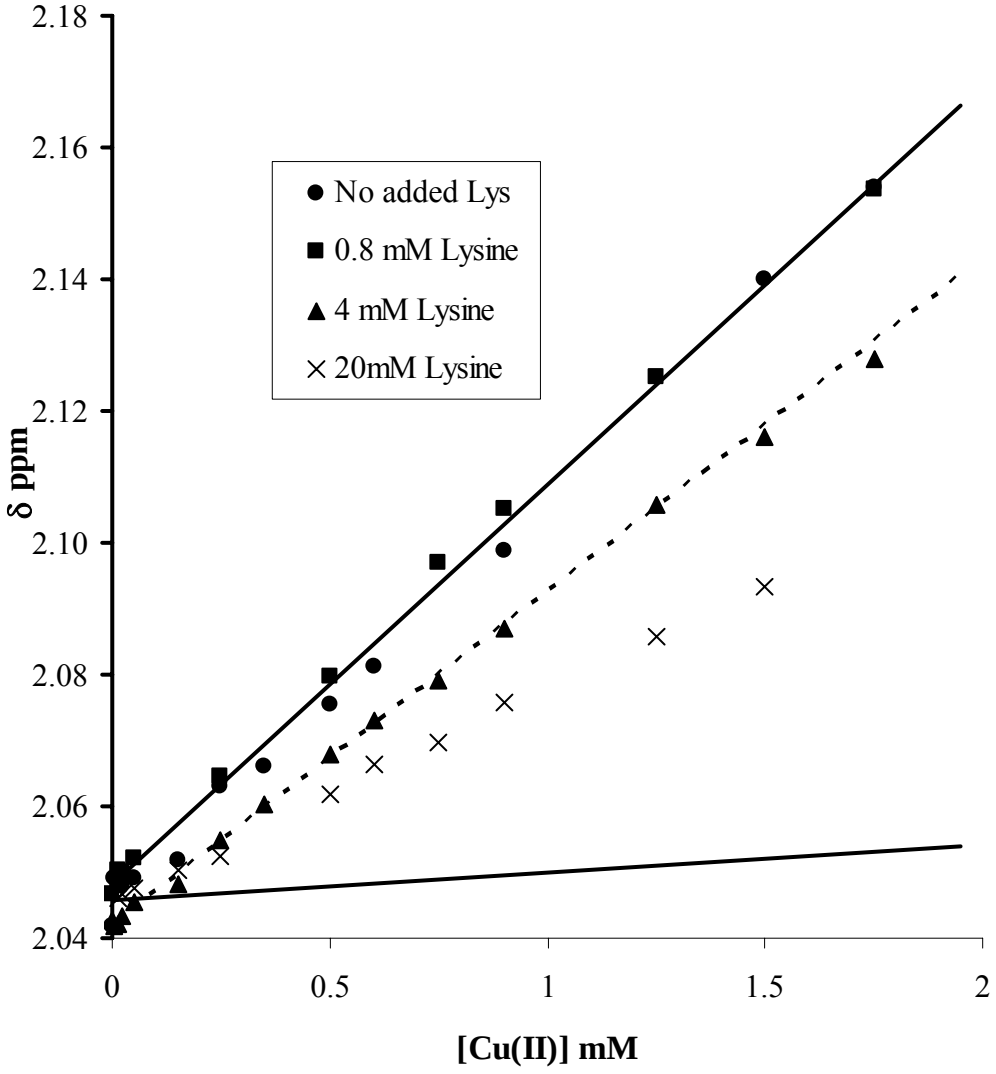

Figure 1.11 Changes in the chemical shift of acetate in rumen liquor with with different amounts of lysine as a function of copper (II) concentrations. Points represent experimental data, while curves represent model predictions [58]

1.14.2 Emmanuel K. Quagraine

Although thiomolybdates formed in the rumen have been implicated in copper deficiency in ruminants, the chemical basis of the interaction between the individual thiomolybdates and both dietary and systemic copper is poorly understood. Also which particular thiomolybdate(s) are formed in the rumen has also been an issue of

contention. Thus a study [102] on the competitive interactions between copper(II) nions, thiomolybdates and some biological ligands was conducted in our group by Emmanuel Quagraine.

In the study, the synthesis of all four TMs was achieved by a single synthetic route using $(NH_4)_2S$ as the sulfide source. TM1 was obtained as the cesium salt, the first time the preparation of this salt in pure form has been reported. Detailed characterization of the the purity of TM products which had been previously lacking was conducted. In the study, the actual amount of TMs in synthesized samples, as well as the expected absorptivities of each pure TM at several wavelengths, were calculated using a computer model based on a non-linear least squares approach to fit the acquired UV/visible spectral data. Also the intensities of ^{95}Mo NMR signals were used to determine the level of cross-contamination of the various TMs, but with lower precision.

Solution chemistry studies was conducted on individual TMs, and their interactions with Cu(II) ions in simple aqueous solutions. These interactions were found to form insoluble products; formation of these was favored by increased ionic strength and reduced pH. The effect of these factors on precipitation was most pronounced for TM4, followed by TM3, TM2, and then TM1. This type of interaction was identified as being kinetically rather than thermodynamically controlled. Both S^{2-} and EDTA compete to some extent with TMs for Cu(II) when they are allowed to react first with the Cu(II) before the TM is added, or when they are added simultaneously with the TMs in solution. However, once Cu(II) reacts with the TMs, neither S^{2-} nor EDTA can strip off the Cu even with a large excess. This is attributed to polymerization of the Cu-TM adduct.

Further experiments were conducted to examine the 3-way interaction between BSA, Cu(II) and TM3. UV/visible spectrophotometric results confirm that this occurs. Ternary complexation occurs for TM3, TM4 and probably TM2. Interestingly, ternary BSA-Cu-TM complex(es) appear soluble in aqueous solution, unlike the Cu-TM complex. To examine the possible involvement of the N-terminal amino acid sequence

in these ternary interactions, some His-containing peptides were synthesized, characterized and used as BSA models to study their acid-base and Cu(II) complexation behavior, and ternary interactions with TMs and Cu(II). It was shown that ternary complexation involving these peptides, Cu(II) and TMs does occur. It was not possible to come to a definitive conclusion with regards to the structure of these ternary complexes, but there was ample evidence to suggest the formation of polymeric species, probably of linear structure for the peptide-Cu-TM4 clusters. The structure and perhaps the strength of the peptide-Cu-TM3 and peptide-Cu-TM2 clusters may be comparable but the TM4 analogue was distinctly different in almost all, if not all the experiments in the study.

1.14.3 Mildred Budu

Copper deficiency has generally been corrected by supplementing diets of ruminants with additional copper. "Chelated" minerals which have been proposed as superior alternatives to inorganic supplements, occurs usually as complexes of amino acids. Although the complexation of copper(II) to amino acids has been extensively studied, the conditions under which the formation constants were obtained are different from what pertains in the rumen. Thus a study [140] was conducted in our group by Mildred Budu to determine the formation constants of with histidine, methionine, lysine and glycine under conditions mimicking rumen conditions. The four amino chosen for the study because these they amino acids are currently being used as copper supplements in bovine diets.

Potentiometric titrations were performed using the gravimetric autotitrator [141] that was previously developed in the group by Min Chen and M. A. Hetherington. The protonation constants for the amino acids; glycine, histidine, methionine and lysine were determined. In addition, formation constants of copper together with these amino acids were at physiological temperature of 38°C in ionic strength of 0.15 **M** KCl. The experimental pH-titration data were analyzed using the HYPERQUAD suite of programs to evaluate the formation constants and species distribution of the individual

ligands with copper. Results generally showed good agreement with literature values, where these were available.

Mixed-ligand complexes of copper(II) with histidine and methionine or lysine were also studied using ^{1}H NMR. The mixed-ligand complexes of copper(II) with histidine and methionine or lysine were chosen for he study. Non-linear expressions made up of ^{1}H NMR chemical shifts and formation constants derived from potentiometry were solved to find the formation constants of the mixed-ligand species. The copper(II)-histidine-methionine case has been previously studied; however, the results of the study in our group were significantly more precise. The copper(II)-histidine-lysine system has not been previously characterized. In both cases the stability of the mixed species were found to be greater than those of their parent complexes. Possible reasons for this are discussed.

The study suggested that, as copper traverses the digestive system, where many potential ligands (such as histidine, methionine and lysine) are likely to compete for metal ions *in vivo*, copper(II) mixed-ligand complexes should be included if a complete picture of the speciation in these systems is desired.

2. EXPERIMENTAL

2.1 COMPUTER MODELING OF SPECIATION

2.1.1 Rumen Model

The rumen fluid model included the major end products of rumen metabolism as potential copper ligands. These are mostly the short chain volatile fatty acids, acetic, propanoic and butanoic, together with ammonia as well as the bicarbonate and phosphate moieties from the saliva. It is difficult to determine exact figures for concentration of the ligands in the rumen, as these are highly dependent on the diet fed to the ruminant. Nevertheless, average values can be assigned after comparison with literature values [59-61, 142, 143] under typical conditions. Table 2.1 shows the analytical concentrations of the ligands used in the present studies.

Table 2.2 shows the set of formation constants used in the rumen model. In setting up the model use was made of complex formation constants measured previously in the group, or selected carefully from the literature. Where literature constants were obtained at different temperatures form what pertains in the rumen, the IUPAC program, Aqueous Solutions was used to correct them as discussed in Section 1.3.

The concentration of copper used for the rumen model was 3.5×10^{-5} **M**, a modest value for the nutritional requirements of a healthy cow [67, 144]. The concentrations of the VFAs were varied in different studies. These are known to vary substantially depending on the diet fed to the ruminant. For instance, diets high in

Table 2.1 Values of ligand concentrations used in rumen model

Ligand	**Concentration** (m**M**)
Acetate	84
Propionate	21
Butyrate	13
i-Butyrate	1
Valerate	0.7
i-Valerate	0.3
Phosphate	20
Carbonate (in all forms)	21
Ammonia (in all forms)	11

concentrates tend to produce fluids that are high in acetic acid but low in propanoic acid, whereas forage diets are known to increase the level of propanoic acid.

Using the concentration of the constituents of rumen fluid in Table 2.1 and the formation constants of the different complexes (Table 2.2) as input values, a computer simulation was performed to determine the distribution of copper with respect to low molecular mass ligands in the rumen fluid. The computer simulation calculations were performed using Microsoft Excel® (Microsoft Corp., WA, USA) spreadsheet program, a powerful numerical analysis package on IBM compatible PC 1.5 GHz (Intel Pentium IV) Gateway microcomputer.

Calculations were performed at average ruminal pH of 6.3 and then from a pH of 5.8 to 6.8, to ensure that the simulation covers normal range of ruminal pH. Also VFA levels are known to vary substantially depending on the diet fed to the ruminant. For instance, diets high in concentrates tend to produce fluids that are high in acetic acid but

Table 2.2 Formation constant (log $\beta = [M_pL_qH_r]/[M]^p[L]^q[H]^r$) data used in rumen simulations [34, 145].

System	p	q	r	log β
Acetic Acid	0	1	1	4.56
Copper Acetate	1	1	0	1.81
	1	2	0	2.83
	1	3	0	3.17
	1	4	0	3.23
Propanoic Acid	0	1	1	4.68
Copper Propanoate	1	1	0	1.70
	1	2	0	2.62
Butanoic Acid	0	1	1	4.62
Copper Butanoate	1	1	0	1.75
	1	2	0	2.70
iso-Butanoic Acid	0	1	1	4.62
Copper iso-Butanoate	1	1	0	1.75
(estimate)	1	2	0	2.70
Valeric Acid	0	1	1	4.62
Copper Valerate	1	1	0	1.75
(estimate)	1	2	0	2.70
Phosphoric Acid	0	1	1	11.40
	0	1	2	18.04
	0	1	3	19.99
Copper Phosphate	1	1	1	3.3
	1	1	2	1.3
Carbonic Acid	0	1	1	9.83
	0	1	2	15.41
Copper Carbonate	1	1	0	6.75
	1	2	0	9.92
	1	1	1	1.3
Ammonia	0	1	1	9.24
Copper Ammonia	1	1	0	4.12
	1	2	0	7.63
	1	3	0	10.51
	1	4	0	12.60

low in propanoic acid, whereas forage diets are known to increase the level of propanoic acid [59]. Speciation calculations were therefore performed under varying concentrations of VFAs.

2.1.2 Cu(II) Supplements in (McDougall's Solution) Bovine Saliva Model

The most prevalent route for administering mineral supplements is the oral one, i.e. in the animal's diet. Saliva is the first fluid that the metal encounters once admitted into the digestive system of the animal. Once ingested, the mineral is transformed into a variety of forms. The relative amounts of these constitute the speciation.

Thus using the concentration of the low molecular mass constituents of McDougall's solution (Table 2.3) and the formation constant of the different complexes (Table 2.4) as input values, a simulation was done to determine the distribution of copper glycine, copper methionine, copper histidine and copper EDTA in McDougall's solution. The formation constants of the copper amino acid complexes (Tables 2.5 and 2.6) were obtained from previous study in our group [58, 140]. The concentration of copper used for the model is 3×10^{-5} **M**, a modest value for the nutritional requirements of a healthy cow [144].

Table 2.3 The composition of McDougall's Solution [146]

Constituent	**Concentration (M)**
$NaHCO_3$	1.67×10^{-1}
Na_2HPO_4	2.61×10^{-2}
KCl	8.04×10^{-3}
NaCl	8.56×10^{-3}
$MgSO_4$	4.06×10^{-4}
$CaCl_2$	3.60×10^{-4}

Table 2.4 Formation constant (log $\beta = [M_pL_qH_r]/[M]^p[L]^q[H]^r$) data used in the saliva simulation studies [34, 145].

System	p	q	r	log β
Phosphoric Acid				
	0	1	1	11.40
	0	1	2	18.04
	0	1	3	19.99
Copper Phosphate				
	1	1	0	3.3
	1	1	1	1.3
Carbonic Acid				
	0	1	1	9.83
	0	1	2	15.41
Copper Carbonate				
	1	1	0	6.75
	1	1	1	1.3
	1	2	0	9.92
Copper Chloride				
	1	1	1	-0.3
Hydrogen Sulfate				
	0	1	1	1.99
Copper Sulfate				
	1	1	1	2.27

Table 2.5 Dissociation Constants of amino acids as obtained at 38 ^{0}C and I = 0.15 **M** (KCl), used in the computer simulation studies [58, 140, 145]

The Glycine System		The Methionine System	
pKa_1	2.450(2)	pKa_1	2.42(2)
pKa_2	9.32(1)	pKa_2	8.98(1)
The Histidine System		The EDTA System	
pKa_1	1.90(1)	pKa_1	1.6
pKa_2	5.86(1)	pKa_2	2.05(5)
pKa_3	8.73(2)	pKa_3	2.79
		pKa_4	6.03(5)
The Lysine System		pKa_5	10.02(7)
pKa_1	2.23(2)		
pKa_2	8.92(2)		
pKa_3	10.48(2)		

2.1.3 Cu(II) Supplements in Bovine Rumen Model

Computer simulations were also conducted as described in Section 2.1.1. However, this time copper was introduced into the rumen model as copper glycine, copper methionine and copper histidine as well as copper peptide complexes. The formation constants of the copper peptide complexes (Table 2.7) were obtained from a previous study in our lab at 25 °C and 0.2 M ionic strength [2] and were thus corrected to the temperature and ionic strength of the rumen using IUPAC Aqueous solutions software (see Section 1.3).

Table 2.6 Stability constants log $\beta_{pqr} = [M_pL_qH_r]/[M]^p[L]^q[H]^r$ as obtained at 38^0C and I = 0.15 **M** (KCl), used in computer simulation studies [58, 140, 145].

p	**q**	**r**	**logβ_{pqr}**
The Copper (II) Glycine System			
1	1	0	8.17(3)
1	2	0	14.12(4)
1	2	-1	3.5(1)
1	1	1	11.78(4)
1	2	1	18.89(8)
The Copper (II) Histidine System			
1	1	0	9.88(1)
1	2	0	18.80(2)
1	1	1	13.93(8)
1	2	1	24.00(2)
1	2	2	27.49(6)
1	2	-1	11.85(3)
The Copper (II) Lysine System			
1	1	0	10.72(8)
1	1	1	18.01(2)
1	2	2	34.69(2)
1	2	1	25.39(7)
1	1	2	21.81(8)
1	2	0	15.30(5)
1	1	-1	.8(1)
The Copper (II) Methionine System			
1	1	0	7.66
1	2	0	14.60
The Copper (II) EDTA System			
1	1	0	18.53(8)
1	1	1	21.38
1	1	2	23.13

Table 2.7 Formation constants log $\beta_{pqr} = [M_pL_qH_r]/[M]^p[L]^q[H]^r$ of copper (II) peptides used in computer simulation studies [102].

p	q	r	logβ_{pqr}	p	q	r	logβ_{pqr}
The Cu(II)-(His-Lys) system				**The Cu(II)-(Asp-Thr(Ac)-His-Lys) system**			
1	1	1	21.55	1	1	2	35.56
1	1	0	18.52	1	1	1	31.71
1	1	-1	12.86	1	1	0	25.58
1	1	-2	3.05	1	1	-1	20.75
1	1	-3	-7.37	1	1	-2	12.73
1	2	2	41.69	1	1	-3	2.46
1	2	1	34.83	0	1	1	10.48
1	2	0	26.18	0	1	2	20.01
2	2	0	42.97	0	1	3	26.74
2	2	-1	27.64	0	1	4	32.26
2	2	-2	19.44	0	1	5	34.31
0	1	1	10.37				
0	1	2	17.67				
0	1	3	22.96				
0	1	4	25.01				
The Cu(II)-(Thr(Ac)-His-Lys) system							
1	1	1	18.54				
1	1	0	8.90				
1	1	-1	-2.42				
1	2	3	41.54				
1	2	2	32.26				
1	2	1	21.89				
1	2	0	12.24				
0	1	1	10.25				
0	1	2	17.26				
0	1	3	22.88				
0	1	4	24.93				

2.2 NMR STUDIES OF RUMEN FLUID

2.2.1 Simulated Rumen Fluid

2.2.1.1 Chemicals, Materials, Reagents

All reagents used were of analytical grade and were used as purchased without any further modifications. Ammonia solution and sodium hydrogen carbonate were obtained from British Drug House (BDH) Chemicals, Toronto; acetic acid Potassium Chloride from EM Science (Affiliate of MERCK); propanoic acid from Fischer Scientific Company, Fair Lawn, NJ, U.S.A.; butanoic acid from Aldrich Chemical Company, Milwaukee, WI, U.S.A.; sodium hydrogen phosphate and L-lysine from Sigma - Aldrich company, St Louis, MO, U.S.A.; and copper (II) chloride from Allied Chemicals, NY, U.S.A. Sodium 2,2-imethyl-2-silapentane-5-sulfonate (DSS) was obtained from Merck Sharp & Dohme (Montreal, Canada).

2.2.1.2 Preparation of Stock solutions

1.0 M stock solutions of acetic, propanoic and butanoic acids as well as sodium hydrogen carbonate and sodium hydrogen phosphate were prepared using ultrapure water obtained from Millpore® Milli-Q gradient A10 system. Similarly 0.01 M copper(II) chloride, 0.1 M lysine solution and 0.3 M potassium chloride stock solutions were prepared using ultrapure water.

2.2.1.3 Preparation of solutions for NMR experiment

Solution mixtures containing concentrations of ligands used in the computer model of the rumen and various copper (II) concentrations were prepared in 100 ml volumetric flasks. The ionic strength were adjusted to 0.15 M using various concentrations of potassium chloride.

10 ml aliquots of the prepared solutions were put into labelled vials and the pH of each solution was adjusted to a pH of 4.00 (± 0.01) using 0.1M $HCl_{(aq)}$.

0.4 ml of each of the solution (with pH adjusted) was put into labelled NMR tubes and 0.05 ml of Dimethyl-2- silapentane-5-sulfonate (D.S.S.) (50%) was added to each tube as an internal standard.

A ^{1}H NMR experiment was conducted to obtain the chemical shift of the methyl proton of acetate on each solution using the bionnomial 1331 pulse sequence technique for water suppression on a Bruker Avance 500 spectrometer at a frequency of 500.13 MHz. All chemical shifts are quoted in ppm versus DSS.

2.2.1.4 pH Measurements

All pH measurements were made with an Accu-pHast standard combination glass body pH electrode (Fisher Catalogue No. 13-60-297) and an Accumet pH meter. The electrode was calibrated by standard U.S. National Institute of Standards and Technology (N.I.S.T.) approved methods, using a set of primary standard solutions whose pH values have been accurately established by the N.I.S.T (formerly known as the National Bureau of Standards) [147]. The primary standard solutions are not stable and were thus used to standardise a set of standard commercial buffers, which are more stable. These standardised buffers were used for routine calibration.

2.2.2 Actual Rumen fluid

2.2.2.1 Rumen Fluid Samples

Fresh rumen fluid samples were obtained from a non-lactating Holstein cow fitted with a flexible rumen fistula. A fistula is one of a number of surgical techniques

that have allowed the collection of rumen content for analysis. It is constructed with an opening in the left side beside the ribs and below the lumbar area. The opening is made through the skin, fascia, muscles and peritoneum and the rumen is sutured to the opening, with the result that adhesions form between the body wall and the rumen wall. With a properly done job, and a plug of good fit, the animals gets by with no apparent discomfort, little or any soreness and only slight amount of leakage.

For the collection of the sample, the plug was removed from the fistulated cow and a glass container was inserted into the rumen (Figure 2.2). The rumen samples were immediately strained through eight layers of cheesecloth (Figure 2.3), to filter the large particles resulting from digestion, then transported to the laboratory in a vacuum flask. The fluid was centrifuged at 10,000g for 1 hr to remove some of the larger biota and colloidal particles. The resulting fluid was then ultracentrifuged at 35,000 g for a further 1 hr to eliminate the finer colloidal particles. Ultracentrifugation was performed with a Beckmann L8-55 Ultracentrifuge at 4^0C.

The resulting fluid was ultrafiltered using an Amicon 8050 Ultrafiltration cell. The Amicon Ultrafiltration cell is a standard commercially available cell. It consists of a pressure inlet valve, a solution compartment, a magnetic stirrer, a membrane support, a retaining stand and a filtrate outlet. This cell has the advantage that it can be used with a variety of membranes of different molecular weight ranges. Once all the components are assembled, the cell can then be slid into the retaining stand. Finally, pressure inlet is attached to the cap. When the cell is pressurized, the cap assembly moves up by itself forming a secure lock with retaining stand. The whole unit is placed on top of a magnetic stirrer. The stirring and flow rates can be varied depending on the viscosity of the solution being filtered. For highly viscous fluids, it is sometimes necessary to increase the stirring, as resistance is high. It is necessary to maintain continuous stirring, and the rate might require altering from time to time. For maximum recovery stirring should be continued a few hours after depressuring.

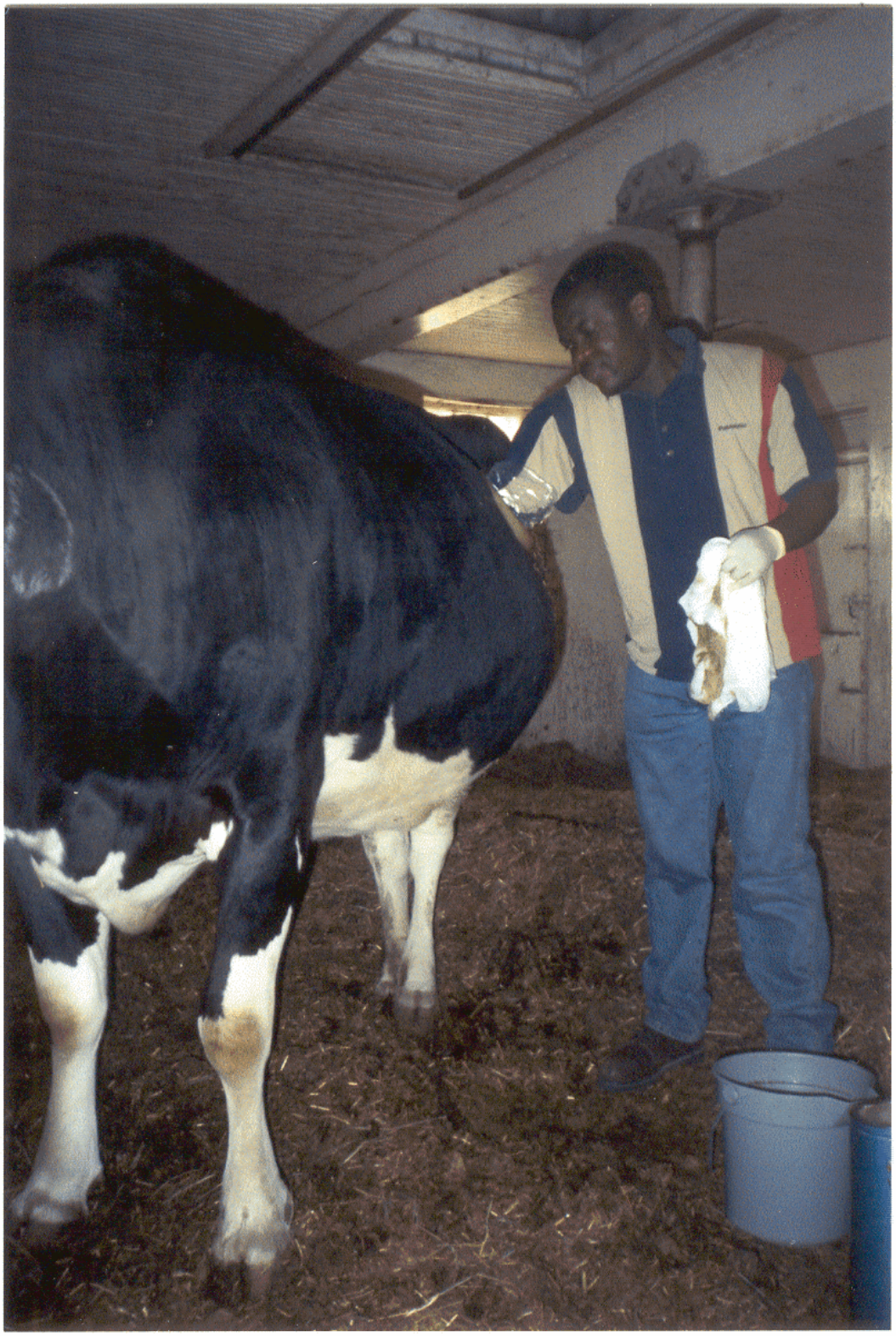

Figure 2.1 Picture of a cow with a rumen fistula

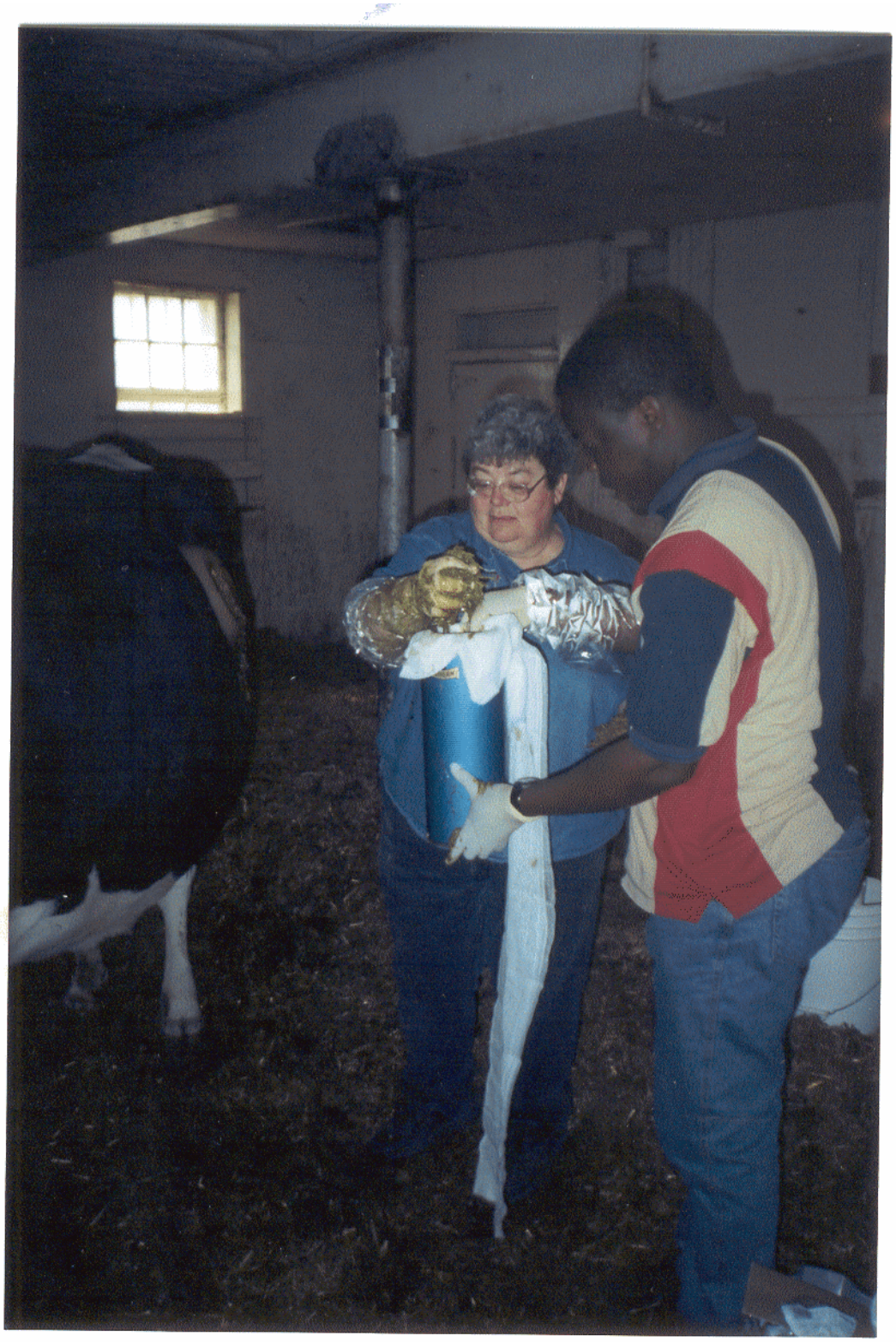

Figure 2.2 Screening of rumen content using cheesecloth

The rumen fluid was first passed through a 0.4 μm filter, then further filtered by successively passing through an Amicon UM10 membrane (Amicon Inc., MA, U. S. A., molecular mass exclusion limit ~10,000) then through an Amicon YC50 membrane (molecular mass exclusion limit ~500). All ultrafiltrations were performed under 55 psi of argon gas at room temperature. Samples for NMR studies were further treated as detailed below.

2.2.2.2 Copper(II) -Rumen Sample NMR Studies

A stock solution containing 0.01 **M** $CuCl_2$ was prepared, with the rumen liquor serving as a solvent. A solution containing DSS was also prepared with the rumen liquor as solvent. Different amounts of the $CuCl_2$ stock solution were added to the rumen sample and the pH adjusted using NaOH and HCl. The concentration of copper(II) was limited by the onset of precipitation of CuS and Cu_2S. It should be noted that copper(II) sulfide is readily precipitated from aqueous Cu(II) solutions in the presence of hydrogen sulfide (being one of the gases produced in the rumen). A stock solution of 0.1 **M** lysine solution was prepared, again using the rumen liquor as solvent. Likewise 0.1 M stock solutions of glycine, methionine and histidine were prepared using rumen liquor as solvent. Finally a solution containing DSS was also prepared with the rumen liquor as solvent.

All solutions for NMR analysis were prepared with the exclusion of oxygen. (Oxygen is paramagnetic and could therefore affect NMR spectral behaviour [134]. In addition, excluding oxygen minimizes the possibility of oxidative breakdown of biological samples.) Solutions were stirred under a slow stream of argon gas. The headspace in each NMR tube was also flushed with a stream of argon gas after the tube was filled. Samples were also filtered through glass wool containing a small magnetic stirrer, to eliminate any particulate paramagnetic impurities.

2.2.2.3 NMR Instrumental Parameters

NMR measurements were performed on a Bruker Avance 500 spectrometer at a frequency of 500.13 MHz. All spectra were acquired using the binomial composite '1-3-3-1' sequence for water suppression (see Section 1.12.5) [135, 148]. The pulse sequence was used to suppress the intense water signal. The offset frequency was set to that of the water resonance. DSS was added to samples as a chemical shift reference. All chemical shifts are quoted in ppm versus DSS (see Section 1.12.4).

2.3 COMPUTER MODELING OF TM FORMATION

Since the chemical reaction mechanism of thiomolybdates (TMs) (see Section 1.10.2) involves reversible unimolecular reactions (i.e. involves elementary steps where one TM species is transformed to another reversibly), the series of rate expressions for each chemical species in the scheme, were represented by a set of linear ordinary differential equations (ODE's) as shown below. However to be able simulate the formation of the TMs with respect to time, the differential equations were solved to obtain an analytical solution using the Laplace transform method.

$$\mathrm{TM0} \underset{k_{10}}{\overset{k_{01}}{\rightleftharpoons}} \mathrm{TM1} \underset{k_{21}}{\overset{k_{12}}{\rightleftharpoons}} \mathrm{TM2} \underset{k_{32}}{\overset{k_{23}}{\rightleftharpoons}} \mathrm{TM3} \underset{k_{43}}{\overset{k_{34}}{\rightleftharpoons}} \mathrm{TM4}$$

$$\begin{aligned}
\frac{d[TM0]}{dt} &= -k_{01}[TM0] + k_{10}[TM1] \\
\frac{d[TM1]}{dt} &= k_{01}[TM0] - (k_{10} + k_{12})[TM1] \\
\frac{d[TM2]}{dt} &= k_{12}[TM1] - (k_{21} + k_{23})[TM2] \\
\frac{d[TM3]}{dt} &= k_{23}[TM2] - (k_{32} + k_{34})[TM3] \\
\frac{d[TM4]}{dt} &= k_{34}[TM3] - k_{43}[TM4]
\end{aligned} \qquad \textbf{(2.1)}$$

The Laplace transform method is a widely established technique for solving simultaneous ordinary linear differential equations. It is a powerful method owing to its generality and straightforward implementation. The basic idea of the method is to substitute the difficult task of solving simultaneous ordinary differential equations (functions of *t*) that describe the rate expressions for each chemical species in a reaction scheme by transforming them into a set of simple polynomial equations (functions of *s*) [149].

Thus initial conditions were applied to the above ODEs (Equation 2.1) and the equations solved to obtain Laplace transform functions corresponding to each chemical species (functions of *s*). Once these were determined, the desired time-dependent function for a given chemical species was found by obtaining the corresponding inverse Laplace transform function (a function of *t*). This was done by simply looking up Laplace transform pairs in extensively compiled tables (see Appendix A.2).

The analytical solutions obtained from the Laplace transform of the ODE representing the rate expressions for each TM species were encoded in Microsoft Excel® spreadsheet and calculated as function of time to obtain time – dependent concentrations of TM. The calculations were done over a three hour period and the values of the rate constants used are as summarized in Table 2.8. The calculation was performed using an IBM compatible PC 1.5 GHz (Intel Pentium IV) Gateway microcomputer.

Table 2.8 Rate constants used in the computer simulation of TM formation [99-101, 150]. See Equation 2.1 for definitions of rate constants.

Rate Constant	Value/s^{-1}
k_{10}	2.0×10^{-2}
k_{01}	2.0×10^{-5}
k_{12}	1.5×10^{-2}
k_{21}	2.0×10^{-5}
k_{23}	6.0×10^{-4}
k_{32}	1.0×10^{-5}
k_{34}	3.5×10^{-5}
k_{43}	5.3×10^{-9}

2.4 POTENTIOMETRIC STUDY OF Cu(II)-TM4 INTERACTIONS USING Cu(II)-ISE

2.4.1 Synthesis of TM4

1.0 g (4.13 mmol) of sodium molybdate dihydrate (BDH Inc.,Toronto) was dissolved in 2 ml of water. 15 ml of ammonium sulfide solution (Sigma Aldrich) was added to the solution, which was stoppered and shaken.. The reaction mixture was then left to stand at room temperature. An orange solution formed and quickly turned red. Red crystals of ammonium tetrathiomolybdate ($(NH_4)_2MoS_4$) formed after less than 45 minutes. To ensure completeness of the reaction, it was left for approximately 3 hours. About 10 ml of cold 1:1 ethanol/ether mixture was added to the solution and kept in an ice-bath for about 30 minutes to increase the yield to 0.7452 g i.e., approximately 69.3 % yield. The crystals were filtered and washed initially with about 10 – 15 ml of cold water. The crystals obtained were dried in vacuo, kept under Ar gas, sealed and stored in the refrigerator [102].

2.4.2 UV/Visible Spectral Analysis

0.1 mM aqueous solution of TM4 was prepared using Millipore water. The UV/visible spectrum of the solution was then taken between 240 and 510 nm. Computer analysis was conducted on the data obtained to determine the percentage purity of the TM4.

2.4.3 Calibration of Copper (II) Ion-Selective Electrode (ISE)

A solid state crystal membrane copper(II) ion-selective electrode obtained from NICO2000, Harrow, Middlesex, U.K. was conditioned in 1000 ppm (0.016 M) $CuSO_4$(aq) solution at 25 ºC for 5 minutes and then calibrated with a series of Cu^{2+}(aq) solutions ranging 0.001 mM to 2.0 mM at 25 ºC. The calibration was repeated at the temperatures of 30 ºC 34 ºC and 38 ºC. The reference electrode used was an Orion double junction Ag/AgCl reference electrode.

2.4.4 Kinetic Study of Cu(II) – TM4 interaction using Cu(II) ISE in unbuffered solutions

0.5 mM $CuSO_4$ and TM4 were prepared respectively using Millipore water. 20 ml of the $CuSO_4$ (aq) solution was introduced into a 100 ml beaker and 20 ml of the Millipore water was added to it. The resulting solution in the beaker was placed in a water bath, set at a temperature of 25 °C. The Cu(II) ISE and the reference electrode were then introduced into the solution and the potential reading taken. 10 ml of the TM4 solution was then introduced into the solution and the concentration of Cu^{2+} monitored over a 3 hour period.

2.4.5 Kinetic Study of Cu(II) – TM4 interaction using Cu(II) ISE in buffered solutions

0.1 M 3(N – morpholino)propanesulfonic acid (MOPS) buffers at pH 4.0, 4.5 and 5.0 were prepared. The buffer solutions were then used to prepare 0.5 mM $CuSO_4$ and TM4 solutions and in effect used as media for the reaction between Cu^{2+} and TM4.

The experiments were conducted as described above (for the unbuffered solution) at a temperature of 25 °C and at a buffer pH of 4.0, 4.5 and 5.0. Experiments were then repeated at temperature of 30 °C, 34°C and 38 °C.

2.5 Cu(II) IN TM-CONTAMINATED RUMEN

The computer simulation of the formation of TMs was extended to include the formation of Cu – TM4 complex according to the scheme below.

$$TM0 \underset{k_{01}}{\overset{k_{10}}{\rightleftharpoons}} TM1 \underset{k_{21}}{\overset{k_{12}}{\rightleftharpoons}} TM2 \underset{k_{32}}{\overset{k_{23}}{\rightleftharpoons}} TM3 \underset{k_{43}}{\overset{k_{34}}{\rightleftharpoons}} TM4 + Cu^{2+} \xrightarrow{k_{45}} CuTM4$$

The rate expressions for each chemical species in the scheme, were similarly represented by a set of linear ordinary differential equations (ODE's) as shown in Equation 2.9. Analytical solutions subsequently obtained using both the Laplace transforms and the integration method were encoded Microsoft Excel® spreadsheet and the time-dependent concentrations of TMs were then calculated. The TM4 produced at each time was then reacted with Cu^{2+} available.

$$\begin{aligned}
\frac{d[TM0]}{dt} &= -k_{01}[TM0] + k_{10}[TM1] \\
\frac{d[TM1]}{dt} &= k_{01}[TM0] - (k_{10} + k_{12})[TM1] \\
\frac{d[TM2]}{dt} &= k_{12}[TM1] - (k_{21} + k_{23})[TM2] \\
\frac{d[TM3]}{dt} &= k_{23}[TM2] - (k_{32} + k_{34})[TM3] \\
\frac{d[TM4]}{dt} &= k_{34}[TM3] - (k_{43} + k_{45})[TM4] \\
\frac{d[CuTM4]}{dt} &= k_{45}[CuTM4]
\end{aligned} \qquad \textbf{(2.2)}$$

To integrate the Cu/TM kinetics with the thermodynamic speciation model, two spreadsheets were developed; one for the Cu/TM kinetics and the other for the thermodynamic speciation model. Cu/TM kinetics spreadsheet was run for fixed time increments of one minute and then the equilibrium model spreadsheet run after each increment and the process repeated. This was done for about 107 minutes (mean residence time of S^{2-} in the rumen).

3. RESULTS AND DISCUSSION

3.1 MODELING OF COPPER(II) SPECIATION IN BOVINE SALIVA AND RUMEN

3.1.1 Development of a Computer Speciation Model

In developing a computer speciation model, the chemical problem is put in an algebraic form using the law of mass action. The mathematical model is chosen on the basis of the known chemistry of the system, using a series of equations to define the system. These equations are then used to generate numerical values for concentrations of the species formed, which are consistent with the known (or assumed) values of the relevant formation constants. At the same time, the sum of each entity (metal or ligand) should also add up to the known total concentration for that entity in all forms.

The general procedure for the calculations will be illustrated using some simple systems as an example. First, consider a system consisting initially only of carbonate species at a specified pH and overall concentration. The relevant reactions can be described in terms of these equations:

$$H_2CO_3 \rightleftharpoons HCO_3^- + H^+$$

$$HCO_3^- \rightleftharpoons CO_3^{2-} + H^+$$

In this system there are four species existing simultaneously in solution, CO_3^{2-}, HCO_3^-, H_2CO_3 and H^+. $[H^+]$ is of course fixed by the pH; the challenge is to find the concentrations of the other three species. The chemistry of carbonic acid can be

described by its dissociation constants: (For the sake of clarity charges have been deliberately omitted)

$$K_{a1} = [HCO_3].[H] / [H_2CO_3]$$
$$K_{a2} = [CO_3].[H] / [HCO_3] \quad \textbf{(3.1)}$$

In solution the sum of the concentrations of individual species will give the total concentration of that species. For the carbonate species in solutions, the total concentration will be given by:

$$\text{Total Carbonate Concentration} = [CO_3] + [HCO_3] + [H_2CO_3] \quad \textbf{(3.2)}$$

$[CO_3]$ and $[H_2CO_3]$ can each be defined in terms of $[HCO_3]$.

$$[H_2CO_3] = [HCO_3].[H] / K_{a1}$$
$$[CO_3] = K_{a2}. [HCO_3]/ [H] \quad \textbf{(3.3)}$$

Substitution into Equation 3.2 then gives an equation with only one unknown. The K_a values are known constants and the $[H^+]$ is fixed by the pH value. A similar analytical solution can be employed to solve for the acid-base forms of any entity. However this approach fails in more complex systems, and numerical approaches are required.

These equations are coded into a Microsoft Excel® spreadsheet, a powerful numerical analysis package. The calculation was performed using an IBM compatible PC 1.5 GHz (Intel Pentium IV) Gateway microcomputer. Spreadsheets are simple yet powerful tools that can be used in manipulating mathematical operations. Arithmetic functions and operations are easily written into the spreadsheet. One of the advantages of using a spreadsheet is that one can see the value at each iteration. Observing progress towards convergence makes the method more understandable, and often reveals some of

the subtleties involved. The spreadsheet utilises a set of input data that includes the total concentration of all the reagents and the relevant formation constants as well as the pH.

When copper(II) ions are introduced into the system, two copper carbonate complexes in addition to free copper are added. The system now contains seven species: CO_3^{2-}, HCO_3^-, H_2CO_3, H^+, Cu^{2+}, $CuCO_3$ and $[Cu(CO_3)_2]^{2-}$. The reactions for the formation of the copper species are

$$Cu^{2+} + CO_3^{2-} \rightleftharpoons CuCO_3$$

$$CuCO_3 + CO_3^{2-} \rightleftharpoons [Cu(CO_3)_2]^{2-}$$

The formation constant expressions for the copper complexes are given by:

$$K_{f1} = [CuCO_3]/[CO_3].[Cu]$$
$$K_{f2} = [Cu(CO_3)_2]/[CuCO_3].[CO_3] \quad \textbf{(3.4)}$$

Mass balance equations can be set up to calculate the total concentration of carbonate species and total concentration of copper species. The mass balance equation for the total copper concentration in the system is

$$\text{Total Copper concentration} = [Cu] + [CuCO_3] + [Cu(CO_3)_2] \quad \textbf{(3.5)}$$

It is necessary to take into consideration the stoichiometric coefficients of the complexes formed; there are 2 carbonate species in each $Cu(CO_3)_2$ complex formed. Accordingly, the new expression for total carbonate in the system is given by:

$$\text{Total Carbonate Conc.} = [CO_3] + [HCO_3] + [H_2CO_3] + [CuCO_3] + 2[Cu(CO_3)_2] \quad \textbf{(3.6)}$$

All the species in this system can be defined in terms of free copper and HCO_3;

$$[H_2CO_3] = [HCO_3].[H]/ K_{a1}$$

$$[CO_3] = [HCO_3].K_{a2}/[H]$$
$$[CuCO_3] = K_{f1}.[Cu].[CO_3]$$
$$[Cu(CO_3)_2] = K_{f1}.K_{f2}.[Cu].[CO_3]^2 \quad \textbf{(3.7)}$$

It is clear that the mass balance equations are no longer linear expressions as the expression for $[Cu(CO_3)_2]$ has resulted in squaring the concentration of the free carbonate $[CO_3]^2$. Solving for these non-linear expressions is not a simple one step approach; an iterative numerical procedure must be found.

The general algorithm used in the numerical procedure involves the assumption of equilibrium concentrations of some input "seed" species, calculation of all other species formed, summation of all species (see Equations 3.5 and 3.6) and comparison with original total concentrations. This is to help in checking how far off the total concentration of species based on that “seed” is from the actual value so as to obtain correction parameter and systematically (iteratively) refine the input concentrations of “seed” species.

Thus the iteration procedure commences with an initial estimate of the concentration of free copper ions and subsequently that of the free carbonate concentration. The concentration of ionic copper is assumed to be one of the lowest components, and hence is ideal for starting the calculation. All other species involved in this equilibrium are defined in terms of free copper and free carbonate. Successive calculations are done in alternate columns using the appropriate equations (see Figure 3.1 for a typical speciation calculation spreadsheet).

A key feature in the algorithm is the definition of all the species in terms of multiplication and division. No addition or subtraction is involved as this helps decrease the size of the round-off. The round-off errors are because a computer stores numbers with a fixed number of digits. When two numbers, nearly equal in value, are subtracted, the difference can be quite small and the result may be insignificant.

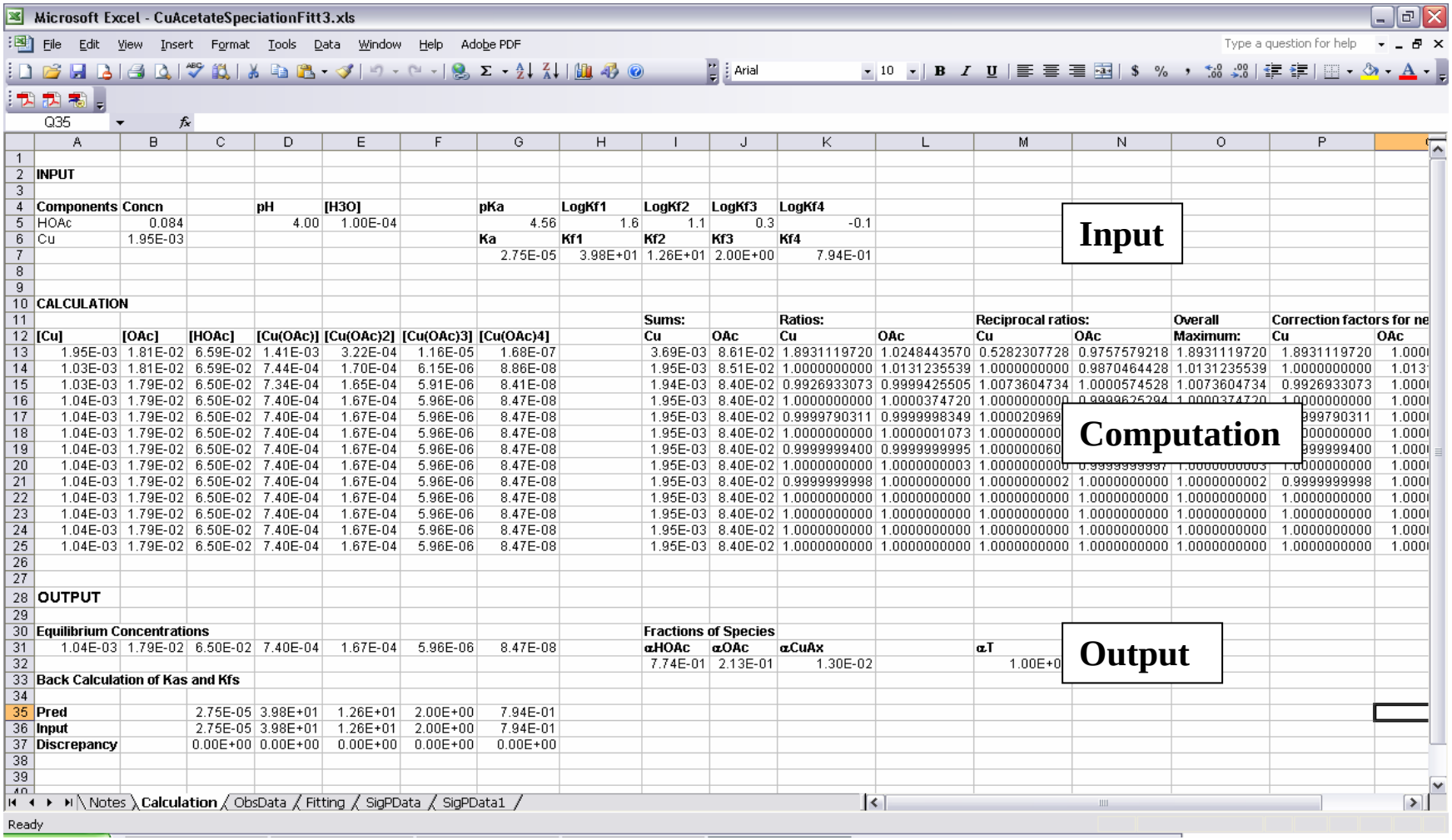

Figure 3.1 A Typical Speciation Calculation Spreadsheet

Instead of varying each concentration of the “seed” species in strict rotation in the iterative method as previously done in our group [58], “a smarter” algorithm is used to select the concentration which is to be corrected in the next line. This was done by the introduction of "concentration ratios" (see Figure 3.2).

"Concentration ratios" are ratios of total concentration of an entity (eg Cu, CO_3 etc) in all forms, calculated from current assumed values of each entity in free form, divided by the actual overall concentration of that entity. The concentration ratios are usually greater than unity since calculated total concentrations are usually greater than actual concentration of each entity in the free form. The reciprocals of the concentration ratios, which are usually less than unity, are also calculated. The idea is to correct the free concentration for the entity showing the greatest discrepancy (either high or low), and recalculate using a correction factor. This is the factor by which the current assumed free entity concentration are divided to get the new values.

To obtain the correction factor, the maximum of all concentration ratios and their reciprocals is found. The maximum of each ratio and its reciprocal is divided by the overall maximum, then truncated. This will yield zero in all cases except where either that ratio or its reciprocal is the overall maximum. In that case, it will yield one. This is "normalized" to yield the value of the maximum (in that case), and one in all other cases, by multiplying by (overall maximum -1) and adding 1 to the result. Finally, this is taken to the power of the sign of the logarithm of the original value to obtain the correction factor. (If the value was < 1, meaning that it was a reciprocal which was the overall maximum, this will result in undoing that reciprocal.).

The correction factor so obtained is used to divide the value of current assumed free entity concentration to get new values in the next row of the spreadsheet. Concentrations of all other species present in the equilibrium are subsequently calculated from the new values and the iterative procedure repeated until all the concentration values of the species have converged. Convergence is rapid initially, however it slows

Sums:		Ratios:		Reciprocal ratios:		Overall	Correction factors for next row:			Resid
Cu	OAc	Cu	OAc	Cu	OAc	Maximum:	Cu	OAc		
3.69E-03	8.61E-02	1.8931119720	1.0248443570	0.5282307728	0.9757579218	1.8931119720	1.8931119720	1.0000000000		1.87E+00
1.95E-03	8.51E-02	1.0000000000	1.0131235539	1.0000000000	0.9870464428	1.0131235539	1.0000000000	1.0131235539		6.80E-04
1.94E-03	8.40E-02	0.9926933073	0.9999425505	1.0073604734	1.0000574528	1.0073604734	0.9926933073	1.0000000000		2.15E-04
1.95E-03	8.40E-02	1.0000000000	1.0000374720	1.0000000000	0.9999625294	1.0000374720	1.0000000000	1.0000374720		5.62E-09
1.95E-03	8.40E-02	0.9999790311	0.9999998349	1.0000209694	1.0000001651	1.0000209694	0.9999790311	1.0000000000		1.76E-09
1.95E-03	8.40E-02	1.0000000000	1.0000001073	1.0000000000	0.9999998927	1.0000001073	1.0000000000	1.0000001073		4.62E-14
1.95E-03	8.40E-02	0.9999999400	0.9999999995	1.0000000600	1.0000000005	1.0000000600	0.9999999400	1.0000000000		1.42E-14
1.95E-03	8.40E-02	1.0000000000	1.0000000003	1.0000000000	0.9999999997	1.0000000003	1.0000000000	1.0000000003		0.00E+00
1.95E-03	8.40E-02	0.9999999998	1.0000000000	1.0000000002	1.0000000000	1.0000000002	0.9999999998	1.0000000000		0.00E+00
1.95E-03	8.40E-02	1.0000000000	1.0000000000	1.0000000000	1.0000000000	1.0000000000	1.0000000000	1.0000000000		0.00E+00
1.95E-03	8.40E-02	1.0000000000	1.0000000000	1.0000000000	1.0000000000	1.0000000000	1.0000000000	1.0000000000		0.00E+00
1.95E-03	8.40E-02	1.0000000000	1.0000000000	1.0000000000	1.0000000000	1.0000000000	1.0000000000	1.0000000000		0.00E+00
1.95E-03	8.40E-02	1.0000000000	1.0000000000	1.0000000000	1.0000000000	1.0000000000	1.0000000000	1.0000000000		0.00E+00

Figure 3.2 Iteration procedure of the speciation calculation

down as it gets closer. The system is deemed to have converged when the value of all the concentration ratios, its reciprocals and the correction factors is 1 x 10^{-14} or less. This is limited by the internal numeric precision of Excel®, which is set at 15 digits. If the number of significant digits in the result is comparable to the number of digits in the computer, further refinement becomes meaningless.

"Resid" is introduced at the end of each step to check for the settling of equilibrium. "Resid" is the sum of squares of the ratios and their reciprocals, minus the number of values. As all values approach unity, this approaches zero.

A similar approach is used for the expanded model where additional ligands are introduced into the system. Chemical entities are used that can provide a complete description of the stoichiometry of the system. The addition of each ligand results in one more mass balance equation. Each species is expressed as the product of a set of chemical components that define the equilibrium position and a formation constant. With each new ligand the expression for the total copper concentration changes to accommodate the new set of species.

When the species have settled at equilibrium, the dissociation and formation constants of the various species are recalculated and compared with the input values to check for discrepancy. This helps ensure that, the results obtained from the model are indeed reliable.

3.1.2 Computer Modeling of Cu(II) Speciation in the Rumen

The results obtained by modeling of the speciation of Cu(II) in the presence of the low molecular mass (LMM) ligands of the bovine rumen environment indicate that the bulk of copper is present as carbonate. This is in spite of the relative high concentrations of volatile fatty acids (VFAs), especially acetic acid, compared to other LMM ligands in the rumen (Table 2.1).

Figure 3.3 illustrates the distribution of copper with respect to the LMM ligands of rumen at the average ruminal pH of 6.3. 60.4% of the copper exists as carbonate species, 23.8% as phosphate, 10.3% as acetate, 3.8% as the other volatile acids, 1.4% as ammonia and 0.2% as aquated copper. $\alpha Cu(CO_3)_x$ represents the fraction of all copper carbonate species; $\alpha Cu(PO_4)_x$, of all copper phospate species; $\alpha Cu(NH_3)_x$, of all copper ammine species; αCu, of "free" ionic copper; $\alpha Cu(OAc)_x$, of all copper acetate species; and $\alpha Cu(OA_x)_x$, of all copper complexes of the other volatile fatty acids (see Tables 2.1 and 2.2) present in the rumen.

The above behaviour results from the relatively higher binding strength of carbonate to copper compared to the rest of the LMM ligands present in the rumen, as detailed in Table 2.2. The result obtained is similar to that obtained for copper speciation in McDougall's solution (bovine saliva) [151]; copper was mainly present as carbonates. This implies that carbonate is able to hold on to copper right from the mouth to the rumen in spite of the myriad LMM ligands it encounters. It is therefore not surprising that copper carbonate has been used as copper supplements for ruminants [152].

Fluctuations in pH, which are common in the rumen, were also incorporated into the model. The changes that occur across the normal ruminal pH range are shown in Figure 3.4. As the pH increases, $\alpha Cu(OAc)_x$ falls off and $\alpha Cu(CO_3)_x$ and $\alpha Cu(PO_4)_x$ dominate up to the highest normal ruminal pH of 6.8, where copper exists mostly as carbonate species. A tiny fraction of the total copper concentration is attached to the rest of the volatile fatty acids – propanoic, butanoic, isobutanoic, pentanoic and isopentanoic, and a very tiny fraction attached to ammonia. Also according to the model copper is virtually completely bound in the rumen fluid, with only trace amounts of "free" ionic copper existing. This is in agreement with other studies that report an immeasurable amount of ionic copper in biological fluids. This is directly attributed to the high complexing ability of the copper(II) ions.

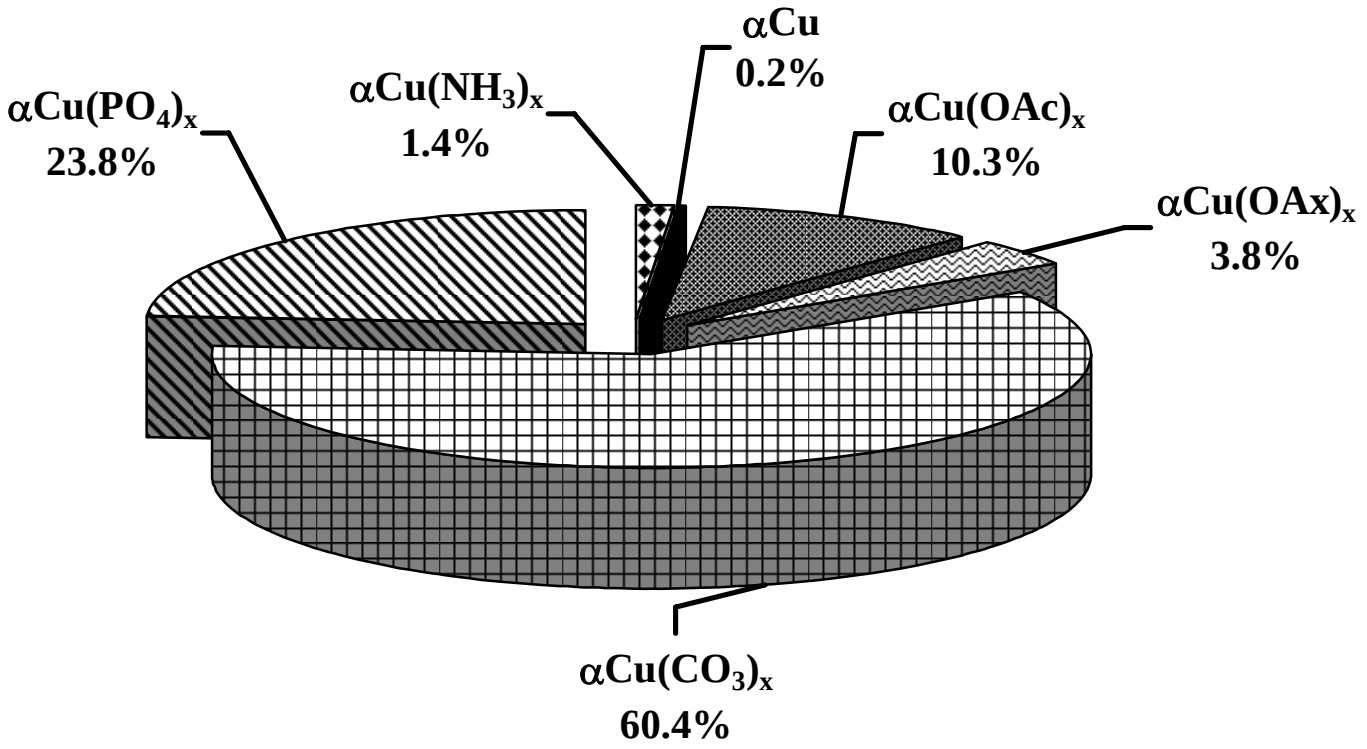

Figure 3.3 Distribution of copper with respect to the LMM ligands in rumen fluid at pH 6.3. Calculation were performed at an ionic strength of 0.15 M; temperature of 38 °C and Cu^{2+} concentration of 3.0 x 10^{-5} M. See Table 2.1 for concentrations of ligand

Concentrations of VFAs in the rumen vary over a wide range with acetic acid being the most dominant [59-63, 142, 143]. The observed proportions of VFAs are related to composition of the diet. Roughage diets high in cellulose give rise to acid mixtures particularly high in acetic acid. As the proportion of concentrates in the diet is increased, the proportion of acetic acid falls and that of propanoic acid rises. Calculations performed under varying concentrations of VFAs did not result in any significant changes in the overall distribution of copper(II), as shown in Figure 3.5. It is known that absorption of volatile fatty acids does in fact take place in the rumen. They are absorbed across the rumen wall in the free form, apparently without active transport (see Section 1.6.1). Since some of complexes copper forms with VFAs are neutral, it might well be that these complexes are absorbed alongside VFAs. This will mean that some copper absorption takes place even prior to its arrival at the small intestine, where most of the copper absorption takes place. However the amount of copper complexes to these acids is minimal and thus the role the copper-VFA complexes play is unlikely to be significant. It is concluded that the proportions of the VFA produced would not markedly affect copper absorption.

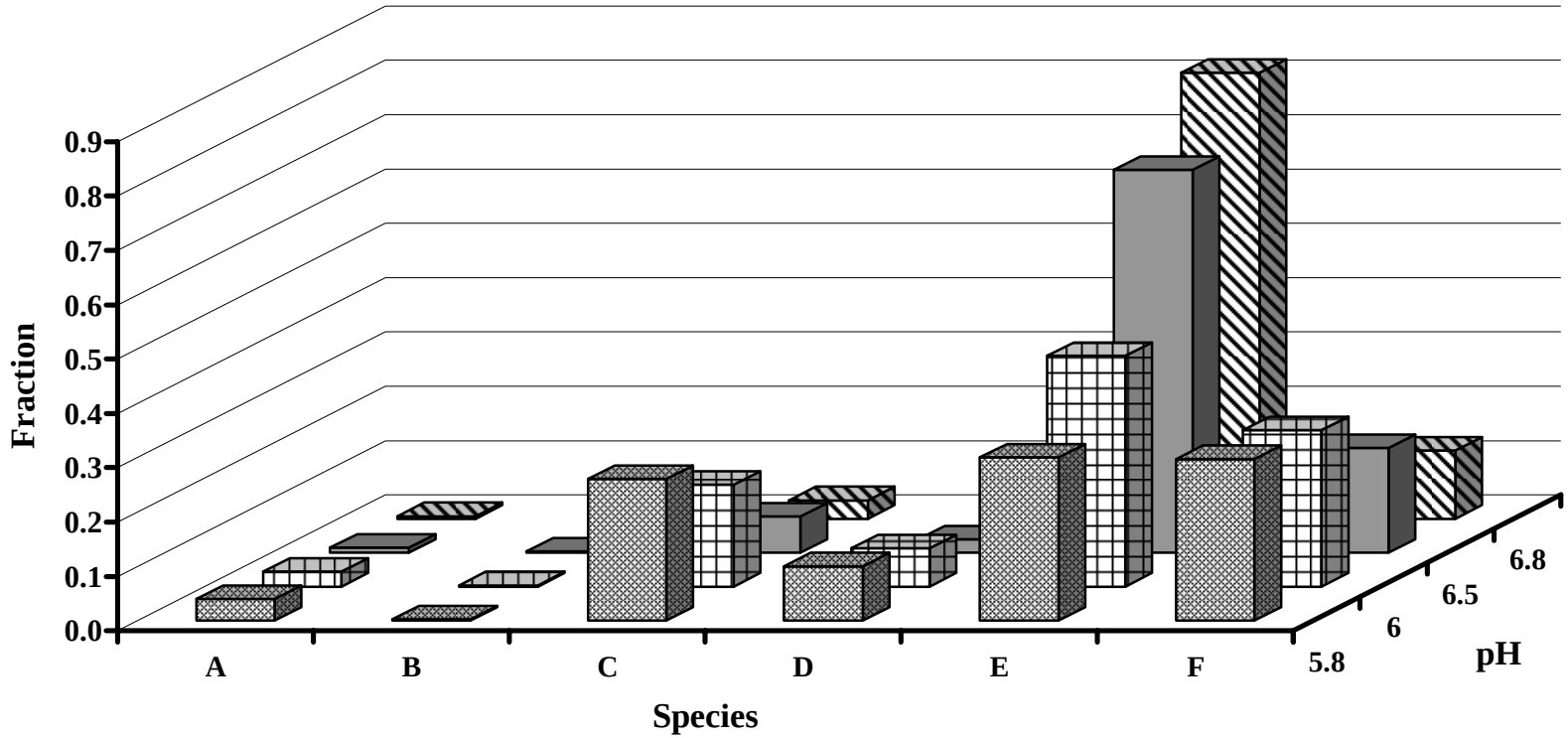

Figure 3.4 Distribution of copper with respect to the LMM ligands in rumen fluids as pH is varied between 5.8 and 6.8. Calculations were performed at an ionic strength of 0.15 M and Cu^{2+} concentration of 3.0×10^{-5} M. See Table 2.1 for concentrations of ligands. **A:** Copper ammonia complexes; **B:** Free Cu^{2+}; **C:** Copper acetate complexes; **D:** Copper VFA complexes; **E:** Copper carbonate complexes; **E:** Copper phosphate complexes.

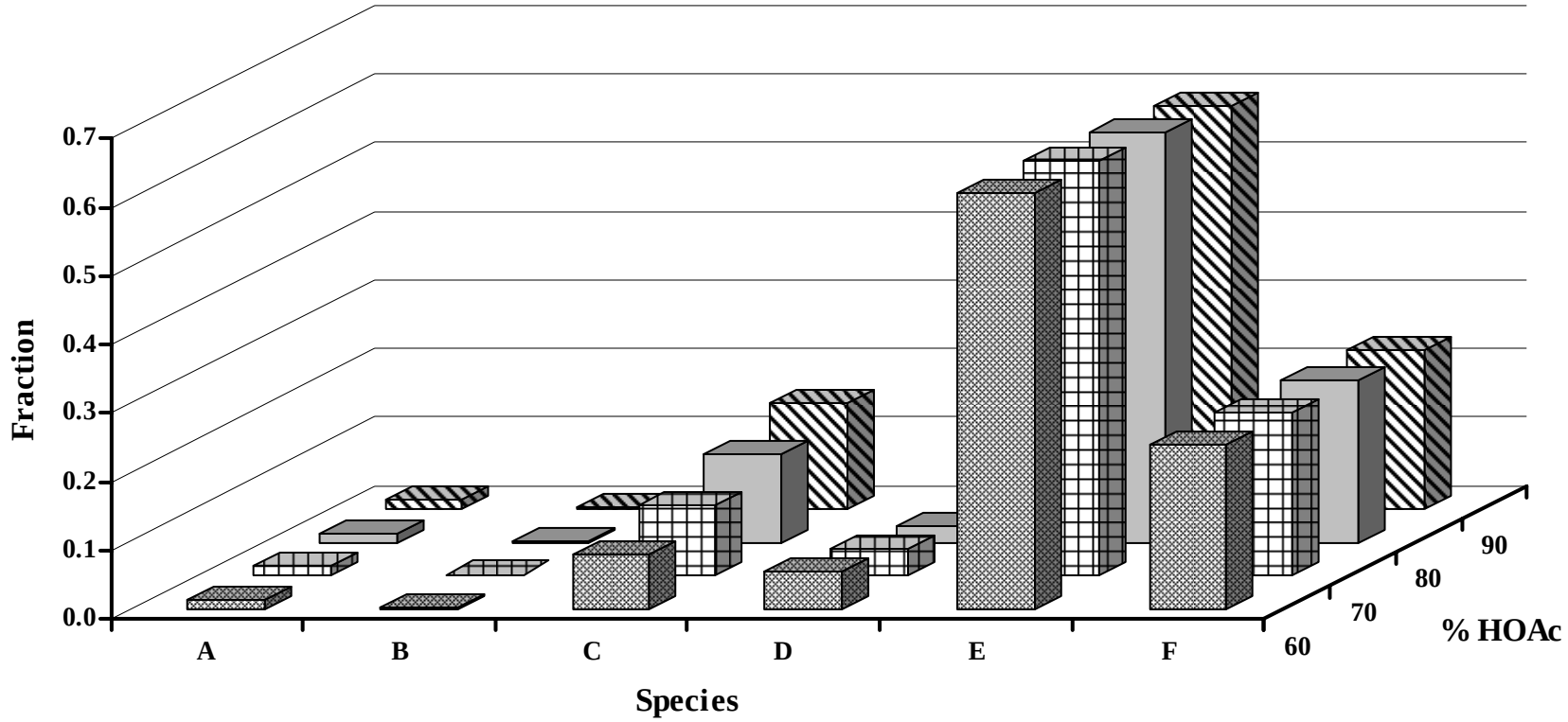

Figure 3.5 Distribution of copper with respect to the LMM ligands in rumen fluid as percentage of acetic acid is varied with respect to other VFAs. Calculations were performed at an ionic strength of 0.15 M and Cu^{2+} concentration of 3.0 x 10^{-5} M. See Table 2.1 for concentrations of ligands. **A:** Copper ammonia complexes; **B:** Free Cu^{2+}; **C:** Copper acetate complexes; **D:** Copper VFA complexes; **E:** Copper carbonate complexes; **E:** Copper phosphate complexes.

3.1.3 Effect of Sulfide, Ca^{2+} and Mg^{2+} on Cu Speciation in the Rumen

3.1.3.1 Effect of Sulfide

To determine the effect of the possible formation of CuS on the distribution of Cu(II) with respect to LMM in the rumen, sulfide was included as ligand in the rumen speciation model.

Using the sulfide concentration of 7.5 x 10^{-4} **M** (see Section 1.11) and the thermodynamic data of 6.82 [145] and 17 [153] representing the pKa_1 and pKa_2 values H_2S respectively as well as pKsp value of 15.2 [145] for the formation CuS, sulfide was included in the copper speciation in rumen fluid model. The result shows that, at an average ruminal pH value of 6.3; 6.3 x 10^{-4} **M** (representing 84 % of the sulfide) exist as H_2S, 1.2 x 10^{-4} **M** (representing 16 % of the sufide) exist as HS^- and very insignificant amount of S^{2-} (2.4 x 10^{-15} **M**). This results supports feed studies [60] that have found that ruminal sulfide occurs mostly as H_2S and HS^-, the proportion depending on rumen pH. Of importance in the result obtained is the fact at average ruminal pH of 6.3, no CuS was found to have been precipitated, even at elevated concentrations representing extreme dietary S intake (see Section 1.11). This is due mainly to the very small amount of S^{2-} present under ruminal pH. Thus the presence of sulfide in the rumen will not alter the distribution of Cu(II) with respect to LMM in the rumen fluid. This finding is in agreement with feed studies [115] in which addition of sulfide to rumen contents in vitro did not change the distribution of Cu between the fluid and solid phases. Thus if CuS is formed at all in the rumen, the amount formed will not significantly affect the distribution of Cu(II) amongst LMM in the rumen.

3.1.3.2 Effect of Ca^{2+} and Mg^{2+}

Since ingesta entering the rumen consist of briefly chewed food, saliva and water, the presence of other mineral ions such as Ca^{2+} and Mg^{2+} in the rumen fluid cannot ignored due to their presence in the ruminant saliva (see Table 2.3) and drinking

water. However due the presence of higher bicarbonate and phosphate in the ruminant saliva (see Table 2.3), most of Ca and Mg enter the rumen already complexed and precipitated as $CaCO_3$, $MgCO_3$, $CaHPO_4$ and $MgHPO_4$ considering the Ksp values of these species [145]. Concentrations in solution are further reduced considering the volume of the bovine rumen (40-100 litres)[61]. Concentrations of Ca and Mg found in the liquid phase of rumen of sheep 2 hours after being feed chaffed alfalfa hay was found to be 2.9 x 10^{-8} M and 3.6 x 10^{-8} M [154] respectively. The low concentrations Mg and Ca in the rumen can also be due to the fact that the rumen has been identified as one of the site for Ca and Mg absorption in the ruminants [67, 155].

Using the concentrations of Ca and Mg mentioned above as conservative estimates, Ca^{2+} and Mg^{2+} were introduced into the copper speciation in rumen fluid model using thermodynamic data of their complextion to various LMM ligands in the rumen, obtained form NIST database [145]. Speciation calculation results obtained in the presence of these ions at concentrations mentioned above coupled with their very low formation constants (LogK of 0.1-0.6)[145] with LMM ligands in the rumen did not have any significant effect on distribution of Cu(II) with respect to LMM in the rumen fluid.

3.1.4 Comparison of Speciation Simulation Model with HySS

The difficulties in analysis of a biological system have meant that computer simulation models are of great advantage to the bioanalytical chemist when studying the metal speciation in a biological system. However, as in any "real life" process studied using simulation techniques, there are three major sources of uncertainty. These have been referred to as "modeling", "data" and "completeness" uncertainties [31] (see Section 1.3).

In principle, completeness uncertainties are unquantifiable, although some allowance can generally be made by extending probability ranges in uncertainity analysis. In simulations of chemical speciation in aqueous media, as has been done in this study, the main source of uncertainty is normally due to the quality of the input,

specifically that of the formation constants and the composition of their associated complexes. Thus it is essential that the formation constants used in any chemical speciation modeling are critically evaluated. In evaluating formation constants from any source, factors that are considered include: experimental method, purity of reagents, background electrolyte, reagent concentrations, ionic strength and computational procedures (see Section 1.3).

The total of these three uncertainties associated with a model can be quantified by combination of uncertainty analysis and exercises in verification and validation. Where possible the model is compared with either experimental results or other computer simulation programs to verify that the results produced are accurate.

Thus in appraising the Cu speciation in rumen fluid model developed above, the results of the model were compared with the results from another computer simulation program called Hyperquad Simulation and Speciation (HySS), a utility program for the investigation of equilibria involving soluble and partially soluble species. HySS is a program written for Windows operating system on personal computers which provides (a) a system for simulating titration curves and (b) a system for providing speciation diagrams (see Section 1.3.1). HySS allows complete flexibility in specifying conditions for speciation calculations, and a simple interface to other Windows applications, such as word-processors or spreadsheets, for the results of the calculations.

Results from the computer simulation of copper speciation in rumen using HySS and the model developed in this study using a spreadsheet is shown in Figure 3.6. Comparison of the distribution of copper with respect to the LMM ligands in rumen fluid at average ruminal pH of 6.3 using both methods show that there is no apparent difference between results (see Table 3.1). To determine whether the two methods differ significantly from each other statistically, the results were subjected to regression analysis (Figure 3.7). Since the slope is insignificantly different from unity (0.9999 ± 5) and the intercept insignificantly different from zero (0.000007 ± 6), we can conclude that the methods do agree. The results from the two methods were further subjected to a

paired t-test, and it was found out that the calculated t value (0.6234) is less than the tabulated value (2.571) for 95 % confidence and 5 degrees of freedom. Thus the two methods are not significantly different at the 95% confidence level [137].

Table 3.1 Concentration fractions of the various species from the computer simulation of copper speciation in rumen using HySS and the method developed in this study.

Concentration Fractions			
Chemical Species(α)	Hyss	This Study	Difference
Cu	0.014372	0.014373	-5.84E-07
$Cu(NH_3)_x$	0.002488	0.002465	2.35E-05
$Cu(OAc)_x$	0.103242	0.103267	-2.54E-05
$Cu(OAx)_x$	0.038397	0.038390	6.81E-06
$Cu(CO_3)_x$	0.603724	0.603658	6.62E-05
$Cu(PO_4)_x$	0.237829	0.237848	-1.90E-05

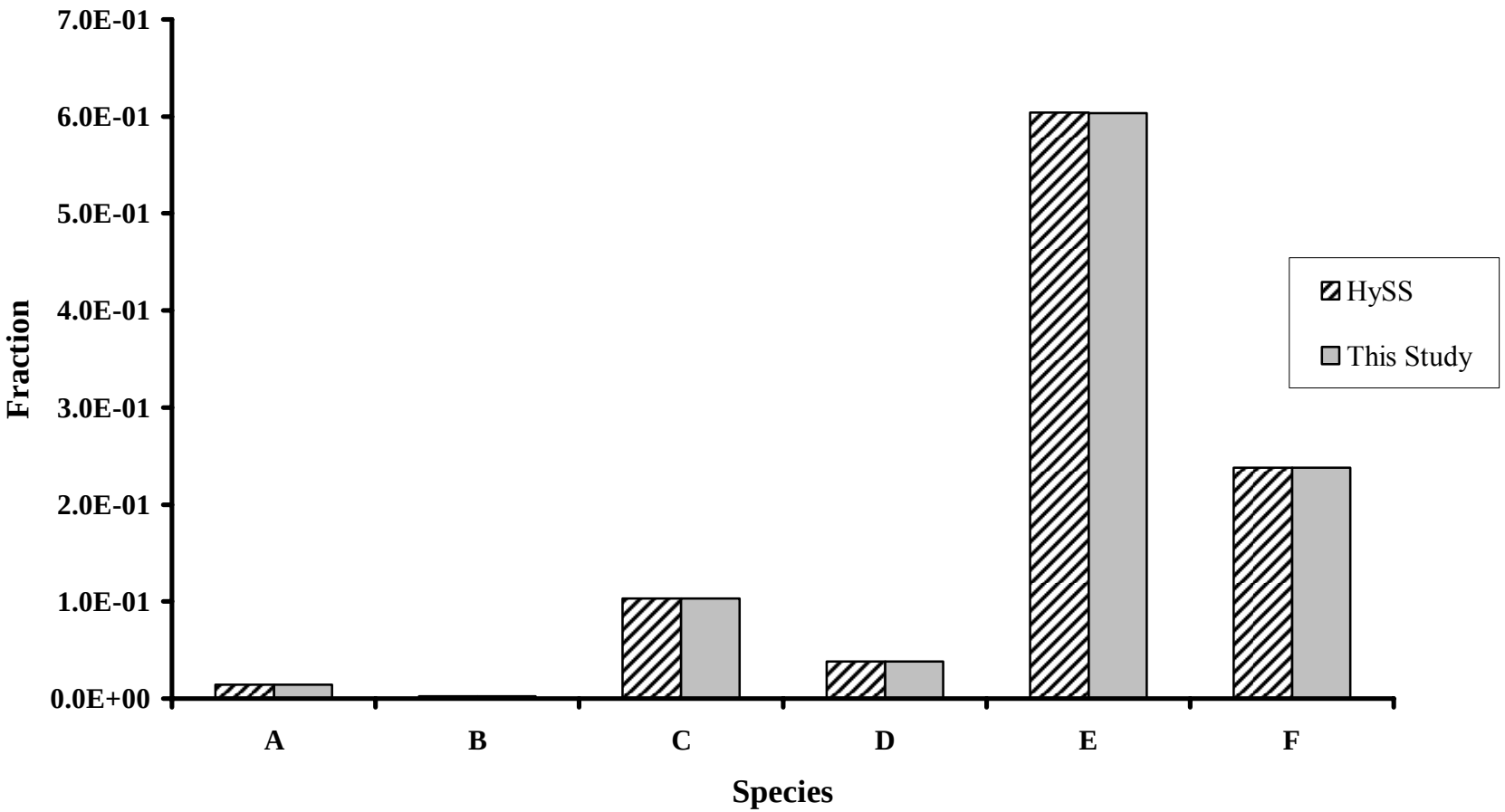

Figure 3.6 Comparison of the distribution of Copper with respect to the LMM ligands in rumen fluid at average ruminal pH of 6.3 calculated using HySS and the method used in this study. Calculations were done at an ionic strength of 0.15 M, temperature of 38 °C and Cu^{2+} concentration of 3.0 x 10^{-5} M. See Table 2.1 for concentrations of ligands. **A:** Copper ammonia complexes; **B:** Free Cu^{2+}; **C:** Copper acetate complexes; **D:** Copper VFA complexes; **E:** Copper carbonate complexes; **E:** Copper phosphate complexes.

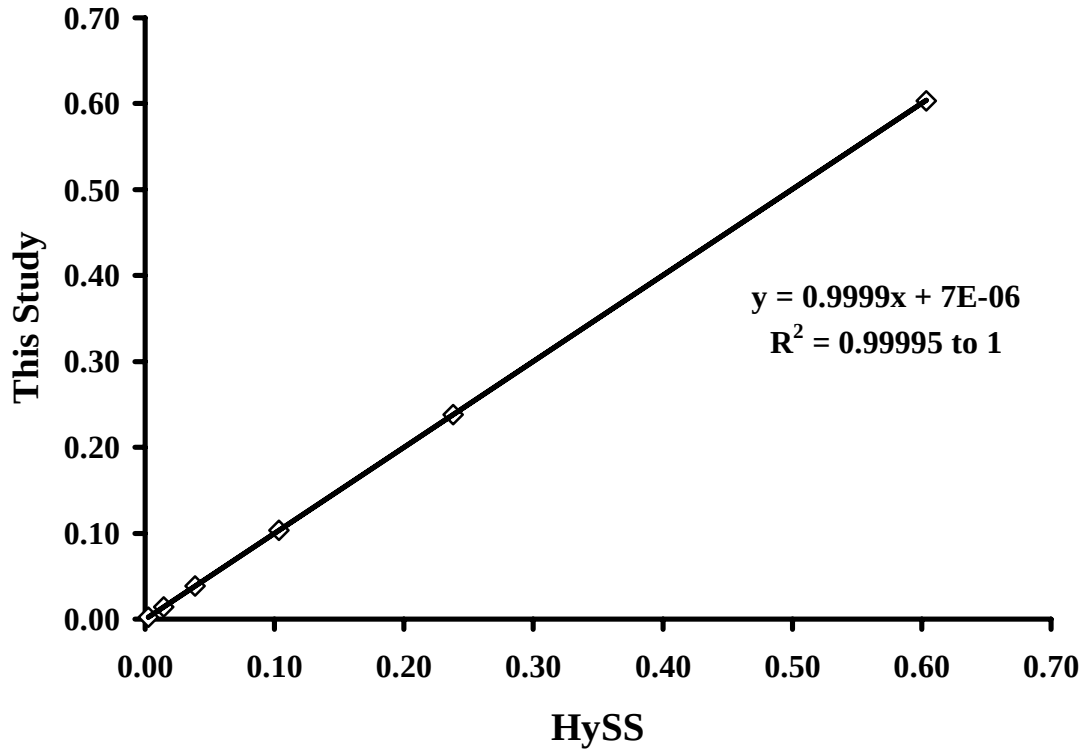

Figure 3.7 A plot of the concentration fraction results of the computer simulation of Cu(II) speciation in the rumen using the method used in this study versus HySS. See Table 3.1 for data)

It can therefore be concluded that the two programs yield the same results. Both programs also have a simple user interface. Using a spreadsheet has the additional advantage that one can watch the value at each iteration. Observing progress towards convergence makes the method more understandable, and often reveals some of the subtleties involved. This is in comparison to the "black box" HySS in which one is only privy to the input data and the output concentration of species and graphs, without understanding the calculations involved in arriving at the results.

Although the two programs yield the same numbers, they could both still be wrong as the results may not reflect the real Cu(II) speciation that pertains in the rumen

fluid. Hence experimental validation is still essential in confirming the computer model description of Cu(II) speciation in rumen fluid (see Section 3.2).

3.1.5 Computer Modeling of Speciation of Chelated Cu(II) Supplements

3.1.5.1 Bovine Saliva (McDougall's Solution)

Mineral supplements are usually administered orally and since the saliva is the first fluid that the metal encounters once admitted into the digestive system of the animal, it is logical that a study of copper speciation in the animal begins with the saliva.

It is well known [156] that the pH of bovine saliva, in the absence of dietary acids, varies throughout the day between 5.5 and 8.0, averaging about 6.0. Thus the speciation of Cu(II) supplements in bovine saliva was calculated over this pH range. All the calculations were done at an ionic strength of 0.15 M and temperature of 38 °C. Figures 3.8, 3.9 and 3.10 show the speciation when the copper is introduced as 1:2 Copper glycine, Copper methionine and Copper lysine complex mixtures ,respectively. The similarities between the figures suggest that there is not much difference in copper speciation in McDougall's solution whether the copper is introduced as Copper glycine, Copper methionine or Copper lysine. This is because in all three cases, the predominant species are copper carbonate species. The result obtained is comparable to an earlier study in our group in which the speciation of copper lysine and copper chloride in McDougall's solution were compared and the predominant species found to be copper carbonate [151].

In all three cases, the concentration of "free" copper at all levels is found to be low, and decreasing with increasing pH values. This is because of the high affinity of copper ions for coordinating ligands. The chloride, sulfate, and the hydroxide ligands do not compete effectively for the copper(II) ions in solution. Although there is a preponderance of chloride ions in saliva, it is not unusual for transition metals to avidly

complex with other ligands instead. In many other biological fluids the chloride is bonded only after all the bidentate and polydentate ligands have been complexed [41].

The amount of copper carbonate species formed rises steadily from about ~20% of the total at a pH of 5.5 to ~90% at a pH of 8.0. The next most predominant species are phosphate complexes, which decrease from about 40% of the total at a pH of 5.5 to almost 0% at a pH of 8.0, in all three systems under discussion. The amounts of copper-amino acid complex species formed differs between the three cases. The copper glycine complexes range from ~12% of the total at a pH of 5.5 to ~3% at a pH of 8.0; copper methionine complexes from ~10% at a pH of 5.5 to 15% at a pH of 8.0; and copper lysine complexes from ~10% at a pH of 5 to 7% at a pH of 8.0.

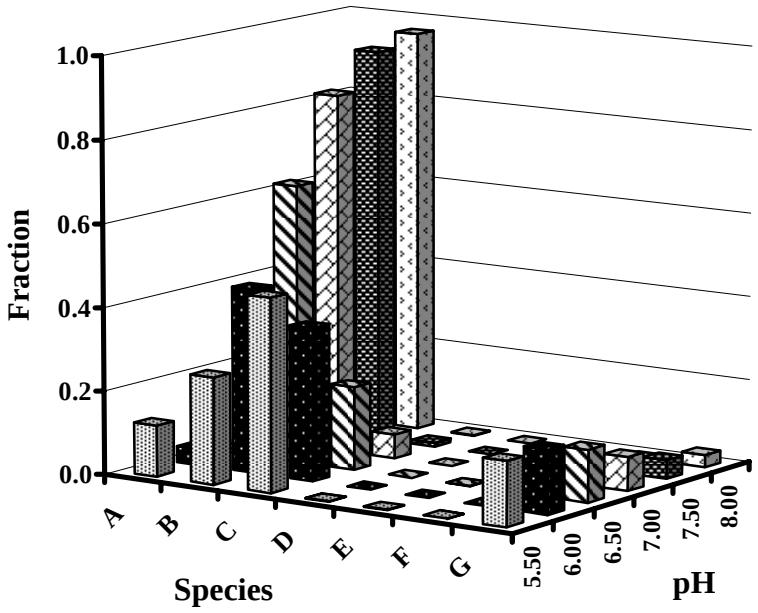

Figure 3.8 Copper speciation in McDougall's solution as function of pH using 1:2 Copper glycine supplement at a copper concentration of 3.0 x 10^{-5} M. **A:** Free Cu^{2+} ; **B:** Copper carbonate complexes ; **C:** Copper phosphate complexes ; **D:** Copper (II) sulfate ; **E:** Copper (II) chloride; **F:** Copper hydroxide complexes; **G:** Copper amino acid complexes

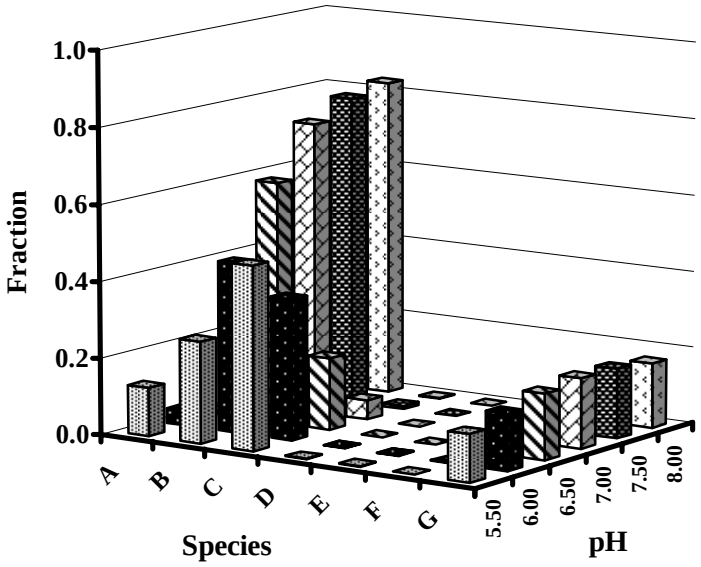

Figure 3.9 Copper speciation in McDougall's solution as function of pH using 1:2 Copper methionine supplement at a copper concentration of 3.0 x 10^{-5}M. For key to species see Figure 3.8

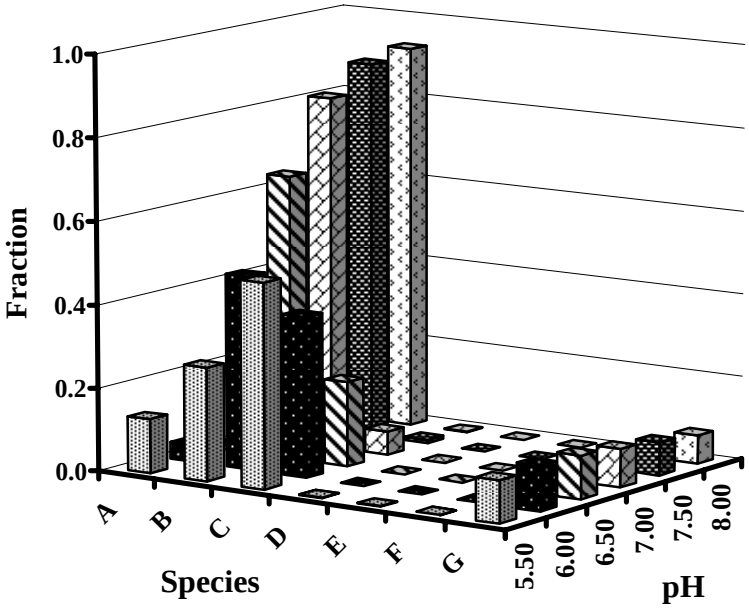

Figure 3.10 Copper speciation in McDougall's solution as function of pH using 1:2 Copper lysine supplement at a copper concentration of 3.0 x 10^{-5}M. For key to species see Figure 3.8

Figures 3.11 and 3.12 show the copper speciation when the copper is introduced as copper histidine and copper EDTA in McDougall's solution. The predicted speciation in both cases suggests that about 90% of the copper will be retained as copper histidine over the entire physiological pH range when copper is introduced as copper histidine. Similarly, almost 100% of the copper is retained in the form of copper EDTA complexes over the entire physiological range when copper is introduced as copper EDTA.

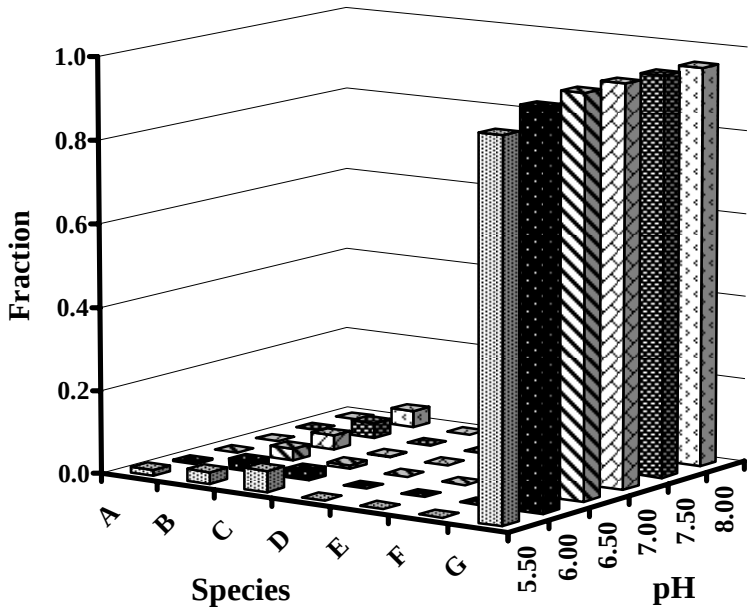

Figure 3.11 Copper speciation in McDougall's solution as function of pH using 1:2 Copper histidine supplement at a copper concentration of 3.0 x 10^{-5}M. For key to species see Figure 3.8

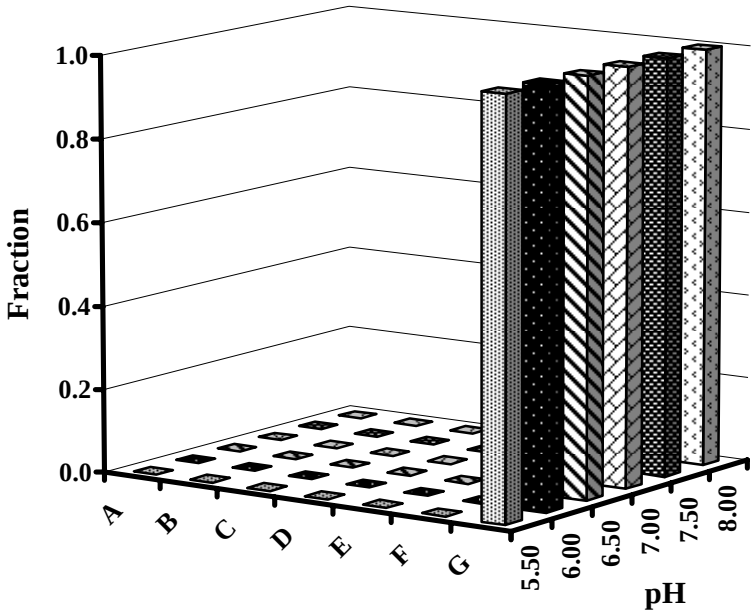

Figure 3.12 Copper speciation in McDougall's solution as function of pH using 1:2 Copper EDTA supplement at a copper concentration of 3.0 x 10^{-5} M. For key to species see Figure 3.8

A comparison of the copper speciation in McDougall's solution at pH 7.0 for the copper supplements discussed above is shown in Figure 3.13. Thus, of all the various copper supplements which have been examined so far, we see that only copper histidine and copper EDTA do not degrade into other species when introduced to bovine saliva. This is because, at a pH of 7, copper complexes of all the four amino acids (glycine, methionine, lysine and histidine) exist as bis complexes (CuL_2) [140], as shown in Figure 3.14. However whereas glycine, methionine and lysine display similar bonding to copper through their carboxylate oxygen and the nitrogen of the amino nitrogen, histidine bonds through its amino and imidazole nitrogens. Since the copper(II) ion is classified as a borderline hard acid, it has a binding preference for nitrogen -based rather than oxygen- based ligands. Thus, histidine has a higher formation constant (see Table 2.6) and hence is able to hold onto copper better than glycine, methionine and lysine in the presence of other competing ligands. EDTA's strong binding to copper (see Table 2.6) can be attributed to the chelate effect; it uses of its four carboxylate oxygens and amine nitrogens for bonding, as shown in Figure 3.15.

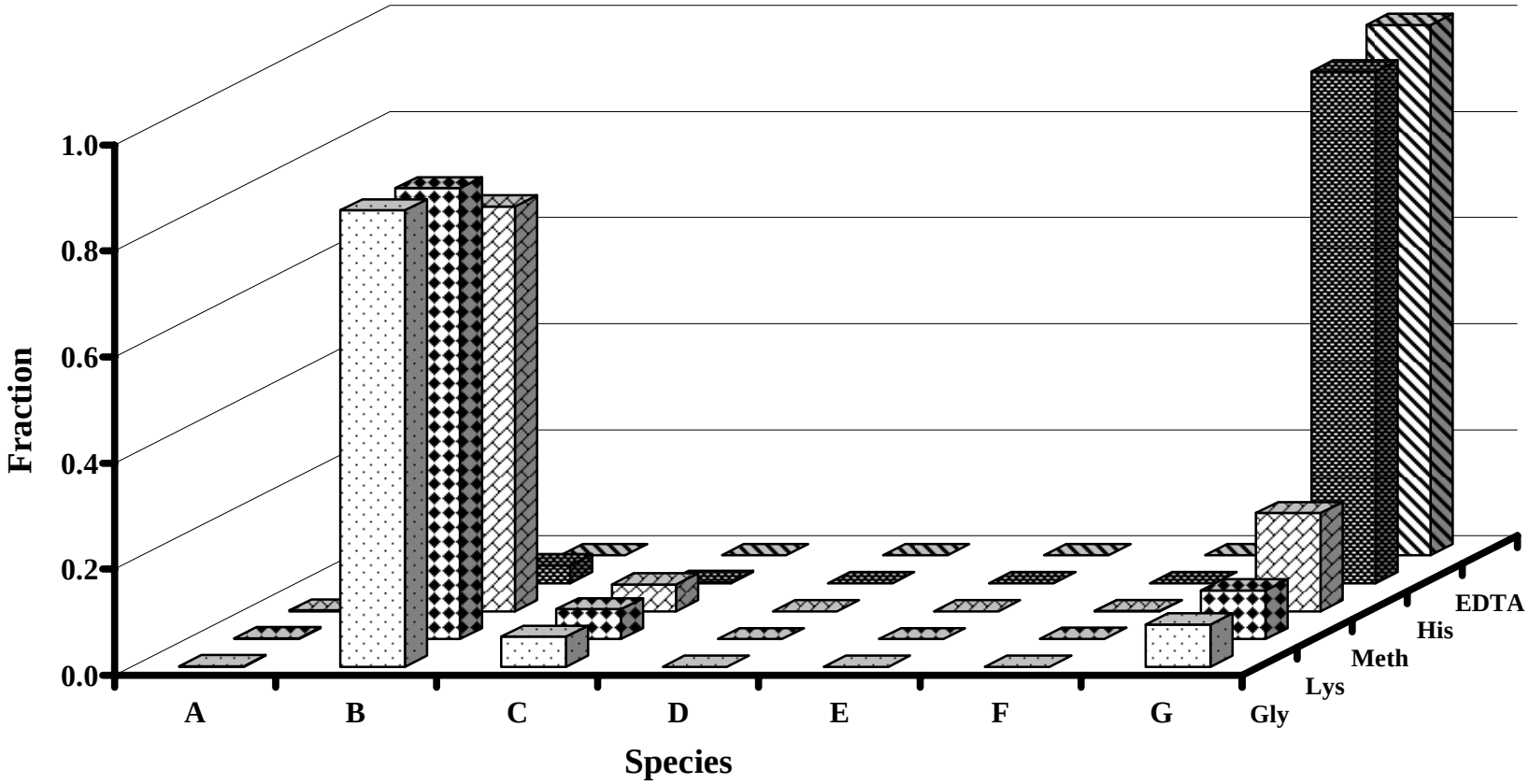

Figure 3.13 Comparison of speciation of copper in McDougall's solution of various copper supplements at physiological pH of 7.0 Calculations were performed at an ionic strength of 0.15 M, temperature of 38 °C and Cu^{2+} concentration of 3.0 x 10^{-5} M. See Table 2.3 for concentrations of ligands. **A:** Free Cu^{2+} ; **B:** Copper carbonate complexes ; **C:** Copper phosphate complexes ; **D:** Copper (II) sulfate ; **E:** Copper (II) chloride; **F:** Copper hydroxide complexes ; **G:** Copper amino acid complexes

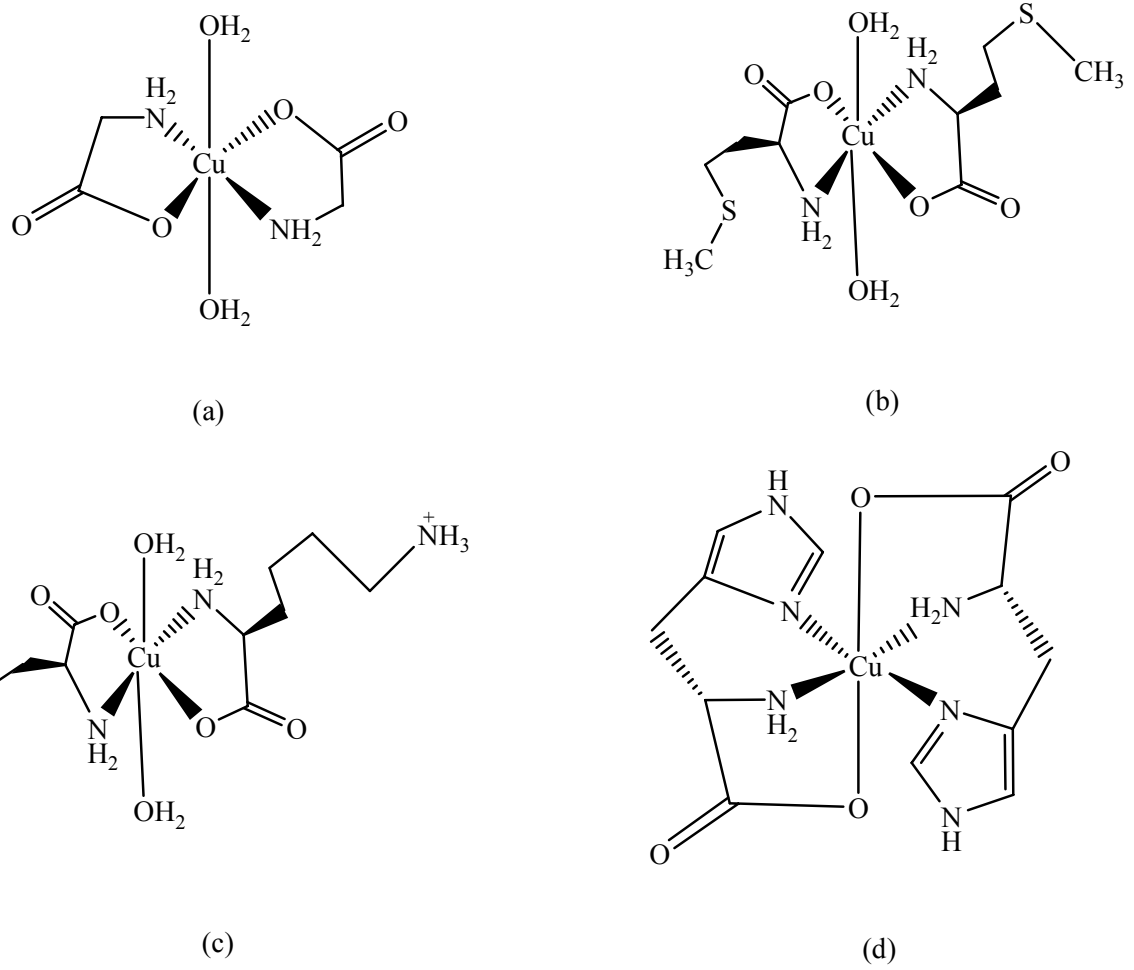

Figure 3.14 Structures of copper (II) biscomplexes of (a) glyine, (b) methionine, (c) lysine and (d) histidine

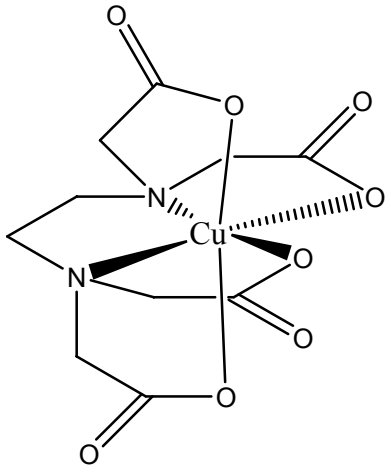

Figure 3.15 Structure of Copper (II) EDTA complex

3.1.5.2 Bovine Rumen (simple ligands)

For proper understanding of the fate of copper(II) amino acid complexes which are widely used as copper supplements, supposedly to enhance the bioavailability of copper [71-73], it is necessary to understand the interactions of copper with the major constituents of the various biofluids encountered down the GI tract. The first of these is rumen fluid.

Since under normal conditions the pH of the contents of the rumen and reticulum is maintained in the range of 5.8 to 6.8 (see Section 1.5.2), the speciation of Cu(II) introduced in the form of various supplements in the bovine rumen were calculated over that entire physiological pH range. Figures 3.16 to 3.18 show the speciation when the copper is introduced as 1:2 (mole ratio) Copper glycine, Copper lysine and Copper methionine mixtures respectively. The speciation for these three copper supplements is similar; at a ruminal pH of 5.8, much of the Cu is attached to acetate (35%), whereas 24% and 10% are attached to carbonate and the amino acids respectively. However as the ruminal pH increases to a 6.8, the Cu attached to acetate gradually reduces to about 6% whereas that of carbonate and the amino acids increases to 60% and 20% respectively for supplements introduced as Copper glycine and Copper lysine. With regards to Copper methionine speciation (Figure 3.16), as the pH increases to a high

ruminal pH of 6.8, the Cu attached to carbonate and methionine increases to 48% and 33% respectively. The results show that when copper supplement is introduced as copper glycine, copper lysine and copper methionine, they do not remain intact, but that a large percentage of the copper is lost to other competing ligands in the rumen.

The outcome of speciation modeling of Copper histidine and Copper EDTA (Figure 3.19 and 3.20 respectively) also show similarity, in that the almost all the copper is attached to the histidine and EDTA respectively over the entire physiological pH range of the rumen. This means that when a copper supplement is introduced as either copper histidine or copper EDTA, it remains almost intact in the rumen. Since Cu bound to the these ligands are exchangeable, it is possible that copper complexes of EDTA and histidine complexes make copper more bioavailable. Indeed it has been found that, from feed studies [157] that copper EDTA given at 3 to 6 months as copper supplements have helped prevent copper deficiency.

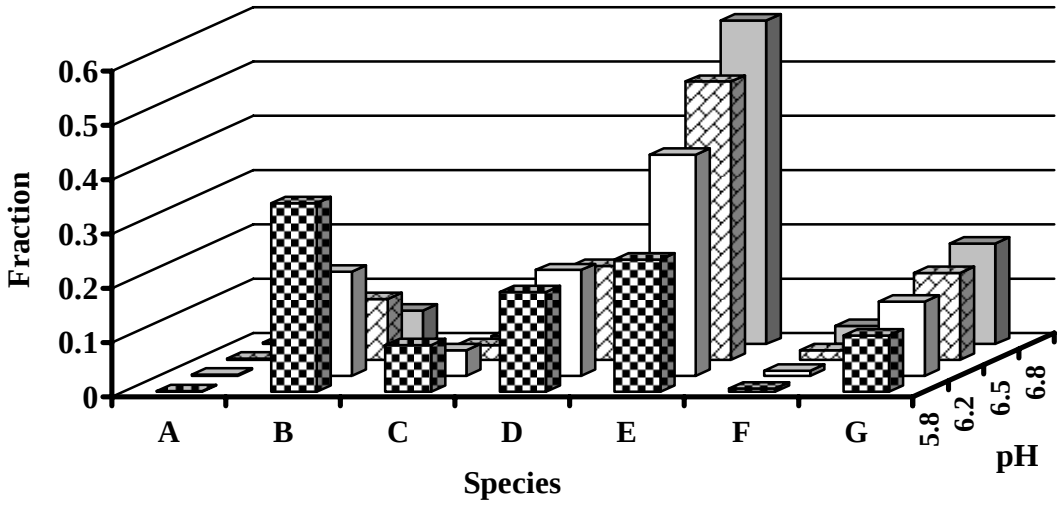

Figure 3.16 Copper speciation in rumen fluid as function of pH using 1:2 Copper glycine supplement at a copper concentration of 3.0 x 10^{-5} M. Calculations were done at Ionic strength of 0.15 M and temperature of 38 °C. **A:** Free Cu^{2+}; **B:** Copper acetate complexes; **C:** Copper VFA complexes; **D:** Copper phosphate complexes; **E:** Copper carbonate complexes; **F:** Copper ammonia complexes; **G:** Copper amino acid complexes.

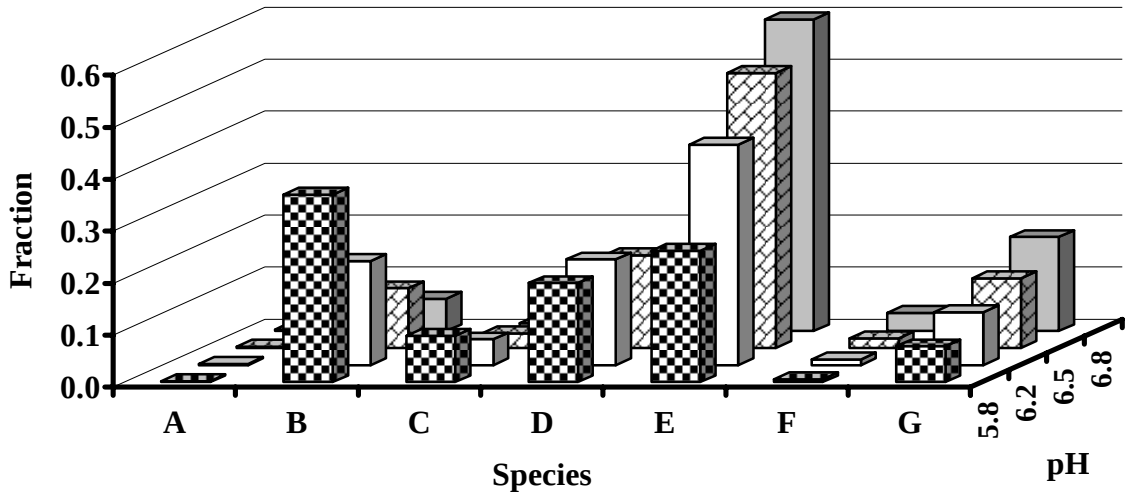

Figure 3.17 Copper speciation in rumen fluid as function of pH using 1:2 Copper lysine supplement at a copper concentration of 3.0 x 10^{-5} M. Calculations were done at Ionic strength of 0.15 M and temperature of 38 °C. For key to species see Figure 3.16

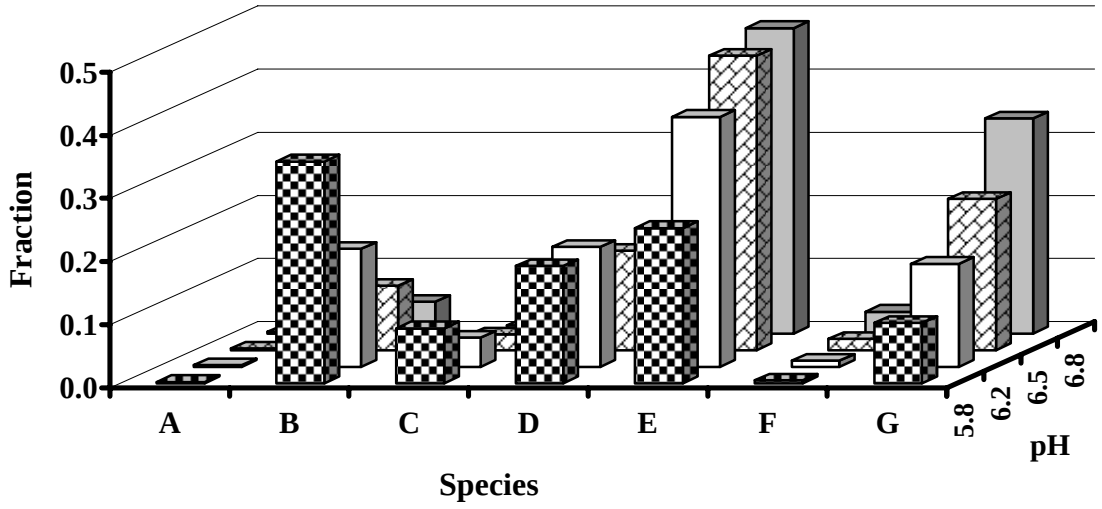

Figure 3.18 Copper speciation in rumen fluid as function of pH using 1:2 Copper methionine supplement at a copper concentration of 3.0 x 10^{-5} M. Calculations were done at Ionic strength of 0.15 M and temperature of 38 °C. For key to species see Figure 3.16

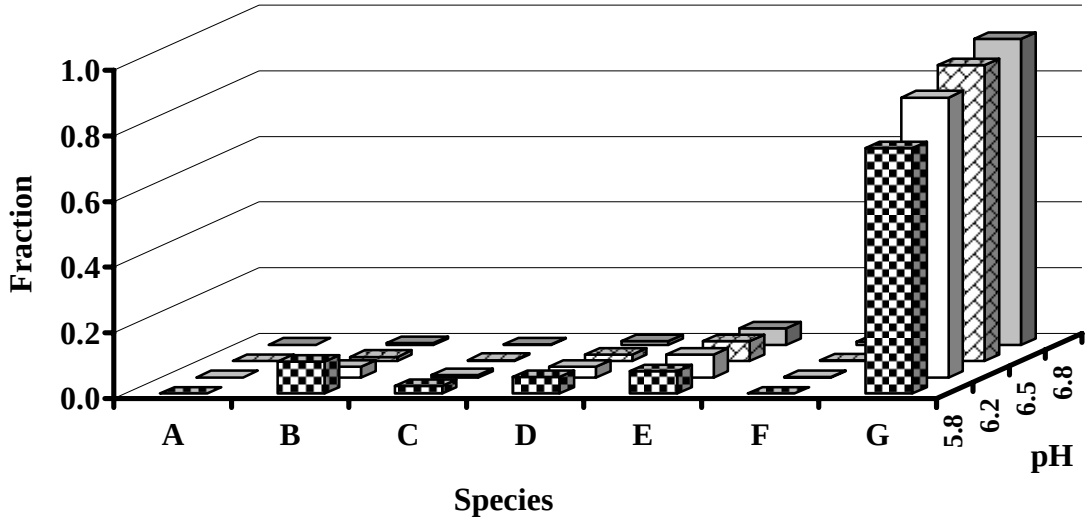

Figure 3.19 Copper speciation in rumen fluid as function of pH using 1:2 Copper histidine supplement at a copper concentration of 3.0 x 10^{-5} M. Calculations were done at Ionic strength of 0.15 M and temperature of 38 °C. For key to species see Figure 3.16

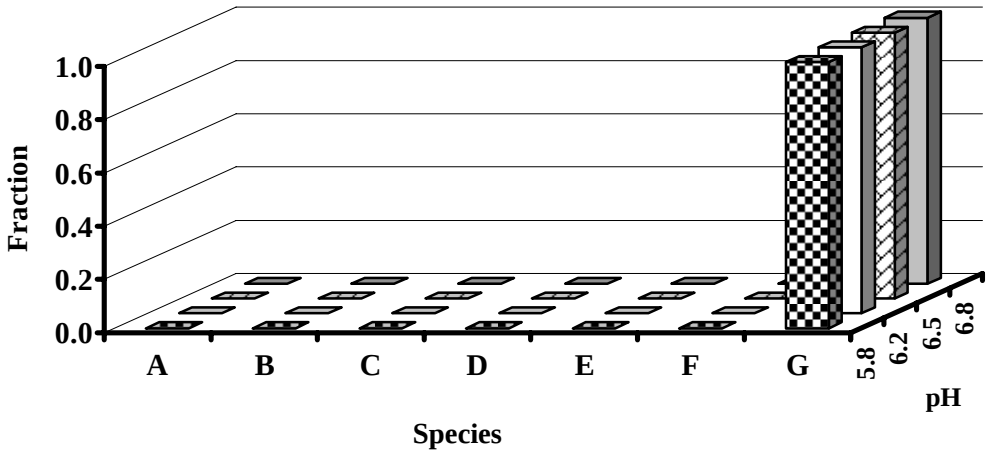

Figure 3.20 Copper speciation in rumen fluid as function of pH using 1:1 Copper EDTA supplement at a copper concentration of 3.0 x 10^{-5} M. Calculations were done at Ionic strength of 0.15 M and temperature of 38 °C. For key to species see Figure 3.16

Comparison of the speciation of copper in rumen fluid of the copper supplements discussed above at average ruminal pH of 6.3 is shown in Figure 3.21. Under these conditions, 14% of the administered copper exists complexed to glycine, 11% to lysine, 19% as methionine, 99 % as histidine and 100% as EDTA in rumen fluid. Thus of all the various copper supplements which have been looked at so far, our present understanding is that copper histidine and copper EDTA seem to be the ones that remains intact in rumen fluid. This observation is similar to what was encountered in bovine saliva (see Section 3.1.3.1).

The speciation profile of myriad of 'free' Cu, as well as net-positively charged (cationic species), net-neutral (neutral species) and net-negatively charged (anionic species) copper complexes as it occurs in rumen fluid is shown in Figures 22 to 25 over an extended pH window. Calculations were performed at an ionic strength of 0.15 M, a temperature of 38 °C and a Cu^{2+} concentration of 3.0×10^{-5} M. At lower pH values, the copper speciation is dominated by cationic complexes. Neutral complexes dominate at neutral pH and anionic complexes at higher pH. This is to be expected because at lower pH, most of the ligands are not fully deprotonated and thus the solution contains mostly uncomplexed Cu^{2+}, protonated ligands and cationic complexes (mostly protonated complexes). However as the pH of solution changes to neutral, most of the protonated complexes loose their proton(s) leading to the formation of (mostly neutral) complexes. Further deprotonation of the complexes occurs as the solution becomes basic, leading to the formation of mainly anionic complexes. This may be significant, because there is some limited absorption of LMM ligands in the rumen [59, 158]. Since it is mainly neutral species that are likely to be absorbed [159], there is the need to understand the charge distribution of the copper species as function of pH so as to get the idea of the amount of copper that is likely to be absorbed. Figure 22 to 25 shows that the charge distribution as function of pH is little affected by whether the copper is introduced into the rumen fluid as an inorganic salt, copper glycine, copper methionine or copper histidine. Thus the extent of neutral species that will be available for absorption will almost be the same whether copper is

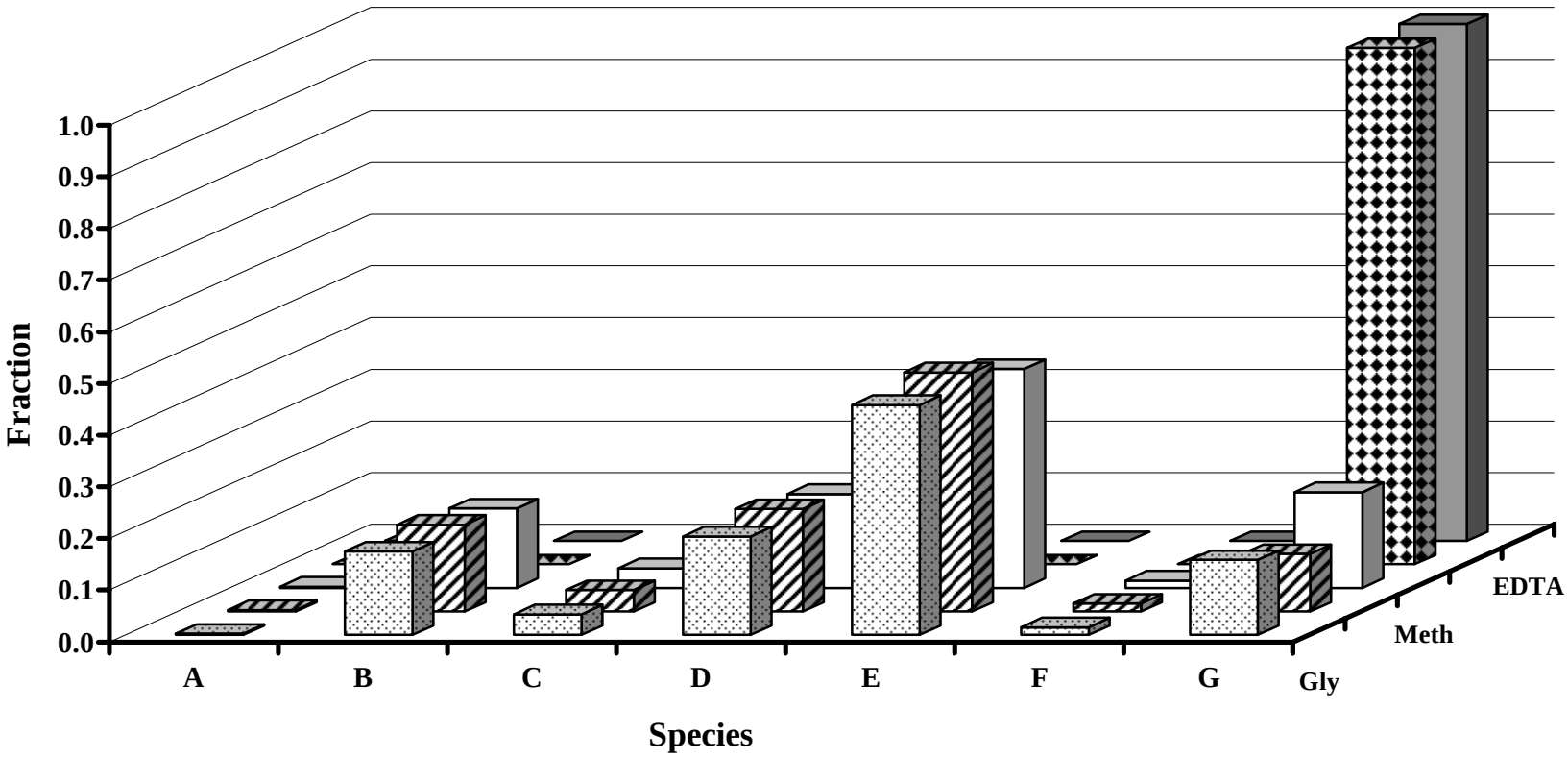

Figure 3.21 Comparison of speciation copper in rumen fluid of various copper supplements at ruminal pH of 6.3. Calculations were done at Ionic strength of 0.15 M; temperature of 38 °C and Cu^{2+} concentration of 3.0 x 10^{-5} M. See table 2.1 for concentrations of ligands. **A:** Free Cu^{2+}; **B:** Copper acetate complexes; **C:** Copper VFA complexes; **D:** Copper phosphate complexes; **E:** Copper carbonate complexes; **F:** Copper ammonia complexes; **G:** Copper amino acid complexes.

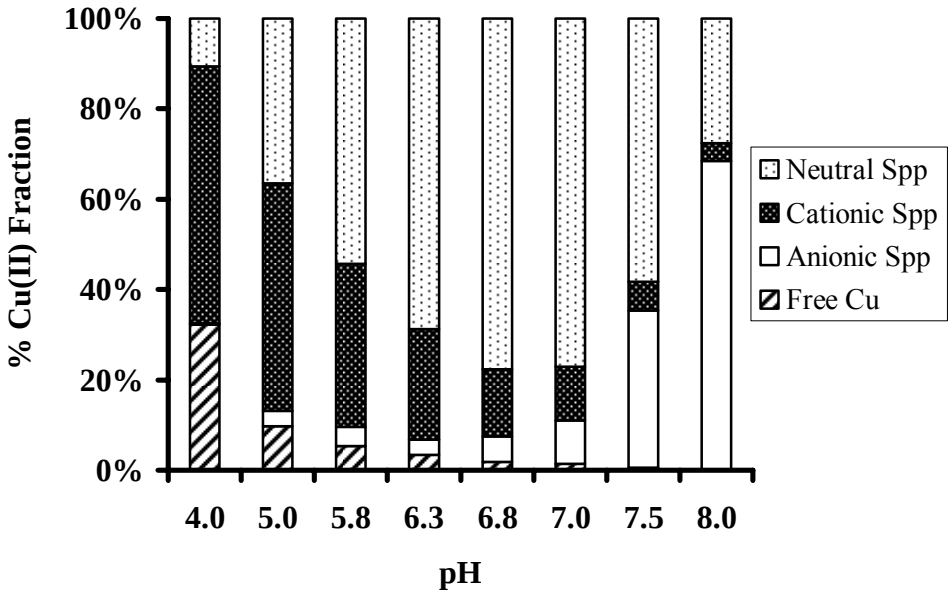

Figure 3.22 Charge distribution of Cu(II) species in rumen fluid. Copper introduced as inorganic salt.

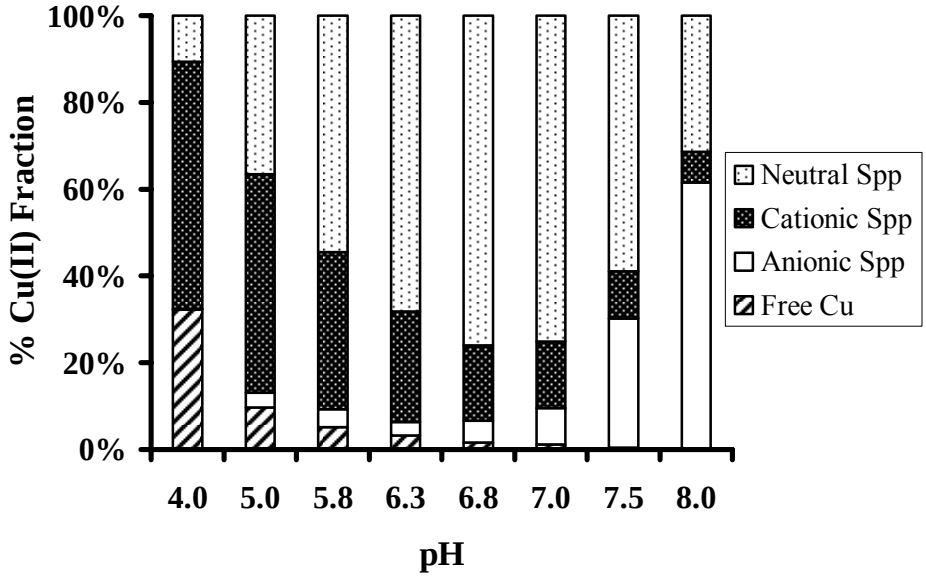

Figure 3.23 Charge distribution of Cu(II) species in rumen fluid. Copper introduced as copper glycine

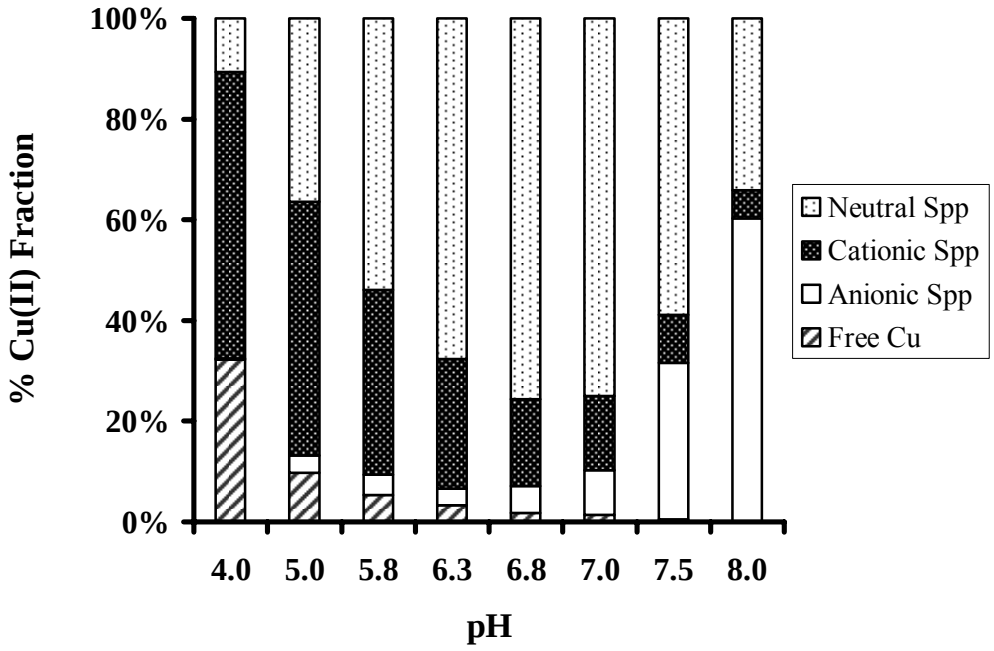

Figure 3.24 Charge distribution of Cu(II) species in rumen fluid. Copper introduced as copper methionine

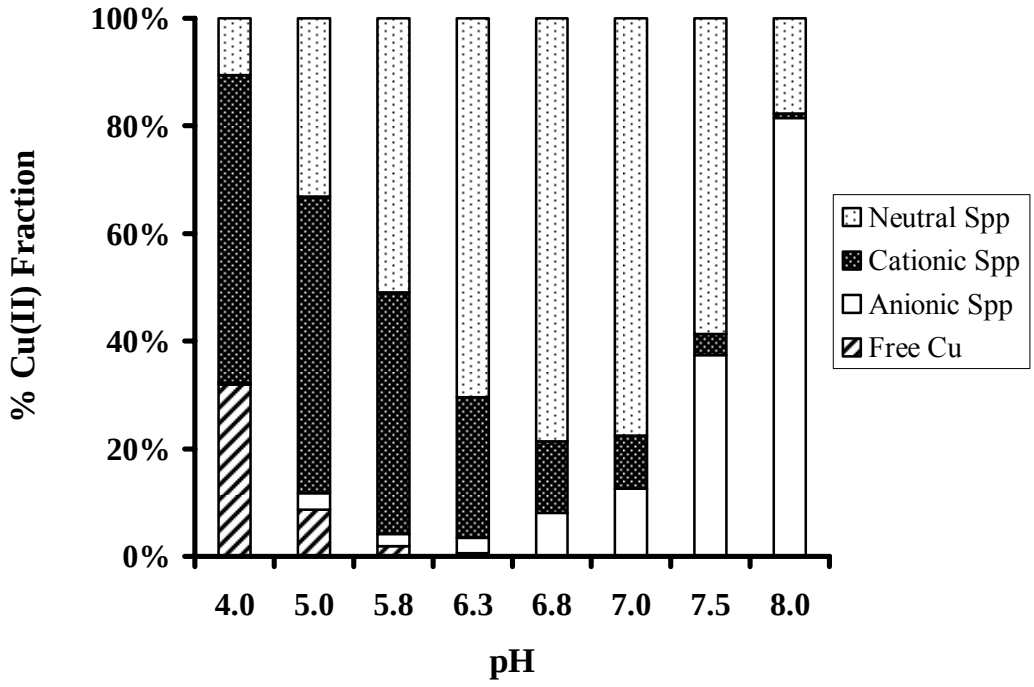

Figure 3.25 Charge distribution of Cu(II) species in rumen fluid. Copper introduced as copper histidine.

introduced as an inorganic salt, copper glycine, copper methionine or copper histidine.

3.1.5.3 Bovine Rumen (peptides)

The study was extended to computer simulations of the speciation of Cu(II)-(His-Lys), Cu(II)-(Thr(Ac)-His-Lys) and Cu(II)-(Asp-Thr(Ac)-His-Lys) in rumen fluid. These peptides have previously [102] been used as models for the N-terminal regions of bovine serum albumin (BSA,) which is responsible for transport of Cu(II) in the blood. The use of the model peptides have proven valuable in elucidating the structural features that contribute to the formation of a BSA-Cu(II) complex. Common forms of commercially complexed copper supplements presently available do not consist only of amino acids but also peptides as ligands to which essential trace metals are complexed [152, 160, 161]. Thus, these BSA models also serve as good candidates of peptide ligands for copper proteinate supplements due to their strong bonding to Cu^{2+} (see Table 2.7).

Results of computer simulation of the Cu speciation of Cu – peptides in rumen fluid (Figure 3.26) show that almost all the copper (>90%) is held by the peptide. This is not surprising considering the high formation constants of Cu(II) – peptide complexes (Table 2.7). Note also the similarity between the amount of copper held by histidine and the peptides. This throws light on the fact histidine play a very important role in the binding of copper. This because in all the three peptides, the imidazole nitrogen of the histidine in the peptide has been found [102] to play a pivotal role in the binding of copper.

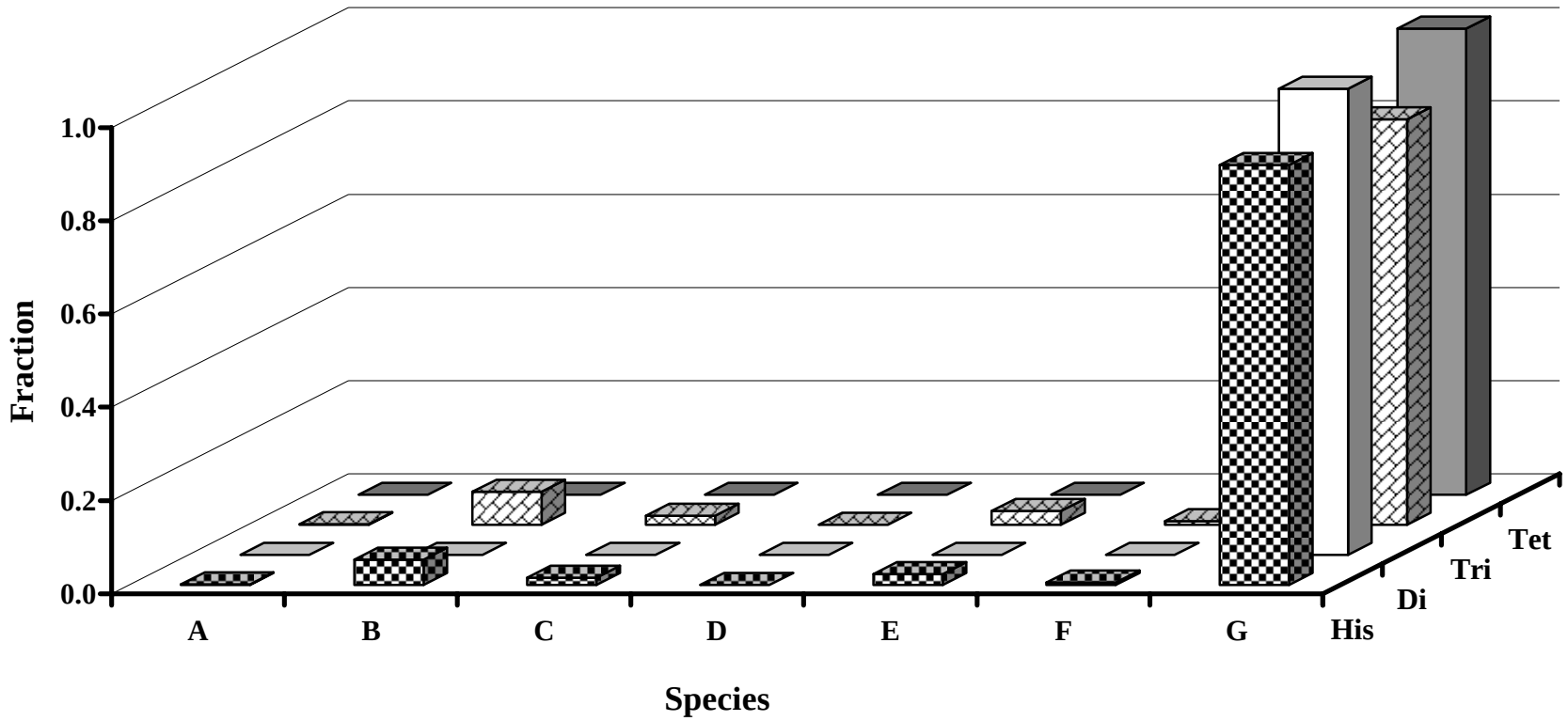

Figure 3.26 Comparison of 1:1 Cu-Peptide Speciation in Rumen fluid at pH of 6.3. Calculations were done at Ionic strength of 0.15 M; temperature of 38 °C and Cu^{2+} concentration of 3.0 x 10^{-5} M. See table 2.1 for concentrations of ligands. **A:** Free Cu^{2+}; **B:** Copper acetate complexes; **C:** Copper VFA complexes; **D:** Copper phosphate complexes; **E:** Copper carbonate complexes; **F:** Copper ammonia complexes; **G:** Copper peptide complexes

3.2 NMR STUDIES OF RUMEN FLUID

3.2.1 NMR Spectrum of Rumen Fluid

The simulated rumen fluid was obtained by putting together accurate concentrations of the various components of the rumen fluid used in the computer simulation described above (see Section 2.2.1 for sample preparation and experimental conditions). The resultant ^{1}H NMR spectrum is as shown in Figure 3.27. Peak assignment for the ^{1}H NMR spectrum was done in a previous study [58]. The large signal at a chemical shift of 2.049 ppm is from the $–CH_3$ group of acetic acid, and as expected it is not coupled to any other group. It has satellite peaks on either side, due to coupling to ^{13}C.

Figure 3.28 shows a typical spectrum of actual rumen fluid. The Binomial 1$\underline{3}$3$\underline{1}$ pulse sequence was employed to suppress the intense water signal. The 1$\underline{3}$3$\underline{1}$ sequence was a good choice of suppression technique; in addition to suppressing the huge water signal, it also helped in eliminating some of the broad signals that are associated with high molecular mass (HMM) ligands. Broad signals by definition in NMR have large spin spin relaxation rates. The rate of relaxation generally varies with size; proteins, being bigger in size than the VFA molecules, will relax faster [126]. The delay time could be such that the protein resonances would be reduced or nulled. After this time has elapsed non-zero responses can still be obtained for other, more slowly relaxing signals.

3.2.2 Monitoring Copper Speciation with the Volatile Fatty Acids

For proper understanding of the fate of the copper supplements in the rumen fluid, it is necessary to understand the interaction of copper with some major constituents of the rumen fluid. As the NMR spectrum has revealed that the major peaks in the spectrum are those of the Volatile Fatty Acid (VFA) components, it was decided to monitor speciation of copper in the rumen through the chemical shift changes that would accompany the addition of the metal to these components.

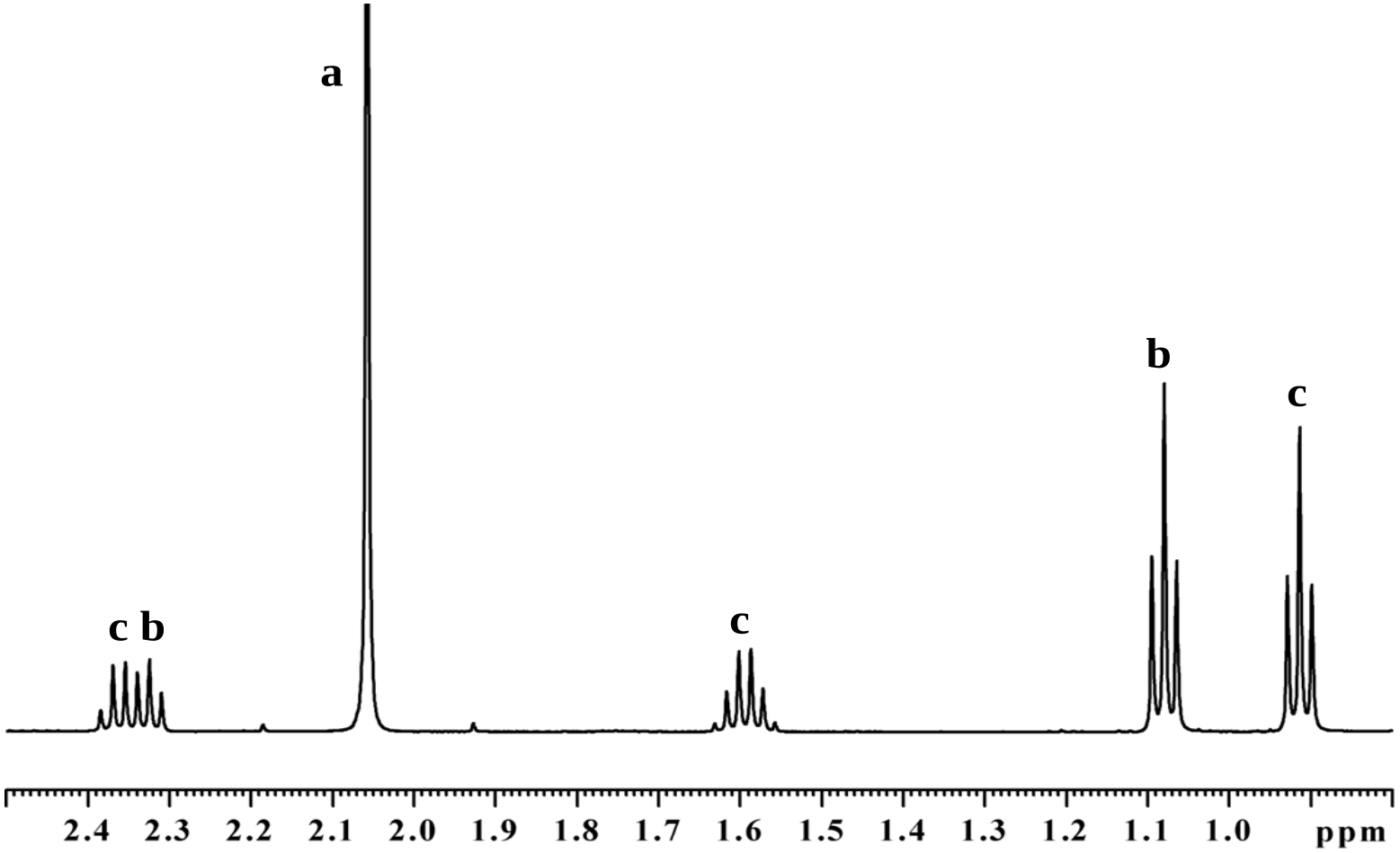

Figure 3.27 ^{1}H NMR spectrum of an artificial rumen liquor sample together with peak assignments, using the Binomial '1331' pulse sequence. (a) Acetic acid (b) Propanoic acid and (c) Butanoic acid

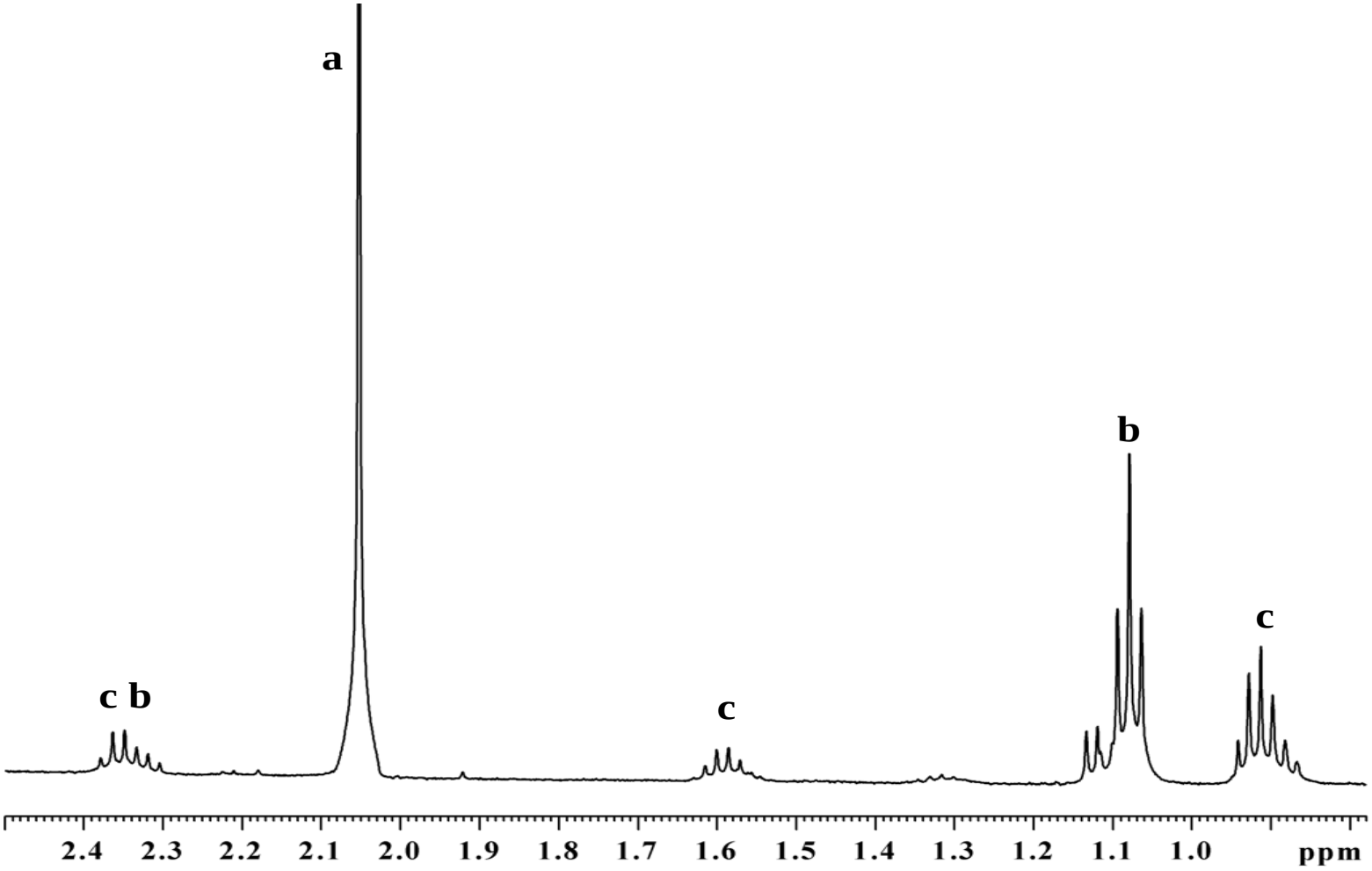

Figure 3.28 ^{1}H NMR spectrum of an actual rumen liquor sample together with peak assignments, using the Binomial '1331' pulse sequence. (a) Acetic acid (b) Propanoic acid and (c) Butanoic acid

To achieve this, it is first necessary to conduct detailed investigations into the NMR spectra of the VFAs and their interaction with Cu(II). This detailed investigation was conducted in a previous study [58]. From a preliminary investigation into the chemical shift changes that accompany the addition of copper to the VFAs, it was noted that the most consistent and pronounced chemical shift changes occur with the acetate methyl proton resonance. In addition, this is the most well-defined NMR peak, and acetic acid is the VFA with the greatest abundance in the rumen fluid samples. The acetate peak was therefore used to monitor the speciation of copper in the rumen fluid.

With the addition of copper(II) ions, Cu complexes are formed rapidly with acetate (see Section 1.4). The maximum concentration of metal ion to be added was limited mostly by the paramagnetic nature of Cu(II) ion, which give rise to efficient NMR relaxation and hence very broad resonances. As a result of which the chemical shifts cannot be established with an acceptable level of confidence (see Section 1.12.3). The amount of copper that can be added is also limited by solubility considerations, though the limitation was principally from the paramagnetic relaxation and not solubility. To minimise the incidence of copper hydrolysis which leads to the formation of insoluble $Cu(OH)_2$, and also to provide a basis for direct comparison with previous studies [58] all the NMR experiments were conducted pH of 4.0.

The complex formed by the acetate ion and copper, though not a particularly strong one, is enough to produce significant changes in the chemical shift of the methyl protons of acetic acid. This is because the unpaired electron of the Cu(II) ion produces a large local magnetic field at all nuclei in its vicinity, leading to substantial changes in chemical shift values (see Section 1.12.3). It is these changes that make the chemical shift of the methyl protons of acetic acid a useful probe in monitoring speciation of Cu(II) in rumen fluid.

The equilibria involved can be expressed as shown on page 134 (A representing acetate):

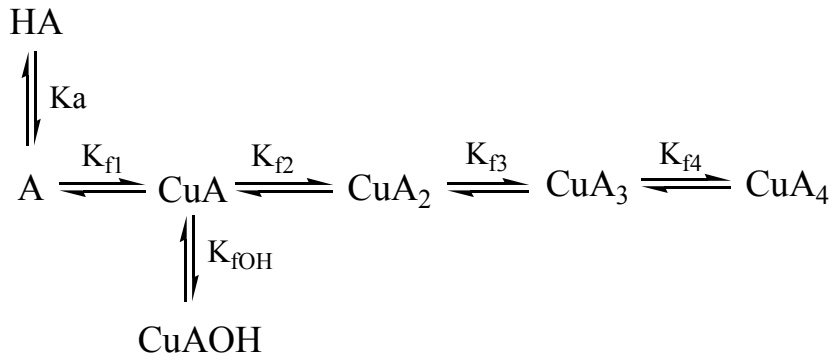

The acetate is mostly present in the free form. This is because of the excess amounts of acetate present in the rumen compared with trace amount of copper coupled with relatively low formation constants of copper-acetate complexes. Thus the amounts of the individual complexes in the sample are small. This is particularly so for the $Cu(A)_3$ and $Cu(A)_4$ and this makes it particularly difficult to establish reliable chemical shift values for each of the individual copper acetate complexes. To simplify the model, we fit instead to a model using a composite of all the copper acetate complexes, CuA_x. This composite contains the sum of all the copper species.

Figure 3.29 shows a plot of the changes in the chemical shift of acetate methyl protons encountered upon the addition of copper(II). The exchange between all the acetate species is fast on the NMR time scale, so only one signal is actually observed in each case. The observed signal is the average of the chemical shifts of the species participating in the equilibria, weighted by their relative amounts. Thus the observed chemical shift is given by

$$\alpha_{obs} = \alpha_A\delta_A + \alpha_{HA}\delta_{HA} + \alpha_{CuAx}\delta_{CuAx} \qquad \textbf{(3.8)}$$

The equations used in computing the α's are

$\alpha_{HA} = [H^+]/R$

$\alpha_A = K_a/R$

$\alpha_{CuA} = K_{f1}.[Cu].[A]/R$

$\alpha_{CuA2} = 2.K_{f1}.K_{f2}.[Cu^{2+}].[A]^2/R$

$\alpha_{CuA3} = 3.K_{f1}.K_{f2}.K_{f3}[Cu^{2+}].[A]^3/R$

$\alpha_{CuA4} = 4.K_{f1}.K_{f2}.K_{f3}.K_{f4}[Cu^{2+}].[A]^4/R$

$\alpha_{CuAx} = \alpha_{CuA} + \alpha_{CuA2} + \alpha_{CuA3} + \alpha_{CuA4}$ **(3.9)**

where R is the sum total of the terms for all the acetate species. It is represented by the formula

$$R = [H^+] + K_a + K_{f1}.[Cu].[A] + 2.K_{f1}.K_{f2}.[Cu^{2+}].[A]^2 + 3.K_{f1}.K_{f2}.K_{f3}.[Cu^{2+}].[A]^3 + 4.K_{f1}.K_{f2}.K_{f3}.K_{f4}.[Cu^{2+}].[A]^4 \quad \textbf{(3.10)}$$

With the help of these equations, the chemical shift values for the individual species were obtained using regression analysis. Values obtained are listed in Table 3.2.

The increased amounts of Cu are predicted to produce a consistent increase in the chemical shift of acetate as the Cu levels is increased. This is explained by the increasing fraction of the Cu- acetate complexes. This is not surprising considering the high chemical shift of the composite acetate copper complex, 16.83 ppm (Table 3.2).

Table 3.2 Calculated chemical shifts for acetate species

Species		**Chemical Shift, ppm**
Acetic acid	A	1.919(3)
	HA	2.071(4)
Copper acetate	[a]CuA_X	16.83(2)

[a]CuA_X refers to a composite of all the different copper acetate complexes.

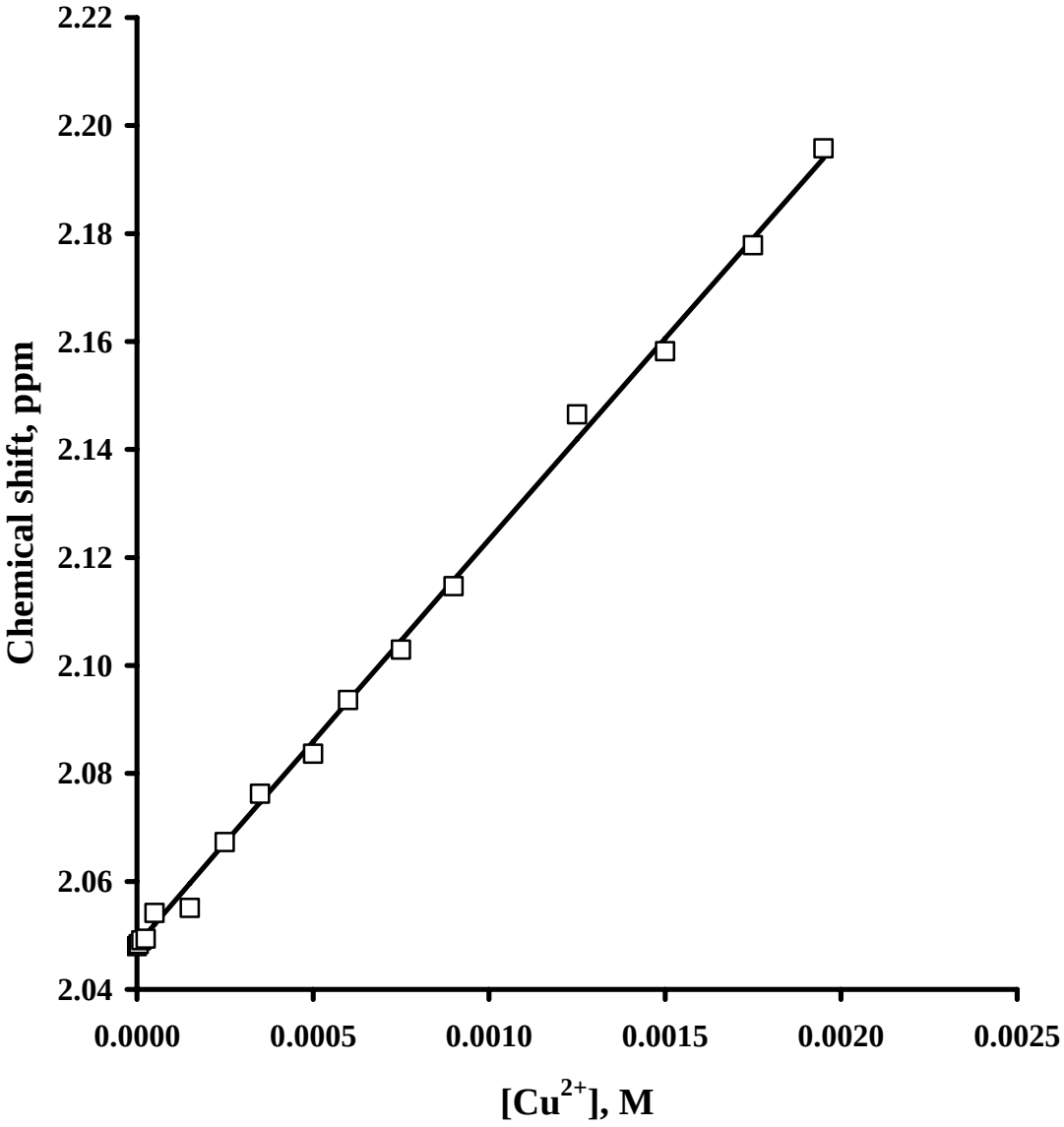

Figure 3.29 Chemical shift of methyl protons of acetic acid as a function of copper(II) concentration. See text for experimental details. Curve shows predicted values and points (□) show experimental values. Data obtained at a pH of 4.0 and a temperature of 38 °C

3.2.3 Validation of Computer Model

3.2.3.1 Speciation of Cu(II) in Rumen

As mentioned in the introduction (see Section 1.2), computer simulation results are incomplete and describe only those aspects that are considered relevant. It therefore becomes necessary to obtain some assurance that the model is a correct representation of the equilibrium in the rumen fluid (see Section 3.1.2). These tests would involve the comparison of calculated and experimentally determined values of some parameter.

From Section 3.2.2, the chemical shift of the acetate methyl protons has been found to respond to changes in the concentration of Cu(II). It was therefore the candidate of choice for monitoring the copper speciation in the rumen fluid by NMR. From knowledge of the species as well as the copper (II) acetate complexes, and using the computer simulation of the copper speciation, it is possible to predict the chemical shift changes that should result from the addition of different amounts of copper (II) solution to the rumen fluid. The chemical shifts changes of acetate in simulated rumen fluid were calculated and compared with experimentally measured values. Results from the model closely fit the information obtained from the experiment. Figure 3.30 shows the fit. It can thus be concluded that the results from the computer model adequately describes the speciation of Cu(II) with respect to LMM in the rumen fluid.

Another study was undertaken where varying amounts of lysine were added as an exogenous ligand to the rumen fluid. The addition of lysine in varying amounts was to stress the model to test for robustness. The choice of lysine is as result of its use to complex copper as chelated copper supplements. The speciation, and hence the chemical shift behaviour was also predicted from the computer model. Figure 3.31 illustrates changes in chemical shift of methyl protons of acetate as a function of copper(II) concentration as different amount of lysine are added. The computer model predicts that the addition of 0.8 m**M** lysine would not alter the speciation significantly, due to the low concentration of the added lysine compared with the concentration of other ligands

present. When actual ^{1}H NMR experiments were conducted this was also the case. The model closely predicts the observed changes in chemical shift. Small deviations are the result of experimental errors in the NMR, and show no systematic trend away from the predicted line.

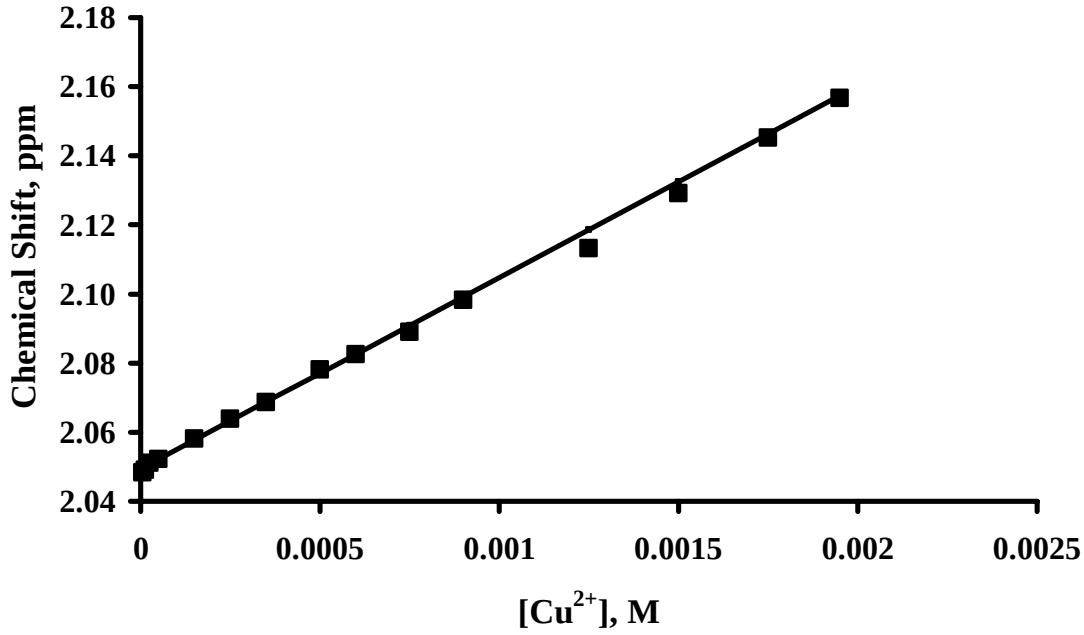

Figure 3.30 Chemical shift of methyl protons of acetic acid in simulated rumen fluid as a function of copper (II) concentration. Curve shows predicted values and points (■) show experimental values.

The computer model predicts a further change in the speciation picture when 4.0 m**M** lysine is added. With this higher concentration of lysine, and considering the strength of the Cu-lysine complexes, lysine should bind more of the Cu(II). This reduces the amount of Cu-acetate complexes, and hence a reduction in the chemical shift of the acetate is predicted. However, when these predictions are compared to the data obtained from an actual ^{1}H NMR experiments, some discrepancy is noted between the model and the experimental values. The reasons for this discrepancy are discussed below.

When 20 m**M** of lysine were added, the model predicts that the bulk of the copper will now be present as copper lysine complexes. The effect on the acetate

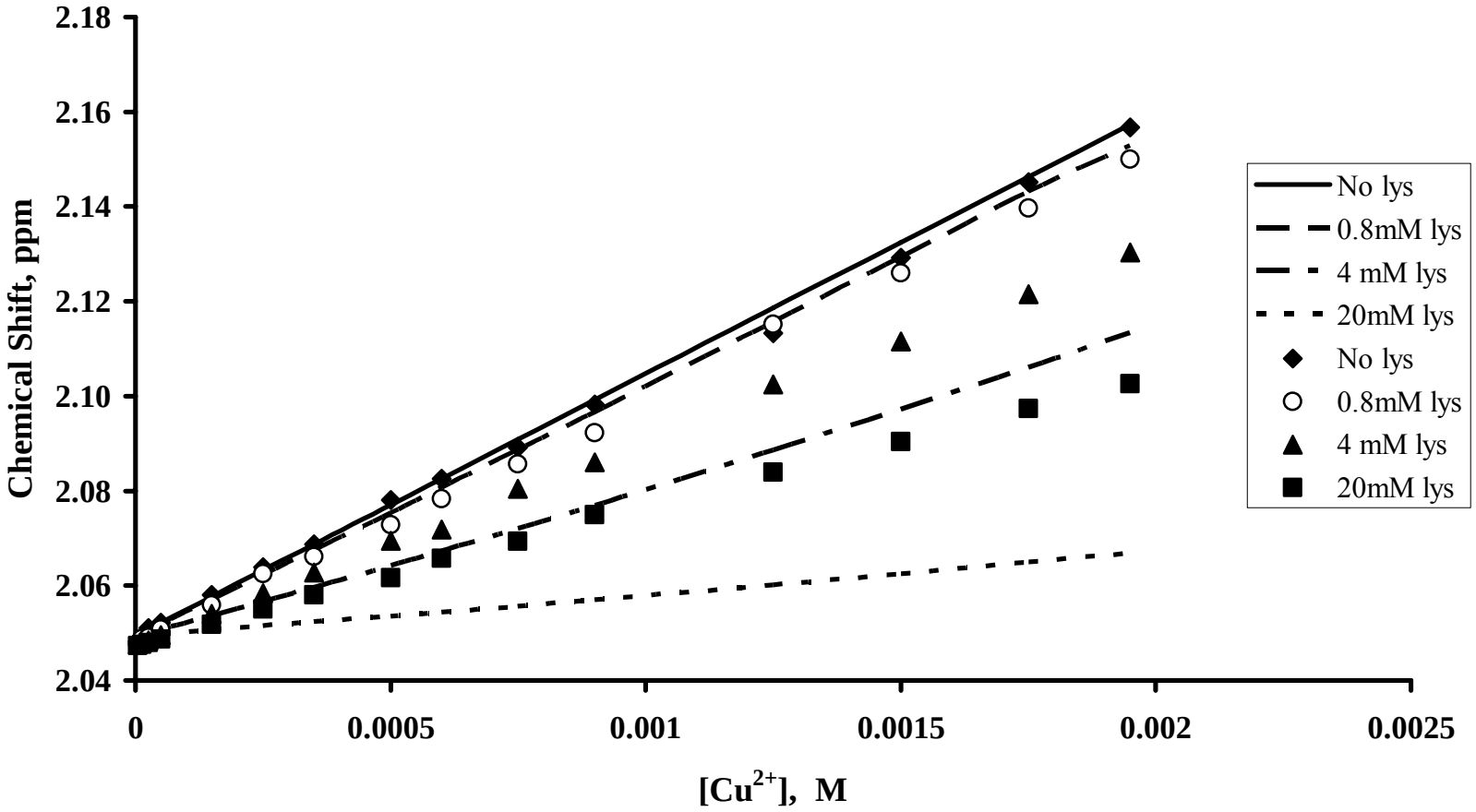

Figure 3.31 Changes in chemical shift of methyl protons of acetate with different amount of lysine as a function of copper(II) concentration in simulated rumen fluid. Points represent experimental data, while curves represent model prediction

chemical shift is similar to that at 4.0 m**M** added lysine, but more pronounced. However, experimental data shows little change in the chemical shift of acetate with the increasing levels of copper. The discrepancy between model and experiment is now pronounced.

It appears that this model does not adequately explain the speciation at this level of lysine. The model seems to predict a lower amount of Cu-acetate complexes than that actually observed. The model underestimates the level of complexation between lysine and Cu; it appears as though there is more lysine complexing the Cu than is actually present. The extent of the discrepancy is more pronounced with increasing levels of copper.

There are a number of reasons that could possibly account for this discrepancy. It could be a result of using values for the metal concentrations that do not accurately reflect those appearing in the model. To explore this possibility, the levels of metals in the fluid were measured using Inductively Coupled Plasma Atomic Emission Spectroscopy in a previous study [58]. The results obtained showed some differences from metal concentration values appearing in the literature. These, however, did not appreciably alter the results obtained from the model, having a minimal effect on the chemical shift variation with added copper levels.

Another possible explanation for the incongruity is that it is due to some interaction of lysine with some species in the rumen liquor. To ascertain whether this was the case, NMR experiments were conducted for increasing lysine concentration in the simulated rumen fluid in a previous study [58] and the results did not show any variation in the chemical shift of the various components of the rumen fluid. Thus a possible interaction of lysine with any of the species in the rumen fluid was ruled out.

The discrepancy could also be due to lack of knowledge of all possible complexes that could form. In particular, the possibility of formation of mixed ligand complexes was explored since formation of mixed ligands are very common in

biofluids [41]. The formation of low molar mass complexes in biofluids results from multimetal-multiligand equilibria involving exchangeable metal ions, amino acids and other biological ligands. Because potential bioligands in rumen fluid exceed Cu(II) ions in number and quantity, the possibility of the formation of Cu(II) mixed ligand complexes will be very high since the Cu(II) ion has been found (see Section 1.3) to form mixed ligands readily. Probable mixed ligand complexes considered in this context include acetopropionatocopper(II), acetadiaminocopper(II) and acetalysinatocopper(II) (Figure 3.32)

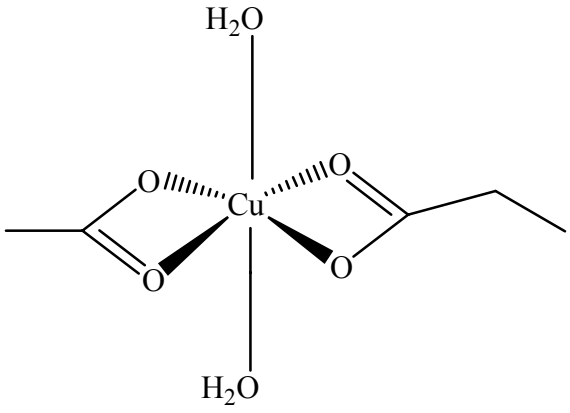

(a) Acetopropionatocopper(II)

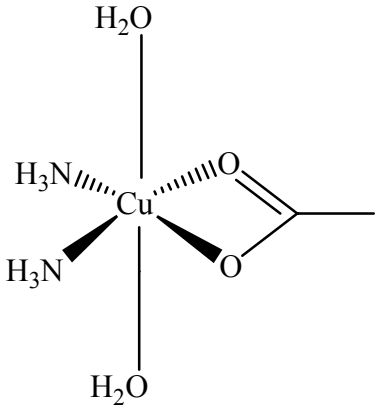

(b)Acetodiaminocopper(II)

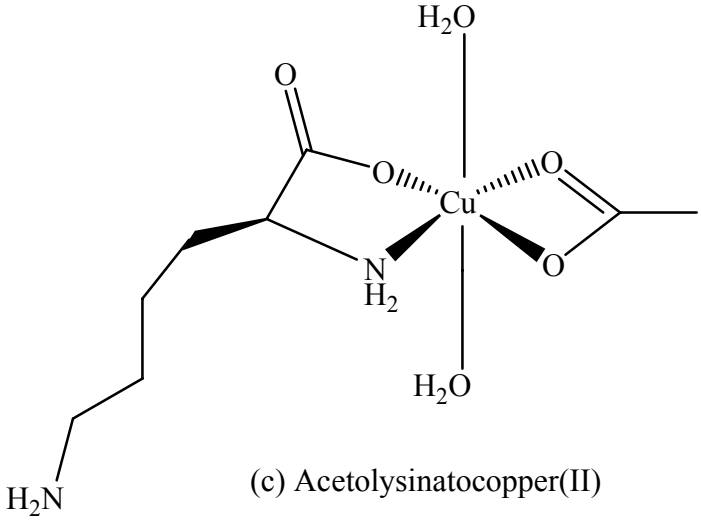

(c) Acetolysinatocopper(II)

Figure 3.32 Possible Mixed ligand complexes of Cu(II) formed in rumen fluid

The choice of acetate as a ligand in all the three mixed ligand complexes considered is a result of it being the most abundant ligand in the rumen and most importantly as it is the candidate of choice for monitoring the copper speciation in the rumen fluid by ^{1}H NMR. Propionate was considered in the mixed ligand complex (a) since it is the second most abundant VFA in the rumen and share similaritires with acetate in the way in which they it bonds to Cu. Since Cu(II) ion is a borderline metal ion according to Pearson's Hard Soft Acid Base (HSAB) concept, it has preference for nitrogen-based ligands. Thus ammonia, although present in rumen fluid in relatively small amounts was considered in another mixed ligand comlex formation (b). The amino acid lysine is known to form stable complexes with Cu(II) with coordination taking place via the α-amino and the carboxylate group so as to form a five membered chelate ring. Since Cu(II) has six coordination sites, the other four remaining sites would be available for coordination by other ligands in the rumen. Thus a mixed ligand of Cu(II), lysine and acetate was considered. This consideration was compnded by the fact that it was the introduction of lysine as exogenous ligand in to the speciation that led to the observed discrepancy.

The mixed ligand species and their formation constants, estimated from their 1:1 copper complex formation constants (Table 3.3) by calculation using Equation 1.11 [46, 47, 162], were introduced into the computer model one after the other. The mixed ligand complex formation involving acetate and lysine introduced into the computer model, gave a much improved fit to the experimental data, as shown in Figure 3.33.

Table 3.3 Estimated formation constant (log $\beta_{pqs} = [M_pL_qA_s]/[M]^p[L]^q[A]^s$) of Mixed ligand complexes of copper, acetate and amino acids used in rumen simulation studies[46, 47, 162].

System	p	q	s	log β_{pqs}
Copper-Acetate-Lysine	1	1	1	8.8
Copper-Acetate-Glycine	1	1	1	9.5
Copper-Acetate-Methionine	1	1	1	8.2

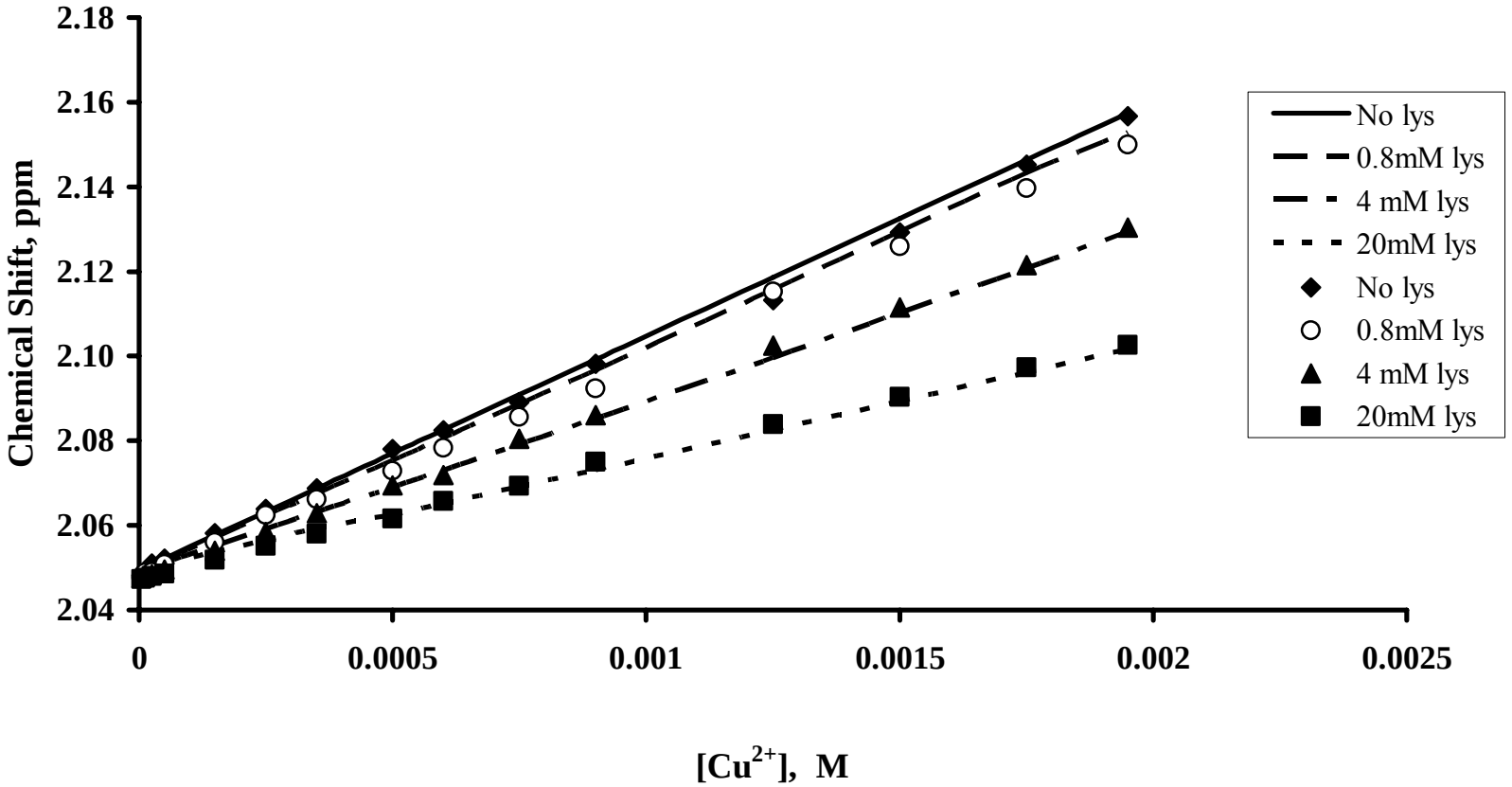

Figure 3.33 Changes in chemical shift of methyl protons of acetate with different amount of lysine as a function of copper(II) concentration in simulated rumen fluid. Model includes mixed-ligand complexes. Points represent experimental data, while curves represent model predictions.

This implies that as lysine is introduced into the rumen fluid, it is unable to strip copper completely off the acetate, but rather forms a mixed ligand complex with it. This complex, which was previously unaccounted for in the computer model, also contributes to overall acetate chemical shift, accounting for the discrepancies observed between the experimental data and the model.

The same experiments were conducted with actual rumen fluid. The results obtained (Figure 3.34) are similar to those obtained for simulated rumen fluid above. As the lysine concentration increases, there is a reduction in the chemical shift of the acetate due to stripping of Cu(II) from the acetate by the stronger-binding lysine. Comparison of the predicted chemical shift of the acetate methyl protons from computer model (which include the mixed ligand complex of copper acetate and lysine) and that obtained from the ^{1}H NMR experiments showed a remarkable agreement. This is in contrast to previous studies, [58, 163] which did not include the Cu(II)-acetate-lysine mixed ligand complex, resulting in a discrepancy between the chemical shifts of the acetate methyl protons predicted from the computer model and those obtained experimentally.

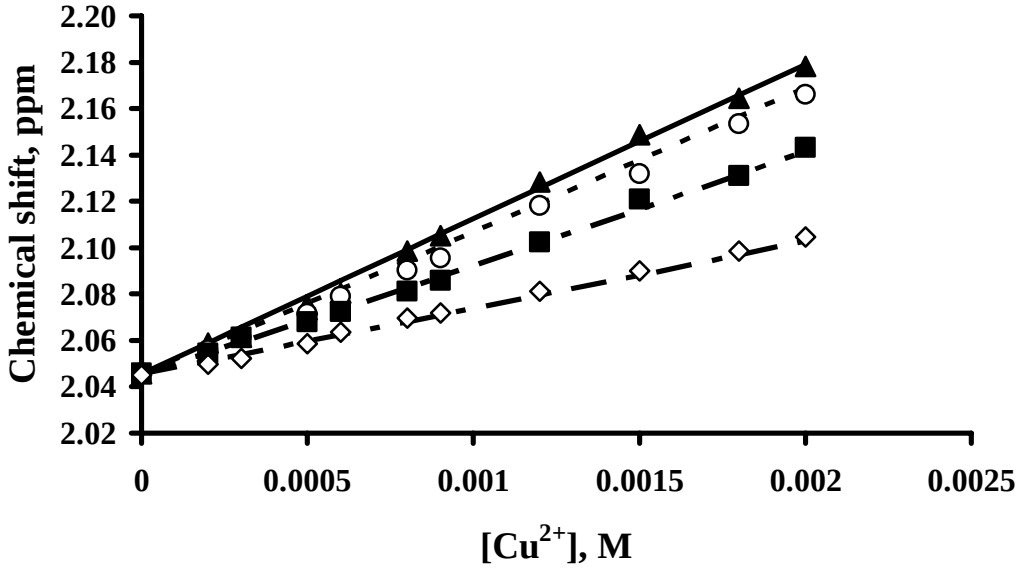

Figure 3.34 Changes in chemical shift of methyl protons of acetate with different amount of lysine in rumen fluid as a function of copper(II) concentration. Points represent experimental data while curves represent model predictions.

3.2.3.2 Speciation of Cu(II) Supplements in Rumen

As reported above for copper lysine, the results of the computer simulations involving copper glycine and copper methionine were also validated with ^{1}H NMR experiments, the monitored parameter being the chemical shift of the methyl protons of acetate as before [58, 163].

Similar to the observation with copper lysine as detailed above, there was an increase in discrepancy between the model-predicted chemical shifts and the observed chemical shifts as the concentration of the amino acid was increased. The implication is again that the model does not adequately explain the speciation of copper at this level. The possibility of formation of mixed ligand complexes was once again explored, as in the lysine case. Mixed-ligand complex formation between copper, acetate and the amino acid, when introduced into the computer models, resulted in a much improved fit to the experimental data, as shown in Figures 3.35 and 3.36.

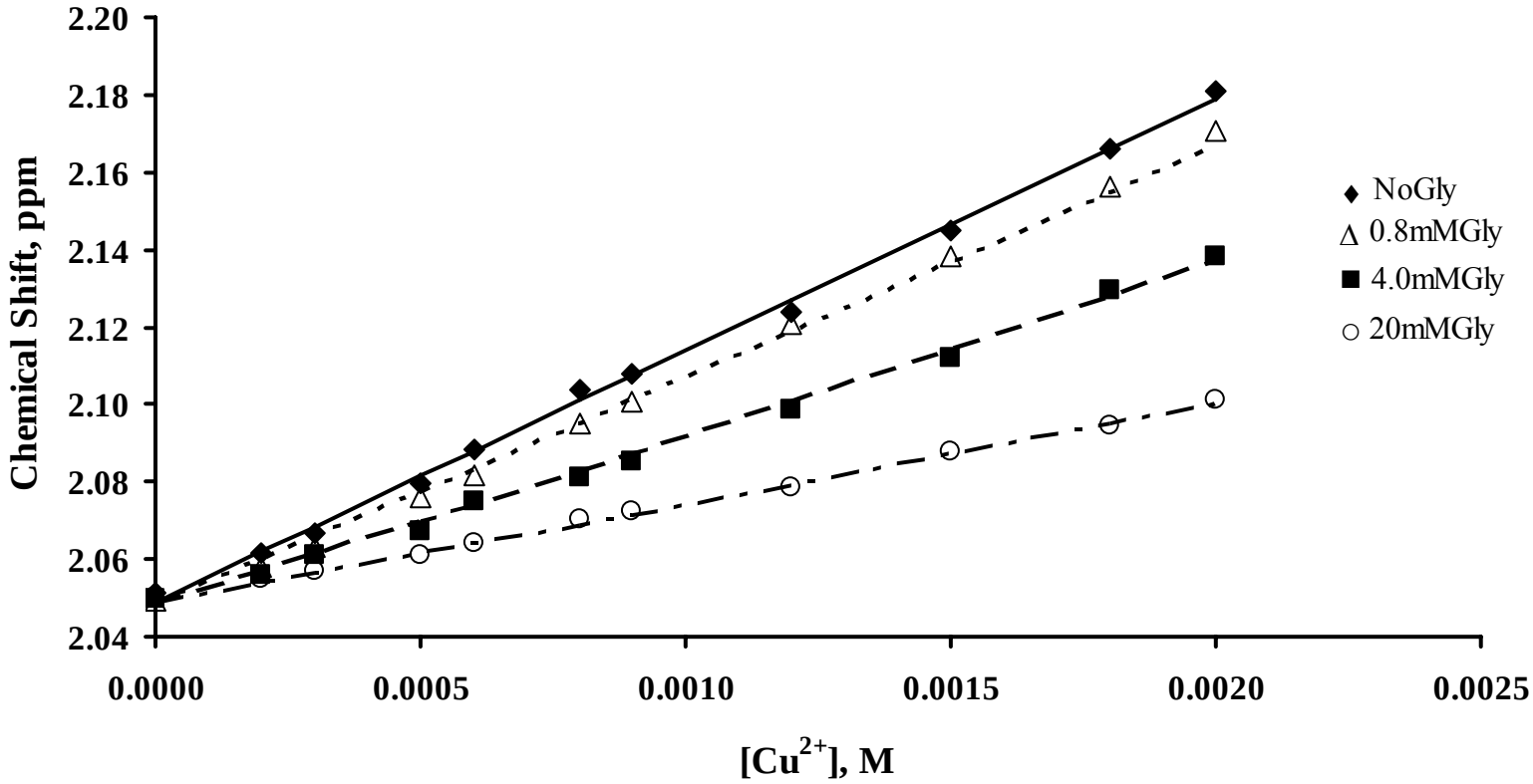

Figure 3.35 Changes in chemical shift of the acetate protons in actual rumen fluid as a function of added copper (II) concentration. Points represent experimental data while curves represent model predictions. Model includes mixed-ligand complexes. Each line represents a different glycine concentration

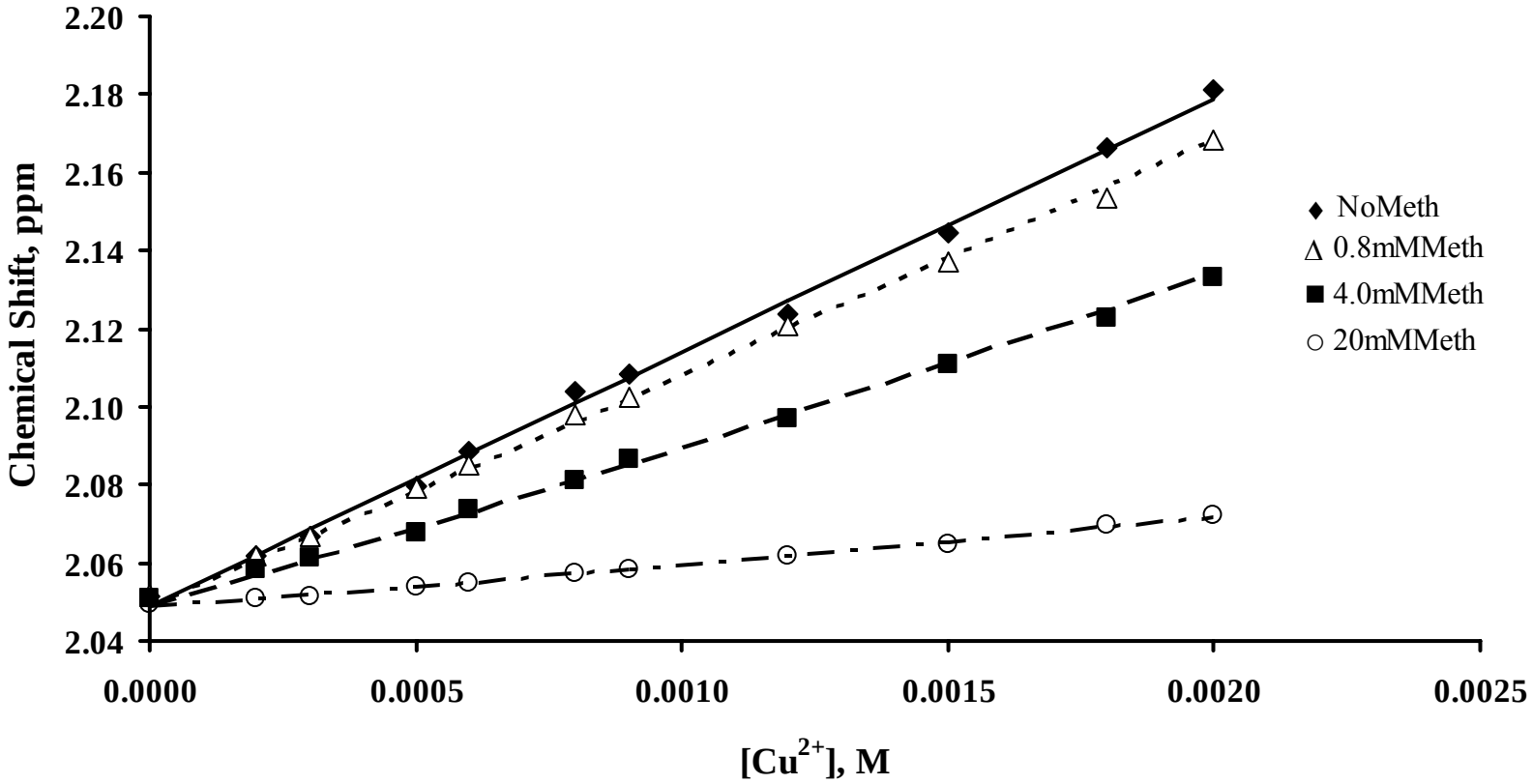

Figure 3.36 Changes in chemical shift of the acetate protons in actual rumen fluid as a function of added copper (II) concentration. Points represent experimental data while curves represent model predictions. Model includes mixed-ligand complexes. Each line represents a different methionine concentration.

3.3 SPECIATION MODELING OF COPPER(II) SPECIATION IN THIOMOLYBDATE – CONTAMINATED RUMEN FLUID

3.3.1 Computer Simulation of the formation of Thiomolybdates in Rumen

Thiomolybdates (TMs) are known to be formed in ruminants. Microbial activity in the rumen can produce sulfides by the reduction of sulfates and from the degradation of sulfur-containing amino acids. Based on numerous feed studies, it has been concluded that the TMs are formed from ingested MoO_4^{2-} and sulfides. This has been confirmed by *in vitro* synthesis of TMs in solution from MoO_4^{2-} and water soluble sulfides and subsequently under simulated rumen conditions (see Section 1.11).

The formation of the TMs has been found to be kinetically controlled; they are formed by the sequential replacement of O^{2-} by S^{2-} ion, to give ultimately the MoS_4^{2-} ion. Kinetic studies done on the formation of TMs have shown that the rate of O^{2-} replacement decreases with increasing S substitution, the reverse reaction rates, giving ultimately the molybdate ion, showing a similar trend *i.e.*, MoS_4^{2-} being the least reactive (see Section 1.10.2).

For the simulation of the TM formation under rumen-like conditions, the forward reaction (formation of TMs) was assumed to proceed through a pseudo first order reaction with respect to TMs, and likewise the backward reaction (hydrolysis of TMs). This is because in modeling the formation of TMs, use was made of kinetic data (see Table 2.8) from the literature [99-101, 150] which were obtained under pseudo first order conditions with respect to molybdate and TMs. That is in most of the TM formation kinetic studies, sulfide concentrations were in excess of the molybdate and the TMs. This is not surprising since in the rumen itself, the ratio of sulfide to molybdenum is usually between 100 and 1000 to 1 [110].

As for any time-dependent physical phenomenon, the series of rate expressions for each chemical species in the TM formation scheme can be represented by a set of ordinary differential equations (ODE's). If (pseudo) first-order behaviour is assumed, these will be linear. These can be then solved to obtain the time-dependent evolution of the concentration of each TM, with boundary constraints defined by the initial concentration of MoO_4^{2-} (see Section 2.3).

Three methods were considered for solution of ODE's include Eulers's method, the Runge – Kutta method and the Laplace transform:

Euler's method is the simplest method of obtaining a numerical solution of a differential equation. It approximates the solution to a first-order linear differential equation with initial values using the forward difference approximation, i.e.:

$$\frac{dy}{dx} = F(x,y) \approx \frac{\Delta y}{\Delta x} = \frac{y_{i+1} - y_i}{x_{i+1} - x_i} \qquad \textbf{(3.11)}$$

The advantage of this method is that it can easily be expanded to handle systems of any complexity. Although it is a simple method, for accurate work like the simulation of TM formation in the rumen, small step sizes are required. This means relatively long computation times, and possibly, incorrect results due to accumulated round-off errors.

The Runge-Kutta method for numerical solution of differential equations numerically integrates ordinary differential equations ($dy/dx = F(x,y)$) by using a trial step at the midpoint of an interval (x_i and x_{i+1}) to cancel out lower-order error terms. The most widely used Runge-Kutta formula involves terms evaluated at x_i, $x_i + \Delta x/2$ and $x_i + \Delta x$. For the purpose of this study, the fourth order Runge-Kutta method was used. The fourth-order Runge-Kutta equations for $dy/dx = F(x,y)$ are

$$y_{i+1} = y_i + \frac{T_1 + 2T_2 + 2T_3 + T_4}{6} \qquad \textbf{(3.12)}$$

where

$$T_1 = F(x_i, y_i)\Delta x$$

$$T_2 = F(x_i + \frac{\Delta x}{2}, y_i + \frac{T_1}{2})\Delta x$$

$$T_3 = F(x_i + \frac{\Delta x}{2}, y_i + \frac{T_2}{2})\Delta x$$

$$T_4 = F(x_i + \Delta x, y_i + T_3)\Delta x$$

If more than one variable appears in the expression, then each is corrected by using its own set of T_1 to T_4 terms. Although this method is reasonably simple and robust and is a good general candidate for numerical solution of differential equations when combined with an intelligent adaptive step-size routine, results obtained from this study showed a significant and unacceptable error in TM formation simulations. After fifteen half lives, the total concentration of TMs present far exceeded the initial concentration of the molybdate which was used as a constraint. Thus the use of this method was abandoned.

This led to the use of the ***Laplace transform,*** as the only one of these methods capable of giving an exact analytical solution for the differential equations describing the formation of TMs.

The Laplace transform, $F(s)$, of a function $f(t)$ is given by the integral

$$F(s) = \int_0^\infty \exp(-st) f(t) dt \qquad \textbf{(3.13)}$$

In this expression the function $f(t)$ is transformed through the integral operation into a function of s and is called the inverse Laplace transform of $F(s)$. The shorthand notation describing the relationship between the Laplace transform pair is given by

$$F(s) = L\{f(t)\}$$

and

$$f(t) = L^{-1}\{F(s)\}$$

The exact analytical solution (see Appendix A.2 for exact analytical solution) obtained from the Laplace transform of the differential equations (see Equation 2.8) of the kinetics of TM formation was encoded in an Excel spreadsheet, and the concentrations of TMs calculated as a function of time using kinetic data obtained from literature (see Table 2.8).

Figure 3.37 shows the results. These bear a resemblance to an earlier experimental observation in which TMs formed from the reaction of Na_2MoO_4 and ammonium sulfide in solution at ruminal conditions (pH 7.0. ionic strength 0.2 M, and temperature 38 °C) was plotted against time after mixing of the reagents (see Figure 1.5).

Within 300 seconds (5 min) 80% of the TM formed is TM2. This is in agreement with an experimental observation [102] that TM2 is rapidly formed from MoO_4^{2-} in the presence of excess sulfide. There is then a steady decline of TM2, with a concomitant increase in TM3. A substantial amount (63%) of the TMs exists as TM3 within 30 minutes. The graphs for the levels of TM2 and TM3 are almost symmetrical, suggesting that TM3 is formed from TM2. The formation of TM4 is slow but noticeable within 30 minutes. TM4 then increases steadily, constituting about 27 % of the TMs after 3 hours.

The mean residence time of sulfide in the rumen of sheep is reported to be 107 minutes at which time 81.5%, 14% and 5% of TMs formed exist as TM3, TM4 and TM2 respectively. This is not surprising, considering the fact that these TMs have all been found to exist in the rumen.

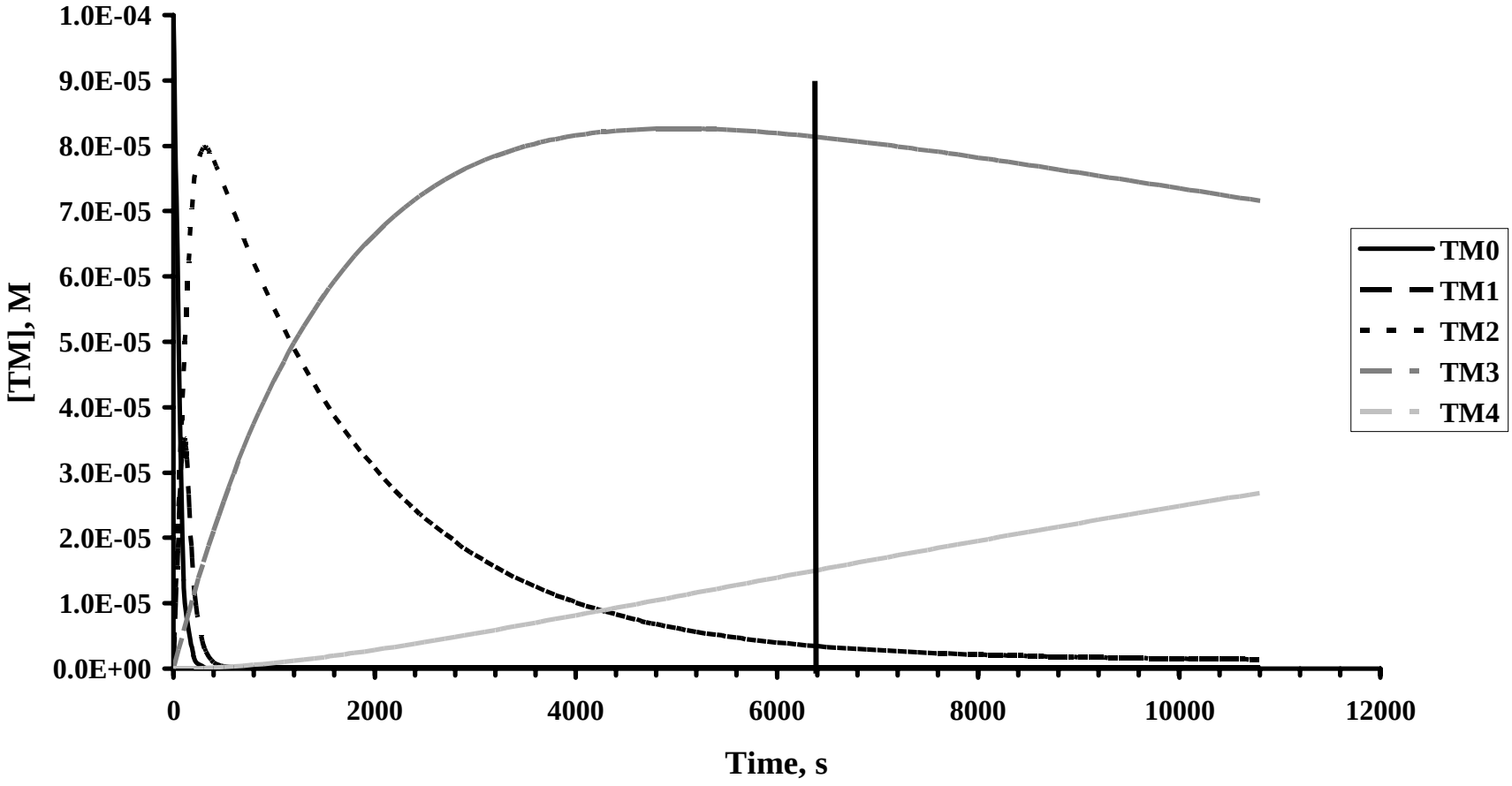

Figure 3.37 Computer simulation of formation of thiomolybdates: TMs as a fraction of total Mo present at different times. The vertical line represents mean residence time of S^{2-} in the rumen. Initial concentration of MoO_4^{2-} is 1.0 x 10^{-4} M.

The lower TMs are generally only present in low concentrations. TM1 forms quickly, rising within ~ 100 s to a peak of approximately 35% of total TMs, but then quickly declines. No appreciable amount of molybdate was present after 300 seconds.

3.3.2 Potentiometric study of Cu(II) – Thiomolybdate interaction using Cu(II) ISE

3.3.2.1 Synthesis of Tetrathiomolybdates

The sequential replacement of O^{2-} by S^{2-} leading to the formation of TM4 was found to be favored by a somewhat lower pH, longer reaction times, higher S : Mo ratios and higher temperatures. This is in agreement with an earlier study [102] in our group. The successful use of ammonium sulfide in these syntheses is consistent with the idea that HS^- is the nucleophile [99], not S^{2-} [120, 164] or H_2S [98, 165]. The first and second acid dissociation constants of H_2S are 1.6 x 10^{-7} and 1.0 x 10^{-17} respectively [166]. Thus, whether sulfur is originally added as H_2S, HS^- or S^{2-}, in aqueous solutions at neutral to moderately alkaline pH values HS^- is the most prevalent species of the three [102].

3.3.2.2 UV/Visible Spectral Analysis

Figure 3.38 shows a typical TM4 UV/visible spectrum with intense absorptions at 468 nm, 317 nm and 241 nm. The 'bump' at the wavelength of 396 nm is due to a small amount of TM3. Purity analysis using data obtained from the UV/visible spectrum shows that TM4 product was 97 % pure. The percentage purity was calculated using a non – linear squares approach to optimize the fit of the acquired UV/Visible spectral data to a Beer's law model.

$$A_{calc}(\lambda) = \alpha_{TM4}A_{TM4}(\lambda) + \alpha_{TM3}A_{TM3}(\lambda) \quad \textbf{(3.14)}$$

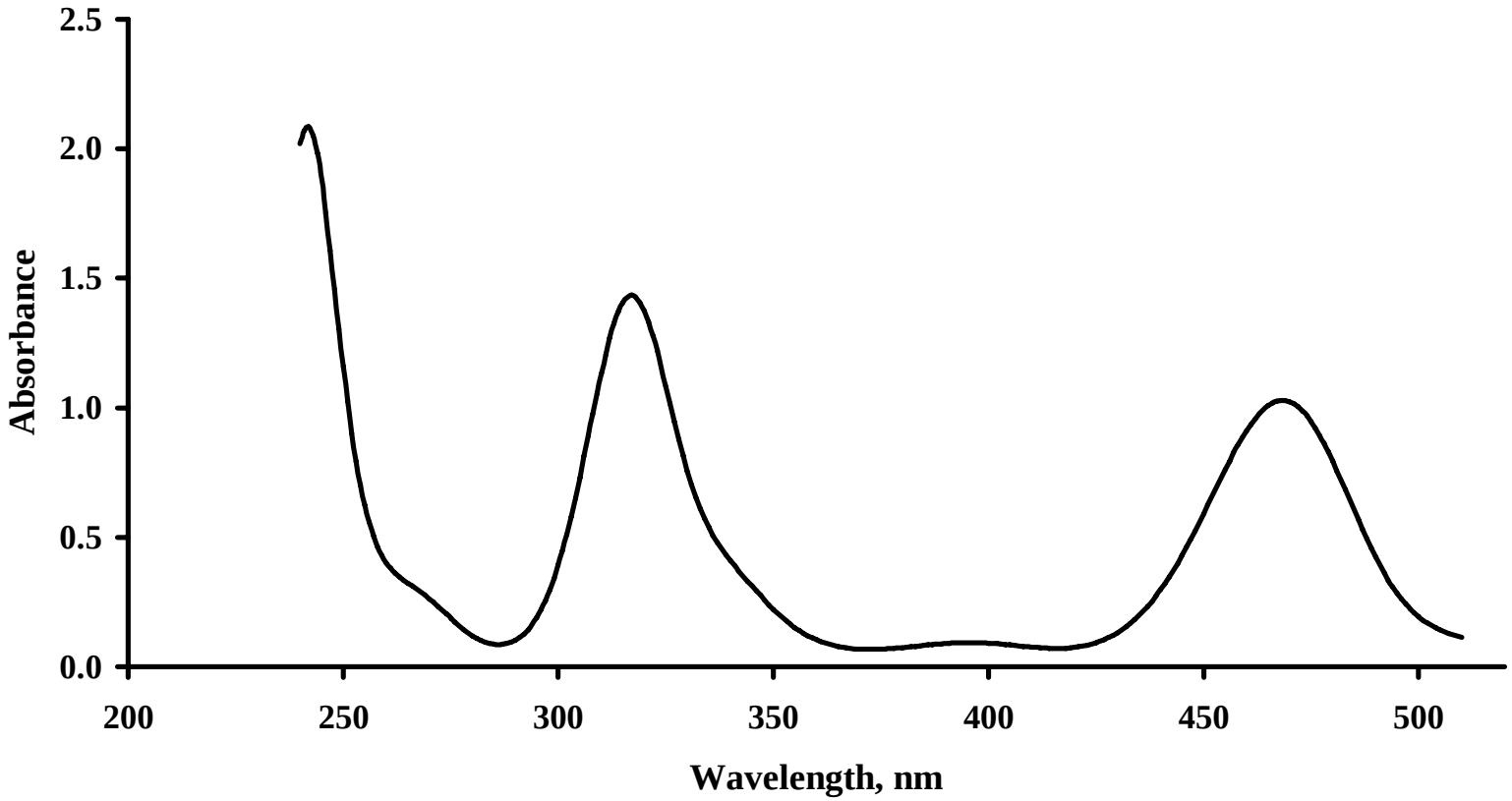

Figure 3.38 UV/visible spectrum of tetrathiomolybdate (TM4) obtained at room temperature. The concentration of TM4 was 0.1 m**M**

where $A_{TM4}(\lambda)$ and $A_{TM3}(\lambda)$ are the individual absorbances at the wavelength λ for TM3 and TM4 respectively, and α_{TM4} and α_{TM3} their mole fractions in the sample [102].

3.3.2.3 Calibration of Copper(II) Ion-Selective Electrode (ISE)

Ion selective electrodes (ISEs) are potentiometric chemical sensors that respond directly, selectively, and continuously to the concentration (strictly, activity) of the free ion of interest in aqueous solution. The ISE technique has additional advantages, such as low cost, sufficient sensitivity and selectivity, wide analytical range of the analyte concentration, insensitivity to optical interferences, and simplicity in assembly [167]. The theory and use of ISEs (and potentiometry in general) are described in Section 1.13.

The copper ion selective employed in this study exhibits pseudo-Nernstian behavior (see Section 1.12) for copper(II) for concentrations of 1.0 to 1.0×10^{-6} M with a detection limit of 1.0×10^{-8} M. The reference electrode used was an Orion double junction Ag/AgCl reference electrode (see Section 2.4.3). [138].

The calibration curve of the Cu(II) ion selective electrode is shown in Figure 3.39. It was obtained at a temperature of 25 °C. The slope of the calibration curve is 26.6, which compares very well with the manufacturer's quoted value of 26 ±3 [11]. Calibration of the electrode was repeated at temperatures of 30 °C, 34 °C and 38 °C. The slopes obtained are 26.6, 27 and 27.2 respectively. These are well within the manufacturer's quoted value, and it is an indication of the proper functioning of the electrode since it is an important diagnostic characteristic of the electrode. Generally the slope of the calibration curves for an ISE, get lower as the electrode gets old or contaminated, and the lower the slope the higher the errors on the sample measurements.

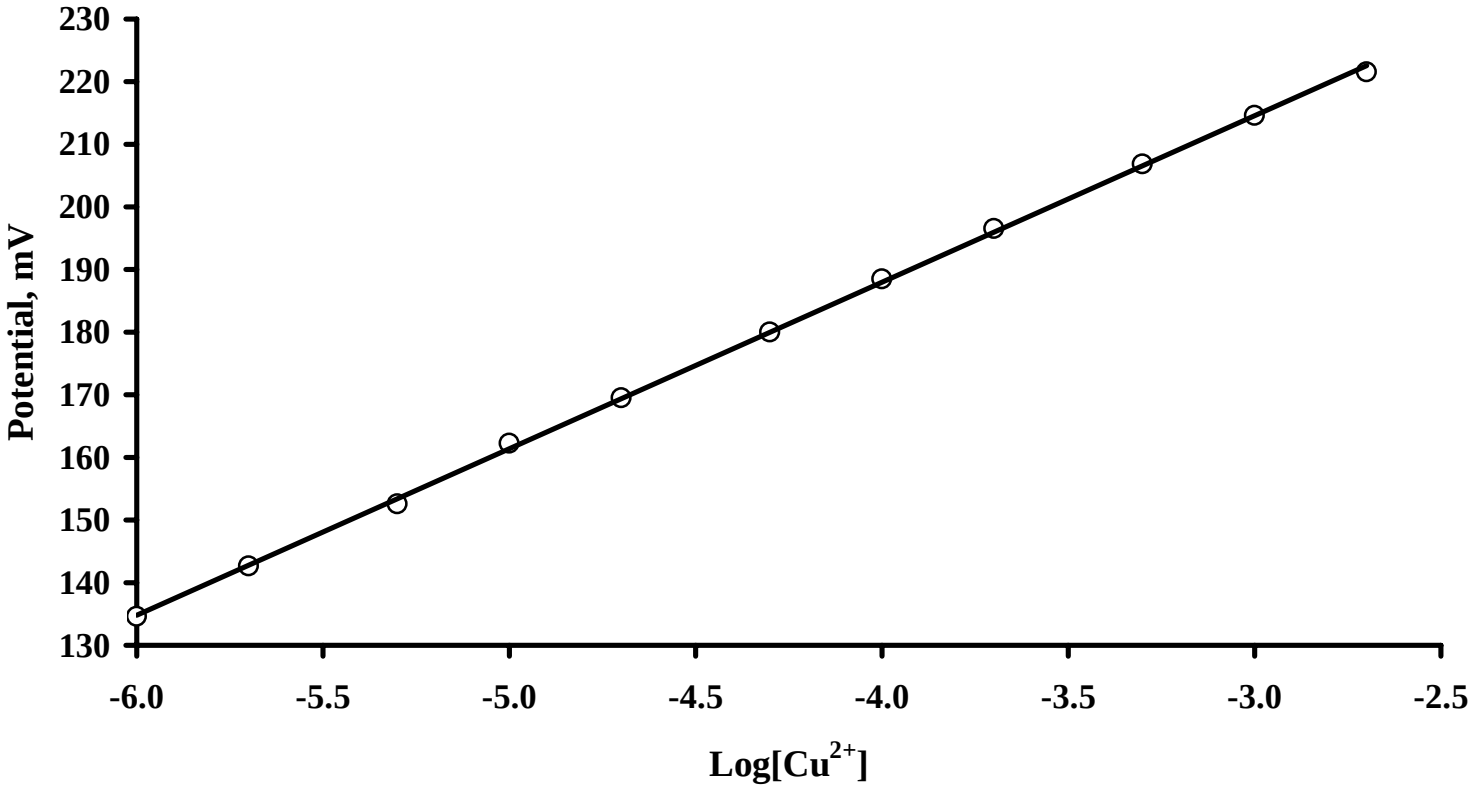

Figure 3.39 The calibration curve of the Cu(II) ISE at 25 °C.

3.3.2.4 Kinetic Study of Cu(II)-TM4 interactions using Cu(II) ISE in unbuffered solution

The aim of this study was to obtain the data required for the kinetic modeling of Cu(II) in the rumen fluid in the presence of TM4, which is lacking in the literature. The experiment was based on the ISE technique because a Cu(II) ion selective electrode is able to directly monitor the free Cu(II) concentration in the presence of the bound Cu(II) and free TM4 without a need for separation processes and without any disturbance of the binding equilibrium (see Section 1.12)

Results from the first experiments, conducted using the Cu(II)-ISE in an unbuffered solution at a temperature of 25 °C, are shown in Figure 3.40. The results obtained cannot be accounted for by a simple model involving the reaction of Cu(II) with TM4 to produce a CuTM4 complex as shown below.

$$Cu^{2+} \xrightarrow[TM4]{k} CuTM4$$

This is because a careful observation shows a biphasic concentration/time curve suggesting a two step reaction. This results compares well with a study in which radioisotope labeled ^{64}Cu was introduced intravenously into sheep which has been fed drenches of varying amounts of molybdenum and sulfur and its radioactivity monitored over time [168]. It was observed that the when ^{64}Cu was introduced, its radioactivity fell rapidly at first, and then more slowly.

This implies that the reaction between Cu^{2+} and TM4 starts with a relatively fast step, followed by a slower step. This result may lead to conclusion that the reaction between Cu^{2+} and TM4 proceeds in a sequential consecutive irreversible reaction as shown below.

$$Cu^{2+} \xrightarrow{k_1} X \xrightarrow{k_2} Y$$

Where k_1 and k_2 are kinetic constants of the first and second step respectively. However whatever the k_1 process is, if it keeps on going, a decay of $[Cu^{2+}]$ to zero should be observed. On the contrary that is not the observation but rather a sequential consecutive reaction as shown below in which the first stage is trying to reach an equilibrium but the second stage (k_2) process "bleeds off" X. The possible identity of the chemical species X and Y will be discussed later.

$$Cu^{2+} \underset{k_{-1}}{\overset{k_1}{\rightleftharpoons}} X \xrightarrow{k_2} Y$$

The set of linear ordinary differential equations corresponding to the above scheme is:

$$\begin{aligned}
\frac{d[Cu^{2+}]}{dt} &= -k_1[Cu^{2+}] + k_{-1}[X] \\
\frac{d[X]}{dt} &= k_1[Cu^{2+}] - (k_{-1} + k_2)[X] \\
\frac{d[Y]}{dt} &= k_2[X]
\end{aligned} \qquad \textbf{(3.15)}$$

These were Laplace transformed as described in Section 2.3 to yield the analytical solution shown below.

$$[Cu^{2+}] = \frac{a}{\gamma_2 - \gamma_1}[(k_{-1} + k_2 - \gamma_1)e^{-\gamma_1 t} - (k_{-1} + k_2 - \gamma_2)e^{-\gamma_2 t}] \qquad \textbf{(3.16)}$$

Where a = initial $[Cu^{2+}]$; γ_1 and γ_2 are roots of the quadratic equation

$$\gamma^2 + \gamma(k_1 + k_{-1} + k_2) + k_1k_2 = 0 \qquad \textbf{(3.17)}$$

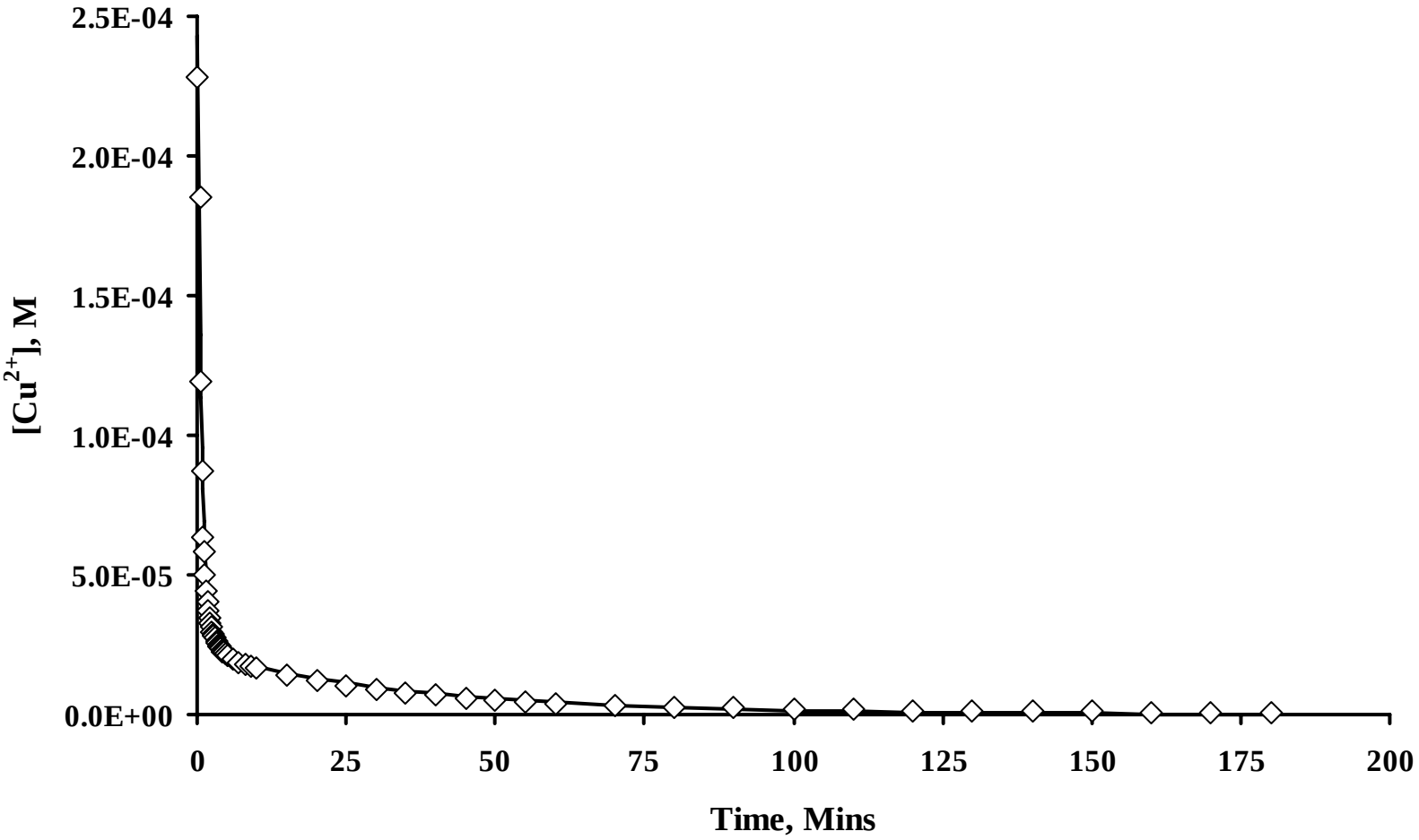

Figure 3.40 Decrease in concentration of Cu^{2+} versus time at 25 °C in an unbuffered solution as Cu^{2+} in complexes with TM4. Points represent experimental data while curves represent fit.

The data from the experiment was fitted to Equation 3.15 using Microsoft Excel® and the data analysis software Origin®. The result is as shown in Figure 3.40. The kinetic constants obtained from the fit are shown in Table 3.4; these confirm an initial reversible fast step followed by a slower step for the reaction of Cu^{2+} and TM4.

Table 3.4 Rate constants obtained from data analysis

k_1 (min^{-1})	k_{-1} (min^{-1})	k_2 (min^{-1})
1.26 ± 0.08	0.14 ± 0.01	0.034 ± 0.009

This implies that the formation of the Cu-TM4 complex consists of two steps. This is in agreement with the conclusion of a study by Clarke and Laurie [169]. In their study, an aqueous solution of TM4 was mixed with $Cu^{2+}_{(aq)}$ and monitored with ESR and UV/Visible spectrometry. Total reduction of Cu(II) to Cu(I) (from ESR measurements) and complete removal of the characteristic UV/Visible spectra of the TM4 occurred at a 1:1 Cu:TM4 ratio. Their results clearly show that any TM4 formed in the rumen would readily react with Cu(II) to produce Cu(I) – TM4 compounds. A mechanism for the formation of Cu(I) – TM4 complex was proposed as shown below; consisting of two steps and giving an overall stoichiometry of 1:1.

$$2Cu(II) + MoS_4^{2-} + 4H_2O \rightarrow 2Cu(I) + MoO4^{2-} + S_2^{2-} + 2HS^- + 6H^+$$

$$2Cu(I) + MoS_4^{2-} \rightarrow CuMoS_4$$

Although the first step in the above mechanism is not an equilibrating step, it suggest that, the initial fast decrease in Cu(II) observed in this study might be as a result of reduction of Cu(II) to Cu(I) followed by complexation reaction between Cu(I) formed and TM4. At which time also the remaining Cu(II) present slowly reduces to Cu(I); accounting for the later slow reduction in Cu(II) concentration observed in this study. If this mechanism is true then the chemical species labeled X mentioned above will be Cu(I) and Y will be CuTM4 complex. Although further studies by Laurie and Pratt

indicated that the Cu(II):TM4 stoichiometric reaction ratio is 1.5:1 and not 1:1 as they earlier suggested, a recent study in our group [102] has found the stoichiometry of Cu(II):TM4 to be indeed 1:1 and further suggested that it is more likely that the excess half equivalent of Cu(II) is only required to drive the reaction to completeness.

Although the above suggested mechanism seems plausible, the exact mechanism involved in the interaction is still unknown and an issue under research. Since the ISE used in the study measures the activity of "free" Cu(II) ions not that of Cu(I), the results obtained also suggest a possible simultaneous redox and complexation followed by a polymerization. That is the first step or process (k_1) involves a relatively fast simultaneous reduction of Cu(II) to Cu(I) and the formation of stable but soluble CuTM4 complex, which try to reach equilibrium with Cu(II) ions (k_{-1}) but the Cu(II) ions "bleeds off" slowly in the second step or process (k_2); possibly reacting further with CuTM4 to give stable and insoluble polymers as suggested in literature [95, 170].

3.3.2.5 Kinetic Study of the Cu(II)-TM4 interaction using Cu(II) ISE in buffered solution

A similar experiment was conducted to look at the effect of pH on the reaction between Cu^{2+} and TM4. To prevent possible reaction of Cu^{2+} with the buffer, 3(N – morpholino)propanesulfonic acid (MOPS) was used. This is because the sulfonate functional group of MOPS reacts very weakly with Cu(II) ions [171]. Results of the data analysis are shown in Table 3.5. The results indicate a mild to no effect on the first step of the reaction between Cu(II) and TM4. Whereas the increase in pH mildly increases the rate of the forward process (k_1) the opposite can be said of the reverse process (k_{-1}). Similar assertion can be made of the second step (k_2) except that at pH of 5.0 at all the temperatures worked at, the k_2 values increases significantly. Hence there is a slight overall increase in rate of reaction between Cu(II) and TM with increase pH.

The observed mild increase in the rate of reaction of Cu^{2+} and TM4 with increased pH suggests the possibility of a competing reaction at lower pH which reduces the rate of Cu^{2+} - TM4 reaction. This is possibly a condensation reaction of TM4 itself,

as the oxidation of inorganic and organic sulfides by metal ions to give disulfide products is well known [172]. In fact, previous studies [173] have shown that at pH of 4.5 and below, TM4 condenses to form products such as $Mo_2S_7^{2-}$ and $Mo_4S_{13}^{2-}$.

It can also be observed from the data that the rate reaction between Cu^{2+} and TM4 increased with increase in temperature with the fastest rate being observed at the average ruminal temperature of 38 °C. This is not surprising as chemical reactions are expected to go faster at higher temperatures. This suggest that the rumen temperature is an essential factor in the interaction between Cu(II) and TM4. Adding to the other ruminal conditions that enhance the reaction between Cu(II) and TM4.

Table 3.5 Rate constants obtained from kinetic data analysis at different temperature and pH values

T, ^oC	pH	k_1 (min^{-1})	k_{-1} (min^{-1})	k_2 (min^{-1})
25	4.0	9.43 ± 0.8	1.62 ± 0.02	0.034 ± 0.002
	4.5	9.45 ± 0.6	1.62 ± 0.01	0.036 ± 0.002
	5.0	9.57 ± 0.6	1.49 ± 0.03	0.141 ± 0.004
30	4.0	11.04 ± 0.7	1.55 ± 0.05	0.169 ± 0.007
	4.5	11.10 ± 0.3	1.24 ± 0.02	0.173 ± 0.003
	5.0	11.11 ± 0.4	1.12 ± 0.02	0.570 ± 0.01
34	4.0	11.48 ± 0.6	1.38 ± 0.04	0.230 ± 0.007
	4.5	11.54 ± 0.2	1.21 ± 0.02	0.376 ± 0.008
	5.0	11.58 ± 0.4	1.02 ± 0.08	0.776± 0.008
38	4.0	11.54 ± 0.9	1.31 ± 0.02	0.376 ± 0.006
	4.5	11.55 ± 0.9	1.02 ± 0.01	0.429 ± 0.006
	5.0	11.70 ± 0.6	0.78 ± 0.03	1.139 ± 0.01

A plot of $\ln k_1$ versus 1/T was obtained for the reaction between Cu^{2+} and TM4 at a pH 4.0, 4.5 and 5.0 (Figure 3.41) with the assumption that the relationship between temperature and rate constant for the forward reaction of the first step of the reaction

between Cu^{2+} and TM4 obeys the Arrhenius equation (Equation 3.17). Activation energy values obtained by calculation from the slope from the Arrhenius plots are shown in Table 3.6. The results show that the activation energy of the forward reaction of the first step of the reaction between Cu^{2+} and TM4 is independent of pH.

$$k = Ae^{-Ea/RT} \qquad \textbf{(3.18)}$$

$$\ln k = \frac{-Ea}{RT} + \ln A$$

Where k is the rate constant for the reaction, A is a proportionality constant that varies from one reaction to another, E_a is the activation energy for the reaction, R is the ideal gas constant in joules per mole kelvin, and T is the temperature in kelvin.

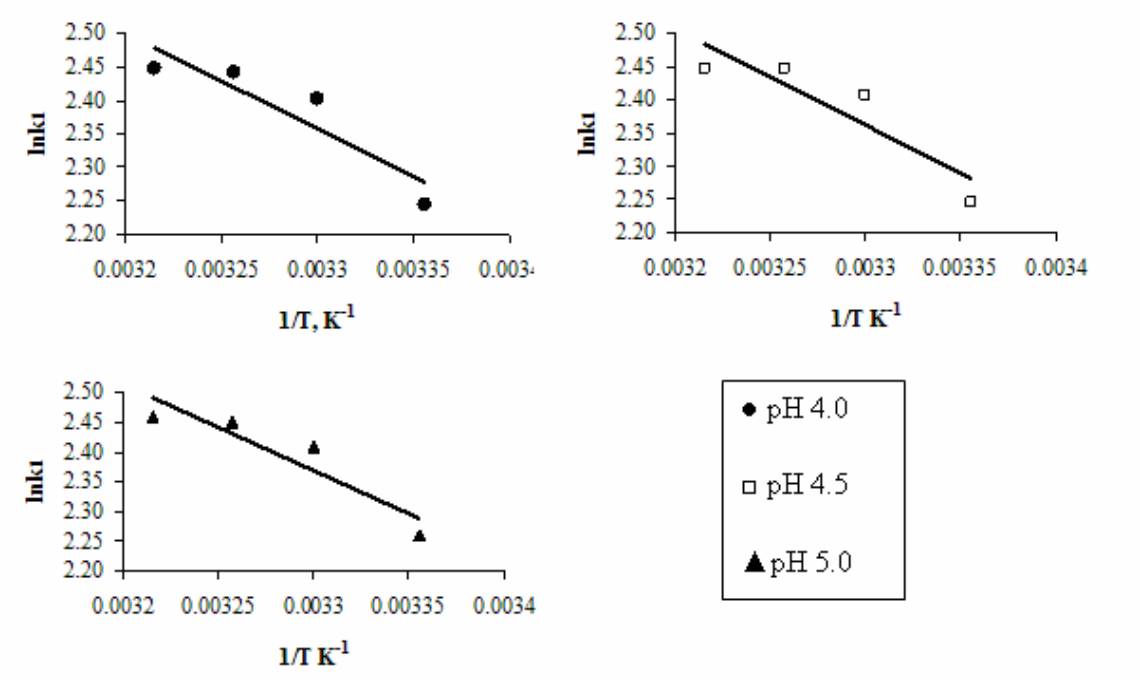

Figure 3.41 Arrhenius plots (lnk_1 vs. 1/T) for Cu^{2+}-TM4 reaction at pH of 4.0, 4.5 and 5.0. Data for the plots were obtained from Table 3.5

Table 3.6 Activation energy of the k_1 process at various pH values calculated from the slope of Arrhenius plots (Figure 3.41)

pH	Activation Energy kJ mol^{-1}
4.0	11.89 ± 0.03
4.5	11.91 ± 0.01
5.0	11.90 ± 0.02

3.3.3 Computer Simulation of Cu(II) in the Rumen Fluid in the Presence of Tetrathiomolybdate (TM4)

3.3.3.1 Computer Simulation of the Interaction between Cu(II) and TM4

The computer simulation of Cu(II) in the rumen fluid in the presence of TM4 was achieved by first modeling the interaction between Cu(II) and TM4. This was done by integrating the formation of CuTM4 into the formation of TMs (see Section 2.5). This did not present any modeling problems as both are kinetic models. The kinetic data obtained at average ruminal temperature of 38 °C in the study discussed in section 3.3.2.5 was used in the modeling. The integration of the models was made in such a way that TM4 produced at each time reacts with Cu^{2+} available. The result is shown in Figure 3.42. The results look similar to that obtained for the formation of TMs. This is because apart from TM4, none of the other TMs was modeled to react with Cu^{2+}. It can however been observed that over 107 minutes, the concentration build up of TM4 has been replaced by that of CuTM4. This means that, almost all TM4 produced reacts with available and that the reaction is effectively almost instantaneous. This is not surprising since in solution chemistry studies [169] involving Cu(II) and TM4, an immediate decrease in the concentrations of both reactants was observed, as evidenced by ESR measurements (for Cu(II)) and reduction of the characteristic UV/Visible spectra of

TM4. Complete removal of the UV/Visible spectra of TM4 (signaling possible reaction completion) was observed to have taken ca 20 minutes at 40 °C. This has been confirmed by a recent study in our group [102].

This may explain why TM4 is usually not observed in UV/Visible analysis of TM contaminated rumen, fluid but mostly TM2 and TM3. As a result of this, the production of TM4 in rumen has been called into doubt although solution chemistry supports its possible production [102]. The implication is that, as TM4 is produced in the rumen, it readily reacts with Cu^{2+} present in the rumen to form insoluble CuTM4 products which become associated with undigested food particles in the solid phase of the rumen and is not detected when rumen fluid is being analyzed for TMs [120]. This is evidenced by the fact CuTM4 products have rather been detected in the faeces of ruminants who were fed on MoO_4^{2-} enriched diets [120].

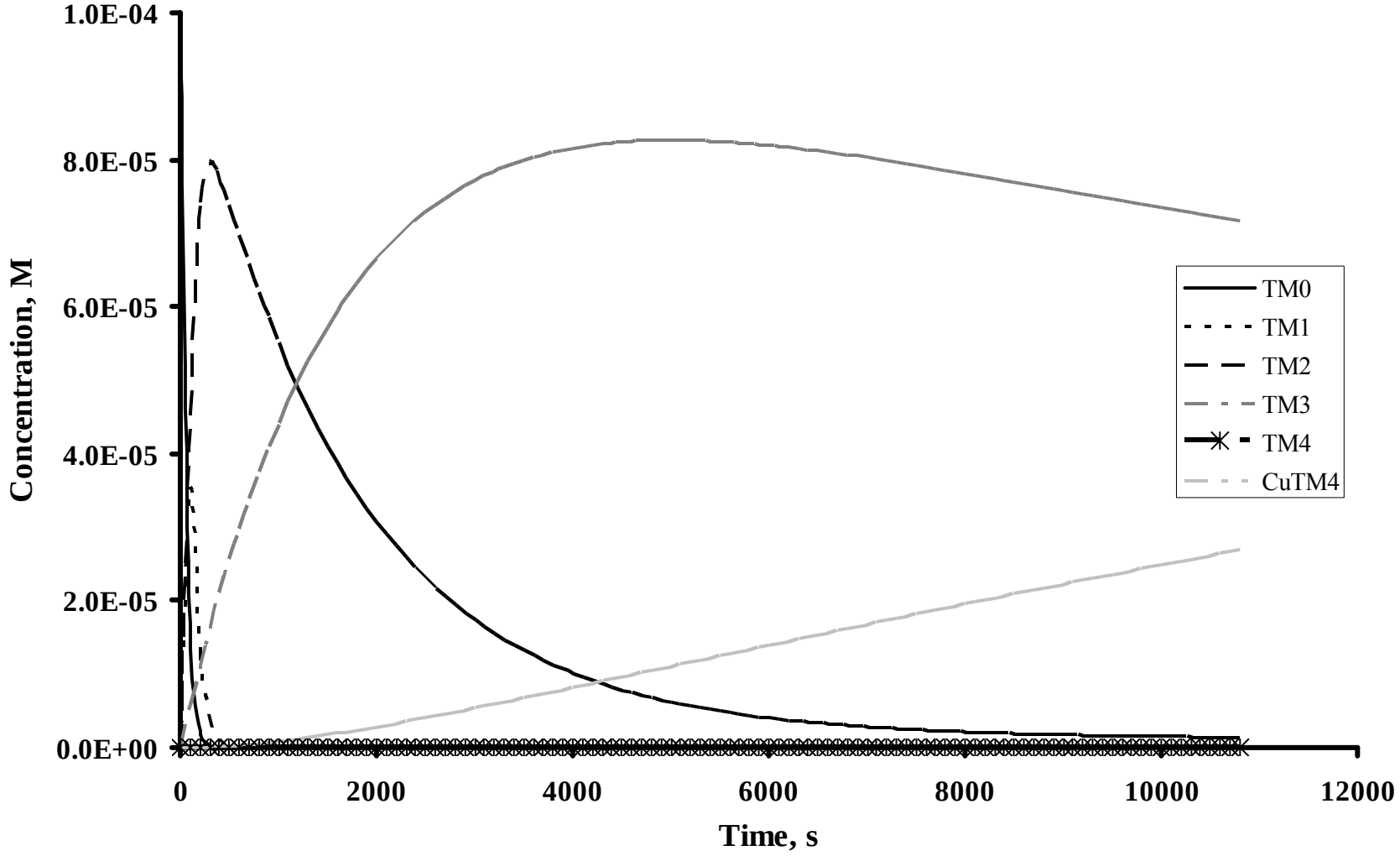

Figure 3.42 Computer simulation of formation of thiomolybdates and CuTM4: TMs as a fraction of total Mo present at different times. Initial concentration of MoO_4^{2-} is 1.0 x 10^{-4} M and that of Cu^{2+} is 3.5 x 10^{-5} M.

3.3.3.2 Integrating Cu(II)/TM4 Kinetics into the Speciation Model

The most challenging task in the computer simulation of Cu(II) in the rumen fluid in the presence of TM4 is the integration of the Cu(II)/TM4 kinetics with the thermodynamic speciation model. This is because kinetic modeling is inherently more difficult than that of thermodynamics, due to the fact that time-dependent processes are path dependent. This dependence on reaction path renders the generalization of the mathematical description of kinetics difficult, and accounts, in part, for the omission of kinetics routines from most speciation codes [174].

To overcome the challenge, two spreadsheets were developed, one for the Cu/TM kinetics and the other for the thermodynamic speciation model. These were linked by the Cu(II) concentration. The Cu/TM4 kinetics spreadsheet was run for fixed time increments of one minute (reduction in the time increments to below one minute did not make any difference in the output) and then the equilibrium model spreadsheet run after each increment. This was possible as a result of the fact that the formation of TM4 and its reaction with Cu(II) occurs slowly (minutes to hours) whereas reaction of Cu(II) with LMM ligands in the rumen is very fast (of the order of nanoseconds). This was done for about 107 minutes (mean residence time of S^{2-} in the rumen) [110]. The effect of TM4 on the bioavailability of Cu is shown in Figure 3.43. The result, compared to that of the speciation model without TM4 (see Section 3.1.1), shows that in the presence of TM4 the Cu(II) bound to low molecular ligands in the rumen is reduced by an average of 76%. The results implies that even in the presence of the myriad ligands present in the rumen, TM4 is able to bind and hold on to most of the Cu(II) available. This has been confirmed by a study [175] in which addition of Cu(II) to a solution of TM4 in strained rumen contents resulted in the loss of the TM4 UV/Visible spectrum, with complete loss of spectrum at an approximately 1:1 Cu:Mo ratio.

Other studies [118] have shown that TM2 and particularly TM3 all have an effect on Cu bioavailability when given intravenously to ruminants and have a reversible inhibitory effect on caeruloplasmin oxidase. Despite these observations, the majority of studies on the biological effects of the thiomolybdate ions have concentrated on TM4

because of its greater aqueous stability. The Cu depletion caused by TM4 appears to result from a decreased absorption from the diet and the formation of a non-bioabsorbable form [95].

The results showed that indeed thiomolybdates and in particular tetrathiomolybdate reacts with Cu(II) and reduces the exchangeable form of Cu(II) in the rumen significantly. This ultimately reduces the the amount of copper likely to be absorbed later in the gastrointestinal tract.

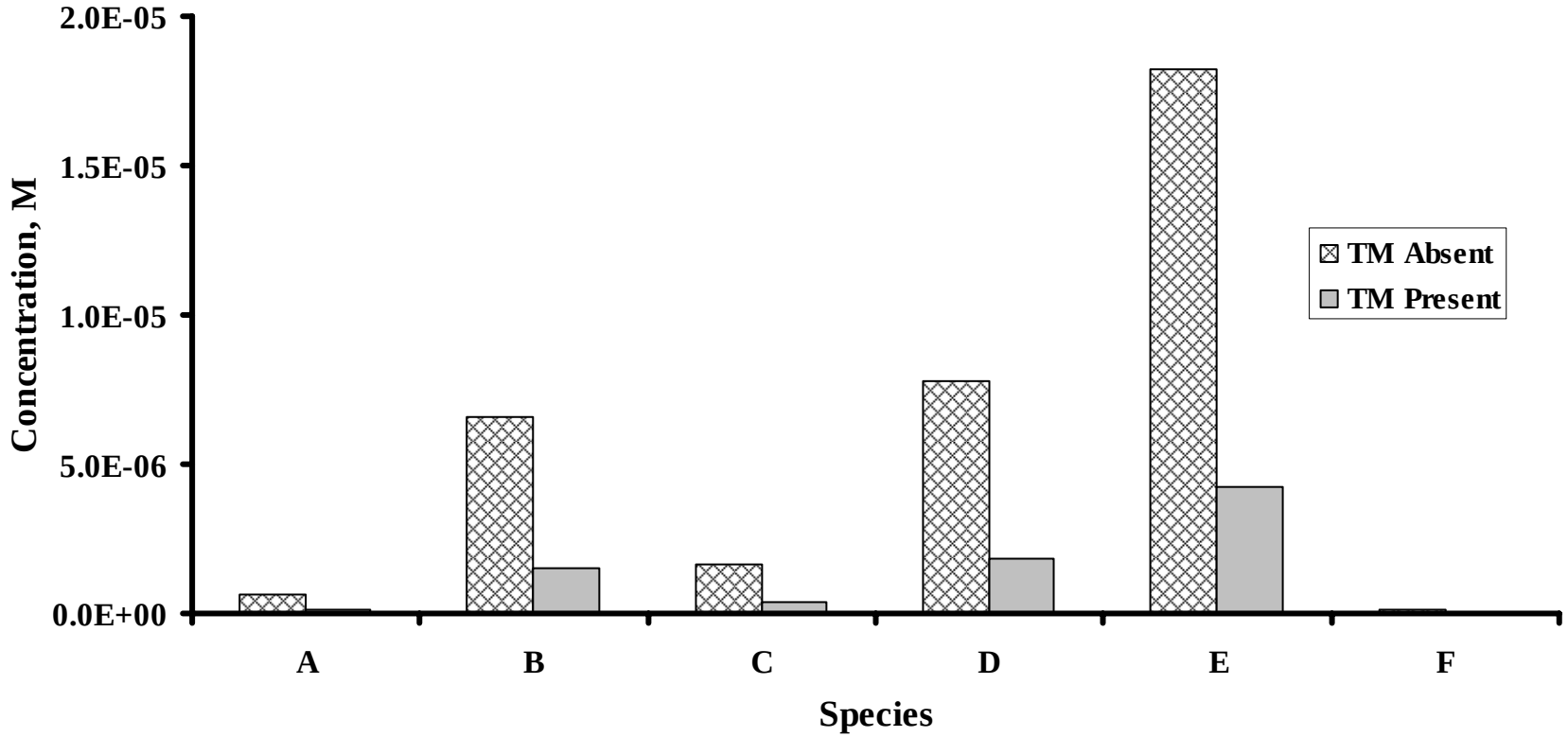

Figure 3.43 Effect of TM4 on the bioavailability of Cu ligand species present in the rumen compared with that of the speciation model without TM4. Initial concentration of MoO_4^{2-} is 1.0 x 10^{-4} M and that of Cu^{2+} is 3.5 x 10^{-5} M. Calculations were done at Ionic strength of 0.15 M; temperature of 38 °C. **A:** Copper ammonia complexes; **B:** Copper acetate complexes; **C:** Copper VFA complexes; **D:** Copper phosphate complexes; **E:** Copper carbonate complexes; **F:** Free Cu^{2+}.

4. SUMMARY, CONCLUSIONS AND FUTURE WORK

4.1 SUMMARY

Copper is an essential trace element for the normal functioning of ruminants. The essentiality of copper is due to its presence in several enzymes and proteins widely distributed in the animals, where it performs central functions in various fundamental biological processes. Thus, distinctive pathologies results from a deficiency in copper resulting in significant economic losses to livestock producers where it occurs. Copper deficiency can result from very low copper in diet (primary copper deficiency) or from interference with Cu absorption in the animal (secondary copper deficiency). The molybdenum-induced secondary copper deficiency that affects ruminants can be attributed to the formation in the rumen of thiomolybdates (TMs) ($MoO_xS_{4-x}^{2-}$; x = 0,1,2 or 3) from molybdate and sulfide. The TMs then react irreversibly with copper, thus reducing its bioavailability.

The objective of the present study is to use computer simulations to develop a Cu(II) speciation model in rumen fluid.The rumen model developed will be expanded to include the formation of thiomolybdates as well interaction of the thiomolybdates with Cu(II) in the presence of the presence myriad ligands present in the rumen. This is to find out the effect of the presence of thiomolybdates in rumen on the bioavailability of Cu(II) in the rumen.

It is difficult to model copper speciation in a biological milieu due to the presence of a myriad of potential ligands which can strongly bind such transition metals. It is important to compute the concentrations of the species that are present at each stage

that the metal passes through, because it is possible that complexes predominating in certain circumstances might prove insignificant in other environments. Though quantitatively the bulk of copper is attached to the macromolecular forms, our main interest lies in the low molecular mass ligands (LMM), as it is in these forms that copper can be transported. In particular, in these forms it can traverse the cell membranes and be readily absorbed.

4.1.1 Computer Modeling of Cu(II) Speciation in the Rumen

Computer simulations were performed with the low molar mass (LMM) ligands which can potentially bind to Cu(II). This included the major end products of rumen metabolism. These are mostly the short chain volatile fatty acids (VFAs), acetic, propanoic and butanoic, together with ammonia as well as the bicarbonate and phosphate moieties from the saliva. It is difficult to determine exact figures for concentration of the ligands in the rumen, as these are highly dependent on the diet fed to the ruminant. Nevertheless, average values can be assigned after comparison with literature values under typical conditions. The concentration of copper used for the model was 3.5×10^{-5} **M**, a modest value for the nutritional requirements of a healthy cow. Speciation calculations were performed at average ruminal pH of 6.3 and then from a pH of 5.8 to 6.8, to ensure that the simulation covers normal range of ruminal pH. Also VFA levels are known to vary substantially depending on the diet fed to the ruminant. Thus speciation calculations were therefore performed under varying concentrations of VFAs. Results of the computer simulation of copper speciation in rumen fluid at average ruminal pH of 6.3 indicate that the copper will be bound largely to the carbonate and the phosphate moieties in the rumen fluid. Though VFAs abounds in rumen fluid, it is the preponderance of these ligands that tilts the equilibrium in their favour. Also as the pH was varied from 5.8 to 6.8, Cu(II) bound to the VFAs falls off and Cu(II) bound to carbonate and phosphate moieties dominate up to the highest normal ruminal pH of 6.8, where copper exists mostly as carbonate species. Calculations performed under varying concentrations of VFAs did not result in any significant changes in the overall distribution of Cu(II).

In appraising the Cu(II) speciation in rumen fluid model developed, the results of the model were compared with the results from another computer simulation program called Hyperquad Simulation and Speciation (HySS), a utility program for the investigation of equilibria involving soluble and partially soluble species. Comparison of the distribution of copper with respect to the LMM ligands in rumen fluid at average ruminal pH of 6.3 using both methods show that there is no apparent difference between the results. Although the two programs yield the same numbers, they could both still be wrong as the results may not reflect the real Cu(II) speciation that pertains in the rumen fluid. Hence experimental validation is still essential in confirming the computer model description of Cu(II) speciation in rumen fluid.

4.1.2 ^{1}H NMR Validation of Computer Model of Cu(II) Speciation in Rumen Fluid

Rumen samples were obtained from a fistulated cow. The rumen sample was filtered, ultracentrifuged and ultrafiltered to eliminate all the macromolecules, leaving a solution consisting essentially of LMM ligands and their metal complexes. NMR spectra were obtained using the 1331 pulse sequence on a Bruker Avance 500 spectrometer at a frequency of 500.13 MHz. A well-resolved spectrum was obtained which consisted mainly of the short chain volatile acids – acetic, propanoic and butanoic acids. These acids are the end products of the metabolism in the rumen. The spectrum indicated that the acetic acid resulting from the fermentation in the rumen was a good probe for monitoring the speciation pattern.

Studies were conducted to monitor the chemical shifts of the acetate species and the Cu(II) acetate complexes. The chemical shifts of the free acetate species were determined. Cu(II) was then added to the acetic acid and the chemical shift of the resulting copper acetate complexes determined using non-linear regression. Due to the low concentration of some of the Cu(II) acetate complexes, a composite value for the complexes was used (see Section 3.2).Using the chemical shift of the acetate and Cu(II) acetate species together with the computer simulation model of the rumen contents, the

changes in chemical shifts that result from the introduction of Cu(II) to the rumen contents were predicted. Comparison was made between experimentally determined and predicted values; the resultant fits were also found to be acceptable.

Another study was undertaken where varying amounts of lysine were added as an exogenous ligand to the rumen fluid. The addition of lysine in varying amounts was to stress the model to test for robustness. With the higher concentration of lysine, and considering the strength of the Cu-lysine complexes, lysine should bind more of the Cu(II). This reduces the amount of Cu-acetate complexes, and hence a reduction in the chemical shift of the acetate is predicted. However, when these predictions are compared to the data obtained from an actual ^{1}H NMR experiments, some discrepancy was noted between the model and the experimental values. The discrepancy between model and experiment were pronounced at higher levels of lysine. It appears that the model does not adequately explain the speciation at this level of lysine. The model seems to predict a lower amount of Cu-acetate complexes than that actually observed. A number of reasons that could possibly account for this discrepancy were considered (see Section 3.2.3.1) including the possible formation of mixed ligands. The mixed ligand complex formation involving acetate and lysine introduced into the computer model, yielded a much improved fit to the experimental data. This means that as lysine is introduced into the rumen fluid, it is unable to strip copper completely off the acetate, but rather forms a mixed ligand complex with it. This complex, which was previously unaccounted for in the computer model, also contributes to overall acetate chemical shift, accounting for the discrepancies observed between the experimental data and the model.

4.1.3 Computer Modeling of Speciation of Chelated Cu(II) Supplements

For better understanding of the speciation and bioavailability of copper in ruminants, there is the need to study the speciation of other copper supplements in biofluids of ruminants so as to establish a good model for copper distribution in ruminants from one body compartments to the other. Thus speciation studies of copper

glycine, copper methionine, copper lysine and Copper EDTA, which are being used as 'chelated' copper supplements (see Section 1.8.1) for ruminants, were conducted in McDougall's solution (simulated bovine saliva) and rumen fluid using computer simulations. The aim of the study was to find out which of the chelated supplements mentioned above holds on to Cu in the presence myriad of competing ligands.

Mineral supplements are usually administered orally and since the saliva is the first fluid that the metal encounters once admitted into the digestive system of the animal, it is logical that a study of copper speciation in the animal begins with the saliva. A comparison results of the copper speciation in McDougall's solution at pH 7.0 for the copper supplements mentioned above shows that only copper histidine and copper EDTA do not degrade into other species when introduced into the bovine saliva. This is due to the strong binding of EDTA and histidine to copper (sec Section 3.1.3). Attention was then focused further down the digestive tract, at the rumen where the ingested food next travels. A comparison results of the speciation of the copper supplements in rumen fluid at an average ruminal pH of pH 6.3 shows that only copper histidine and copper EDTA do not degrade into other species when introduced into rumen fluid despite the presence of myriad amounts of ligands compared to bovine saliva. Thus of all the various copper supplements which have been looked at so far, our present understanding is that copper histidine and copper EDTA seem to be the ones that remain intact from the oral cavity to the rumen.

4.1.4 Computer Simulation of Speciation of Cu(II) in the Rumen fluid in the Presence of Thiomolybdates

The rumen model developed was expanded to include the formation of thiomolybdates as well as theinteraction of the thiomolybdates with Cu(II) in the presence of the presence myriad ligands present in the rumen. This was to find out the effect of the presence of thiomolybdates in rumen on the bioavailability of Cu(II) in the rumen.

Since the chemical reaction mechanism of thiomolybdates (see Section 1.9.2) involves reversible pseudo first order reactions (i.e. involves elementary steps where one thomolybdate species is transformed to another reversibly), the series of rate expressions for each chemical species in the scheme, were represented by a set of linear ordinary differential equations (ODE's). To simulate the formation of the thiomolybbdates with respect to time, the differential equations were solved to obtain an analytical solution, using the Laplace transform method. The analytical solutions obtained from the Laplace transform of the ODE representing the rate expressions for each thiomolybdate species, were encoded in a Microsoft Excel® spreadsheet and calculated as function of time to obtain time-dependent concentrations of thomolybdates. Kinetic data for the simulation were obtained from the literature. Results show that at the mean residence time of sulfide in the rumen of sheep is reported to be 107 minutes at which time 81.5%, 14% and 5% of TMs formed exist as TM3, TM4 and TM2 respectively. This is not surprising, considering the fact that these TMs have all been found to exist in the rumen.

The computer simulation of the formation of thiomolybdates was extended to include the formation of Cu – TM4 complex. The kinetic data used for the simulation of the formation of Cu-TM4 complex was obtained from the kinetic study of Cu-TM4 interaction using Cu(II)-ISE (see Section 3.3.2). The integration of the formation Cu-TM4 to the TM formation model was made in such a way that TM4 produced at each time reacts with Cu^{2+} available. This did not present any modeling problems as both are kinetic models. The result look similar to that obtained for the formation of thiomolybdates. This is because apart from TM4, none of the other TMs was modeled to react with Cu^{2+}. It was however observed that over 107 minutes, the concentration build up of TM4 has been replaced by that of CuTM4. This means that, almost all TM4 produced reacts with Cu(II) available and that the reaction is effectively almost instantaneous leading to the formation of insoluble CuTM4 products. This may explain why TM4 is usually not observed in UV/Visible analysis of thiomolybdate contaminated rumen fluid but mostly TM2 and TM3.

The most challenging task in the computer simulation of Cu(II) in the rumen fluid in the presence of TM4 is the integration of the Cu(II)/TM4 kinetics with the thermodynamic speciation model. This is because kinetics modeling is inherently more difficult than that of thermodynamics, mainly due to the fact that time-dependent processes are path dependent (see Section 3.3.3.2). To overcome the challenge, two spreadsheets were developed; one for the Cu/TM kinetics and the other for the thermodynamic speciation model. These were linked by the Cu(II) concentration. Cu/TM4 kinetics spreadsheet was run for fixed time increments of one minute and then the equilibrium model spreadsheet run after each increment. This was done for about 107 minutes (mean residence time of S^{2-} in the rumen). The result, compared to that of the speciation model without TM4 (see Section 3.1.1), shows that in the presence of TM4, the Cu(II) bound to low molecular ligands in the rumen is reduced by an average of 76%. The results implies that even in the presence of the myriad ligands present in the rumen, TM4 is able to bind and hold on to most of the Cu(II) available. Rendering Cu(II) non-bioavailable since it results in the formation of insoluble products which are binds unto non digestible part of the animal's food excreted by through it faeces.

4.2 CONCLUSIONS

It used to be a common assumption that the nutritional value of a trace elements depends largely on the total concentration of the nutrients as measured by analytical methods. However recent research in chemical speciation of trace element in biological systems has shown that it is the form in which the trace element occurs that influences it bioavailability but not the total concentartion. Speciation modelling and measurement can help in formulating supplements of higher bioavailabilities. These models can be used as a convenient and cost effective tool in evaluating metal supplement bioavailabilities. As with most modelling techniques, it is also important to validate such models by experimental means.

In this study computer simulation has been used to effectively model the speciation of Cu(II) in rumen fluid. The essence of the study is to help understand the distribution of copper in biofluids of ruminants with ultimate aim of helping combat copper deficiency; a problem that confronts farmers daily. Comparison of the speciation of copper glycine, copper methionine, copper lysine and Copper EDTA, which are being used as 'chelated' copper supplements for ruminants shows that only copper histidine and copper EDTA do not degrade into other species when introduced into the bovine saliva and rumen fluid. The study has shown that knowledge of the chemical form supplied could be of limited value as the many interactions in the gastro-intestinal tract could alter the chemical form ingested considerably. The form eventually absorbed could be significantly different, and might bear no resemblance to that ingested. ^{1}H NMR experiments were used to validated the computer model results.

Since thiomolybdates which form in the rumen has been identified as antagonists to the absorption of copper, the rumen speciation model was expanded to include the formation of thiomolybdates and the reaction between tetrathiomolybdate and Cu(II). The study showed that indeed thiomolybdates and in particular tetrathiomolybdate reacts with Cu(II) and reduces the exchangeable form of Cu(II) in the rumen significantly. This ultimately reduces the the amount of copper likely to be absorbed later in the gastrointestinal tract. This compliment solution studies and feed studies that has shown that thiomolybdates particularly TM4 is responsible for secondary copper deficiency in ruminants that graze on molybdenum rich soils or are feed diet rich in molybdenum.

The importance of these models lies in considering the effects of other factors that might enhance or inhibit metal absorption. They can contribute to a better understanding of the different processes that take place prior to absorption and consequently to a better prediction of metal bioavailabilities. It is difficult to consider computer simulated distribution to be completely reliable, as many of the inputs are not yet reliable enough to fully and adequately answer some of the important questions posed. The prediction of physiological uptake and distribution patterns from analytical data, such as that obtained in this thesis is premature at this stage. All the same, they

could prove useful insights, which are difficult, if not altogether impossible to obtain in any other way. It is however ultimately important to check the relevant predictions of speciation models with *in vivo* data from animal studies if available. It is hoped that the results presented here will help in enabling stake holders in the livestock industry make a rational and informed choice between the known alternatives.

4.3 FUTURE WORK

Currently, we have a good understanding of the copper speciation in bovine rumen fluid in the absence of thiomolybdates as well as the extent to which presence of thiomolybdates particularly TM4 affects bioavalability of Cu(II) in the rumen. However many questions which are chemical in nature, and are yet to be explored. The methods used here could be used in conjunction with knowledge from previous studies and other disciplines in fully understanding how thiomolybdates interfere with Cu(II) absorption in the rumen with the ultimate aim of designing optimal copper supplements.

For instance, TM3 has also been identified as likely to react irreversibly with Cu(II) just like TM4. The rumen model develop in this study can thus be expanded to include CuTM3 interaction. This will help in appreciating the extent to which TM3 and TM4 can affect Cu bioavalability in the rumen. Also modelling of chelated copper supplements, particularly copper histidine and copper EDTA, in the presence of TM4 and TM3 in rumen fluid could be explored to understand the level to which strong Cu(II) ligands such as EDTA and histidine can compete with TMs for Cu. To be able to achieve the above mentioned modelling effectively, reliable kinetic data determined under conditions mimicking that of the rumen is essential.

Since the diet of ruminants influence the types and amounts of potential Cu(II) ligands in the rumen, the model can be expanded to include the effect of diet on Cu speciation in rumen fluid in the presence of thiomolybdates. This could be done by further refining the model to closely reflect other minor ligands that may be present in

the rumen. Potentiometric work can be carried out to determine the formation constants with higher precision, as these are critical for the conclusions to be valid.

Tracking Cu(II) further down the digestive tract could extend the work done in this thesis. These investigations can be done by methods similar to those outlined in the thesis. The abomasum and the small intestine are two good candidates. Speciation in the small intestine is particularly important, as the form reaching there is likely to be absorbed, as it is the major site of absorption. It is also instructive to consider the *in vivo* redox chemistry of copper in more details.

To understand completely the processes involved in thiomolybdate interference of copper absorption and metabolism, a multi-disciplinary effort will be required. Nevertheless, it is felt that a significant start has been made in applying rigorous chemical investigative techniques to this important area.

REFERENCES

(1) Yule, L.; Quinn, G. W.; Taylor, D. M.; Williams, D. R. In *Metal Compounds in Environment and Life*; Merian, E., Haerdi, W., Eds.; Science and Technology Letters: Northwood, 1992; Vol. 4, pp 421-428.

(2) Katz, S. A.; Salem, H. *The Biological and Environmental Chemistry of Chromium*; VCH: New York, 1994.

(3) Templeton, D. M.; Ariese, F.; Cornelis, R.; Danielsson, L.-G.; Muntau, H.; Leeuwen, H. P. V.; Lobinski, R. *Pure and Applied Chemistry* **2000**, *72*, 1453-1470.

(4) Williams, D. R. *Coordination Chemistry Reviews* **1999**, *185-186*, 177-188.

(5) Deighton, N.; Goodman, B. A. In *Chemical Speciation in the Environment*; Ure, A. M., Davidson, C. M., Eds.; Blackie Academic & Professional: Glasgow, 1995.

(6) Florence, T. M. In *Trace Element Speciation: Analytical Methods and Problems*; Batley, G. E., Ed.; CRC Press Inc.: Boca Raton, 1989.

(7) Roat-Malone, R. M. *Bioinorganic Chemistry*; Wiley InterScience: Toronto, 2002.

(8) Taylor, D. M.; Williams, D. R. *Trace Element Medicine and Chelation Therapy*; The Royal Society of Chemistry: Cambridge, 1995.

(9) Gardiner, P. H. E. In *Handbook of Metal-Ligand Interactions in Biological Fluids: Bioinorganic Chemistry*; Berthon, G., Ed.; Marcel Dekker, Inc: New York, 1995; Vol. 2.

(10) Barnett, M. I.; Duffield, J. R.; Evans, D. A.; Findlow, J. A.; Griffths, B.; Morris, C. R.; Vesey, J. A.; Williams, D. R. *Nutr. Availability: Chem. Biol. Aspects* **1989**, *72*, 97.

(11) Smith, W. R.; Missen, R. W. *Chemical Reaction Equilibrium Analysis: Theory and Algoriths*; Krieger: Malabar, FL, 1991.

(12) Ingri, N.; Kakalowicz, W.; Sillen, L. G.; Warnqvist, B. *Talanta* **1967**, *14*, 1261.

(13) Perrin, D. D.; Sayce, I. G. *Talanta* **1967**, *14*, 833.

(14) May, P. M. In *Handbook of Metal-ligand Interactions in Biological Fluids: Bioinorganic Chemistry*; Berthon, G., Ed.; Marcel Dekker: New York, 1995; Vol. 2.

(15) May, P. M.; Linder, P. W.; Williams, D. R. *J. Chen. Soc., Dalton Trans* **1977**, 588.

(16) Westall, J. C.; Zachary, J. L.; Morel, F. M. M.; Dept of Civil Engineering, MIT: Cambridge MA, 1976.

(17) Sayce, I. G. *Talanta* **1968**, *15*, 1397.

(18) Kharaka, Y. K.; Barnes, I.; NTIS: Springfield,VA, 1973.

(19) Baxter, A. C.; Williams, D. R. *J.Chem.Soc.,Dalton Trans.* **1974**, 1117.

(20) Martell, A. E. *Inorg.Chim.Acta* **1985**, *103*, 73-82.

(21) May, P. M.; Murray, K.; Williams, D. R. *Talanta* **1985**, *32*, 483.

(22) Mattigold, S. V.; Sposito, G. In *Chemical Modeling in Aqueous Systems*; Jenne, E. A., Ed.; ACS Symposium Series No. 93: Washington, 1979, pp 837.

(23) May, P. M.; Murray, K. *J. Chem. Eng. Data* **2001**, *46*, 1035.

(24) May, P. M.; Murray, K. *Talanta* **1991**, *38*, 1409 and 1419.

(25) May, P. M.; Murray, K. *Talanta* **1993**, *40*, 819.

(26) Gustafsson, J. P., 2.50 ed.; Dept. of Land & Water Resources Engineering: Stockholm, 2006.

(27) Verweij, W., 6.0 ed.; Wilko Verweij: Netherlands, 2006.

(28) Gans, P.; Alderighi, L.; Ienco, A.; Peters, D.; Sabatini, A.; Vacca, A. *Coordination Chemistry Reviews* **1999**, *184*, 311-318.

(29) Parkhurst, D. L.; Thorstenson, D. C.; Plummer, L. N.; U S Geol. Survey, 1985, pp 80-96.

(30) Wolery, T. J.; Lawrence Livermore National Laboratory: Livermore CA, 1985.

(31) Duffield, J. R.; Marsicano, F.; Williams, D. R. *Polyhedron* **1991**, *10*, 1105-1111.

(32) Duffield, J. R.; Williams, D. R. *Chem. Soc. Rev.* **1986**, *15*, 291.

(33) Martell, A. E.; Smith, R. M. *Critical Stability Constants*; Plenum Press: New York, 1974-1989.

(34) May, P. M.; Murray, K.; Mayhem Unit Trust and The CSIR, Pretoria, South Africa.: Perth, 2003.

(35) Lumsdon, D. G.; Evans, L. J. In *Chemical Speciation in the Environment*; Ure, A. M., Davidson, C. M., Eds.; Blackie Academic & Professional: Glasgow, 1995.

(36) Sukhno, I. V.; Buzko, V. Y.; D.Pettit, L.; IUPAC and Academic Software: UK, 2004.

(37) Gans, P.; Sabatini, A.; Vacca, A., 2006 ed.; Protonic Software: Leeds, UK, 1998-2006.

(38) Diamond, D.; Hanratty, V. C. A. *Spreadsheet Applications in Chemistry using Microsoft Excel*; John Wiley & Sons, Inc: New York, 1997.

(39) Hill, M.-. *McGraw - Hill Concise Encyclopedia of Chemistry*; M. D. Licker The McGraw - Hill Companies, Inc.: Toronto, 2004.

(40) Hathaway, B. J. In *Comprehensive Coordination Chemistry*; Wilkinson, G., Gillard, R. D., McCleverty, J., Eds.; Pergamon Press: Oxford, 1987; Vol. 5.

(41) Jameson, R. F. In *Metals in Biological Sysytems*; Sigel, H., Ed.; Marcel Dekker, Inc: New York, 1981.

(42) Cotton, F. A.; Wilkinson, G.; Gaus, P. L. *Basic Inorganic Chemistry*, Third ed.; John Wiley & Sons: Toronto, 1995.

(43) Cotton, F. A.; Wilkinson, G.; Murillo, C. A.; Bochmann, M. *Advanced Inorganic Chemistry*, Sixth ed.; John Wiley & Sons, Inc: Toronto, 1999.

(44) Martell, A. E.; Hancock, R. D. *Metal Complexes in Aqueous Solution*; Plenum Press: New York, 1996.

(45) McMasters, W. B. S. a. D. L. *Journal of the American Chemical Society* **1961**, *83*, 4699

.

(46) Yamauchi, O. In *Handbook of Metal-Ligand Interactions in Biological Fluids: Bioinorganic Chemistry*; Berthon, G., Ed.; Marcel Dekker: New York, 1995; Vol. 1.

(47) Sigel, H. *Mixed-Ligand Complexes*; Marcel Dekker: New York, 1973.

(48) Khurana, S. C.; Nigam, I. J.; Saxena, S. P.; Gupta, C. M. *Aust. J. Chem.* **1975**, *28*, 1617-1620.

(49) Grenthe, I.; Puigdomenech, I.; Hummel, W. In *Modelling in Aquatic Chemistry*; Grenthe, I., Puigdomenech, I., Eds.; OECD Nuclear Energy Agency: Paris, 1997.

(50) Georgievskii, V. I.; Annenkov, B. N.; Samokhin, V. T. *Mineral Nutrition in Animals*; Butterworths: London, 1982.

(51) Bertini, I.; Messori, L.; Viezzoli, M. S. In *Handbook of Metal-Ligand Interactions in Biological Fluids: Bioinorganic Chemistry*; Berthon, G., Ed.; Marcel Dekker: New York, 1995; Vol. 1.

(52) Silva, F. J. J. R. d.; Williams, R. J. P. *The Biological Chemistry of the Elements*; Clarendon Press: Oxford, 1991.

(53) Linder, M. C. *Biochemistry of Copper*; Plenum Press: New York, 1991.

(54) Harris, E. D. In *Handbook of Nutritionally Essential mineral Elements*; O'Dell, B. L., Sunde, R. A., Eds.; Marcel Dekker, Inc: New York, 1997, pp 231.

(55) Turnland, J. R. In *Modern Nutrition in Health and Disease,* 9th ed.; Shills, M. E., Olson, J. A., Shike, M., Ross, A. C., Eds.; Lippincott Williams and Wilkins: Philadelphia, 1999, pp 241.

(56) Halcrow, M. A.; Knowles, P. F.; Phillips, S. E. V. In *Handbook on Metalloproteins*; Bertini, I., Sigel, A., Sigel, H., Eds.; Marcel Dekker, Inc: New York, 2001.

(57) Wattiaux, M. A.; Howard, W. T. In *Dairy Essentials*; Babcock Institute for International Dairy Research and Development, University of Wisconsin-Madison.

(58) Attaelmannan, M. A. PhD, Saskatchewan, 1999.

(59) Church, D. C., Ed. *The Ruminant Animal, Digestive Physiology and Nutrition*; Prentice-Hall: New Jersey, 1988.

(60) Soest, P. J. V. *Nutritional Ecology of the ruminant*, Second ed.; Comstock: Ithaca, 1994.

(61) Czerkawski, J. W. *Introduction to Rumen Studies*; Pergamon Press: Oxford, 1986.

(62) Pond, W. G.; Church, D. C.; Pond, K. R. *Animal Nutrition and Feeding*, Fourth ed.; John Wiley and Sons: New York, 1995.

(63) Smith, S. *The Microbiology and Biochemistry of The Rumen*; Munton and Fisson Limited: England, 1973.

(64) McArthur, J. M.; Miltimore, J. E. *Can J. Anim. Sci.* **1961**, *41*, 187.

(65) Berthon, G., Ed. *Handbook of Metal-Ligand Interactions in Biological Fluids, Bio-Inorganic Chemistry*; Marcel Dekker, Inc: New York, 1995.

(66) Angyal, S. J. *Adv. Carbohyd. Chem. Biochem.* **1989**, *47*, 1.

(67) McDowell, L. R. *Minerals in Animal and Human Nutrition*; Academic Press: San Diego, 1992.

(68) Gooneratne, S. R.; Buckley, W. T.; Christensen, D. A. *Canadian Journal of Animal Science* **1989**, *69*, 819-845.

(69) Smart, M. E.; Cymbaluk, N. F.; Christensen, D. A. *Can. Vet. J.* **1992**, *33*, 163-170.

(70) NRC *Nutrient Requirements of Beef Cattle*; National Academy of Sciences, National Research Centre: Washington D.C., 1996.

(71) Spears, J. W. *The Journal Of Nutrition* **2003**, 1506S-1509S.

(72) AAFCO; Association of American Feed Control Officials, Georgia Dept of Agriculture: Atlanta, Ga. 30334, 1990.

(73) Hidiroglou, M. H.; Ivan, M.; McDowell, L. M., Salvador, Balima Brazil 1990; 19-30.

(74) Chapman, H. L.; Bell, M. C. *J. Anim Sci* **1963**, *22*, 82.

(75) Wittenberg, K. M., University of Alberta, Alberta 1993; 62.

(76) Kincaid, R. In *Feedstuffs*, 1989, pp 22.

(77) Ho, S. K.; Ruminant Subcommittee Expert Committee on Animal Nutrition: Winnepeg, Manitoba, 1977.

(78) Patton, R. S. In *Feedstuffs*, 1990; Vol. 62, pp 14.

(79) Kincaid, R. L.; Blanickel, R. M.; Crowrath, J. D. *J. Dairy Sci.* **1986**, *69*, 160.

(80) Nockels, C. F.; DeBonis, J.; Torrent, J. *J. Anim. Sci* **1993**, *71*, 2539.

(81) Du, Z.; Henken, R. W.; Clarke, T. W. *J. Dairy Sci.* **1993**, *76(supp. 1)*, 306.

(82) Kirchgessner, M.; Grassman, E. In *Trace Element Metabolism in Animals*; Mills, C. F., Ed.; E. S. Livingstone: Deinburbhy, 1970.

(83) DeBonis, J.; Nockels, C. F. *J. Anim Sci* **1992**, *70 (Suppl)*, 314(Abst).

(84) Baker, D. H.; Olde, J.; Funk, M. A.; Wielad, B. *Poult. Sci.* **1991**, *70*, 177.

(85) Ward, J. D.; Spears, J. W. *J. Anim. Sci.* **1991**, *69(Suppl)*, 5549.

(86) Ward, J. D.; Spears, J. W. *J. Dairy Sci.* **1993**, *76*, 2994.

(87) Kegley, E. B.; Spears, J. W. *J. Anim Sci* **1994**, *72*, 2728.

(88) Wittenberg, K. M.; Boila, R. J.; Shariff, M. A. *Can J. Anim. Sci.* **1990**, *70*, 859.

(89) Ellwood, L. S. M. Sc. Dissertation, University of Saskatchewan, Saskatchewan, 1997.

(90) Aoyagi, S.; Baker, D. H. *Poult. Sci.* **1993**, *72*, 165-171.

(91) Langlands, J. P.; Donald, G. E.; Bowles, J. E.; Smith, A. J. *Austr. J. Agric. Res* **1989**, *40*, 187-193.

(92) CRC *Handbook of Chemistry and Physics*; CRC Press: Boca Raton, 1988.

(93) Johnson, J. L. In *Handbook of Nutrionally Essential Mineral Elements*; O'Dell, B. L., Sunde, R. A., Eds.; Marcel Dekker: New York, 1997.

(94) Price, J.; Will, A. M.; Paschaleris, G.; Chester, J. K. *Br. J. Nutr.* **1987**, *58*, 127-138.

(95) Laurie, S. H. *Eur. J. Inorg. Chem.* **2000**, 2443 - 2450.

(96) Berzelius, J. J. *Poggendorfs Ann. Phys. Chem.* **1826**, *7*, 262.

(97) Mellor, J. W. *A Comprehensive Treatise on Inorganic and Theoretical Chemistry*; Longmans: London, 1922.

(98) Muller, A.; Diemann, E.; Jostes, R.; Bogge, H. *Angew. Chem. Int. Ed. Engl.* **1981**, *20*, 934.

(99) Harmer, M. A.; Sykes, A. G. *Inorg. Chem.* **1980**, *19*, 2881.

(100) Brule, J. E. PhD, Brown University, Providence, 1982.

(101) Clarke, N. J.; Laurie, S. H. *Inorganic Chimica Acta* **1987**, *130*, 79-83.

(102) Quagraine, E. K. PhD, University of Saskatchewan, 2002.

(103) Clarke, N. J.; Laurie, S. H. *Journal of Inorganic Biochemistry* **1980**, *12*, 1980.

(104) Mason, J.; Kellerher, C. A.; Letters, J. *Br. J. Nutr.* **1982**, *48*, 391-397.

(105) Hynes, M.; Lamand, M.; Montel, G.; Mason, J. *Br. J. Nutr.* **1984**, *52*, 149.

(106) Hynes, M.; Wood, M.; Poole, D.; Rogers, P.; Mason, J. *Journal of Inorganic Biochemistry* **1985**, *24*, 279

.

(107) Woods, M.; Mason, J. *Journal of Inorganic Biochemistry* **1987**, *30*, 261.

(108) El-Galland, T. T.; Mills, C. F.; Bremmer, I.; Summers, R. *Journal of Inorganic Biochemistry* **1983**, *18*, 323.

(109) Bray, A. C.; Suttle, N. F.; Field, A. C. *Proc. Nutr. Soc* **1982**, *41*, 67A.

(110) Gawthorne, J. M.; Nader, C. J. *Br. J. Nutr.* **1976**, *35*, 11.

(111) George, G. N.; Pickering, I. J.; Harris, H. H.; Gailer, J.; Klein, D.; Lichtmanneger, J.; Summer, K.-H. *Journal of the American Chemical Society* **2000**, *125*, 1704-1705.

(112) Dick, A. T. *Aust. Vet. J.* **1953**, *29*, 233-239.

(113) Dick, A. T.; Dewey, D. W.; Gawthorne, J. M. *J. Agric. Sci* **1975**, *85*, 567-568.

(114) Suttle, N. F. *Br. J. Nutr.* **1975**, *34*, 411-420.

(115) Allen, J. D.; Gawthorne, J. W. *Br. J. Nutr.* **1987**, *58*, 265-276.

(116) El-Gallad, T. T.; Mills, C. F.; Brenner, I.; Summers, R. *Journal of Inorganic Biochemistry* **1983**, *18*, 323.

(117) Clarke, N. J.; Laurie, S. H.; Pratt, D. E. *Inorganic Chimica Acta* **1987**, *138*, 103.

(118) Mason, J.; Lannon, B. *Journal of Inorganic Biochemistry* **1986**, *26*, 107.

(119) Bristow, S.; Garner, C. D.; Haygard, S. K.; Morris, G. A.; Nicholson, J. R.; Mills, C. F. *J. Chem. Soc. Chem. Commun* **1985**, 479.

(120) Suttle, N. F. *Annu. Rev. Nutr.* **1991**, *11*, 121-140.

(121) Suttle, N. F. *Br. J. Nutr.* **1974**, *32*, 559-568.

(122) Huisingh, J.; Matrone, G. In *Molydenum in the environment*; Chappell, W. R., Peterson, K. K., Eds.; Marcel Decker: New York, 1976; Vol. 1.

(123) Suttle, N. F. *Ann. N. Y. Acad. Sci* **1980**, *355*, 195-207.

(124) Golfman, L. S.; Boila, R. J. *Can J. Anim. Sci.* **1990**, *70*, 905-920.

(125) Hornak, J. P.; Joseph P. Hornak, 1999.

(126) Sanders, J. K. M.; Hunter, B. K. *Modern NMR Spectroscopy*, Second ed.; Oxford University Press: New York, 1993.

(127) Abragam, A. *Principles of Nuclear Magnetism*; Oxford University Press, 1983.
(128) Wikipedia, t. f. e.; Wikimedia Foundation, Inc., 2006.

(129) Skoog, D. A.; Holler, F. J.; Nieman, T. A. *Principles of Instrumental Analysis*, Fifth ed.; Saunders College Publishing: Orlando, 1998.

(130) Leyden, D. E.; Cox, R. H. *Analytical Applications of NMR*; John Wiley and Sons: New York, 1977.

(131) Hetherington, M. A. M.Sc., University of Saskatchewan, 1995.

(132) Wuthrich, K. *NMR in Biological Research*; North-Holland Publishing Co.: Amsterdam, Netherlands, 1976

(133) Berliner, L. J.; Reuben, J. *Biological Magnetic Resonance*; Plenum Press: New York, 1987.

(134) Hore, P. J. *J. Magn. Reson* **1983**, *54*, 539
.
(135) Hore, P. J. *J. Magn. Reson* **1983**, *55*, 283.

(136) Nic, M.; Jirat, J.; Kosata, B. *IUPAC Compendium of Chemical Terminology-The Gold Book*, Electronic version ed.; International Union of Pure and Applied Chemistry, 2006.

(137) Harris, D. C. *Quantitative Chemical Analysis*, Fifth ed.; W. H. Freeman and Company: New York, 1999
.
(138) Rundle, C. C.; Nico2000 Ltd, London, UK, 2005.

(139) Koryta, J. *Annual Reviews of Materials Science* **1986**, *16*, 13-27.

(140) Budu, M. MSc, University of Saskatchewan, 2004
.
(141) Hetherington, M. A. MSc, University of Saskatchewan, Saskatchewan, 1995.

(142) Hungate, R. E. *The Rumen and its Microbes*; Academic Press: New York, 1966.

(143) Haresign, W.; Cole, D. J. A. *Recent Developments in Ruminant Nutrition*; Butterworth: Toronto, 1981.

(144) McDonald, P.; Edwards, R. A.; Greenhaugh, J. F. D. *Animal Nutrition*, Fourth ed.; John Wiley and Sons: New York, 1988.

(145) Martell, A. E.; Smith, R. M.; Motekaitis, R. J., Seven ed.; National Institute of Standards and Technology: Gaithersburg, MD, 2003.

(146) McDougall, E. I. *Biochem* **1948**, *43*.

(147) Bates, R. B. *pH: Theory and Practice*, Second ed.; John Wiley and Sons: New York, 1973.

(148) Derome, A. E. *Modern NMR Techniques for Chemistry Research*; Pergamon: Oxford, 1987.

(149) Andraos, J. *Journal of Chemical Education* **1999**, *76*, 1578.

(150) Brule, J. E.; Hayden, Y. K.; Callahan, K. P.; Edwards, J. O. *Gazetta Chimica Italiana* **1988**, *118*, 93-99.

(151) Attaelmannan, M. A.; Reid, R. S. *Journal of Inorganic Biochemistry* **1996**, *64*, 215 - 224.

(152) Ward, J. D.; Spears, J. W.; Kegley, E. B. *J. Dairy Sci.* **1996**, *79*, 127-132.

(153) Licht, S.; Forouzan, F.; Longo, K. *Analytical Chemistry* **1990**, *62*, 1356-1360.

(154) Joblin, K. N.; Lee, J. *J. Anim Sci* **1990**, *68*, 2067-2074.

(155) Wadhwa, D. R.; Care, A. D. *J Comp Physiol B* **2000**, *170*, 581-588.

(156) Kay, R. N.; Hobson, P. N. *J. Dairy Res.* **1963**, *30*, 261.

(157) Underwood, E. J. *The Mineral Nutrition of Livestock*, Second ed.; Commonwealth Agrcultural Bureaux: Slough, UK, 1981.

(158) Ammerman, C. B.; Baker, D. H.; Lewis, A. J. *Bioavailability of Nutrients for Animals: Amino acids, Minerals and Vitamins*; Academic Press Inc: San Diego, 1995.

(159) Jones, P. W.; Taylor, D. M.; Webb, L. M.; Williams, D. R. *Applied Radiation and Isotopes* **2002**, *57*, 159-165.

(160) Kincaid, R. L.; Blauwiekel, R. M.; Cronrath, J. D. *J. Dairy Sci.* **1986**, *69*, 160-163.

(161) Eckert, G. E.; Greene, L. W.; Carstens, G. E.; Ramsey, W. S. *J. Anim. Sci.* **1999**, *77*, 244-249.

(162) Grenthe, I.; Plyasunov, A. V.; Spahiu, K. In *Modelling in Aquatic Chemistry*; Grenthe, I., Puigdomenech, I., Eds.; NEA-OCED: Paris, 1997.

(163) Attaelmannan, M. A.; Reid, R. S. *Journal of Inorganic Biochemistry* **1998**, *69*, 59-65.

(164) Sarkar, S.; Mishra, S. B. S. *Coordination Chemistry Reviews* **1984**, *59*, 239.

(165) Aymonino, P. J.; Ranade, A. C.; Diemann, E.; Muller, A. *Z. Anorg. Allg. Chem.* **1969**, *371*, 300.

(166) Weber, K. M.; Leaver, D. D.; Wedd, A. G. *Br. J. Nutr.* **1979**, *41*, 403.

(167) Liu, J. *Journal of Chemical Education* **2004**, *81*, 395-397.

(168) Weber, K. M.; Boston, R. C.; Leaver, D. D. *J. Agric. Res.* **1983**, *34*, 295-306.

(169) Clarke, N. J.; Laurie, S. H. *Inorganic Chimica Acta* **1982**, *66*, L35-L38.

(170) Ecclestone, T.; Harvey, I.; Laurie, S. H.; Symons, M. C. R.; Taiwo, F. A. *Inorganic Chemistry Communications* **1998**, *1*, 460-462.

(171) Liana, Z.-X.; Li, H.-H. *Acta Crystallographica Section E* **2007**, *63*, M853-M855.

(172) Kuehn, C. G.; Iseid, S. S. *Prog. Inorg. Chem.* **1980**, *27*, 153.

(173) Saxena, R. S.; Jain, M. C.; Mittal, M. L. *Austr. J. Chem* **1968**, *21*, 91.

(174) Waite, T. D. In *Trace Element Speciation: Analytical Methods and Problems*; Batley, G. E., Ed.; CRC Press: Boca Raton, 1990.

(175) El-Gallad, T. T.; Mills, C. F.; Bremmer, I.; Summers, R. *Journal of Inorganic Biochemistry* **1983**, *18*, 323.

APPENDIX

A.1 CORRECTION OF STABILITY (EQUILIBRIUM) CONSTANTS

A.1.1 Ionic Strength Correction using Davies Equation

The stability (concentration equilibrium) constant is a function of ionic strength, e.g.

$$K = [ML]/[M][L] = K^{o} / (\gamma_{ML}/\gamma_{M}.\gamma_{L})$$

or for the reaction $pM^{2+} + qH^{+} + rL^{n-1} = MpHqLr^{(pz + q - m)}$

$$\beta_{p,q,r} = [MpHqLr]/[M]^{p}[H]^{q}[L]^{r} = \beta^{o}_{p,q,r} / (\gamma_{MpHqLr}/\gamma_{Mp}.\gamma_{Hq}.\gamma_{Lr})$$

If we use the Davies equation for the mean ionic activity coefficient:

$$Log\gamma_{i} = -Az_{i}^{2}[I^{1/2} / (1+I^{1/2}) - 0.3I]$$

then for the above general reaction, the stability constants at one ionic strength can be related to the value at zero ionic strength ($\beta^{o}_{p,q,r}$)

$$Log\beta_{p,q,r} = Log\beta^{o}_{p,q,r} + a_{i} [I^{1/2}/ (1 + I^{1/2}) - 0.3I]$$

where $a_{i} = A\Sigma z^{2}$ and A denotes the Debye - Huckel limiting slope (0.509 $M^{-1/2}$) and Σz^{2} is the square of the charge on each species summed over the formation reaction.

Example: For the reaction of Fe^{2+} with Nitrilotriacetate (NTA^{3-}), $N(CH_2COO^{-})_3$;

$$Fe^{2+} + L^{3-} = FeL^{-}$$

$log\beta_{1,0,1}$ is 8.82 in 0.1 M KCl at 25 ºC. The value at I = 0.0 M can be calculated by first determining the value for Σz^{2} and applying the Davies equation to calculate ($\gamma_{ML}/\gamma_{M}.\gamma_{L}$).

For this reaction

$$\Sigma z^{2} = (1 - 9 - 4) = -12 \text{ and } A\Sigma z^{2} = 6.12$$

and $log\beta^{o}_{p,q,r} = log\beta_{p,q,r} + 6.12[0.1^{1/2}/(1+0.1^{1/2}) - 0.3(0.1)] = 8.82 + 1.29 = 10.11$

The value of $log\beta_{1,0,1}$ at any other ionic strength I' ($log\beta'_{1,0,1}$) can be calculated from

$$Log\beta_{p,q,r} = Log\beta^{o}_{p,q,r} + a_{i} [I^{1/2}/ (1 + I^{1/2}) - 0.3I]$$

and $\text{Log}\beta'_{p,q,r} = \text{Log}\beta^{o}_{p,q,r} + a_i\,[I'^{1/2}/(1 + I'^{1/2}) - 0.3I']$

and hence

$\text{Log}\beta'_{p,q,r} = \text{Log}\beta_{p,q,r} + a_i\,[I'^{1/2}/(1 + I'^{1/2}) - 0.3I'] - a_i\,[I^{1/2}/(1 + I^{1/2}) - 0.3I]$

It must however be noted that the Davies equation cannot be used for ionic strength corrections above I = 0.2 M.

Above I = 0.2 M it is necessary to use Specific Ion Interaction Theory which requires coefficients for each specific ion pair interaction.

According to Specific Ion theory the activity coefficient of an ion *i* of charge z_i at ionic strength I is given by:

$\log \gamma_i = - Az_i^2\, I^{½}/(1 + 1.5\, I^{½}) + \sum_k \varepsilon_{(j,k)}\, m_k$

Where the summation extends over all ions k present in solution (at molality m_k) and the interaction coefficients $\varepsilon_{(j,k)}$ are zero if the two ions have the same charge.

A major limitation with this theory is that the individual interaction coefficients are not available *a priori* and must be derived from experiments.

A.1.2 Temperature Correction Using van't Hoff Equation

If the value of ΔH is known from calorimetry then it may be used in the van't Hoff equation to calculate the stability constant at one temperature (T_2) from a published value at another temperature (T_1). On integration the van't Hoff equation gives:

$\log K_1/K_2 = - (\Delta H/2.303R)[1/T_1 - 1/T_2]$

Calculations show that the effect on the lg K value from a 10 °C temperature change is likely to be small.

Example: for the reaction

$Cu^{2+} + NH_3 = [Cu(NH_3)]^{2+} \qquad \Delta H = - 46.0 \text{ kJ mol}^{-1}$

log K is 7.76 at 25 °C; what is the value of log K at 37 °C?

Substitution in the van't Hoff equation:

$\log K_1/K_2 = - (\Delta H/2.303R)[1/T_1 - 1/T_2]$

gives:

$$\log K(T = 37°C) = \log K(T = 25°C) - \left(\frac{46.0 \times 10^3}{2.303 \times 8.314}\right)[1/310 - 1/298]$$

$$= 7.76 - (-0.31) = 8.07$$

It is assumed that ΔH is constant within the temperature range T_1 to T_2.

The above corrections of stability constants using Davies equation, Specific Ion interaction theory and van't Hoff equation have been incorporated into an IUPAC sanctioned suite of software programs called Aqua Solution Software (Aq_Solutions).

The programs were developed by Igor V. Sukhno, Vladimir Y. Buzko (Chemistry Department, Kuban State University, Krasnodar, Russia (email: sukhno@chem.kubsu.ru) and Leslie D.Pettit, Academic Software, UK (e-mail: pettit@acadsoft.co.uk)

Copies of the program can be obtained from http://public.kubsu.ru/aquasolsoft/ and http://www.iupac.org/projects/2000/2000-003-1-500.html

A.2 APPLICATION OF LAPLACE TRANSFORMATION TO CHEMICAL KINETICS SYSTEMS

The basic idea of the method is to substitute the difficult task of solving simultaneous ordinary differential equations (functions of t) that describe the rate expressions for each chemical species in a reaction scheme by transforming them into a set of simple polynomial equations (functions of s).

Initial conditions are applied and these equations can then be readily solved to obtain Laplace transform functions corresponding to each chemical species (functions of s).

Once these are determined, the desired time-dependent function for a given chemical species is found by obtaining the corresponding inverse Laplace transform function (a function of t).

In practice this is done by simply looking up Laplace transform pairs in extensively compiled tables

The method is illustrated in full detail for the following reaction scheme

$$TM0 \underset{k_2}{\overset{k_1}{\rightleftharpoons}} TM1 \underset{k_4}{\overset{k_3}{\rightleftharpoons}} TM2$$

with initial conditions [TM0] = $[TM0]_0$, [TM1] = 0, and [TM2] = 0 at time zero. The corresponding rate laws are given by the following set of differential equations

$$\frac{d[TM0]}{dt} = -k_1[TM0] + k_2[TM1] \quad \textbf{(1a)}$$

$$\frac{d[TM1]}{dt} = k_1[TM0] - (k_2 + k_3)[TM1] + k_4[TM2] \quad \textbf{(1b)}$$

$$\frac{d[TM2]}{dt} = k_3[TM1] - k_4[TM2] \quad \textbf{(1c)}$$

Letting
[TM0] = x; [TM1] = y; [TM2] = z; and $[TM0]_0 = a$ leads to simplification of the Equations in (1a-c) to

$$x'(t) + k_1x(t) - k_2y(t) = 0 \quad \textbf{(2a)}$$

$$y'(t) - k_1x(t) + (k_2+k_3)y(t) - k_4z(t) = 0 \quad \textbf{(2b)}$$

$$z'(t) - k_3y(t) + k_4z(t) = 0 \quad \textbf{(2c)}$$

Applying Laplace transforms to Equations 2a–c yields

$$L\{x'(t) + k_1x(t) - k_2y(t)\} = 0 \quad \textbf{(3a)}$$

$$L\{y'(t) - k_1x(t) + (k_2+k_3)y(t) - k_4z(t)\} = 0 \quad \textbf{(3b)}$$

$$L\{z'(t) - k_3y(t) + k_4z(t)\} = 0 \quad \textbf{(3c)}$$

or

$$sx(s) - x(0) + k_1x(s) - k_2y(s) = 0 \quad \textbf{(4a)}$$

$$sy(s) - y(0) - k_1x(s) + (k_2+k_3)y(s) - k_4z(s) = 0 \quad \textbf{(4b)}$$

$$sz(s) - z(0) - k_3y(s) + k_4z(s) = 0 \quad \textbf{(4c)}$$

Further applying the initial condition criteria to Equations 4a–c yields

$$[s + k_1]x(s) - k_2y(s) = a \quad \textbf{(5a)}$$

$-k_1x(s) + [s + k_2 + k_3]y(s) - k_4z(s) = 0$ **(5b)**

$[s + k_4]z(s) - k_3y(s) = 0$ **(5c)**

The matrix method of determinants or Cramer's method with the help of MapleSoft® (multipurpose mathematics software tool) was used to solve for x(s), y(s), and z(s) in Equations 5a–c. Solving the equations in succession yields.

$$x(s) = \frac{a[s^2 + s(k_2 + k_3 + k_4) + k_2k_4]}{s^2 + s(k_1 + k_2 + k_3 + k_4) + k_1k_3 + k_2k_4 + k_1k_4} \quad \textbf{(6a)}$$

$$y(s) = \frac{ak_1(s + k_4)}{s^2 + s(k_1 + k_2 + k_3 + k_4) + k_1k_3 + k_2k_4 + k_1k_4} \quad \textbf{(6b)}$$

$$z(s) = \frac{ak_1k_3}{s^2 + s(k_1 + k_2 + k_3 + k_4) + k_1k_3 + k_2k_4 + k_1k_4} \quad \textbf{(6c)}$$

As is apparent, Equations 6a-c have the same denominator. This can be converted by factoring to $(s + \gamma_1)(s + \gamma_2)$, if one recognizes $\gamma 1$ and $\gamma 2$ as the negative roots of the quadratic equation

$$\gamma^2 + \gamma(k_1 + k_2 + k_3 + k_4) + k_1k_3 + k_2k_4 + k_1k_4 = 0 \quad \textbf{(7)}$$

Hence

$$x(s) = \frac{a[s^2 + s(k_2 + k_3 + k_4) + k_2k_4]}{(s + \gamma_1)(s + \gamma_2)} \quad \textbf{(8a)}$$

$$y(s) = \frac{ak_1(s + k_4)}{(s + \gamma_1)(s + \gamma_2)} \quad \textbf{(8b)}$$

$$z(s) = \frac{ak_1k_3}{(s + \gamma_1)(s + \gamma_2)} \quad \textbf{(8c)}$$

The corresponding inverse Laplace transforms of x(s), y(s), and z(s) found from tables of transforms yield the functions x(t), y(t), and z(t):

$$x(t) = a\left[\frac{k_2k_4}{\gamma_1\gamma_2} - \frac{k_1(\gamma_1 - k_3 - k_4)}{\gamma_1(\gamma_2 - \gamma_1)}e^{-\gamma_1 t} - \frac{k_1(k_3 + k_4 - \gamma_2)}{\gamma_2(\gamma_2 - \gamma_1)}e^{-\gamma_2 t}\right] \quad \textbf{(9a)}$$

$$y(t) = ak_1\left[\frac{k_4}{\gamma_1\gamma_2} + \frac{k_4-\gamma_1}{\gamma_1(\gamma_1-\gamma_2)}e^{-\gamma_1 t} + \frac{k_4-\gamma_2}{\gamma_2(\gamma_2-\gamma_1)}e^{-\gamma_2 t}\right] \quad \textbf{(9b)}$$

$$z(t) = ak_1k_3\left[\frac{1}{\gamma_1\gamma_2} + \frac{1}{\gamma_1(\gamma_1-\gamma_2)}e^{-\gamma_1 t} - \frac{1}{\gamma_2(\gamma_1-\gamma_2)}e^{-\gamma_2 t}\right] \quad \textbf{(9c)}$$

Finally, the set of equations 9a–c can be rewritten in the familiar form

$$[TM0]_t = [TM0]_0\left[\frac{k_2k_4}{\gamma_1\gamma_2} - \frac{k_1(\gamma_1-k_3-k_4)}{\gamma_1(\gamma_2-\gamma_1)}e^{-\gamma_1 t} - \frac{k_1(k_3+k_4-\gamma_2)}{\gamma_2(\gamma_2-\gamma_1)}e^{-\gamma_2 t}\right] \quad \textbf{(10a)}$$

$$[TM1]_t = [TM0]_0 k_1\left[\frac{k_4}{\gamma_1\gamma_2} + \frac{k_4-\gamma_1}{\gamma_1(\gamma_1-\gamma_2)}e^{-\gamma_1 t} + \frac{k_4-\gamma_2}{\gamma_2(\gamma_2-\gamma_1)}e^{-\gamma_2 t}\right] \quad \textbf{(10b)}$$

$$[TM2]_t = [TM0]_0 k_1k_3\left[\frac{1}{\gamma_1\gamma_2} + \frac{1}{\gamma_1(\gamma_1-\gamma_2)}e^{-\gamma_1 t} - \frac{1}{\gamma_2(\gamma_1-\gamma_2)}e^{-\gamma_2 t}\right] \quad \textbf{(10c)}$$

An important realization is that the method of Laplace transforms cannot be applied to chemical systems involving bimolecular transformations because there is no distributive property for product functions; that is, the Laplace transform of a product of functions does not equal the product of the Laplace transforms of those functions:

$$L\{f(t)g(t)\} \neq L\{f(t)\}L\{g(t)\} \quad \textbf{(11)}$$

Differential equations describing bimolecular transformations are classified as nonlinear and are generally solved by numerical methods. Further information can be found in literature [146]